

**Commission on the Protection
of the Black Sea Against Pollution**

**State of the Environment
of the Black Sea**

(2001-2006/7)

© 2008, Commission on the Protection of the Black Sea Against Pollution

ISBN 978-9944-245-33-3

For bibliographic purposes this document may be cited as:

BSC, 2008. State of the Environment of the Black Sea (2001-2006/7). Edited by Temel Oguz. Publications of the Commission on the Protection of the Black Sea Against Pollution (BSC) 2008-3, Istanbul, Turkey, 448 pp.

This document has been prepared with the financial assistance of the European Union.

The designations employed and the presentation of the material in this publication do not imply the expression of any opinion whatsoever on the part of the Commission on the Protection of the Black Sea Against Pollution nor of the European Union concerning the legal status of any country, territory, city or area or of its authorities, or concerning delimitation of its frontiers or boundaries. Moreover, the views expressed do not necessarily represent the decision or the stated policy of the Commission on the Protection of the Black Sea Against Pollution nor of the European Union, nor does citing of trade names or commercial processes constitute endorsement.

This publication may be reproduced in whole or in part and in any form for educational or non-profit purposes without special permission from the copyright holder, provided acknowledgement of the source is made. Commission on the Protection of the Black Sea Against Pollution would appreciate receiving a copy of any publication that uses this publication as a source.

No use of this publication may be made for resale or for any other commercial purpose whatsoever without prior permission in writing from the Permanent Secretariat of the Black Sea Commission on the Protection of the Black Sea Against Pollution.

Cover design: Nilufer Akpınar

Cover images: Photos of *Mnemiopsis leidyi* and *Beroe ovata* by Ahmet E. Kideys; Satellite images are from EC-Joint Research Centre, Global Environment Monitoring Unit Ocean Colour Archive, <http://oceancolour.jrc.ec.europa.eu/>; as presented in Fig. 2.4.8a of this report.

Published by Referans Çeviri Hizmetleri, Yazılım ve Yayıncılık Ltd. on behalf of the Commission on the Protection of the Black Sea Against Pollution.

Printing and binding: Artus Basım Tel: (0212) 289 88 80

Referans

Referans Çeviri Hizmetleri, Yazılım ve Yayıncılık San. ve Tic. Ltd. Şti.
Recep Paşa Cad. Ataköy İş Merkezi No: 5 Kat:3 34437 Taksim-Beyoğlu/İstanbul
Tel: (0212) 361 50 71 (Pbx) Faks: (0212) 361 44 29
info@referanscevirisi.com



Commission on the Protection of the Black Sea Against Pollution



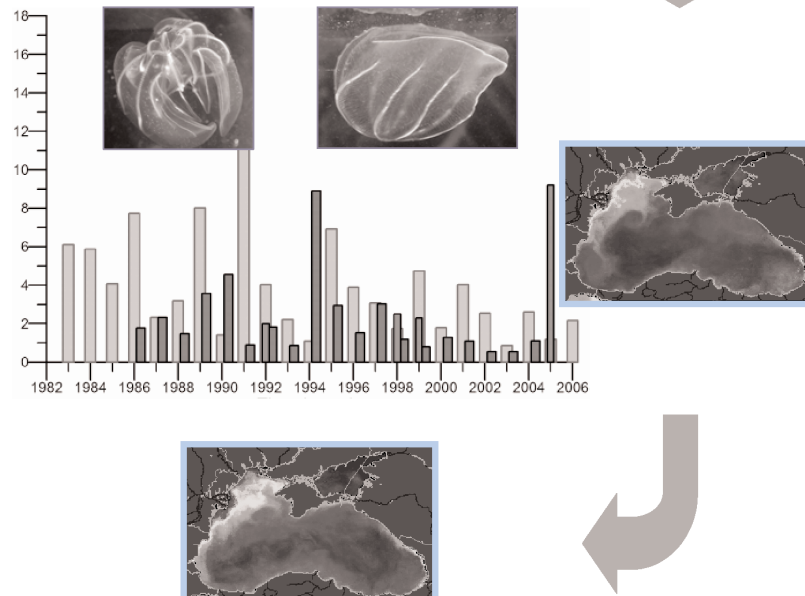
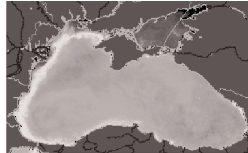
State of the Environment of the Black Sea

(2001-2006/7)

Chief Editor

Temel Oguz

Institute of Marine Sciences,
Middle East Technical University, Erdemli, Turkey



Istanbul, Turkey
2008

Authors of the State of Environment Report

Valeria **Abaza**, *National Institute for Marine Research and Development "Grigore Antipa" (NIMRD), Constanta, Romania*
abaza@alpha.rmri.ro

Vladimir **Akatov**, *Maykop State Technological University, Maykop, Russia*

Yelda **Aktan**, *Faculty of Fisheries, Istanbul University, Istanbul, Turkey*
yaktan@istanbul.edu.tr

Elena **Arashkevich**, *P.P.Shirshov Institute of Oceanology Russian Academy of Sciences, Russian Federation*
aelena@ocean.ru

Alexei **Birkun, Jr.**, *Brema Laboratory, Simferopol, Ukraine*
alexeibirkun@home.cris.net

Laura **Boicenco**, *National Institute for Marine Research and Development "Grigore Antipa" (NIMRD), Constanta, Romania*
laura_boicenco@cier.ro

Margarita V. **Chikina**, *P.P.Shirshov Institute of Oceanology, RAS, Moscow, Russia*

Adriana **Cociasu**, *National Institute for Marine Research and Development (NIMRD), Constanta, Romania*
acociasu@alpha.rmri.ro

Georgi M. **Daskalov**, *CEFAS Lowestoft laboratory, Lowestoft, Suffolk, United Kingdom*
georgi.daskalov@cefas.co.uk

Kristina **Dencheva**, *Institute of Oceanology, Bulgarian Academy of Sciences, Varna, Bulgaria,*

Yury **Denga**, *Ukrainian Scientific Centre of the Ecology of Sea, Odessa, UKRAINE*
lawmd@te.net.ua

Camelia **Dumitrache**, *National Institute for Marine Research and Development "Grigore Antipa" (NIMRD), Constanta, Romania*
iulia@alpha.rmri.ro

Victor N. **Egorov**, *The A.O. Kovalevsky Institute of Biology of the Southern Seas, NASU, Sevastopol, Ukraine*
v.yegorov@ibss.org.ua

Sergei B. **Gulin**, *The A.O. Kovalevsky Institute of Biology of the Southern Seas, NASU, Sevastopol, Ukraine*

Vakhtang **Gvakharia**, *Gamma, Tbilisi, GEORGIA*

Tsiuri **Gvarishvili**, *Georgian Marine Ecology and Fisheries Research Institute (MEFRI), Batumi, Georgia*
ciuri-gvarishvili@rambler.ru

Ludmila **Kamburska**, *Institute of Oceanology, Bulgarian Academy of Sciences, Varna, Bulgaria*
lyudmila.kamburska@jrc.it

Mery **Khalvashi**, *Georgian Marine Ecology and Fisheries Research Institute, Batumi, Georgia*
merikhal@rambler.ru

Ahmet Erkan **Kideys**, *Bahcelievler Mahallesi, Aki Sokak, No 11, Uskudar, Istanbul, Turkey*
kideys@gmail.com

Douglas **Knowler**, *School of Resource and Environmental Management Simon Fraser University, Burnaby, British Columbia, Canada*
djk@sfu.ca

Tzenka **Konsulova**, *Institute of Oceanology, BAS, Varna, Bulgaria*
konsulova@io-bas.bg

Alexander **Korshenko**, *State Oceanographic Institute, Moscow, RUSSIA*
korshenko@mail.ru

Nikita V. **Kucheruk**, *P.P.Shirshov Institute of Oceanology, RAS, Moscow, Russia*
kucheruk@ocean.ru

Gennady V. **Laptev**, *Ukrainian Hydrometeorological Institute, Kiev, Ukraine*

Nino **Machitadze**, *Gamma, Tbilisi, Georgia*
n_machitadze@yahoo.com

Olga V. **Maximova**, *P.P.Shirshov Institute of Oceanology RAS, Moscow, Russian Federation*

- Eteri **Mickashavidze**, *Georgian Marine Ecology and Fisheries Research Institute (MEFRI), Batumi, Georgia*
- Veselina **Mihneva**, *Institute of Fishing Resources, Varna, Bulgaria*
- Alexander **Mikaelyan**, *P.P.Shirshov Institute of Oceanology RAS, Moscow, Russia*
mikael@ocean.ru
- Galina **Minicheva**, *Odessa Branch, Institute of Biology of the Southern Seas, NASU, Odessa, Ukraine*
minicheva@eurocom.od.ua
- Natalia Yu. **Mirzoyeva**, *The A.O. Kovalevsky Institute of Biology of the Southern Seas, NASU, Sevastopol, Ukraine*
- Snejana **Moncheva**, *Institute of Oceanology, Bulgarian Academy of Sciences, Varna, Bulgaria*
snejm@mail.varna.techno-link.com
- Natalia A. **Moruchkova**, *P.P.Shirshov Institute of Oceanology RAS, Moscow, Russian Federation*
- Eteri **Musaeva**, *P.P.Shirshov Institute of oceanology Russian Academy of Sciences*
- Dina **Nesterova**, *Odessa Branch, Institute of Biology of the Southern Seas, NASU, Odessa, Ukraine*
- Alexei I. **Nikitin**, *SE SPA "Typhoon" of Roshydromet, Obninsk, Russia*
- Temel **Oguz**, *Institute of Marine Sciences, Middle East Technical University, Erdemli, Turkey*
oguz@ims.metu.edu.tr
- Andra **Oros**, *National Institute for Marine Research and Development, Constanta, Romania*
andra@alpha.rmri.ro
- Iolanda **Osvath**, *Marine Environment Laboratories, International Atomic Energy Agency, Monaco*
I.Osvath@iaea.org
- Bayram **Ozturk**, *Turkish Marine Research Foundation (TUDAV), Istanbul, Turkey*
ozturkb@istanbul.edu.tr
- Nicolae **Panin**, *National Institute of Marine Geology and Geo-ecology - GeoEcoMar, Romania*
panin@geoecomar.ro
- G.G. **Polikarpov**, *The A.O. Kovalevsky Institute of Biology of the Southern Seas, NASU, Sevastopol, Ukraine*
- Leonid **Polishchuk**, *Odessa Branch, Institute of Biology of the Southern Seas, NASU, Odessa, Ukraine*
- Nikolai **Revkov**, *Institute of Biology of the Southern Seas, NASU, Sevastopol, Ukraine*
nrevkov@yandex.ru
- Fatih **Sahin**, *Sinop University, Fisheries Faculty, 57000 Sinop, Turkey*
fthshn@hotmail.com
- Alis **Sburlea**, *National Institute for marine research and development "Grigore Antipa", Constanta, Romania,*
- Murat **Sezgin**, *Sinop University, Faculty of Fisheries, Sinop, Turkey*
msezgin@omu.edu.tr
- Tamara **Shiganova**, *P.P.Shirshov Institute of oceanology Russian Academy of Sciences*
shiganova@ocean.ru
- Vladislav A. **Shlyakhov**, *YugNIRO, Kerch, Crimea, Ukraine*
fish@kerch.com.ua
- Uliana V. **Simakova**, *P.P.Shirshov Institute of Oceanology RAS, Moscow, Russian Federation*
- Kremena **Stefanova**, *Institute of Oceanology, Bulgarian Academy of Sciences, Varna, Bulgaria*
stefanova@www.io-bas.bg
- Nikolai A. **Stokozov**, *The A.O. Kovalevsky Institute of Biology of the Southern Seas, NASU, Sevastopol, Ukraine*
- Ahmet Nuri **Tarkan**, *Mugla University, Faculty of Fisheries Mugla, Turkey*
tarkann@mu.edu.tr
- Florin **Timofte**, *National Institute for Marine Research and Development "Grigore Antipa" (NIMRD), Constanta, Romania*
- Valentina **Todorova**, *Institute of Oceanology, BAS, Varna, Bulgaria*
vtodorova@io-bas.bg
- Funda **Ustun**, *Sinop University, Fisheries Faculty, Sinop, Turkey*
fundaustun@hotmail.com

Madonna **Varshanidze**, *Georgian Marine Ecology and Fisheries Research Institute (MEFRI), Batumi, Georgia*
mvarshanidze@yahoo.com

Violeta **Velikova**, *29 Inebolu Sokak, Kabatas, Istanbul, Turkey*
velikova_violeta@yahoo.com

Alexander **Vershinin**, *P.P. Shirshov Institute of Oceanology Academy of Sciences, Russian Federation*
alexander.vershinin@yahoo.com

Oleg V. **Voitsekhovych**, *Ukrainian Hydrometeorological Institute, Kiev, Ukraine*
voitsekh@voi.vedos.kiev.ua

Preface and Acknowledgements

More than 60 prominent scientists working on the Black Sea ecosystem have contributed to this report. Despite this is the most comprehensive report on the State of Environment of the Black Sea for the period 2001-2007, limitation in the systematically collected data and indicators, makes a conclusive inference difficult on the real state of the ecosystem of this sea.

Chapter 1, within two sub-chapters, presents introductory information on the Black Sea physico-chemical characteristics and geology/history. Chapter 2 deals with one of the most important problems of the Black Sea, the Eutrophication. Chapter 3, dealing with Chemical Pollution, has several subchapters of different pollutant groups. Radioactive pollution is dealt in Chapter 4. States of phytoplankton, zooplankton, macrophytobenthos, zoobenthos are presented in Chapters 5, 6, 7 and 8, respectively. The fisheries is the subject of Chapter 9 and mammals of Chapter 11. Socio-economic pressures and impacts are included in Chapter 11. The overall assessment of the report summarizing all these issues is given in Chapter 12.

Contributions to Chapter 4 were provided with partial support from the International Atomic Energy Agency's Technical Co-operation Project RER/2/003 for "Marine Environmental Assessment in the Black Sea Region".

Thanks to UNDP/GEF BSERP Project personnel and earlier Permanent Secretariat staff for their support at the initial stages of the preparation of this report, all authors and especially to the chief editor Prof Temel Oguz for their scientific contributions, to the Advisory Group members of the Commission on the Protection of the Black Sea Against Pollution for their comments, Mr Kiril Iliev for formatting, Ms Nilufer Akpınar for preparing for printing and all other organizations and people who kindly provided data, information and other input. Special thanks go to Dr Violeta Velikova, not only for her personal scientific contribution in the entire report, but also for her organizational and thorough efforts making compilation of this comprehensive report possible.

Prof Ahmet E. Kideys

Executive Director
Permanent Secretariat
Commission on the Protection of the Black Sea Against Pollution
Dolmabahçe Sarayı, 2. Hareket Köşkü,
34353 Beşiktaş, İstanbul, Turkey

Table of Contents

Table of Contents	9
List of Tables	13
List of figures	19
CHAPTER 1A. GENERAL OCEANOGRAPHIC PROPERTIES: PHYSICO-CHEMICAL AND CLIMATIC FEATURES (T. Oguz)	39
1A.1. Main physical and chemical features	39
1.2.2. Circulation characteristics	45
1.2.3. Climatic properties	48
CHAPTER 1B GENERAL OCEANOGRAPHIC PROPERTIES: GEOGRAPHY, GEOLOGY AND GEOCHEMISTRY (N. Panin)	61
1B.1 Geographic position and physiography	61
1B.2. Geology of the Black Sea	62
1B.3. Water and sediment supply from rivers	63
1B.4. Sedimentary systems of the Black Sea	64
1B.5. Past environmental and sea level changes in the Black Sea	67
CHAPTER 2 THE STATE OF EUTROPHICATION (T. Oguz <i>et al.</i>)	83
2.1. Introduction	83
2.2. Long-term changes in river nutrient loads	83
2.3. Long-term changes in nutrient concentrations	87
2.4. Surface chlorophyll concentration	99
2.5. Surface and near-bottom oxygen concentrations	105
2.6. Conclusions and key assessments	109
CHAPTER 3 THE STATE OF CHEMICAL POLLUTION (A. Korshenko <i>et al.</i>)	113
3.1. The State Of Total Petroleum Hydrocarbons (TPHs)	113
3.1.1. Water	113
3.1.2. Bottom Sediments	123
3.2. The State Of Chlorinated Pesticides	129
3.2.1. Water	129
3.2.2. Bottom Sediments and Biota	134
3.3. The State Of Trace Metals	150
3.3.1. Ukrainian sector of the Black Sea - Northwestern region	150
3.3.2. Russian sector of the Black Sea - Northeastern region	155
3.3.3. Georgian sector of the Black Sea - Southeastern region	157
3.3.4. Romanian sector of the Black Sea - Western region	159
CHAPTER 4 THE STATE OF RADIOACTIVE POLLUTION (V. Egorov <i>et al.</i>)	163
4.1. Introduction	163
4.2. Concentrations and inventories of radionuclides in the water column	163
4.3. Concentrations and inventories of radionuclides in sediment	166
4.4. Radionuclides in marine biota	168
4.5. Conclusions	170
CHAPTER 5 THE STATE OF PHYTOPLANKTON (D. Nesterova <i>et al.</i>) ..	173
5.1. Introduction	173
5.2. Species composition	174

5.3. Long-term changes in algal blooms	181
5.4. Seasonal dynamics	189
5.5. Conclusions and recommendations	191
Appendix	192
CHAPTER 6 THE STATE OF ZOOPLANKTON (T. Shiganova <i>et al.</i>)	201
6.1. Introduction	201
6.2. Ukrainian shelf area	202
6.3. Romanian shelf area	211
6.4. Bulgarian shelf area	215
6.5. Turkish shelf area	224
6.6. Georgian shelf area	227
6.7. Northeastern shelf area	228
6.8. Conclusions	242
CHAPTER 7 THE STATE OF MACROPHYTOBENTHOS (G. Minicheva <i>et al.</i>)	247
7.1. Introduction	247
7.2. Ukrainian shelf area	247
7.3. Romanian shelf area	252
7.4. Bulgarian shelf area	256
7.5. Turkish shelf area	261
7.6. Northeastern (Russian) shelf area	263
7.7. Conclusions	269
CHAPTER 8 THE STATE OF ZOOBENTHOS (N. Revkov <i>et al.</i>)	273
8.1. Introduction	273
8.2. Ukrainian shelf area	274
8.3. Romanian shelf area	288
8.3.1. Peculiarities of zoobenthos during the previous state of ecosystem	288
8.3.2. Peculiarities of zoobenthos during the present state of ecosystem	291
8.4. Bulgarian shelf area	297
8.4.1. Characteristics of major zoobenthic communities	297
8.4.2. Spatial patterns of diversity, abundance and biomass distribution	300
8.4.3. Assessment of recent ecological state	302
8.4.4. Long-term trends in species diversity, abundance and biomass	303
8.5. Turkish Shelf waters	306
8.6. Georgian shelf area	309
8.7. Russian Shelf Waters	312
8.8. Conclusions	314
CHAPTER 9 THE STATE OF MARINE LIVING RESOURCES	
(V. Shlyakhov & G. Daskalov)	321
9.1. Introduction	321
9.2. The state of key anadromous fishes	321
9.2.1. Sturgeons	322
9.2.2. Pontic shad	327
9.3. The state of key pelagic fishes	329
9.3.1. Sprat	330
9.3.2. Black Sea anchovy	332
9.3.3. Horse mackerel	335
9.3.4. Ecosystem effects on pelagic fisheries	336

9.4. The state of populations of key demersal fishes	337
9.4.1. Whiting	338
9.4.2. Picked dogfish	343
9.4.3. Turbot	345
9.4.4. Striped and red mullets	349
9.4.5. Mulletts (<i>Mugilidae</i>)	351
9.5. Commercial mollusks	353
9.5.1. Mediterranean mussel	353
9.5.2. Sea snail (<i>Rapana</i> spp.)	354
9.5.3. Clams	356
9.6. Water plants	357
9.7. Conclusions	358
CHAPTER 10 THE STATE OF CETACEAN POPULATIONS (A. Birkun)	365
10.1. Introduction	365
10.2. Harbour porpoise (<i>Phocoena phocoena relicta</i> Abel, 1905)	366
10.2.1. Taxonomy and genetics	366
10.2.2. Distribution	366
10.2.3. Abundance	368
10.2.4. Habitat and ecology	369
10.2.5. Life history	373
10.2.6. Past and ongoing threats	374
10.2.7. Population trend	375
10.3. Short-beaked common dolphin (<i>Delphinus delphis ponticus</i>)	376
10.3.1. Taxonomy and genetics	376
10.3.2. Distribution	376
10.3.3. Abundance	376
10.3.4. Habitat and ecology	377
10.3.5. Life history	377
10.3.6. Past and ongoing threats	377
10.3.7. Population trend	378
10.4. Common bottlenose dolphin (<i>Tursiops truncatus ponticus</i>)	378
10.4.1. Taxonomy and genetics	378
10.4.2. Distribution	379
10.4.3. Abundance	379
10.4.4. Habitat and ecology	380
10.4.5. Life history	381
10.4.6. Past and ongoing threats	381
10.4.7. Population trend	383
10.5. Conservation tools and strategies	383
10.5.1. National instruments	384
10.5.2. International and regional instruments	385
10.5.3. The IUCN status	387
10.5.4. Conservation plan for Black Sea cetaceans	387
10.6. Conclusions	389
Appendix A. Examples of cetacean research and conservation projects implemented in the Black Sea region in 2002-2006	396
Appendix B. Conservation Plan for Black Sea Cetaceans: aims of actions proposed	398
Appendix C. Conservation Plan for Black Sea Cetaceans: actions and activities of high priority	399

CHAPTER 11 SOCIO-ECONOMIC PRESSURES AND IMPACTS (D. Knowler)	401
11.1. Introduction	401
11.2. Valuing the Environmental Goods and Services Provided by the Black Sea	402
11.3. Socio-economic and Institutional Pressures	404
11.4. Consequences of Environmental Change in the Black Sea	407
11.4.1 Fisheries	407
11.4.2 Tourism	410
11.4.3 Health	412
11.5. Sustainability: Progress and Prospects	412
11.6. Conclusions	414
CHAPTER 12 OVERALL ASSESSMENT OF THE PRESENT STATE OF BLACK SEA ECOSYSTEM (T. Oguz et al.)	417
12.1. Introduction	417
12.2. Mesoscale variability of the circulation system	418
12.3. Climatic regulation of the Black Sea	419
12.4. Eutrophication/Nutrient enrichment	421
12.5. Chemical pollution	428
12.6. Biodiversity change, habitat destruction, alien species invasions	431
12.7. Status of marine living resources	442
12.8. Conclusions	444

List of Tables

Table 1B.1. Fluvial water and sediment discharge into the Black Sea. *Data from Balkas et al. (1990); ** multiannual mean discharge before damming the River Danube after Bondar (1991); Panin (1996).	63
Table 1B.2. Stratigraphy and correlations of Upper Quaternary phases for the coastal and inner shelf zones (with slight modification from Fedorov, 1978).	71
Table 1B.3. Stratigraphy and correlations of Upper Quaternary phases for shelf and bathyal zones (with slight modification from Scherbakov et al., 1979)	74
Table 2.2.1. The sources and causes of nutrient enrichment in the western coastal waters of the Black Sea.	84
Table 2.2.2 Annual-mean river-borne nutrient loads (in kilotonnes y ⁻¹) into the Black Sea from each country during 2003-2005 (from TDA, 2007). The superscripts (a) and (b) denote the estimates based on the TNMN measurements at Reni and the NMRD measurements at Sulina discharge point, respectively.	84
Table 2.3.1. Multi-annual mean surface nutrient concentrations (μM) in Constanta (after Velikova and Cociasu, 2004)	89
Table 2.3.2. Annual and regional-mean concentrations of phosphorus and nitrogen species in Bulgarian coastal waters during 2001-2003. TP, TN and ON refer to total phosphorus, total nitrogen and organic nitrogen, respectively. All values are expressed in μM (after Velikova and Cociasu, 2004).	93
Table 2.3.3. Multi-annual mean nutrient ratios in Romanian surface coastal waters, the Bay of Varna and Bulgarian coastal waters (BW) as an average of all measurements within the 50 km zone (after Velikova and Cociasu, 2004)	99
Table 3.1.1. The average concentration of TPHs (mg/l) in different part of the Black Sea measured during the September-October 2000 IAEA Cruise.	114
Table 3.1.2. The average and maximum concentrations of TPHs (mg/l) in Ukrainian part of the Black Sea, 2000-2005.	115
Table 3.1.3. Annual average (above) and maximum concentrations (below) of TPHs (mg/l) in Ukrainian coastal waters of the Black Sea, 2000-2004 [4].	116
Table 3.1.4. The average and maximum concentration of TPHs (mg/l) in the surface coastal waters of Romanian part of the Black Sea, 2001-2005.	117
Table 3.1.5. TPHs concentrations in different water layers along the Russian coast in 2002-2006.	120
Table 3.1.6. Mean concentration of TPHs (mg/l) and number of measurements (in parantheses) in the different zones of Russian coastal waters in 2002 - 2006.	121
Table 3.1.7. Annual variation of the mean concentration of TPHs (mg/l) in Russian coastal waters in 2002 - 2006.	121
Table 3.1.8. Seasonal variation of the mean concentration of TPHs (mg/l) in Russian coastal waters in 2002 - 2006.	121
Table 3.1.9. Maximum and mean concentration of Total Petroleum Hydrocarbons (mg/l) in the Black Sea waters in 1992 - 2006.	122

Table 3.1.10. The mean concentration of TPHs ($\mu\text{g/g}$) and number of measurements within monitoring programme in the different sites of Romanian coast in 2005.	125
Table 3.1.11. The concentration of TPHs ($\mu\text{g/g}$) and other physical and chemical parameters of the bottom sediments of the Georgian part of the Black Sea in June 2006 [9].	127
Table 3.1.12. Maximum and mean concentration of TPHs ($\mu\text{g/g}$) in the bottom sediments of the Black Sea in 1995 - 2006.	129
Table 3.2.1. Maximum and average concentration of pesticides (ng/l), and number of observations (in parantheses) in marine waters of the Black Sea in 1992 - 2005.	132
Table 3.2.2. The average concentration of chlorinated pesticides (ng/l) in the different zones of Russian costal waters in July 2005.	134
Table 3.2.3. The average concentration of pesticides in the bottom sediments in the North-Western Shelf of Ukrainian waters, ng/g	136
Table 3.2.4. The concentration (ng/g) of organic pollutants in biota and bottom sediments along the Russian coast in August-September 2003.	140
Table 3.2.5. Maximum and mean concentration of pesticides (ng/g), and number of measurements (in parentheses) in the bottom sediments of the Black Sea in 1993 - 2006.	144
Table. 3.2.6. The repetitions of high $\gamma\text{-HCH}$ concentration in the bottom sediments exceeds the PL 0.05 ng/g in the different sets of samples (in per cent).	146
Table. 3.2.7. The repetitions of high DDTs concentration in the bottom sediments exceeds the PL 2.5 ng/g in the different sets of samples (in per cent).	148
Table 3.3.1. The trace metals concentration ($\mu\text{g/l}$) in Ukrainian waters of the Black Sea in December 2004 - January 2005 (25th cruise of R/V "Vladimir Parshin").	151
Table 3.3.2. The trace metals concentration ($\mu\text{g/g}$) in the bottom sediments of Ukrainian part of the Black Sea in December 2004 - January 2005 (25 cruise of R/V "Vladimir Parshin").	154
Table 3.3.3 The trace metal concentration ($\mu\text{g/g}$) in the bottom sediments of Phyllophora field and NW Shelf of the Black Sea in July-August 2007 (26 cruise of R/V "Vladimir Parshin").	157
Table 3.3.4 Metal concentration ($\mu\text{g/g}$) in bottom sediments measured during June-July 2002 to the south of Taman.	157
Table 3.3.5. The metals concentration ($\mu\text{g/g}$) in the bottom sediments of Georgian shelf in 1993-1995 and 2000.	157
Table 4.1. The dynamics of ^{137}Cs and ^{90}Sr levels (Bq m^{-3}) in surface waters of the North-Eastern Black Sea near the Russian Coast.	166
Table 4.2. The ranges of ^{137}Cs and ^{90}Sr concentrations in marine biota ($\text{Bq kg}^{-1} \text{ w.w.}$) from coastal measurements performed by the riparian countries in the years 2000-2005.	170
Table 5.1. Taxonomic composition of Black Sea phytoplankton in Ukraine waters	175
Table 5.2. Phytoplankton species distributed along the Turkish Coast of Black Sea.	179
Table 5.3. Mean phytoplankton density and biomass in the shallow waters in front of Constanta and number of blooms registered in Romanian marine waters during different periods.	184

Table 5.4. Abundance (cells/l) and biomass (mg·m ⁻³) of dominant and blooming phytoplankton species along the Bulgarian shelf in different periods.	192
Table 5.5. Maximum abundance (million cells/l) of species that caused phytoplankton blooms in the northwestern Black Sea in the 1954-1960s and in 1973-2005.	197
Table 6.1. Long-term dynamics of biomass (mg·m ⁻³) of the main species of zooplankton of the northwestern Black Sea (provided by Polischuk and Nastenka (1998) and Polyshchuk (2005) up to 1999, modified by L. Polishchuk afterwards).	205
Table 6.2. Average multiyear biomass (mg·m ⁻³) of total zooplankton and its main components in the 0-100 m layer in offshore areas near the southern Crimean coast.	206
Table 6.3. Biomass (mg·m ⁻³) of main groups of dominating zooplankton species in the Danube estuary area in May and November 2004-2005.	207
Table 6.4. Long-term changes in annual and/or multi-annual average abundance (ind·m ⁻³) of main zooplankton species in the Sevastopol Bay.	209
Table 6.5. Mean density (ind·m ⁻³) and biomass (mg·m ⁻³) of <i>Noctiluca scintillans</i> along the Romanian continental shelf during the 1970s and 1980s.	212
Table 6.6. Taxonomic composition of dominant groups in spring-summer at 3 miles station at Cape Galata (st. 301) including Varna Bay	217
Table 6.7. Number of zooplankton species (S), the Shannon-Wiener index (H) and the Pielou's evenness index (J) by years in summer-autumn in the Varna Bay.	218
Table 6.8. Summer mean abundance of dominant taxonomic groups [ind·m ⁻³] at 3 miles offshore of the Cape Galata.	220
Table 6.9. Mesozooplankton biomass statistics by areas (shelf, open sea) during summer period 1998-2001 (number of observations, n=250).	221
Table 6.10. Annual changes of the trophic zooplankton biomass (mg·m ⁻³) in the south-eastern part of the Black Sea.	227
Table 7.1. Number of macroalgae species (underlined) and its percentage (bold) in the total floristic composition of the northwestern coastal waters of the Black Sea (Milchakova, 2007; Eremenko, Minicheva, Kosenko, 2006).	248
Table 7.2. Long term changes in the species composition of algae of the Zernov Phyllophora Field.	249
Table 7.3. Variability of morphological structure of thallus for some common macroalgae of the Ukrainian coast.	250
Table 7.4. The periods of alteration of community structural-functional organization for the macrophytobenthos of northwestern part of the Black Sea.	252
Table 7.5. Number of macroalgal species at the Romanian coast, between 1977 and 2005 by different authors	252
Table 7.6. Changes in species structure of different types of macrophytes in Varna Bay.	257
Table 7.7. Changes in saprobic structure of macrophytes in Varna Bay in the years of investigation.	257
Table 7.8. Bulgarian and Black Sea macroalgae taxonomic composition.	258
Table 7.9. Comparison of floristic indices along the Bulgarian coastline.	258

Table 7.10. Benthic algae and macrophytes diversity from different areas in the Black Sea coast of Turkey (Aysel <i>et al.</i> , 2005).	262
Table 7. 11. Dominancy in division level among of Black Sea coast of Turkey (Aysel <i>et al.</i> , 2005).	262
Table 8.1. Basic taxa of macrozoobenthos along the NW and Crimean coastlines.	275
Table 8.2. Quantity indicators of development of bottom biocenoses on the NWS shelf during 1983 - 2003 (Sinegub, 2006).	281
Table 8.3. Quantity indicators of development of bottom biocenoses at the Crimean shores during 1980 - 2004.	282
Table 8.4. Habitat features, average \pm conf. lev. 95 % of the number of species (S), abundance, biomass, and Shannon-Wiener community diversity H' index of soft bottom macrozoobenthic communities on the Bulgarian Black Sea shelf, summer 1998-2002.	299
Table 8.5. Species richness of zoobenthos over the Black Sea and along the Anatolian coast (Sezgin <i>et al.</i> , unpublished data)	307
Table 8.6. Some indicator zoobenthic species in the southern Black Sea.	308
Table 8.7. Quantitative characteristics of the benthic communities in Georgian Black Sea waters in 2003-05.	311
Table 8.8. Number of stations made during surveys on R/V "Akvanavt"	312
Table 9.1. The total and individual populations of the Russian and Starred sturgeon and Beluga in the Rivers Dnieper and Danube in 1996 - 2006, in million individuals per year. Data sources: for RO - R. Reinartz (2002), for BG and UA - BSIS (2007).	324
Table 9.2. Length-weight and age characteristics of mature Russian and starred sturgeons in the Ukrainian Danube in 2003	325
Table 9.3. Mean annual and unreported catches and total abundance of Russian sturgeon according to the data of trawl surveys in 1988 - 2005 in the Sea of Azov (assessments of unreported catch were taken from Shlyakhov <i>et al.</i> , 2005).	326
Table 9.4. Whiting and picked dogfish catches in the Black Sea according to the official statistics. The last three rows provide the average catches for the periods indicated in the subscripts.	339
Table 9.5. Whiting stock in the Russian waters in the northeastern Black Sea (thousand tons) (taken from the TDA Technical Task Team National Experts - Russian Federation Report, 2006).	341
Table 9.6. Fish stocks protection measures for whiting implemented by the Black Sea countries.	342
Table 9.7. Commercial stock of picked dogfish in the Black Sea and along the coast of the former USSR and in the water of Ukraine in 1989 - 2005, thousand tons	344
Table 9.8. Turbot catches in the Black Sea in 1989 - 2005 in tons. The last three rows show the average catches for the years indicated in the subscripts.	346
Table 9.9. Some studies carried out in the Black Sea regions on turbot stocks.	347
Table 9.10. Biomass and catches of the turbot of the Black Sea in the waters of Ukraine in 1996 - 2006 (tons), mean fishing mortality, relevant to its official catches in 1992 - 1995 and 1996 - 2005.	348
Table 9.11. Landings of mullets in the Black Sea according to the official statistics (tons).	350

Table 9.12. Landings of Mediterranean mussel and sea snail in the Black Sea (tons).	355
Table 9.13. Indicators for the fisheries in the Black Sea for 1970 - 2005 (Caddy's method)	359
Table 10.1. Taxonomic status of Black Sea marine mammals	366
Table 10.2. Geographic range of Black Sea cetaceans	367
Table 10.3. Estimates of Black Sea cetaceans density (individuals per 1 km^2) and absolute abundance in the selected maritime areas (values of 95% confidence interval are enclosed in brackets)	370
Table 10.4. Target fish species of Black Sea cetaceans (+ - prey species confirmed by identification of food residues in stomach contents of the cetaceans; ± - suspected prey species listed on base of indirect evidences)	371
Table 10.5. Life history parameters of Black Sea cetaceans	372
Table 10.6. Known (documented) threats to Black Sea cetaceans ¹	373
Table 11.1. Estimated Value of Black Sea Coastal Wetlands (US\$/ha/yr)	403
Table 11.2. Living Marine Resources of the Black Sea and their Values	403
Table 11.3. Demographic Data for the Black Sea Countries and their Coastal Zones, Selected Years	405
Table 11.4. Selected Economic Data for the Black Sea Countries, 1995 to 2000 and 2001 to 2005.	406
Table 11.5. Potential Long Run Profits in the Black Sea Anchovy Fishery for the Pre- <i>Mnemiopsis</i> and <i>Mnemiopsis</i> Periods (US\$ thousands, 1989/90 prices)	409
Table 11.6. Fishery Statistics for the Black Sea during 1995-2000 and 2001-2005	409
Table 11.7. General Tourism Statistics for Black Sea Countries	410
Table 11.8. Estimated Annual Loss of Tourism Value from Environmental Deterioration of the Black Sea in the Mid-1990s	411
Table 11.9. Degree of Health Risk Associated with Various Aspects of Black Sea Pollution	413
Table 11.10. Preliminary Socio-economic Indicators for the Black Sea	415
Table 12.1. Ranges and average values of Chl-a concentration ($mg.m^{-3}$) near the Zmeiny Island of the northwestern shelf during summer months of 2003-2007 (after Kovalova et al., 2008).	425

List of figures

Fig. 1A.2.1. Vertical variations of temperature (°C) and density (expressed in terms of sigma-t, kg m ⁻³) at various locations of the interior basin during different months representing different types of vertical structures (the data are retrieved from the IMS-METU data base; http: sfp1.www.ims.metu.tr/ODBMSDB/).	39
Fig. 1A.2.2. O ₂ and H ₂ S profiles (left) and NO ₃ , NO ₂ and NH ₄ profiles (right) versus density expressed in sigma-t (kg m ⁻³) in the center of the eastern gyre of the Black Sea during May 2003. The data source: http://www.ocean.washington.edu/cruises/Knorr2003/index.html	41
Fig. 1A.2.3. Vertical distribution of temperature (T), salinity (S), transmission (Trans), oxygen (O ₂), hydrogen sulfide (H ₂ S), total manganese (Mn ₂ ⁺), silicates (Si), nitrates (NO ₃), nitrites (NO ₂), ammonia (NH ₄), urea (Urea), phosphates (PO ₄), and organic phosphorus (Porg) at a summer station near Gelendzhik, along the eastern coast of the Black Sea. Concentrations of chemical parameters are in µM (after Yakushev et al., 2005).	42
Fig. 1A.2.4. A typical structure of the upper layer circulation field deduced from a circulation model using assimilation of altimeter sea level anomaly data as described by Korotaev et al. (2003).	45
Fig. 1A.2.5. SeaWiFS chlorophyll distributions showing two alternative forms of circulation structure in the northwestern shelf; (a) a southward coastal current system during days 152-155 (early June) and (b) a closed circulation system confined into its northern sector during days 194-197 (mid-July), 1998 (from Oguz et al., 2001).	47
Fig. 1A.2.6 Schematic diagram for major quasi-permanent/recurrent features of the upper layer circulation identified by synthesis of hydrographic studies and analysis of the sea level anomaly altimeter data (modified from Korotaev et al. 2003).	48
Fig. 1A.2.7 Long-term variations of the river discharge, precipitation, evaporation (km ³ y ⁻¹) for the Black Sea together with net water flux and the corresponding net Bosphorus inflow from the Black Sea (after Ilyin et al., 2006).	49
Fig. 1A.2.8. Yearly changes of the Danube discharge (km ³ y ⁻¹) during 1960-2005 (data provided by A. Cociasu).	49
Fig. 1A.2.9. Monthly changes of the Danube discharge (km ³ y ⁻¹) during 1993-2005 (blue) and its annual-mean variations (green) (data provided by A. Cociasu).	50

Fig. 1A.2.10. Long-term variations of the basin-averaged winter-mean (December-March) Sea Surface Temperature (SST) during 1960-2005 using the monthly data sets of Hadley Centre-UK Meteorological Office (blue), GISST (Kasmin and Zatsepin, 2007; red), NCEP-Reynolds 1° resolution AVHRR (violet), Pathfinder5 4 km resolution AVHRR (black), minimum temperature of the Cold Intermediate Layer for the mean of May - November period (green), and the winter-mean (December-March) SST measured near Constanta (Romanian coast). All these data were plotted after smoothed by the three point moving average.	51
Fig. 1A.2.11. The mean SST distribution in February for 2001 and 2003 obtained from 9 km monthly-mean, gridded NOASS/NASA AVHRR Oceans Pathfinder data set (after Oguz et al., 2003). The curve (in white colour) shows 200 m bathymetry.	52
Fig. 1A.2.12. Annual-mean (triangles) and August (dots) SST variations obtained by the basin-averaging of 9 km monthly-mean, gridded NOASS/NASA AVHRR Oceans Pathfinder data, and annual-mean (stars) and August (squares) SST variations measured at Constanta (Romanian coast) and along the northeastern coastal waters (crosses; Shiganova, 2005).	52
Fig. 1A.2.13a. Long-term variations of the detrended sea level anomaly (blue) after high frequency oscillations have been filtered by the three point moving average and its comparison with annual mean sea level anomaly retrieved from satellite altimeter measurements (after Oguz et al., 2006).	53
Fig. 1A.2.13b. Comparison of the detrended monthly-mean sea level anomaly obtained from the basin-averaged altimeter data (black) and the mean of 12 coastal sea level stations around the basin (blue) (after Goryachkin et al., 2003).	53
Fig. 1A.2.14. Monthly (blue) and yearly (green) SLA changes in the Black Sea during 1993-2006 together with its long-term trend (brown) and two shorter term trends (yellow) for 1993-1999, 1999-2003, and 2003-2006.	54
Fig. 1A.2.15. Winter (December-March) mean air temperature anomaly variations measured at the meteorological station near the Kerch Strait (red) and obtained by averaging of the GISST data for the basin (green), and winter (December-March) mean surface atmospheric pressure (hPa) obtained by averaging ERA40 data over the basin (blue). High frequency oscillations in the data have been filtered by the three point moving average.	54

Fig. 1A.2.16. Long-term variations of the winter North Atlantic Oscillation index (blue), East Atlantic-West Russia (EAWR) index (green) and Iceland sea surface temperature (red). High frequency oscillations in the data have been filtered by the five point moving average.	56
Fig. 1B.1. Geomorphologic zoning of the Black Sea (after Ross et al., 1974, Panin and Ion, 1997).	61
Fig. 1B.2. Tectonic sketch of the Black Sea Region (after Dinu et al., 2003; Panin et al., 1994).	62
Fig. 1B.3. The decreasing trend of the Danube River sediment discharge after damming (Iron Gates I barrage in 1970, Iron Gates II barrage in 1983).	64
Fig. 1B.4. Main sedimentary environments in the northwestern Black Sea (after Panin et al., 1998).	65
Fig. 1B.5. Repartition of litho-stratigraphic units on the sea floor in the NW Black Sea (from S. Radan, unpublished data).	66
Fig. 1B.6. Plaeo-geographic reconstruction of the Black Sea during the Karangatian phase (Riss-Würmian or Mikulinian interglacial) (after Tchepalyga, 2002).	68
Fig. 1B.7. Palaeo-geographic reconstruction of the Black Sea during the Neoeuxinian phase (Upper Würmian) (after Tchepalyga, 2002).	69
Fig. 1B.8. The scenario of the Black Sea water level fluctuation since the Last Glacial Maximum (after Lericolais et al., 2006, Final Report of the EU project "Assemblage")	70
Fig. 2.2.1 Relative contributions of different point and diffuse sources to the emissions of (a) total nitrogen (N) and (b) total phosphorus averaged over 5 year bins and amounts of total nitrogen and phosphorus fertilizer consumption in the Danube catchments basin (solid circles). Redrawn from daNUbs Project Final Report (2005).	85
Fig. 2.2.2 Annual DIN and P-PO4 loads measured at Sulina discharge point of the River Danube to the sea and at Reni located at the upstream end of the Sulina branch.	85
Fig. 2.2.3. BOD5 load from the Danube River and other rivers (Dniester, Dniepr and Bug) discharging into the northwestern shelf during 1995-2005.	86
Fig. 2.3.1. Spatial distribution of surface temperature, salinity and nitrate concentration (μM) in Romanian coastal and offshore waters during September 2002 (Horstmann and Davidov, 2002).	87
Fig. 2.3.2 Annual DIN concentration measured at Sulina discharge point of the River Danube to the sea and at Reni located at the upstream end of the Sulina branch.	87

Fig. 2.3.3. Amalgamated annual-mean surface N-NO ₃ and P-PO ₄ concentration changes in Romanian waters (re-drawn from Parr et al., 2007).	88
Fig. 2.3.4. Decadal variability of surface dissolved inorganic nitrogen (DIN) concentration along the western and eastern coastal waters of the NWS based on the averaging of available data from several stations at 5-year bins (after Loveya et al., 2006).	88
Fig. 2.3.5. Annual-mean surface concentrations of N-NO ₃ (green) and N-NH ₄ (blue) at Constanta station (A. Cociasu, per. com).	89
Fig. 2.3.6. Monthly changes of surface NO ₃ (squares) and NH ₄ (dots) concentrations and the trend of NO ₃ concentration at Constanta monitoring station during 2000-2006.	90
Fig. 2.3.7. Annual-mean N-NO ₃ (left) and N-NH ₄ (right) concentrations (μM) at various sites along northwestern Ukrainian waters during 2000-2006 (After PMA AG and AC Activities and Reporting, 2007).	90
Fig. 2.3.8a. Monthly changes of surface NO ₃ concentration at the Mamia beach and 5 m and 20 m isobaths further offshore during 2000-2005.	91
Fig. 2.3.8b,c. Monthly changes of surface NO ₃ and NH ₄ concentrations at Ahtopol and Burgaz monitoring stations during 2000-2005.	91
Fig. 2.3.8d. Monthly surface NO ₃ concentration (blue) and total nitrogen (organic + inorganic) concentration (green) (μM) at the Bosphorus northern entrance during 1996-2003 (redrawn after Okus, 2005).	92
Figure 2.3.9. Decadal variability of surface dissolved organic nitrogen (DON) concentration along the western and eastern coastal waters of the NWS based on the averaging of available data from several stations at 5-year bins.	92
Figure 2.3.10. Ranges of mean nitrate (NO ₃ -N) concentrations during 2000-2005 in surface waters (0-10 m) along the coast of the Black Sea (modified from TDA Report, 2007).	94
Fig. 2.3.11. Temporal variations of the subsurface peak nitrate concentration within the interior basin computed by averaging of all available data (after Konovalov and Murray, 2001, modified with the recent data by T. Oguz).	94
Fig. 2.3.12. Annual-mean P-PO ₄ concentration measured at Sulina discharge point of the River Danube to the sea and at Reni located at the upstream end of the Sulina branch.	95
Fig. 2.3.13a. Decadal variability of surface phosphate (P-PO ₄) concentration along the western and eastern coastal waters of the NWS based on the averaging of available data from several stations (redrawn from Loveya et al., 2006).	95
Fig. 2.3.13b. Annual-mean P-PO ₄ concentration (μM) at various sites of northwestern Ukrainian coastal waters during 2000-2006 (After PMA AG and AC Activities and Reporting, 2007).	95

Fig. 2.3.14. Annual-mean surface concentrations of PO_4 (right hand side axis) and SiO_4 (left hand side axis) at Constanta station.	96
Fig. 2.3.15. Surface concentrations of P-PO_4 in near-shore waters of the Gelendzhik area during 2003-2004 (redrawn from Kucheruk, 2005).	96
Fig. 2.3.16. Ranges of mean concentrations of phosphate (P-PO_4) during 2000-2005 in surface waters (0-10m) along the coast of the Black Sea (After TDA Report, 2007).	96
Fig. 2.3.17. Long-term changes of nutrient concentration ratios at (a) Sulina discharge point, Romanian shelf and Bosphorus exit region, and (b) Ukranian coastal waters.	97
Fig. 2.3.18. Long-term changes of nutrient concentration ratios at (a) Constanta monitoring station, and (b) monthly changes in Bulgarian coastal waters during 2001-2003.	98
Fig. 2.3.19. Vertical profiles of N/P and Si/N ratios at different locations of the interior basin during different months and years.	98
Fig. 2.4.1. The regions of the western basin used for the analysis of SeaWiFS chlorophyll concentration variations.	100
Fig. 2.4.2. Average surface chlorophyll concentration for five regions of the western Black Sea basin obtained from 8-daily 9 km resolution SeaWiFS ocean colour products after the original data is smoothed by 5 point moving average. The axis on the right hand side applies for the region 1, and the axis on the left hand side for all other regions.	100
Fig. 2.4.3. Monthly surface chlorophyll concentration variations (mg m^{-3}) at Constanta station during 2001-2005.	101
Fig. 2.4.4. Monthly surface chlorophyll concentration during 1987-2001 measured in the Burgaz Bay (red dots) and the Bosphorus northern exit (green squares), and the SeaWiFS ocean color data for the region 4 (bold lines). The dashed line shows decreasing trend of peak Chl concentration since the 1980s. The field data are provided by Hibaum (2005); Moncheva (2005) and Okus (2005) and satellite data by daily-8, 9 km resolution SeaWiFS ocean colour product.	101
Fig. 2.4.5. Surface chlorophyll-a concentration measured along the Crimean topographic slope zone (dots; after Churilova et al., 2005), near the Cape Sinop at the central part of the southern coast (triangles; after Feyzioglu, 2006; Bat et al., 2007), and Surmene Bay near the southeastern corner of the sea (squares; after Feyzioglu, 2006).	102
Fig. 2.4.6. Long-term changes of surface chl-a concentrations in the interior Black Sea (depth >1500m) for May-November period, 1978-1999. Each data point represents a single measurement taken from Yunev et al. (2002) (blue symbols) and Churilova et al (2004) (red symbols). This data set is complemented by	

the monthly-average 9 km gridded May to September-mean SeaWiFS data for the interior basin defined by 31-41°E longitudes and 41.5-44°N latitudes (green symbols).	103
Fig. 2.4.7. Annual-mean surface chlorophyll concentration for five regions of the western Black Sea basin obtained from 8-daily 9 km resolution SeaWiFS ocean colour product. The colour code for the regions are as shown in Fig.2.4.2.	103
Fig. 2.4.8. Monthly composites of surface chlorophyll concentration derived from daily-2km resolution SeaWiFS (NASA) ocean colour products for 2001, 2003 and 2005 (<i>EC-Joint Research Centre, Global Environment Monitoring Unit Ocean Colour Archive, http://oceancolour.jrc.ec.europa.eu/</i>).	104
Fig. 2.4.8. (continued) Monthly composites of surface chlorophyll concentration derived from daily -2km resolution SeaWiFS (NASA) ocean colour products for 2001, 2003 and 2005 (<i>EC-Joint Research Centre, Global Environment Monitoring Unit Ocean Colour Archive, http://oceancolour.jrc.ec.europa.eu/</i>).	105
Fig. 2.5.1. Long-term variations of spatial coverage of hypoxia in the northwestern shelf (redrawn from Loyeva et al., 2006), average chlorophyll concentration (mg m^{-3}) for the northern part of the NWS provided by daily-8 km SeaWiFS ocean color sensor and the River Danube N-NO_3 discharge.	106
Fig. 2.5.2. Vertical distribution of oxygen saturation ratio along the Sulina transect during September 2001 and 2003, July 2002 (after Velikova and Cociasu, 2004).	107
Fig. 2.5.3. Temporal variations of surface dissolved oxygen concentration in Constanta since the 1960s.	108
Fig. 2.5.4. SOL thickness measured as the difference between the sigma-t surfaces of 20 μM dissolved oxygen and 5 μM hydrogen sulphide concentrations deduced by all available data from the deep interior basin (after Konovalov et al., 2005), average dissolved oxygen concentration within the layer of $\sigma_t \sim 14.45$ and 14.6 kg m^{-3} surfaces in the region off the eastern coast (after Yakushev et al., 2005), and annual-mean surface dissolved oxygen concentration in northwestern coastal waters.	108
Fig. 3.1.1. Average Total Petroleum Hydrocarbons distribution (mg/l) at 11-20 September 1998.	114
Fig. 3.1.2. Average Total Petroleum Hydrocarbons distribution (mg/l) at 22 September - 9 October 2000. The anomalous high concentration 3.27 mg/l near town Feodosiya is not shown on the map.	115
Fig. 3.1.3. Division of the Russian coastal waters in terms of TPHs pollution.	119

Fig. 3.1.4. The oil spills in the Black Sea for period 2000-2004. Map of oil spills based on images taken by Synthetic Aperture Radars (SARs) of European satellites ERS-2 and Envisat. The oil spill density has been spatially normalized to the spill widths and the number of images available for the detection http://serac.jrc.it/midiv/maps/ .	122
Fig. 3.1.5. Oil spills in the northeastern part of the Black Sea in 2006 and 2007.	123
Fig. 3.1.6. Total Petroleum Hydrocarbons distribution in the bottom sediments of coastal area of the Black sea in September-December 1995 [8].	124
Fig. 3.2.1. The maximum concentration of γ -HCH (ng/g) in the different regions of the Black Sea (the maximums 4.5 ng/g in Ukrainian waters 1992 and 29.0 ng/g in Romanian water 1993 are not presented in the figure). The duplication of some years means different seasons of expeditions.	143
Fig. 3.2.2. The repetition factor of exceeding of PL by average concentration of γ -HCH (ng/g) in the bottom sediments of different regions of the Black Sea. The outstanding 2.78 ng/g in Romania 1993 is not presented in the figure. The duplication of some years means different seasons of expeditions. The Permission Level is 0.05 ng/g.	147
Fig. 3.2.3. The maximum concentration of pesticides DDTs group (ng/g) in the bottom sediments of different regions of the Black Sea (the maximum 63950 ng/g in Ukrainian waters 2003 is not presented in the figure). The duplication of some years means different seasons of expeditions. Total number of analyzed bottom sediments samples is 217.	147
Fig. 3.2.4. The "hot spot" sites in the coastal zone of the Black Sea with total DDTs concentration in sediments exceeding the level of Extremely High Pollution (12.5 ng/g) level during 1993-2006.	148
Fig. 3.3.1 Concentration of cadmium ($\mu\text{g/l}$) in Ukrainian marine waters in 1995-2000.	150
Fig. 3.3.2 Concentration of mercury ($\mu\text{g/l}$) in Ukrainian marine waters in 1995-2000.	151
Fig. 3.3.3. Concentration of lead ($\mu\text{g/l}$) in Ukrainian marine waters in 1995-2000.	152
Fig. 3.3.4 Concentration of zinc ($\mu\text{g/l}$) in Ukrainian marine waters in 1995-2000.	152
Fig. 3.3.5 Concentration of copper ($\mu\text{g/l}$) in Ukrainian marine waters in 1995-2000.	153
Fig. 3.3.6 Concentration of arsenic ($\mu\text{g/l}$) in Ukrainian marine waters in 1995-2000.	153
Fig. 3.3.7 Concentration of chromium ($\mu\text{g/l}$) in Ukrainian marine waters in 1995-2000.	153
Figure 3.3.8. The high copper and chromium concentration ($\mu\text{g/g}$) in the bottom sediments of Ukrainian part of the Black Sea.	156

Fig. 3.3.9. Trace metal average values (2000 - 2005) in seawater along Romanian littoral	159
Fig. 3.3.10. Trace metal average values (2000 - 2005) in sediments along Romanian littoral	160
Fig. 3.3.10. (cont'd) Trace metal average values (2000 - 2005) in sediments along Romanian littoral	160
Fig. 4.1. Vertical distributions of ^{137}Cs (on top) and ^{90}Sr (below) concentrations in the Black Sea central basin in 1986-2000 (circles), curve-fitted profiles (solid lines) and average levels of ^{137}Cs concentration in the 0-200 m layer and ^{90}Sr in the 0-50 m layer before the Chernobyl NPP accident (dashed lines) (Stokozov and Egorov, 2002)	164
Fig. 4.2. Temporal evolution of the ^{137}Cs inventory in the 0-50 m water layer of the Black Sea after the Chernobyl NPP accident: estimates based on measured water concentrations (circles) and modeling (solid and dashed lines) (Egorov et al., 1993). A corresponding average environmental half-life of 5-7 y can be estimated for ^{137}Cs in surface waters.	165
Fig. 4.3. Vertical distributions of ^{134}Cs , ^{137}Cs activities (Bq kg^{-1} d.w.) and the $^{238}\text{Pu}/^{239+240}\text{Pu}$ activity ratio versus sediment depth (cm) in the Danube delta region in 1997.	167
Fig. 4.4. Temporal evolution of ^{137}Cs (on the right) and ^{90}Sr (on the left) concentrations in water (a), algae <i>Cystoseira crinita</i> (b), mollusc <i>Mytilus galloprovincialis</i> (c) and fish <i>Merlangius merlangus euxinus</i> (d) in the Sevastopol bays in 1986-2005.	169
Fig. 5.1. Phytoplankton species diversity by taxonomic classes in the Bulgarian shelf.	176
Fig. 5.2. Long-term changes in phytoplankton taxonomic structure by biomass (mg/m^3) in percentage in spring (3 nm Cape Galata)	176
Fig. 5.2.a. Seasonal phytoplankton taxonomic structure by numerical abundance (cells/l^{-1}) averaged for the period 2000-2006 for the Bulgarian shelf waters	177
Fig. 5.2b. Percentage of main algal groups in density (upper) and biomass (lower) in front of Constanta waters during 1986-2005.	178
Fig. 5.3. Phytoplankton community structure within the interior basin in different seasons prior to 1985, during 1985-1994 and after 1994.	180
Fig. 5.4. Changes in phytoplankton biomass in 1954-1960s and in 1973 - 2005s in the northwestern Black Sea shelf.	181
Fig. 5.5a. Change in abundance ($\text{million cells.l}^{-1}$) and phytoplankton biomass (g.m^{-3}) of the Danube estuarine area (1988-2004).	182
Fig. 5.5b. Change in abundance (blue bars; $\text{million cells.l}^{-3}$) and phytoplankton biomass (red bars; g.m^{-3}) of the Danube estuarine area (2003-2008).	183
Fig. 5.5c. Number of blooming species in the coastal area of the Odessa Bay.	183

Fig. 5.6. Change in annual-mean density and biomass of phytoplankton in 1983-2006 in Constanta.	184
Fig. 5.7. Number of phytoplankton species contributing to blooms in Romanian waters between 1960 and 2005.	185
Fig. 5.8. Phytoplankton species contributing to summer blooms in Bulgarian coastal area between 1975 and 2005	186
Fig. 5.9. Long term changes of phytoplankton biomass at 3 nm away from the Cape Galata. The data prior to 1970 were taken from Petrova-Karadjova (1984 and 1990).	187
Fig. 5.10. Frequency of EQ classess of summer phytoplankton blooms averaged for 1990-2000 (indicated by "90") and 2000-2007 (indicated by "20") for coastal stations (201 near the Cape Kaliakra and 301 near the Cape Galata, and VB-Varna Bay).	187
Fig. 5.11. Comparison of phytoplankton abundance during two contrasting periods (i.e. stagnant and non-stagnant) in 1989-2005.	187
Fig. 5.12. Average annual abundance and biomass of phytoplankton in Georgian waters in 1992-2005.	188
Fig. 5.13. Long-term changes of total phytoplankton biomass within the water column of interior basin (g m^{-2}) compiled from all available measurements at locations deeper than 100 m during May-September, and the December-March mean SST ($^{\circ}\text{C}$) as an average of various data sets (Hadley, Reynolds-NCEP, Pathfinder), and the mean temperature of CIL during May-October.	189
Fig 5.14. Monthly changes of mean phytoplankton biomass in the northwestern coastal waters during 1975-2005.	190
Fig. 5.15. Long term changes of phytoplankton biomass at different seasons 3 nm away from the Cape Galata.	190
Fig. 6.1a. Long-term biomass changes of <i>Aurelia</i> , <i>Mnemiopsis</i> (left axis) and edible zooplankton (right axis) in the northwestern sector of Ukrainian shelf waters. No <i>Aurelia</i> biomass data were reported after 2001. Data source: YugNIRO, Kerch, Ukraine, sorted out by Dr. A. Grishin, see Velikova V. and Chipev N. 2005.	203
Fig. 6.1b. Long-term changes in abundance (%) of mesozooplankton species in the Northwest part of the Black Sea (after Temnykh et al. 2006).	204
Fig. 6.1c. Long-term changes of mesozooplankton abundance (ind. m^{-3}) in the Northwest part of the Black Sea (after Temnykh et al. 2006).	204
Fig. 6.1d. Biomass ($\text{mg}\cdot\text{m}^{-3}$) of edible zooplankton and <i>Noctiluca scintillans</i> in the Ukrainian (UK) coastal waters of the northwestern Black Sea (NWS) during 1953-2007.	207

Fig. 6.2. The regions studied most extensively in the NWS coastal waters during 2000-2007: 1 - Danube river mouth (Ukrainian part of the Danube Delta), 2 - Odessa Bay area, 3 - Grygorivsky Liman, 4 - Yagorlytska Bay, 5 - Tendrivska Bay.	208
Fig. 6.3. Edible, gelatinous, and <i>Noctiluca</i> biomass changes during 2003-2007 in the Danube discharge and Odessa regions.	208
Fig. 6.4a. <i>Mnemiopsis</i> predation impact on mesozooplankton during July in Sevastopol Bay. Data source: Finenko et al. (2007).	210
Fig. 6.4b. Meroplankton and Crustacean abundances during spring-autumn 1999-2002 in the Sevastopol Bay. Data source: Finenko et al. (2007).	210
Fig. 6.5. Changes in <i>Penilia avirostris</i> and <i>Pleurobrachia pileus</i> abundances in Constantza region during 1982-2003.	213
Fig. 6.6. Annual variations of edible zooplankton biomass (left) and relative abundances of edible zooplankton and <i>Noctiluca</i> (right) in the Romanian littoral zone 0-10 m layer.	214
Fig. 6.7. Seasonal changes of trophic zooplankton along the Romanian littoral zone in the upper 10 m layer during 1994-2007.	214
Fig. 6.8. Interannual variations of total zooplankton abundance (ind. m ⁻³) and percent share of key taxonomic groups in Varna Bay.	218
Fig. 6.9. Vertical distribution of total edible zooplankton abundance and biomass by taxonomic groups [in %] in surface homogeneous layer (SHL) and the sub-thermocline layer (TK) off the Bulgarian Black Sea coast during summer period 1998-2001.	219
Fig. 6.10. Long-term changes of Copepoda+Cladocera, <i>M. leidy</i> and <i>B. ovata</i> abundances (log transformed) and SST anomaly at 3 miles off the Cape Galata during summer 1967-2005 (from Kamburska et al., 2006b).	220
Fig. 6.11. Long-term changes of annual-mean edible zooplankton biomass at 3 miles off the Cape Galata and its average over the Bulgarian coastal waters.	221
Fig. 6.12. Mean and maximum abundances of <i>Mnemiopsis leidy</i> [ind.m ⁻³] in the Bulgarian shelf and open sea areas during summer 1998-2005 (number of observations n=172).	222
Fig. 6.13. <i>N. scintillans</i> spring-autumn mean abundance (ind.m ⁻³) along the Bulgarian coastal waters.	222
Fig. 6.14a. Seasonal changes of trophic zooplankton abundance along the Bulgarian shelf waters in 2002-2006.	223
Fig. 6.14b. Seasonal changes of <i>Noctiluca scintillans</i> abundance along the Bulgarian shelf waters in 2002-2006.	223
Fig. 6.14c. Monthly changes of <i>Aurelia aurita</i> biomass (g m ⁻²) along the Bulgarian shelf waters in 2002-2007 (with data from the north-western region in 09.2004). The red line depicts the average of all monthly data in Bulgarian waters.	224

Fig. 6.14d. Monthly changes of <i>Mnemiopsis leidyi</i> biomass (g m^{-2}) along the Bulgarian shelf waters in 2002-2006 (with data from the north-western region in 09.2004). The red line depicts the average of all monthly data in Bulgarian waters.	224
Fig. 6.15. Annual mean biomass (mg.m^{-3}) of the total zooplankton, fodder zooplankton and <i>Noctiluca scintillans</i> off the Cape Sinop (in the central sector of the southern coast) during 1999-2005. Data sources: Unal, (2002), Ustun (2005), Bat et. al. (2007), Ustun et. al. (2007).	225
Fig. 6.16. Monthly biomass (g.m^{-2}) changes of edible zooplankton and <i>Noctiluca scintillans</i> off the Cape Sinop (in the central sector of the southern coast) during 2002-2004. Data source: Ustun (2005).	225
Fig. 6.17. Abundance (ind.m^{-3}) variations of trophic zooplankton and <i>N. scintillans</i> off the Cape Sinop (in the central sector of the southern coast) during 1999-2005.	226
Fig. 6.18. Annual variation of zooplankton community structure abundance (%) in in the sea off Sinop.	226
Fig. 6.19. Variations of edible zooplankton and jelly abundance (ind.m^{-3}) and sea surface temperature off the Cape Sinop (in the central sector of the southern coast) during 2002-2004.	226
Fig 6.20. Annual-mean trophic zooplankton (Protozoa, Copepoda, Cladocera) biomass (mg m^{-3}) variations in the Georgian waters during 1955-1957 and 1990-2002 within the upper 100 m layer.	227
Fig. 6.21. Interannual variations of summer <i>M. leidyi</i> and <i>N. scintillans</i> abundances indicating their negative correlation for (a) inshore waters ($r = -0.3$) and (b) offshore waters ($r = -0.4$ $p < 0.02$) of the north-eastern basin.	228
Fig. 6.22. Interannual variations of <i>Aurelia aurita</i> abundance in near-shore and offshore waters during (a) spring and (b) summer months, as well as of the mean spring and summer temperatures. The data are compiled from various sources: Shushkina and Musaeveva (1983); Shushkina and Arnautov (1987); Flint, Arnautov, and Shushkina (1989); Shiganova et al. (2003, 2006).	229
Fig. 6.23. Interannual variations of <i>Aurelia aurita</i> and <i>Mnemiopsis leidyi</i> abundances in coastal and offshore waters of the northeastern basin during (a) spring, (b) summer months.	230
Fig. 6.24. Interannual variations of zooplankton biomass (mg m^{-2}) and <i>M. leidyi</i> abundance (ind. m^{-2}) before the <i>B. ovata</i> appearance.	231
Fig. 6.25. Interannual variations of species composition and abundance of edible zooplankton in the inshore waters in August after the introduction of <i>M.leidyi</i> : (A) coldwater and eurythermal species, and (B) thermophilic species.	233

Fig. 6.26. Interannual variations in the species composition and abundance of edible zooplankton in the open sea waters in August after the introduction of <i>M.leidy</i> : (A) coldwater and eurythermal species and (B) thermophilic species.	234
Fig. 6.27. Interannual variations in zooplankton biodiversity index of edible zooplankton (as an average of the inshore and offshore data) in the spring and August after the introduction of <i>M. leidy</i>	234
Fig. 6.28. Interannual variations of <i>Mnemiopsis</i> and <i>Beroe</i> abundances (ind.m ⁻²) in August and September, respectively.	235
Fig. 6.29. Interannual variations in the species composition and abundance of edible zooplankton in the inshore waters in August: (A) coldwater and eurythermal species and (B) thermophilic species.	236
Fig. 6.30. Interannual variations in the species composition and abundance of zooplankton in the open sea waters in August: (A) coldwater and eurithermal species and (B) thermophilic species.	237
Fig. 6.31. Long-term changes of edible zooplankton biomass in the northeastern Black Sea during August-September, 1978-2004. The data for 1978-1991 were taken by Vinogradov et al. (1992) and for 1993-2004 by Shiganova et al. (2004).	238
Fig. 6.32. Interannual variations in the species composition and abundance of edible zooplankton in the spring: (A) in the inshore zone and (B) in the open sea waters.	239
Fig. 6.33. long-term changes of edible zooplankton biomass within the deep interior basin of the Black Sea. The data shown by dots and triangles are provided by Kovalev et al. (1998) and Arashkevich et al. (2008a) for the northeastern basin.	240
Fig. 6.34. Inter-annual biomass (g m ⁻²) variations of dominant zooplankton groups during 1998-2008 (after Arashkevich et al., 2008a).	240
Fig. 6.35. The relation between mesoscale variability of the circulation system (left) and zooplankton biomass distribution (right) along an offshore-onshore transect in the NE basin. Zooplankton biomass was expressed by its normalized difference with respect to the mean biomass of each set of measurements (after Arashkevich et al., 2008a).	241
Fig. 6.36. Monthly changes of gelatinous predators <i>Aurelia</i> , <i>Mnemiopsis</i> , and <i>Pleurobrachia</i> as the mean of measurements at three stations within the northeastern coastal waters during 2005-2007 (after Araskevich et al., 2008b).	242
Fig. 7.1. Photos for the brown algae <i>Cystoseira barbata</i> (left), <i>Desmarestia viridis</i> (center) and the red algae <i>Polysiphonia elongata</i> (right).	248
Fig. 7.1A. Dynamics of changes in surface index (SI _{cm}) and average value of specific surface (S/W) of species composition of phytobenthos of the Danube-Dnepr interfluves.	250
Fig. 7.2. Annually dynamic of biomass and production of macrophytes community of Danube-Dnepr interfluves.	252

Fig. 7.3. Location of sampling stations along the Romanian Black Sea coast during 2000-2005 observations (left) and quantitative proportion of red and green algae along the Romanian Black Sea shore (right).	255
Fig. 7.4. Annual evolution of biomass (g.m^{-2}) of green and red algae along the Romanian littoral between 1996 and 2005 (Bologa and Sava, 2006).	256
Fig. 7.5. Biomass distribution of macrophytes along the investigated transects in 1994.	259
Fig. 7.6. Average multi-annual specific surface values ($\text{m}^2.\text{kg}^{-1}$) along the Bulgarian coastline during 1999-2002.	260
Fig. 7.7. Average multi-annual biomass values (g.m^{-2}) along the Bulgarian coastline during 1999-2002.	261
Fig. 7.8. Map for the coastal regions along the Turkish coast of the Black Sea.	262
Fig. 7.9. Taxonomic composition of North Caucasian bottom algoflora in the 1970s (Kalugina-Gutnik, 1975) and the present decade.	264
Fig. 7.10. <i>Cystoseira</i> biomass dynamics (1970s: Kalugina-Gutnik, 1975)	265
Fig. 7.11. <i>Phyllophora</i> biomass dynamics. Data source for 1970s: Kalugina-Gutnik (1975).	266
Fig. 8.1. Relative contribution of basic zoobenthos groups in the NWBS and at the Crimea coast during 1967 - 2005 (without taking into account Oligochaeta and Turbellaria).	274
Fig. 8.2. Species numbers (in %) of basic zoobenthos groups in different regions of the Ukrainian sector of the Black Sea. The data used for the NWBS correspond to 1973 - 2003. For Sevastopol and Karadag, the measurement period covered observations prior to 1973.	276
Fig. 8.3. Changes in macrozoobenthos species diversity on the soft bottoms along the coast of Crimea during different periods.	278
Fig. 8.4. Total number of macrozoobenthos species in different areas of the NW Black Sea: blue - Bivalvia, black - Gastropoda, green - Crustacea, red - Polychaeta (from Ukrainian National Report, 2007).	279
Fig. 8.5. Macrozoobenthos biomass (g m^{-2}) in different areas of the NW Black Sea: blue - Bivalvia, black - Gastropoda, green - Crustacea, red - Polychaeta (from Ukrainian National Report, 2007).	279
Fig. 8.6. Benthic belts of the Black Sea shelf (from Zaika, 1998, with additions).	280
Fig. 8.7. Vertical profiles of the total zoobenthos biomass in the biocenosis <i>Chamelea gallina</i> (A) (according to 157 stations) and the biomass <i>Chamelea gallina</i> (B) (310 stations) at the coast of Crimea for the period 1980 - 1990s.	283
Fig. 8.8. Vertical profiles of the total zoobenthos biomass in biocenosis <i>Mytilus galloprovincialis</i> (A) (according to 86 stations) and	

the biomass <i>Mytilus galloprovincialis</i> (B) (370 stations) at the coast of Crimea for the period 1980 - 1990s.	283
Fig. 8.9. Long-term dynamics of zoobenthos biomass in Sevastopol Bay - with consideration of all macrozoobenthos (A), and without <i>Mytilus galloprovincialis</i> which is not a typical soft bottom species of the Sevastopol Bay (B).	284
Fig. 8.10. Long-term changes of macrozoobenthos biomass at the western coast of Crimea.	285
Fig. 8.11. Rank-'Density index' curves for the first 10 macrozoobenthos species at the western coast of Crimea.	286
Fig. 8.12. Long-term changes of 'Density index' values with respect to populations of <i>Ch. gallina</i> , <i>M. galloprovincialis</i> and <i>M. phaseolina</i> at the western coast of Crimea. The 'Density index' axes on the left and right are marked by L and R, respectively, in the figure.	287
Fig. 8.13. Index of Biomass of benthic groupings per different years. Range of depths in groupings: a - (sandy zone) - 1 - 12 m, b - (silty-sand) - 13 - 25 m, c - (mussel silt) - 26 - 50 m, d - (phaseolina silt) - 51 - 110 m.	288
Fig. 8.14. Change in species diversity in the muddy bottom biocoenosis of <i>Modiolus phaseolinus</i> during 1981-2001 that was the most characteristic biocoenosis along the Romanian coast from 55m to 120 m.	291
Fig. 8.15. The change in species diversity of the macrobenthic fauna in the pre-Danubian sector of Romanian coastline during 1993-2005.	291
Fig. 8.16. Changes in the average abundances of macrozoobenthos at different depths in the pre-Danubian sector.	292
Fig. 8.17 - Changes in zoobenthic average biomass at different depths in the pre-Danubian sector.	293
Fig. 8.18. Change of species diversity in the Constanta marine sector between 1993 and 2002.	293
Fig. 8.19. Average zoobenthos abundance (ind. m ⁻² , left) and biomass (g m ⁻² , right) at 10-30m and 30-50m depth ranges in the Constanta sector of the Romanian shelf waters during 1990-99 and 2000-02.	293
Fig. 8.20. Changes in the average abundance (ind m ⁻²) and biomass (g m ⁻²) of macrozoobenthic populations in the central (Constanta) sector at 5-20 m depth range.	294
Fig. 8.21. Change of species diversity in the Southern (Mangalia) marine sector between 1993 and 2007.	295
Fig. 8.22. Average zoobenthos abundance (ind. m ⁻² , left) and biomass (g m ⁻² , right) at 30-50m depth range in the Mangalia sector of the Romanian shelf waters during 1994-2002.	295
Fig. 8.23. Average abundance (ind. m ⁻²) and biomass (g m ⁻²) of	

macrozoobenthic populations in the southern sector at 0-20 m depth range.	296
Fig. 8.24a. Average abundance (ind. m ⁻²) and biomass (g m ⁻²) of macrozoobenthic populations during 2002-2006 at 0-20 m depth range of the northern, central, southern sectors of Romanian littoral zone.	296
Fig. 8.24b. Change in number of macrozoobenthic species during 1992-2007 in the northern, central, southern sectors of Romanian littoral zone.	297
Fig. 8.25. Map of the studied area with sampling locations and communities as differentiated according to the cluster analysis: S - infralittoral sand community, C - infralittoral silt community, M - upper circalittoral silt community with <i>Melinna palmata</i> , T - impoverished circalittoral silt community, P - lower circalittoral clay community with <i>Modiolula phaseolina</i>	298
Fig. 8.26. Distribution of the average number of macrozoobenthos species (S) on the Bulgarian shelf and average Shannon-Wiener community diversity (H') index at sampling stations, summer 1998-2002.	301
Fig. 8.27. Distribution of average macrozoobenthos abundance on the Bulgarian Black Sea shelf and abundance structure at sampling stations, summer 1998-2002.	301
Fig. 8.28. Distribution of average macrozoobenthos biomass on the Bulgarian Black Sea shelf and biomass structure at sampling stations, summer 1998-2002.	302
Fig. 8.29. AMBI values (mean ±st. error) at sampling stations (according to Fig. 8.26) on the Bulgarian Black Sea shelf, summer 1998-2002 and thresholds for five ecological state categories.	303
Fig. 8.30. Alterations in (a) total number of species (S) and (b) taxonomic structure of benthic macrofauna over the "pristine" period 1954-1957, the intensive anthropogenic eutrophication period 1982-1985, and the recent period 1998-2002.	304
Fig. 8.31. Alterations in (a) total abundance and (b) percent abundance structure for the "pristine" period 1954-1957, the intensive anthropogenic eutrophication period 1982-1985, and the recent period 1998-2002.	305
Fig. 8.32. Seasonal changes of macrozoobenthos abundance (ind.m ⁻²) at 16 coastal stations along the Georgian shelf waters in 2003-2004.	309
Fig. 8.33. Species number of main macrozoobenthic group registered in 1990 and 2003-04 observations along the Georgian coast.	310
Fig. 8.34. Location of sampling transects in 2001-2007.	312
Fig. 8.35. Long-term changes in biomass of dominant macrozoobenthic species at 10-30 m depth range in the southern Caucasian coastal zone.	313

Fig. 9.1. Commercial exploitation of Marine Living Resources in the Black Sea in 1996 - 2005.	322
Fig. 9.2. Total capture production of Marine Living Resources in the Black Sea in 1989 - 2005.	322
Fig. 9.3. Total capture production of main anadromous fishes in the Black Sea during 1989 - 2005.	323
Fig. 9.4. The total abundance (in million of individuals) of three anadromous sturgeon species in the north-western Black Sea according to the data of YugNIRO trawl surveys and mathematical modeling (taken from Shlyakhov, 2003). Red bars: Russian sturgeon; blue bars: Starred sturgeon; yellow line: Beluga.	325
Fig. 9.5. Changes in Pontic shad catches in the Black Sea basin in 1989 - 2005.	328
Fig. 9.6. Turkish and the sum of Bulgarian, Romanian and Ukrainian catch variations of Pontic shad in the Black Sea as well as its biomass estimation in the Ukrainian Danube region.	329
Fig. 9.7. Total catch of main pelagic fishes in the Black Sea during 1989-2005.	330
Fig. 9.8. Time-series of recruitment, spawning stock biomass (SSB), catch and fishing mortality of Black Sea sprat.	332
Fig. 9.9. Time-series of recruitment, spawning stock biomass (SSB), catch and fishing mortality of the Black Sea anchovy.	334
Fig. 9.10. Time-series of recruitment, spawning stock biomass (SSB), catch and fishing mortality of the Black Sea horse mackarel.	337
Fig. 9.11. Total catch of main demersal fishes in the Black Sea during 1989 - 2005.	338
Fig. 9.12. Long-term changes of CPUE for three demersal species in Turkish waters of the Black Sea in 1989 - 2005 (from the TDA Technical Task Team National Experts - Turkey Report, Duzgunes, 2006).	340
Fig. 9.13. Whiting landings and average length of whittings harvested in the eastern Black Sea region of Turkey. (Taken from Knudsen and Zengin, 2006).	340
Fig. 9.14. Whiting biomass by age groups (in thousand tons) in the western part of the Black Sea during the period of 1971 - 1997. (Taken from Prodanov and Bradova, 2003).	341
Fig. 9.15. Biomass of picked dogfish in the Black Sea-BBS (Prodanov <i>et al.</i> , 1997), in the waters of Ukraine- BUA (Shlyakhov, Charova, 2006) and the mean standard length (l average) in trawl catches of picked dogfish in the northwestern part of the sea: Trend lines are shown for the BUA and l average data series.	344
Fig. 9.16. Mean length and weight of turbot in the northwestern Black sea and its landings by Ukraine in 1997 - 2005.	349
Fig. 9.17. Landings of striped mullet in the Black Sea waters of Turkey (according to data of the TDA Technical Task Team National Experts - Turkey, Duzgunes, 2006).	351

Fig. 9.18. Biomass and mean length changes of golden mullet in the Crimean waters of Ukraine during 1996-2005.	352
Fig. 9.19. Total catch of main mollusks in the Black Sea in 1989 - 2005.	352
Fig. 9.20. Harvesting of striped venus in the Black Sea along the Turkish coasts.	356
Fig. 9.21. Total capture production of main water plants in the Black Sea in 1989 -2005.	357
Fig. 10.1. Operational units of the Ukrainian National Network for Cetaceans Monitoring and Conservation (Birkun, 2006b).	384
Fig. 11.1. Modified D-P-S-I-R model showing the Relationship between Drivers (D), Pressures (P), State Changes (S), Impacts (I) and Responses (R), with the Addition of Institutional Barriers. Source: Mee (2005).	404
Fig. 11.2. Annual Population Growth in the Black Sea Countries, 1995 to 2005. data source: World Bank Development Indicators website (accessed November 27, 2007) at http://web.worldbank.org	406
Fig. 11.3. Sustainability Indicators: Adjusted Net Saving in the Six Black Sea Countries, 1996 - 2004. Data source: World Bank website (accessed November 27, 2007) at http://web.worldbank.org	414
Fig. 12.1. Schematic representation of the Black Sea pelagic and benthic ecosystem transformations along the Black Sea western coast (after Friedrich <i>et al.</i> , 2006).	417
Fig. 12.2. A typical structure of the upper layer circulation field deduced from a circulation model using assimilation of altimeter sea level anomaly data. (after Korotaev <i>et al.</i> , 2003).	418
Fig. 12.3. SeaWiFS chlorophyll distributions showing two alternative forms of circulation structure in the northwestern shelf; (a) a southward coastal current system during days 152-155 (early June) and (b) a closed circulation system confined into its northern sector during days 194-197 (mid-July), 1998 (after Oguz <i>et al.</i> , 2002).	419
Fig. 12.4. Annual-mean sea surface temperature (SST) anomaly changes obtained by <i>in situ</i> measurements at 3 nm offshore of Cape Galata (Bulgaria, after Kamburska <i>et al.</i> , 2006; right axis, in red colour) and the basin averaging (left axis, in blue colour) of the Hadley-2 data, and their comparison with the globally-averaged SST fluctuations based on Hadley-2 data (in green; left axis). The Hadley-2 data is described by Rayner <i>et al.</i> (2003). All data show both the unsmoothed and smoothed (by three-year moving averaging) variations.	420
Fig. 12.5. The changes of annual-mean, basin-averaged sea surface temperature (SST) anomaly and the North Atlantic Oscillation and the East Atlantic-West Russia climate indices.	421

Fig. 12.6. River Danube annual dissolved inorganic nitrogen (DIN), phosphate (P-PO ₄) and silicate (SiO ₄) loads into the Black Sea based on the measurements conducted at Sulina. The data are taken from Cociasu <i>et al.</i> (2008).	422
Fig. 12.7a. Decadally-averaged changes of surface dissolved inorganic nitrogen (DIN) concentration along the western and eastern coastal waters of the NWS as well as surface N-NO ₃ concentration in the Romanian shelf (red bars) and the Sulina exit of the River Danube solid dots). The data except at Sulina are amalgamated from several stations.	422
Fig. 12.7b. Decadally-averaged changes of surface dissolved nitrogen (DON) concentration along the western and eastern coastal waters of the NWS.	423
Fig. 12.8. Temporal variations of the subsurface peak nitrate concentration within the interior basin.	423
Fig. 12.9. Decadally-averaged changes of N-NO ₃ /P-PO ₄ ratios in the Ukrainian and Romanian shelf based on the amalgamated data (see Chapter 2 of this report).	424
Figure 12.10. Average surface chlorophyll concentration for the northwestern shelf and the interior basin obtained from 8-daily 9 km resolution SeaWiFS and Modis ocean colour products after the original data is smoothed by 5 point moving average.	425
Fig.12.11. Long-term variations of spatial coverage of hypoxia in northwestern coastal waters. The data are taken from the Ukrainian National Reports, UkrNCEM.	426
Fig. 12.12. Changes in summer oxygen saturation values of bottom waters at three locations along the Sf. Georghe transect immediately to the south of Danube discharge zone (after GEF-UNDP Project Report, 2006).	426
Fig. 12.13. Long-term variations of winter dissolved oxygen concentration within the layer of density surfaces $\sigma_t \sim 14.45\text{--}14.6 \text{ kg m}^{-3}$ in the offshore region the eastern coastal waters during 1984-2004 and summer-autumn mean CIL temperature of the interior basin. The oxygen data are provided by Yakushev <i>et al.</i> (2008).	427
Fig. 12.14. Total of number of oil spills and amount of oil spilt during 1996-2006 on the basis of data reported by countries to the BSC.	428
Fig. 12.15. Composite map of oil spill anomalies in the Black Sea during 2000-2002 and 2004 based on the images taken by Synthetic Aperture Radars (SARs) of European satellites ERS-2 and Envisat (http://serac.jrc.it/midiv/maps/). The oil spill density has been spatially normalized to the spill widths. The darker areas signify the high anomaly regions.	429
Fig.12.16. Mean concentration of total petroleum hydrocarbons in surface waters (0-10m depth) around the Black Sea periphery during 2000-2005 (after TDA, 2007).	429

Fig. 12.17. Mean concentrations of total petroleum hydrocarbons in sediments around the periphery of the Black Sea during 1996-2006 (after TDA, 2007).	430
Fig.12.18a. Long-term variations of annual-mean phytoplankton biomass (g m^{-3}) averaged over all stations in the Romanian (RO), Bulgarian (BG), Georgian (GE) shelves as well as the coastal northwestern sector of Ukrainian shelf (NWS-UA, after Nesterova, 1987, see Chapter 5 of this report).	431
Fig. 12.18b. Long-term variations of summer-autumn mean phytoplankton biomass (g m^{-2}) (vertical bars; after Mikaelyan, 2005), the mean CIL temperature ($^{\circ}\text{C}$) (blue dots; after Belikopitov, 2005) averaged over all stations within interior basin and mean winter (December-March) sea surface temperature (SST) as an average of Hadley2, NCEP-Reynolds and Pathfinder5 data sets. The phytoplankton biomass is expressed in terms of euphotic zone integrated values.	432
Fig. 12.19a. Long-term changes in species number contributing to annual phytoplankton biomass along the Bulgarian coastal waters (after Moncheva, 2005).	432
Fig. 12.19b. Long-term changes annual-mean phytoplankton to edible zooplankton biomass ratio along the Bulgarian coastal waters (after Moncheva, 2005).	433
Fig. 12.20. Long-term change in percentage of biomass of main algal groups in Constanta monitoring station during 1986-2005 (after Boicenco, see Chapter 5 of this report).	433
Fig. 12.21a. Long term annual-mean changes of bacterioplankton abundance in the surface layer of northwestern and Bulgarian coastal waters (redrawn from Kovalova <i>et al.</i> , 2008).	434
Fig. 12.21b. Long term monthly-mean changes of bacterioplankton abundance in the surface layer of northwestern coastal waters in the Black Sea (redrawn from Kovalova <i>et al.</i> , 2008).	435
Fig.12.22. Long-term variations of the annual-mean edible zooplankton biomass in the northeastern basin (g m^{-2}) and the western coast (mg m^{-3}) obtained by averaging the Romanian, Bulgarian, and the northwestern Ukrainian data sets. Also included for comparison is the edible zooplankton biomass (g m^{-2}) measured near the Cape Sinop in central part of the Turkish coast (after Shiganova <i>et al.</i> , see Chapter 6 of this report).	435
Fig. 12.23. Distribution of summer edible zooplankton biomass (mg m^{-3}) during 1954-1995 (after Temnykh, 2006).	436
Fig. 12.24. Mean <i>Mnemiopsis leidyi</i> abundance (ind.m^{-3}) in the Northeastern (NE), North-Western (NW), and Western (W) Black Sea inshore and offshore waters during the summer 1998-2004 (redrawn from Kamburska <i>et al.</i> 2006).	437

Fig. 12.25a. Long-term change of total macrophyte biomass (kg m^{-2}) in the northwestern shelf dominated by small, opportunistic species (after Minicheva, see Chapter 7 of this report).	438
Fig.12.25b. <i>Cystoseira</i> spp. biomass at different depths along the northeastern coastal zone during 1970, 1988 and 2005 (after Kucheruk, 2006).	438
Fig.12.25c. Changes in floristic diversity of macrophyte communities in Zernov's <i>Phyllophora</i> field (after Friedrich et al., 2008).	439
Fig. 12.26. Temporal changes in species diversity of total macrozoobenthos community in the Romanian pre-Danubian and Constanta sectors (left) and the Bulgarian shelf (right) (after Abaza, Todorova <i>et al.</i> , see Chapter 8 of this report).	439
Fig. 12.27. Recent ecological state of the northwestern and western shelves according to the AMBI classification. Yellow and green colours signify moderate and good ecological state, whereas the brown spots are degraded regions of macrozoobenthos (after GEF-UNDP Project Report, 2006).	440
Fig. 12.28a. Changes in dominant zoobenthos species biomass (g m^{-2}) at the 10-30 m depth range of northeastern Black Sea coast during 1936-2005 period (after Kuchreruk, 2006).	441
Fig. 12.28b. Species rank of macrozoobenthic population indicating its overwhelming domination by worms in the northwestern shelf (after Friedrich et al., 2008).	441
Fig. 12.29. Total catches of main anadromous, demersal and small pelagic fishes in the Black Sea during 1989-2005. The demarsal and pelagic fish catch values need to be multiplied by 10 and 100 to get the observed magnitudes, respectively (after Shlyakhov and Daskalov, see Chapter 9 of this report)	442
Fig. 12.30. Total catch of main mollusks in the Black Sea in 1989 -2005 (after Shlyakhov and Daskalov, see Chapter 9 of this report).	443
Fig. 12.31. Long-term changes of Q-value defined as the ratio of pelagic fish catch (in ktons y^{-1}) to phytoplankton biomass (in mg m^{-3}) as a measure of ecosystem vulnerability to the changes by external stressors (after Yunev <i>et al.</i> , 2008).	445

CHAPTER 1A. GENERAL OCEANOGRAPHIC PROPERTIES: PHYSICO-CHEMICAL AND CLIMATIC FEATURES (T. Oguz)

Temel Oguz

Institute of Marine Sciences,
Middle East Technical University, Erdemli, Turkey

1A.1. Main physical and chemical features

The Black Sea is a strongly stratified system; its stratification within the upper 100 m layer (10% of the entire water column) varies up to a density of $\sigma_t \sim 5 \text{ kg m}^{-3}$ (Fig. 1A.2.1) and is an order of magnitude greater than, for example, in the neighboring Mediterranean Sea. The pycnocline corresponding to the density surface $\sigma_t \sim 16.2 \text{ kg m}^{-3}$ approximately conforms to 150 m depth within the interior cyclonic cell or may extend to 200 m within coastal anticyclones. The deep homogenous layer that has a thickness of 2000 m within the abyssal plain of the sea possesses almost vertically uniform characteristics below 200 m within the range of values of temperature (T) of $\sim 8.9\text{-}9.1^\circ\text{C}$, salinity (S) of $\sim 22\text{-}22.5$, and $\sigma_t \sim 17.0\text{-}17.3 \text{ kg m}^{-3}$. The deepest part of the water column approximately below 1700 m involves homogeneous water mass formed by convective mixing due to the bottom geothermal heat flux during the last several thousands of years (Murray et al., 1991).

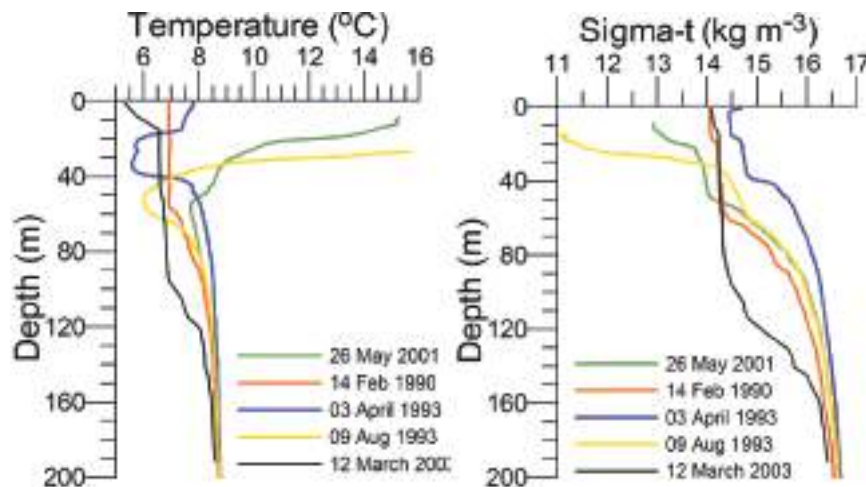


Fig. 1A.2.1. Vertical variations of temperature ($^\circ\text{C}$) and density (expressed in terms of sigma-t, kg m^{-3}) at various locations of the interior basin during different months representing different types of vertical structures (the data are retrieved from the IMS-METU data base; <http://sfp1.www.ims.metu.tr/ODBMSDB/>).

The upper 50-60 m is homogenized in winter with $T \sim 6\text{-}7^\circ\text{C}$, $S \sim 18.5\text{-}18.8$, $\sigma_t \sim 14.0\text{-}14.5 \text{ kg m}^{-3}$ when the northwestern shelf and near-surface levels of the deep basin exposed to strong cooling by successive cold-air outbreaks, intensified wind mixing, and evaporative loss. Two examples are depicted in Fig. 1A.2.1 for the interior cyclonic cell at the time of intermediate level convection event during 14 February, 1990 and immediately after one of the most severe winters of the last century (April 3,

1993) during which the mixed layer temperature reduced to $\sim 5.5^{\circ}\text{C}$. Yet another observation of winter convection event within an anticyclonic eddy closer to the southern coast (41.39°N , 30°E) during March 2003 is shown in Fig. 1A.2.1. This event cooled the surface mixed layer to 6.5°C within 90 m layer that is roughly twice deeper than those observed in the cyclonic interior basin.

As the spring warming stratifies the surface water, the remnant of the convectively-generated cold layer is confined below the seasonal thermocline and forms the Cold Intermediate Layer (CIL) of the upper layer thermohaline structure (Fig. 1A.2.1). Following severe winters, the CIL may preserve its structure for the rest of the year, but it may gradually warm up and lose its character in the case of warm winter years. These alternative structures are shown in Fig. 1A.2.1. Stratification in summer months comprises a surface mixed layer with a thickness of 10-20 m with $T \sim 22\text{-}26^{\circ}\text{C}$, $S \sim 18\text{-}18.5$ and $\sigma_t \sim 10.5\text{-}11.5 \text{ kg m}^{-3}$.

An important feature of the upper layer physical structure is the intensity of diapycnal mixing that controls ventilation of the CIL and oxygen deficient zone and nutrient entrainment from its subsurface source in winter months. According to the recent microstructure measurements (Gregg and Yakushev, 2005 and Zatsepin et al. 2007), the vertical diffusivity attains its maximal values on the order of $10^{-3}\text{-}10^{-4} \text{ m}^2 \text{ s}^{-1}$ in the surface mixed layer (0-15 m), but decreases to $10^{-5}\text{-}10^{-6} \text{ m}^2 \text{ s}^{-1}$ across the seasonal thermocline (15-30 m). An increase in the diapycnal diffusivity is observed in the CIL to the range $2\text{-}6 \times 10^{-5} \text{ m}^2 \text{ s}^{-1}$. Below the base of the CIL, it rapidly decreases to its background values of $1\text{-}4 \times 10^{-6} \text{ m}^2 \text{ s}^{-1}$. Consequently, turbulent fluxes near the base of CIL are too weak to renew the oxygen deficient Suboxic Layer (SOL).

The Mediterranean underflow that is characterized typically by $T \sim 13\text{-}14^{\circ}\text{C}$ and $S \sim 35\text{-}36$ upon issuing from the Bosphorus modifies considerably by mixing with the upper layer waters and enters the shelf with $T \sim 12\text{-}13^{\circ}\text{C}$ and $S \sim 28\text{-}30$. In the shelf, its track is regulated by small scale topographic variations. As it spreads out as a thin layer along the bottom, it is diluted by entrainment of relatively colder and less saline CIL waters and is barely distinguished by its slight temperature and salinity differences from the ambient shelf waters up on issuing the shelf break. The modified Mediterranean water is then injected in the form of thin multiple layers at intermediate depths (150-250 m) (Hiscock & Millero, 2006; Glazer et al, 2006). Signature of the Mediterranean inflow within the interior parts of the basin can be best monitored up to 500 m, where the residence time of the sinking plume varies from ~ 10 years at 100 m depth to ~ 400 years at 500 m (Ivanov and Samodurov, 2001; Lee et al., 2002).

The upper layer biogeochemical structure that overlies the deep and lifeless anoxic pool (except anaerobic bacteria) involves four distinct layers (Fig. 1A.2.2). The uppermost part extending to the depth of 1% light level (a maximum thickness of nearly 50 m) characterizes active biological processes (e.g. nutrient uptake, plankton grazing, mortality, microbial loop, etc.), high oxygen concentrations ($\sim 300 \mu\text{M}$) and seasonally varying nutrient and organic material concentrations supplied laterally from rivers and coastal zones and vertically from sub-surface levels through vertical mixing. In the interior basin, surface mixed layer waters are poor in nutrients for most of the year except occasional incursions from coastal regions and by wet precipitation. Below the seasonal thermocline and in the deeper part of the euphotic zone, nutrient concentrations

increase due to their recycling as well as continuous supply from the nutricline. Nitrate accumulation in this light-shaded zone generally supports summer subsurface phytoplankton production. In winter, nutrient stocks in the euphotic zone are renewed from the nutricline depths through upwelling, vertical diffusion and seasonal wind and buoyancy-induced entrainment processes and depleted by biological utilization.

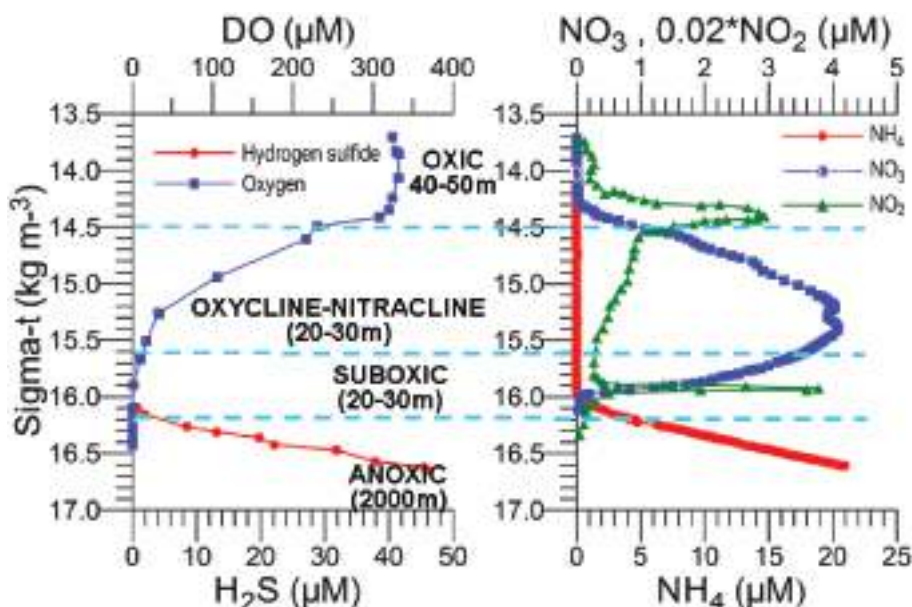


Fig. 1A.2.2. O_2 and H_2S profiles (left) and NO_3 , NO_2 and NH_4 profiles (right) versus density expressed in sigma-t ($kg\ m^{-3}$) in the center of the eastern gyre of the Black Sea during May 2003. The data source: <http://www.ocean.washington.edu/cruises/Knorr2003/index.html>.

The euphotic layer oxygen concentration undergoes pronounced seasonal variations within a broad range of values from about 250 to 450 μM . The period from the beginning of January until mid-March exhibits vertically uniform mixed layer concentrations of ~ 300 – $350\ \mu M$, ventilating the upper $\sim 50\ m$ of the water column as a result of convective overturning. The rate of atmospheric oxygen input in the ventilation process is proportional to the excess of saturated oxygen concentration over the surface oxygen concentration. The maximum contribution of oxygen saturation is realized towards the end of February during the period of coolest mixed layer temperatures, coinciding with the maximum and deepest winter oxygen concentrations during the year. After March, initiation of the warming season is accompanied by oxygen loss to the atmosphere and decreasing solubility, thus reducing oxygen concentrations within the uppermost 10 m to 250 μM during the spring and summer months. A subsequent linear trend of increase across the seasonal thermocline links low near-surface oxygen concentrations to relatively higher sub-thermocline concentrations. Depending on the strength of summer phytoplankton productivity, the sub-thermocline concentrations exceed 350 μM in summer.

The upper boundary of oxycline where oxygen concentration starts decreasing from $\sim 300\ \mu M$ corresponds to $\sigma_t \sim 14.4$ – $14.5\ kg\ m^{-3}$ (35–40 m) isopycnal surfaces in cyclonic regions (Fig. 1A.2.2) and $\sigma_t \sim 14.0$ – $14.2\ kg\ m^{-3}$ (70–100 m) in coastal anticyclonic regions (Fig. 1A.2.3). The lower boundary of oxycline is defined by 10 μM oxygen concentration located generally at $\sigma_t \sim 15.6\ kg\ m^{-3}$. Oxygen concentrations

finally vanish above the anoxic interface located at $\sigma_t \sim 16.2 \text{ kg m}^{-3}$. The oxygen deficient ($\text{O}_2 < 10 \mu\text{M}$), non-sulfidic layer having a thickness of 20-to-40 m coinciding with the lower nitracline zone is referred to as the "Suboxic Layer (SOL)" (Fig. 1A.2.2). Since identified by Murray et al. (1989, 1991), it has been observed consistently all over the basin with almost similar characteristics. Analyzing the available data after the 1960s, Tugrul et al. (1992), Buesseler et al. (1994) and Konovalov and Murray (2001) showed that the suboxic zone was present earlier, but it was masked in the observations because of low sampling resolution and contamination of water samples with atmospheric oxygen. These earlier observations measured dissolved oxygen concentrations more than $10 \mu\text{M}$ inside the sulfidic layer (Sorokin, 1972; Faschuk, et al., 1990; Rozanov et al., 1998).

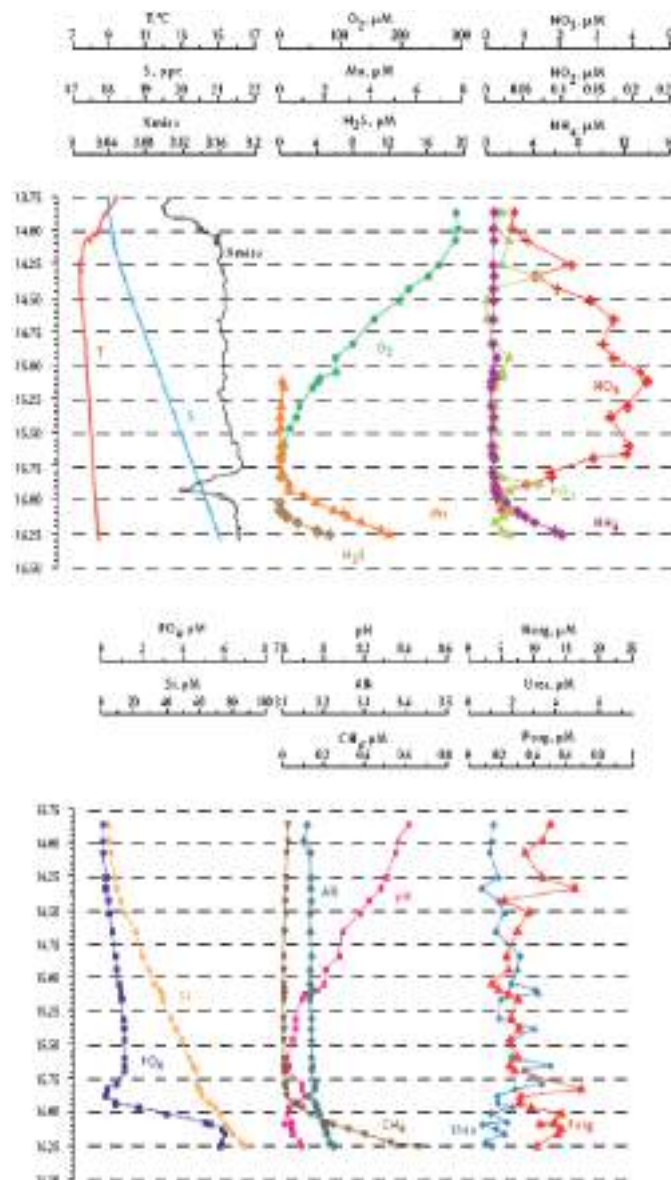


Fig. 1A.2.3. Vertical distribution of temperature (T), salinity (S), transmission (Trans), oxygen (O_2), hydrogen sulfide (H_2S), total manganese (Mn^{2+}), silicates (Si), nitrates (NO_3), nitrites (NO_2), ammonia (NH_4), urea (Urea), phosphates (PO_4), and organic phosphorus (Porg) at a summer station near Gelendzhik, along the eastern coast of the Black Sea. Concentrations of chemical parameters are in μM (after Yakushev et al., 2005).

The SOL structure is subject to temporal and regional modifications during the periods of enhanced phytoplankton production in the surface layer. For example, the R.V Knorr May-June 2001 survey conducted within the western basin during a phytoplankton bloom episode (Oguz and Ediger, 2007) showed gradual change in the position of the oxycline and the upper boundary of the SOL up to $\sigma_t \sim 15.15 \text{ kg m}^{-3}$ within less than a month. On the other hand, the oxygen profiles in the southwestern Black Sea shelf-slope region displayed another extreme case with lenses of high oxygen content ($\sim 20 \text{ }\mu\text{M}$) within the Suboxic Layer and its interface with the anoxic layer due to the intrusions of relatively oxygen rich Mediterranean underflow (Hiscoock & Millero, 2006; Glazer et al, 2006). In anticyclones, the upper boundary of SOL is located at deeper levels ($\sim 15.8 \text{ kg m}^{-3}$) and therefore the SOL is relatively shallow (around 10-20 m) (Oguz et al., 2003).

Only a small fraction ($\sim 10\%$) of particulate flux is exported to deeper anoxic part of the sea (Lebedeva and Vostokov, 1984; Karl and Knauer, 1991). This loss is compensated excessively by lateral nitrogen supply mainly from the River Danube, by wet deposition and nitrogen fixation. The nutrient fluxes of anthropogenic origin are transported across the shelf and around the basin through the Rim Current system, and spread ultimately over the interior basin and form a major source of nitrate enrichment of the euphotic zone, while some is lost through Bosphorus surface flow (Polat and Tugrul, 1995). The river influence markedly weakens toward the south along the coast and offshore for most of the year due to photosynthetic consumption of dissolved inorganic nutrients and sedimentation within the northwestern and western shelves. The river supply gives rise to a high N/P ratio within northwestern-western shelf that makes phosphate as the primary limiting nutrient along the coastal zone. The outer shelf appears to possess weakly nitrogen or phosphorus limited system, but the interior basin and major part of the sea is strongly nitrogen limited.

When nitrate profiles are plotted against density, the position of its peak concentration ($6.0 \pm 2.0 \text{ }\mu\text{M}$) coincides approximately with the $\sigma_t \sim 15.5 \pm 0.1 \text{ kg m}^{-3}$ level (Figs. 1.2.2 and 1.2.3). Some degree of variability is, however, observed in its position and concentration in the western interior basin particularly in the vicinity of the wide topographic slope zone adjacent to the northwestern shelf. The nitrate structure is accompanied by occasional peaks of ammonium and nitrite on the order of $0.5 \text{ }\mu\text{M}$ and $0.1 \text{ }\mu\text{M}$, respectively, near the base of the euphotic zone due to inputs from excretion and aerobic organic matter decomposition following subsurface plankton production (Fig. 1A.2.2). They, however, rapidly deplete below the euphotic zone.

Within the oxygen deficient layer below $\sigma_t \sim 15.6 \text{ kg m}^{-3}$, organic matter decomposition via denitrification, and oxidation of reduced manganese and iron result in a sharp decrease of nitrate concentration to trace values at $\sigma_t \sim 16.0 \text{ kg m}^{-3}$ isopycnal surface (Figs. 1.2.2 and 1.2.3). As nitrate is reduced to nitrogen gas, nitrite formed as an intermediate product marks the limits of denitrification zone; its peak concentration up to $0.2 \text{ }\mu\text{M}$ is usually observed at $\sigma_t \sim 15.85 \text{ kg m}^{-3}$ (Fig. 1A.2.2 and 1.2.3). Nitrite is often used to oxidize ammonium (the anammox reaction; $\text{NO}_2^- + \text{NH}_4^+ \rightarrow \text{N}_2$) as documented recently (Kuypers et al., 2003). The deep sulphide-bearing waters contain no measurable nitrate, but constitute large pools of ammonium and dissolved organic nitrogen. Ammonium concentration increases sharply below $\sigma_t \sim 16.0 \text{ kg m}^{-3}$, reach at values of $10 \text{ }\mu\text{M}$ at 150 m ($\sigma_t \sim 16.5 \text{ kg m}^{-3}$) and $20 \text{ }\mu\text{M}$ at 200 m ($\sigma_t \sim 16.8 \text{ kg m}^{-3}$) (Fig.

1A.2.3). The gradient of ammonium profiles in the vicinity of the suboxic-anoxic interface suggests no ammonium supply to the euphotic zone from the anoxic region.

The vertical structure of phosphate concentration resembles nitrate in the upper layer but has a more complex structure in the suboxic-anoxic layers (Fig. 1A.2.3). Phosphate concentrations increase gradually within the deeper part of euphotic layer up to a maximum value of 1.0-1.5 μM around $\sigma_t \sim 15.6 \text{ kg m}^{-3}$, and then decreases to minimum of about 0.5 μM at $\sigma_t \sim 15.9 \text{ kg m}^{-3}$ where nitrite locally displays a peak. It then increases abruptly to peak values of 5.0-8.0 μM near $\sigma_t \sim 16.2 \text{ kg m}^{-3}$ that coincides with the first appearance of sulfide in the water column and therefore coincides with the anoxic boundary. Formation of this peak has been explained by dissolution of phosphate-associated iron and manganese oxides. Silicate possesses a relatively simple vertical structure with a steady increase of concentrations below the euphotic layer up to about 70-75 μM at $\sigma_t \sim 16.2 \text{ kg m}^{-3}$ and then to about 150 μM at $\sigma_t \sim 16.8 \text{ kg m}^{-3}$ (Fig. 1A.2.3).

The boundary between the suboxic and anoxic layers involves a series of complicated redox processes. As dissolved oxygen and nitrate concentrations vanish, dissolved manganese, ammonium and hydrogen sulfide concentrations begin to increase (Fig. 1A.2.3). Marked gradients of particulate manganese around this transition zone near $\sigma_t \sim 16.0 \text{ kg m}^{-3}$ reflect the role of manganese cycling. The deep ammonium, sulfide and manganese pools have been accumulating during the last 5000 years as a result of organic matter decomposition after the Black Sea has been converted into a two-layer stratified system.

The anaerobic sulfide oxidation and nitrogen transformations coupled to the manganese and iron cycles form the first-order dynamics maintaining stability of the interface structure between the suboxic and anoxic layers. The upward fluxes of sulfide and ammonium are oxidized by Mn(III, IV) and Fe(III) species, generated by Mn(II) and Fe(II) oxidation in reactions with nitrate. The upward flux of ammonium is also oxidized by NO_2^- via anammox reaction (Kuypers et al., 2003). These oxidation-reduction reactions are microbially catalyzed, but dissolved chemical reduction may also play a role in Mn(IV) reduction with sulfide. Trouwborst et al. (2006) have recently shown the key role of soluble Mn(III) in manganese catalytic redox cycle. Mn(III) acquires a second peak at the top of the SOL, just below the layer where O_2 disappears and particulate and dissolved manganese starts increasing with depth.

Anaerobic photosynthesis is an additional mechanism contributing to the oxidation-reduction dynamics near the anoxic interface. The reduced chemical species (HS^- , Mn^{2+} , Fe^{2+}) are oxidized by anaerobic phototrophic bacteria in association with phototrophic reduction of CO_2 to form organic matter. This mechanism was supported by the discovery of large quantities of bacteriochlorophyll pigments near the suboxic-anoxic boundary (Repeta et al., 1989; Repeta and Simpson, 1991; Jorgensen et al., 1991; Jannasch et al., 1991). A particular bacterium is capable of growth using reduced S (H_2S or S^0) at very low light levels ($\ll 0.1\%$ of the incident radiation at the surface). Its contribution, however, is mostly limited to cyclonic regions where the anoxic interface zone is shallow enough to be able to receive sufficient light to maintain photosynthetic activity. The third mechanism is direct oxidation of H_2S by oxygen and

particulate manganese near the interface layer. Konovalov and Murray (2001) show that more than 50% of the upward flux sulfide could be consumed by this pathway.

1.2.2. Circulation characteristics

The upper layer waters of the Black Sea are characterized by a predominantly cyclonic, strongly time-dependent and spatially-structured basin-wide circulation. Many details of the circulation system have been explored by the recent hydrographic data (Oguz et al., 1994; 1998; Oguz and Besiktepe, 1999; Gawarkiewicz et al., 1999; Krivosheya et al., 2000), Lagrangian floats (Afanasyev et al., 2002; Poulain et al., 2005; Oguz et al., 2006), the satellite AVHRR and ocean color data (Oguz et al., 1992; Sur et al., 1994, 1996; Sur and Ilyin, 1997; Ozsoy and Unluata, 1997; Ginsburg et al., 2000, 2002a,b; Afanasyev et al., 2002; Oguz et al., 2002a; Zatsepin et al., 2003), altimeter data (Korotaev et al., 2001 and 2003; Sokolova et al., 2001), as well as modeling studies (e.g. Oguz et al., 1995; Stanev and Beckers, 1999; Besiktepe et al., 2001; Staneva et al., 2001; Beckers et al., 2002; Korotaev et al., 2003).

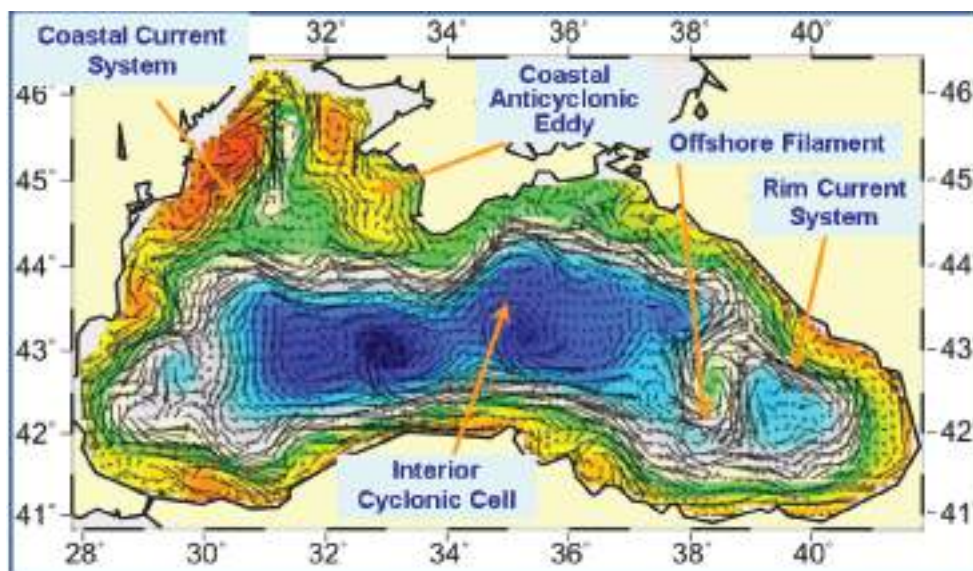


Fig. 1A.2.4. A typical structure of the upper layer circulation field deduced from a circulation model using assimilation of altimeter sea level anomaly data as described by Korotaev et al. (2003).

These analyses reveal a complex, eddy-dominated circulation with different types of structural organizations of water masses within the interior cyclonic cell, the Rim Current jet confined mainly along the abruptly varying continental slope and margin topography around the basin, and a series of anticyclonic eddies along onshore side of the Rim Current (Fig. 1A.2.4). The interior circulation consists of several sub-basin scale gyres, each of which is formed by several cyclonic eddies. They evolve continuously by interactions among each other, as well as with meanders and filaments of the Rim Current. The overall basin circulation is primarily forced by the curl of wind stress throughout the year, and further modulated by the seasonal evolution of the surface thermohaline fluxes and mesoscale features arising from the basin's internal dynamics. The strong topographic slope together with the coastline configuration of the basin governs the main pattern of the Rim Current system but it modulates seasonally

from a more coherent structure in the winter and spring to more turbulent structure in the late summer and autumn. The fresh water discharge from the Danube contributes to buoyancy-driven component of the basin-wide cyclonic circulation system. Baroclinic instability processes are responsible by introducing considerable variability of the Rim Current in the form of eddies, meanders, filaments, offshore jets that propagate cyclonically around the basin. Over the annual time scale, westward propagating Rossby waves further contribute to the complexity of basin wide circulation system (Stanev and Rachev, 1999). Eddy dynamics and mesoscale features evolving along the periphery of the basin as part of the Rim Current dynamic structure appear to be the major factor for the shelf-deep basin exchanges. They link coastal biogeochemical processes to those beyond the continental margin, and thus provide a mechanism for two-way transports between near shore and offshore regions.

The ship mounted Acoustic Doppler Current Profiler (ADCP) and CTD measurements in the western Black Sea (Oguz and Besiktepe, 1999), carried out soon after an exceptionally severe winter conditions in 1993, provided striking findings in regards to the intensity and vertical structure of Rim Current in the western basin. The data has shown a vertically uniform current structure in excess of 50 cm/s (maximum value ~ 100 cm/s) within the upper 100 m layer, followed by a relatively sharp change across the pycnocline (between 100 and 200 m) and the vertically uniform sub-pycnocline currents of 20 cm/s (maximum value ~ 40 cm/s) up to 350 m being the approximate limit of ADCP measurements. The cross-stream velocity structure exhibited a narrow core region (~ 30 km) of the Rim Current jet that was flanked by a narrow zone of anticyclonic shear on its coastal side and a broader region of cyclonic shear on its offshore side. Such exceptionally strong sub-pycnocline currents of the order of 20-40 cm/s should be largely related with the severity of the winter conditions that was indeed one of the most severe winters of the last century (Oguz et al., 2006). The corresponding geostrophically-estimated currents from the CTD measurements were relatively weak due to the lack of ageostrophic effects and barotropic component of the current.

Contrary to the jet-like flow structure over the continental slope along the southern coast, the currents measured by ADCP over the northwestern shelf (NWS) were generally weaker than 10 cm/s (Oguz and Besiktepe, 1999). Relative weakness of the shelf currents is consistent with the fact that the continental slope acts as an insulator limiting the effects of Rim Current and mesoscale features propagating over the wide topographic slope zone between the NWS and the deep interior.

Apart from complex eddy-dominated features, larger scale characteristics of the upper layer circulation system possess a distinct seasonal cycle (Korotaev et al., 2003; Poulain et al., 2005). The interior cyclonic cell in winter months involves a well-defined two-gyre system surrounded by a rather strong and narrow jet without much lateral variations. This system gradually transforms into a multi-centered composite cyclonic cell surrounded by a broader and weaker Rim Current zone in summer. The interior flow field finally disintegrates into smaller scale cyclonic features in autumn (September-November) in which a composite Rim Current system is hardly noticeable. The turbulent flow field is rapidly converted into a more intense and organized structure after November-December.

The basic mechanism which controls the flow structure in the surface layer of the northwestern shelf is spreading of the Danube outflow. Wind stress is an additional modifier of the circulation. The Danube anticyclonic eddy confines within a narrow band along the coast between Odessa and Constanta and is introduced by the wind forcing prevailing for almost half of the year during spring and summer months (Fig. 1A.2.5a,b). It sometimes expands and occupies almost the whole NWS region (Fig. 1A.2.5b). The Constanta and Kaliakra anticyclones located further south have a typical lifespan of 50 days and are observed for about 190 days per year.

An alternative configuration of the River Danube plume is the southward coastal current system (Fig. 1A.2.5a). The leading edge of this plume protrudes southward (i.e. downstream) as a thin baroclinic boundary current along the western coastline. The flow system is separated from offshore waters by a well defined front as inferred from the large contrast between the chlorophyll concentrations in the figure. Its offshore flank may display unstable features, exhibits meanders and spawns filaments extending across the wide topographic slope zone (Fig. 1A.2.5b). Except such small scale features, there is almost no exchange between shelf and interior basin.

All available finding of the Black Sea circulation system suggest that the most notable quasi-persistent and/or recurrent features of the circulation system, as schematically presented in Fig. 1A.2.6, include (i) the meandering Rim Current system cyclonically encircling the basin, (ii) two cyclonic sub-basin scale gyres comprising four or more gyres within the interior, (iii) the Bosphorus, Sakarya, Sinop, Kizilirmak, Batumi, Sukhumi, Caucasus, Kerch, Crimea, Sevastopol, Danube, Constanta, and Kaliakra anticyclonic eddies on the coastal side of the Rim Current zone, (iv) bifurcation of the Rim Current near the southern tip of the Crimea; one branch flowing southwestward along the topographic slope zone and the other branch deflecting first northwestward into the shelf and then contributing to the southerly inner shelf current system, (v) convergence of these two current systems near the southwestern coast, (vi) presence of a large anticyclonic eddy within the northern part of the northwestern shelf.

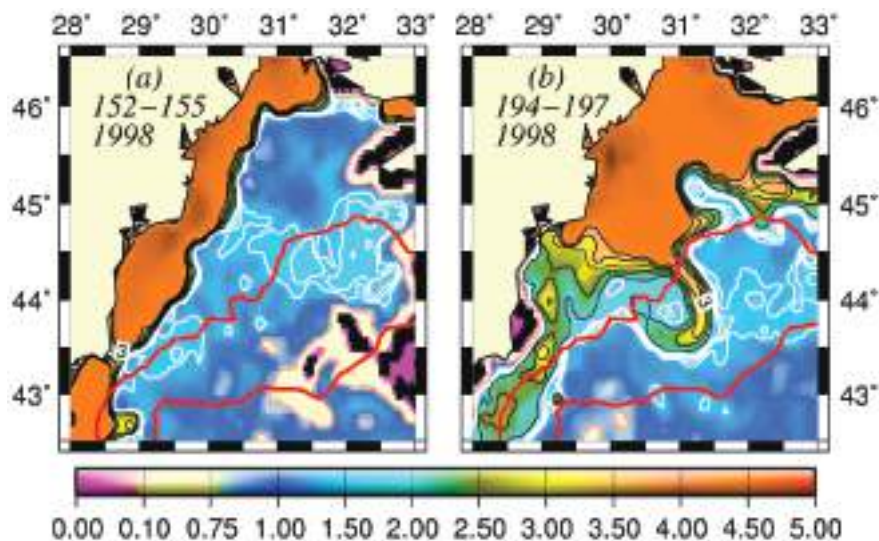


Fig. 1A.2.5. SeaWiFS chlorophyll distributions showing two alternative forms of circulation structure in the northwestern shelf; (a) a southward coastal current system during days 152-155 (early June) and (b) a closed circulation system confined into its northern sector during days 194-197 (mid-July), 1998 (from Oguz et al., 2001).

Lagrangian subsurface current measurements by three autonomous profiling floats deployed into the intermediate layer and deep layers permitted new insights on strength and variability of the flow field (Korotaev et al., 2006). They, for the first time provided direct, quantitative evidence for strong currents and a well organized flow structure that changed the traditional views built on a rather sluggish deep circulation of the Black Sea. The data suggested active role of mesoscale features on the basin-wide circulation system at 200 m similar to the case observed in the upper layer (<100 m) circulation system. The currents reach a maximum intensity of 15 cm s^{-1} along the Rim Current jet around the basin, which is consistent with the findings of ADCP measurements (Oguz and Besiktepe, 1999).

The magnitudes of deep currents may reach to 5 cm s^{-1} at 1500 m depth along the steep topographic slope (Korotaev et al., 2006). The combination of float and altimeter data suggests that deep currents are steered by the steep topographic slope and well-correlated with the structure of surface currents at seasonal and longer time scales. The deep layer currents flow along the strong topographic slope following constant potential vorticity isoclines due to the topographic β -effect. The wind stress, as the main driving force, can introduce a barotropic flow on the order of 5 cm s^{-1} as further supported by the numerical modeling studies (Stanev, 1990; Oguz et al., 1995; Stanev and Beckers, 1999). The floats at the intermediate (750 m) and deep (1550 m) layers also delineate the importance of mesoscale eddies on the flow field.

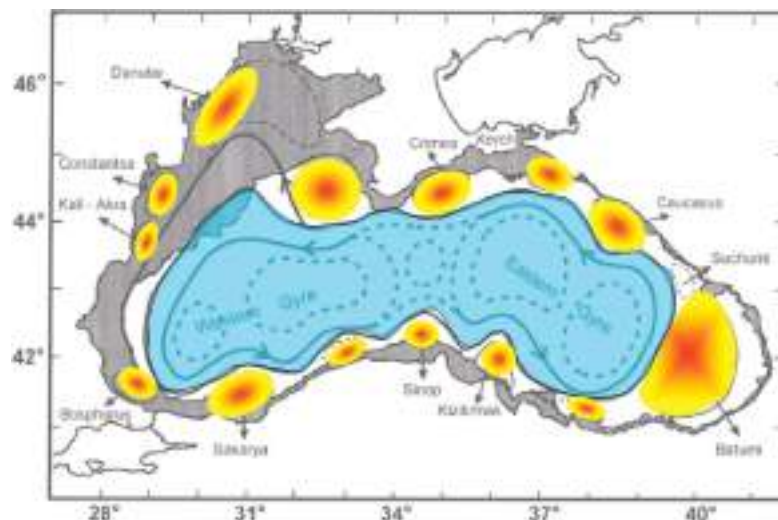


Fig. 1A.2.6 Schematic diagram for major quasi-permanent/recurrent features of the upper layer circulation identified by synthesis of hydrographic studies and analysis of the sea level anomaly altimeter data (modified from Korotaev et al. 2003).

1.2.3. Climatic properties

Water budget: On the basis of available data since the 1920s (Ilyin et al., 2006), the total river discharge and precipitation into the sea show weak but opposite trends that compensate each other and therefore their sum remain uniform at $\sim 550 \text{ km}^3 \text{ y}^{-1}$ (Fig. 1A.2.7). Evaporation varied slightly around $400 \text{ km}^3 \text{ y}^{-1}$ up to the mid 1970s (except 15% increase in the 1940s), and then decreased steadily to $\sim 300 \text{ km}^3 \text{ y}^{-1}$ during the subsequent 15 years and stabilized at this value afterwards. The net fresh water flux into the sea,

therefore, revealed an increasing trend from $\sim 120 \text{ km}^3 \text{ y}^{-1}$ in the early 1970s to $\sim 300 \text{ km}^3 \text{ y}^{-1}$ in the mid-1990s with additional fluctuations of $\sim 100 \text{ km}^3 \text{ y}^{-1}$. Its difference from the temporal volume change of the sea (which in fact may be calculated by the sea level data) implies a nearly two-fold change in the net outflow from the Black Sea into the Bosphorus during the second half of the 1990s with respect to the 1960s.

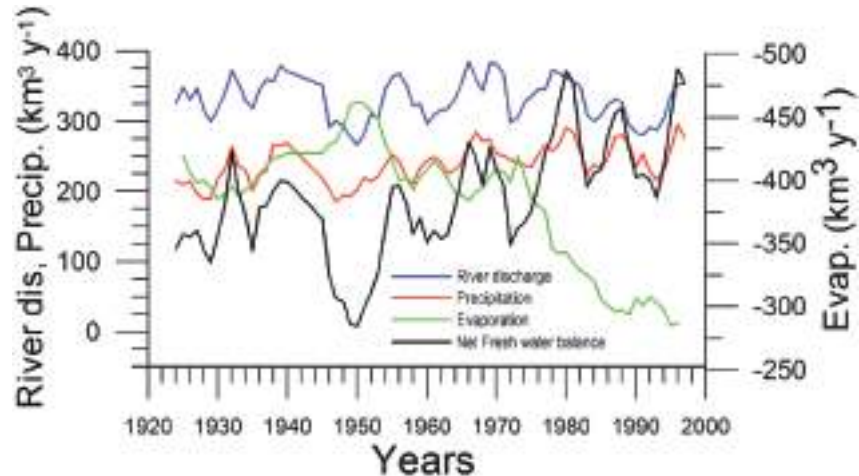


Fig. 1A.2.7 Long-term variations of the river discharge, precipitation, evaporation ($\text{km}^3 \text{ y}^{-1}$) for the Black Sea together with net water flux and the corresponding net Bosphorus inflow from the Black Sea (after Ilyin et al., 2006).

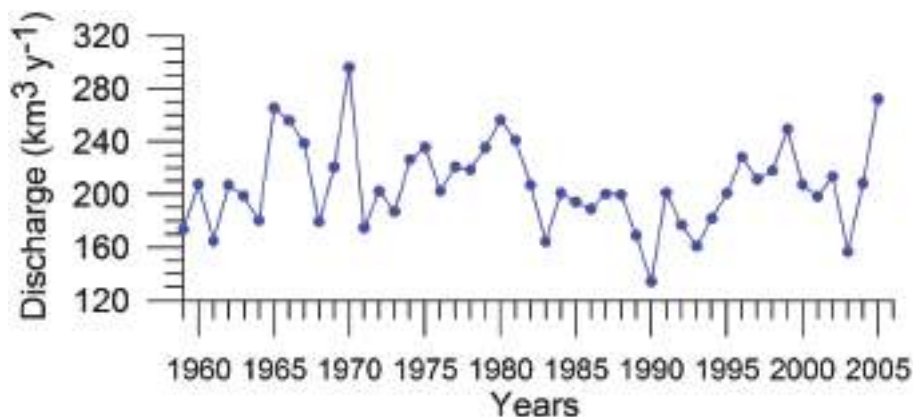


Fig. 1A.2.8. Yearly changes of the Danube discharge ($\text{km}^3 \text{ y}^{-1}$) during 1960-2005 (data provided by A. Cociasu).

One of the implications of water budget analysis is a continuous trend of decrease of the total river discharge from the early 1980s to the mid-1990s and then an increase during the rest of the 1990s. The Danube discharge was mainly responsible for these changes as it decreased to $100 \text{ km}^3 \text{ y}^{-1}$ in the 1980s (up to 1993) and started increasing again by the same amount during the 1990s (Fig. 1A.2.8). A similar reduction took place once again during 2000-2003, but 2004-2005 was a recovery phase to the level in the 1999. A closer inspection of its monthly variations (Fig. 1A.2.9) in fact reveals two different modes of variations depending on the regional climatic variations. Some years (e.g. 1993, 1995, 2000, 2001, 2002, 2004, and 2005) were characterized only by the spring peak. The years 1994, 1996-1999 attained both winter and spring peaks, whereas no spring discharge occurred in 2003. A limited Danube inflow took place previous autumn

and winter months of this particular anomalous year and therefore the Black Sea received the lowest discharge rate from the Danube since the beginning of the 1990s.

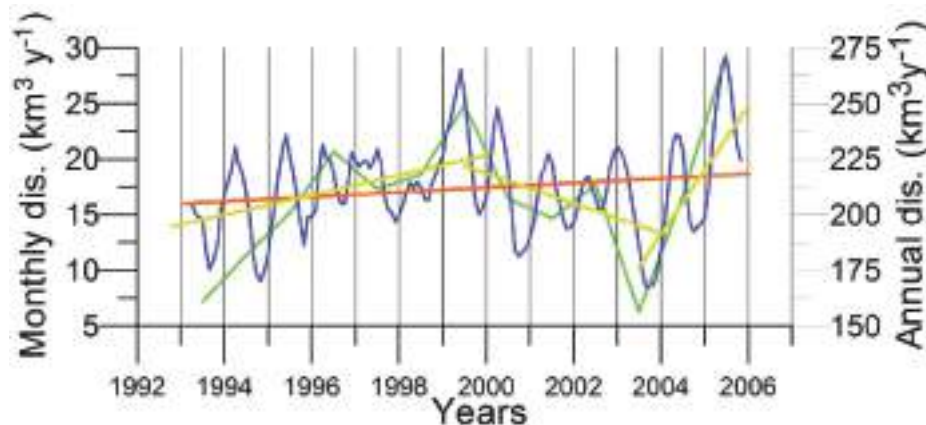


Fig. 1A.2.9. Monthly changes of the Danube discharge ($\text{km}^3 \text{y}^{-1}$) during 1993-2005 (blue) and its annual-mean variations (green) (data provided by A. Cociasu).

Sea Surface Temperature: The winter-mean (December-March) sea surface temperature (SST) variations shown in Fig. 1A.2.10 were described by different monthly-mean data sets. The first one was compiled by Hadley Centre, UK Meteorological Office from all available in situ measurements within the interior part of the basin with depths greater than 1500 m and Advanced Very High Resolution Radiation (AVHRR) satellite observations (Rayner et al., 2003). The second data set was provided by the Global Ice-Sea Surface Temperature, version 2.2 data set (GISST2.2) for the region confined by 42° - 44°N latitude range and 29° - 39°E longitude range during 1950-1994 (Kazmin and Zatsepin, 2007). Other data sets include the NCEP-Reynolds 1° resolution monthly AVHRR night-time measurements for 1983-2006 and 4 km resolution weekly Pathfinder5 AVHRR night-time measurements for 1987-2005. Fig. 1A.2.10 also shows the minimum Cold Intermediate Layer temperature variation (characterized by temperatures less than 8°C below the seasonal thermocline) as the mean of all available data from the interior basin for May-November period of 1950-1995 (Belokopytov, 1998) and from the regular measurements along several cross-sections within the eastern Black Sea during July-September period of 1990-2004 (Krivosheya et al., 2005).

The winter GISST data reveal an approximately 1.0°C cooling trend from 9.0°C in 1970 to 8.0°C in 1985. The Hadley SST data instead remain uniform at $8.7 \pm 0.1^\circ\text{C}$ during the 1960s and 1970s and then decreased abruptly from about 8.5°C at 1981 to 7.7°C at 1984. The cooling phase persists up to 1994 and switches abruptly to the warming mode until 2002 that was then replaced by a cooling mode up to the present. The NCEP-Reynolds data that form a part of the Hadley data set are similar to the Hadley one after 1993. The more recent and refined Pathfinder data set was also similar to the NCEP-Reynolds data after the beginning of the 1990s. The accompanying CIL data support reliability of the Hadley winter SST data because the minimum CIL temperature in summer months reflects signature of the winter SST. Approximately 0.7°C difference between the sub-surface summer CIL temperature and the winter Hadley SST should probably arise from different spatial averaging of the variable data sets.

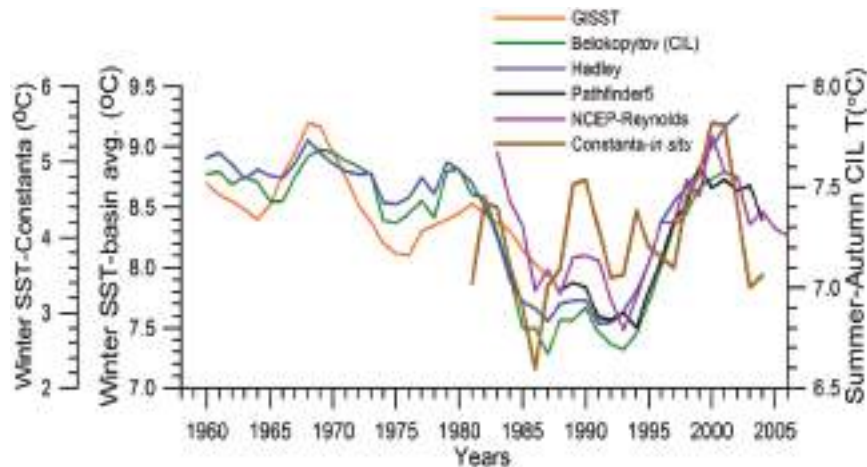


Fig. 1A.2.10. Long-term variations of the basin-averaged winter-mean (December-March) Sea Surface Temperature (SST) during 1960-2005 using the monthly data sets of Hadley Centre-UK Meteorological Office (blue), GISST (Kasmin and Zatsepin, 2007; red), NCEP-Reynolds 1° resolution AVHRR (violet), Pathfinder5 4 km resolution AVHRR (black), minimum temperature of the Cold Intermediate Layer for the mean of May - November period (green), and the winter-mean (December-March) SST measured near Constanta (Romanian coast). All these data were plotted after smoothed by the three point moving average.

Considerable regional variability up to 2°C between the colder interior basin and warmer peripheral zone irrespective of the interannual variability is a striking feature of the Black Sea (Fig. 1A.2.11). In general, regional meteorological conditions in the eastern part favour milder winters and warmer winter temperatures in the surface mixed layer. Thus the decadal warming signature was felt more pronouncedly in the eastern basin during the 1990s. The western coastal waters receiving the freshwater discharge from Danube, Dniepr and Dniestr Rivers correspond to the coldest parts of the Black Sea that are roughly twice colder than the southeastern corner of the basin irrespective of the year (Fig. 1A.2.11).

Consistency between the summer-autumn mean CIL temperature and the winter SST variations in terms of both timing and duration of the warm and cold cycles implies propagation of the winter warming/cooling events to 50-60 m depths during rest of the year. The existence of sharp thermocline helps to preserve the CIL signature throughout the year irrespective of the surface mixed layer temperature structure. The high correlation ($r=0.89$ with significance level=0.99) between the summer-autumn mean CIL temperature and the winter (December-March) mean winter SST allows a rough estimate of the former from the satellite data using the empirical relationship $T(\text{CIL})=0.619 \cdot \text{SST}+2.063$.

The summer SST variations differ from the winter ones to a considerable extent (Fig. 1A.2.12; blue). For example, cold winters of 1991-1992 are followed by relatively warm summers with $\text{SST} \geq 25^\circ\text{C}$ in August. Contrary to a steady rise of the winter SST after 1994, summer SSTs remain relatively low (below 24.5°C) until 1998, and fluctuates between 25°C and 26°C afterwards. In-situ measurements along the northeastern coast (Shiganova, 2005) generally support these features (blue line in Fig. 1A.2.12). On the other hand, the annual-mean basin-averaged SST reveals a warming trend from $\sim 14.8^\circ\text{C}$ in 1989 to 15.6°C in 2005 with some oscillations along the trend (green line in Fig. 1A.2.12). In particular, 1992, 1993, 1997, 2003 and 2004 emerge as cold years.

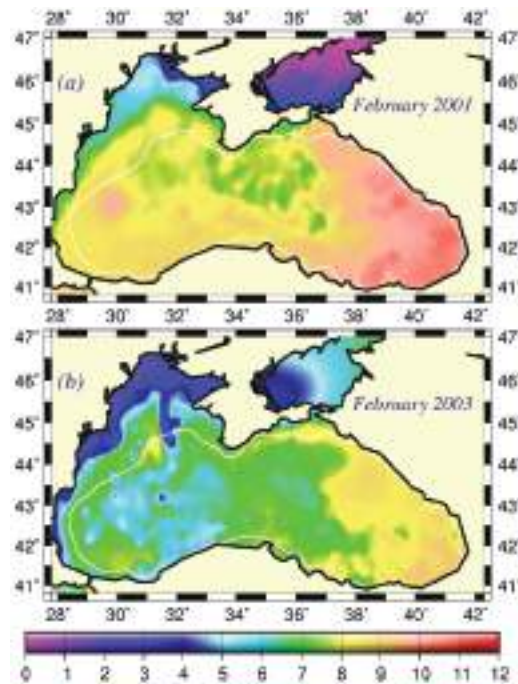


Fig. 1A.2.11. The mean SST distribution in February for 2001 and 2003 obtained from 9 km monthly-mean, gridded NOASS/NASA AVHRR Oceans Pathfinder data set (after Oguz et al., 2003). The curve (in white colour) shows 200 m bathymetry.

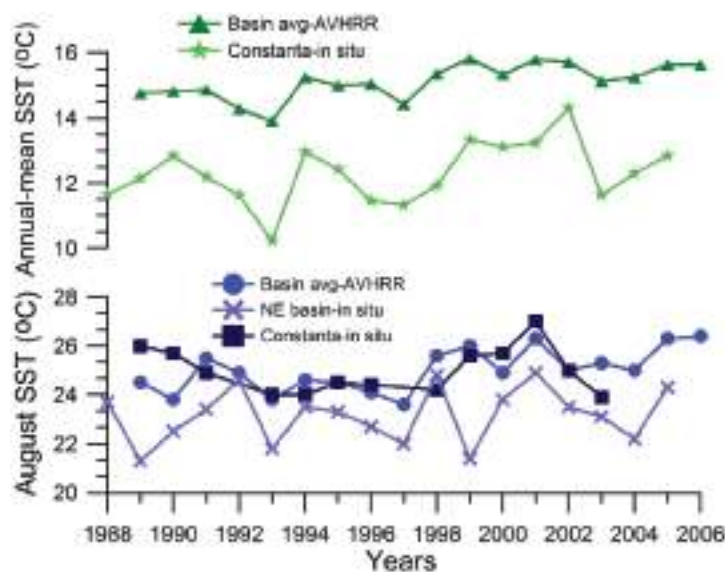


Fig. 1A.2.12. Annual-mean (triangles) and August (dots) SST variations obtained by the basin-averaging of 9 km monthly-mean, gridded NOASS/NASA AVHRR Oceans Pathfinder data, and annual-mean (stars) and August (squares) SST variations measured at Constanta (Romanian coast) and along the northeastern coastal waters (crosses; Shiganova, 2005).

Sea level: It is a prominent feature of global warming as well as large scale atmospheric systems in regional seas. Sea level change provide best response of the physical climate to atmospheric forcing, because the link includes an overall response of the changes in the surface atmospheric pressure through the inverse barometer effect, water density

changes in response to temperature and salinity variations (steric effects), precipitation, evaporation and river runoff. The detrended sea level anomaly (SLA) time series (Reva 1997, Tsimplis and Josey 2001, Stanev and Peneva 2002), as an average of the measurements at 12 coastal stations around the Black Sea, oscillate within the range of 10 cm (Fig. 1A.2.13a). Its higher (lower) values coincide with the warm (cold) cycles of the water temperature indicating that a part of the observed sea level change has a thermal origin due to the thermo-steric effect. The annual-mean tide-gauge data show a high degree of consistency with the altimeter SLA data as well (Fig. 1A.2.13b). They both exhibit a rising trend of 3 cm y^{-1} from 1993 to the mid-1999 followed by -3.0 cm y^{-1} declining trend for 07/1999-12/2003 in consistent with the cooling phase indicated by the winter SST data. When monthly variations of the SLA are resolved, the linear trend of rise increases to 20 cm during 1992-1999 (Fig.1.2.14) that was roughly 3 cm higher than the estimate based on the coastal tide gauge data (Tsimplis and Josey, 2001; Stanev and Peneva 2002). Good agreement between the monthly SLA changes and the Danube discharge rates suggest its predominant role on the basin-scale sea level oscillations.

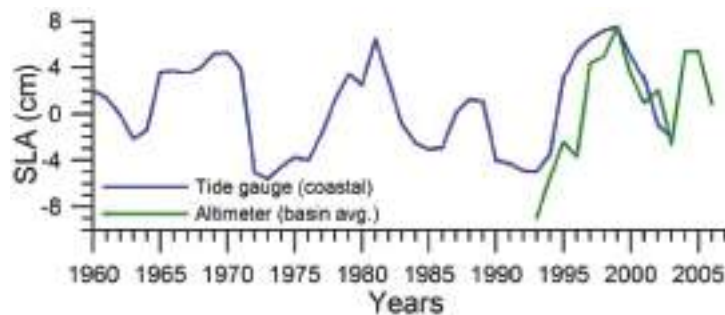


Fig. 1A.2.13a. Long-term variations of the detrended sea level anomaly (blue) after high frequency oscillations have been filtered by the three point moving average and its comparison with annual mean sea level anomaly retrieved from satellite altimeter measurements (after Oguz et al., 2006).

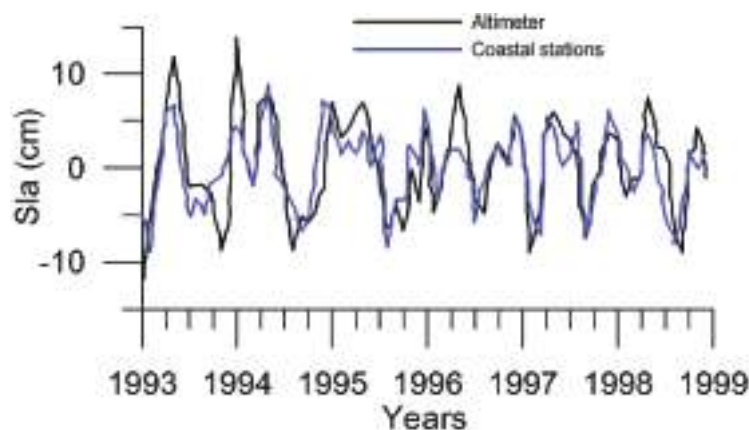


Fig. 1A.2.13b. Comparison of the detrended monthly-mean sea level anomaly obtained from the basin-averaged altimeter data (black) and the mean of 12 coastal sea level stations around the basin (blue) (after Goryachkin et al., 2003).

Air Temperature and surface atmospheric pressure: The winter-mean air temperature anomaly data from various coastal stations around the periphery of the basin (Titov,

2000; 2002) exhibit similar temporal variations, even though the mean temperatures and their range of variations may differ from the western to eastern end of the basin. Fig. 1A.2.15 provides an example along the northern coast of the central Black Sea. Fig. 1A.2.15 also includes the spatially averaged 2° resolution data retrieved from the URL site <ftp://data.giss.nasa.gov/pub/gistemp/txt/>.

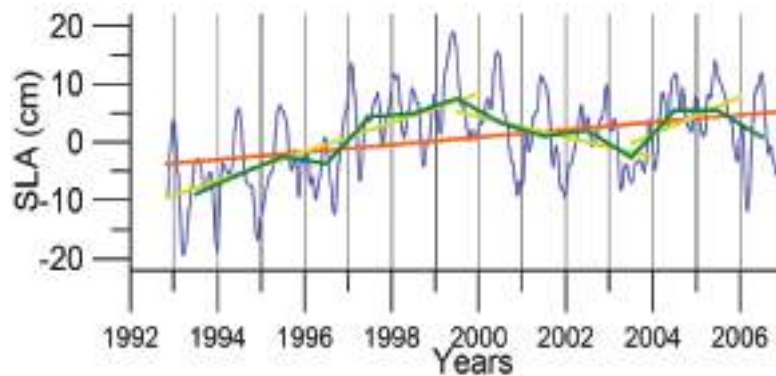


Fig. 1A.2.14. Monthly (blue) and yearly (green) SLA changes in the Black Sea during 1993-2006 together with its long-term trend (brown) and two shorter term trends (yellow) for 1993-1999, 1999-2003, and 2003-2006.

In general, the long-term AT anomaly data since 1885 exhibit a linear warming trend with the overall temperature rise of 0.9°C (Oguz et al., 2006). It is consistent with the warming observed in winter temperature over Eurasia that was explained partly by temperature advection from the North Atlantic region (i.e. connected to the NAO) and partly by the radiative forcing due to increased greenhouse gases (Hurrell, 1996). The last two decades have been subject to its abrupt variations over 10 year cycles (Fig. 1A.2.15). In particular, according to the GISST data set, the winter AT anomaly decreased 2.0°C during the mid-1970s and 1985-1995. The former was less whereas the latter was more pronounced for the coastal station data. Both the timing and duration of the warm and cold cycles fit reasonably well with the winter-mean (December-March) SST and the summer-autumn (May-November) mean CIL temperature time-series (Fig. 1A.2.10). The agreement between the winter-mean AT anomaly and SST is particularly good for the GISS-based data sets.

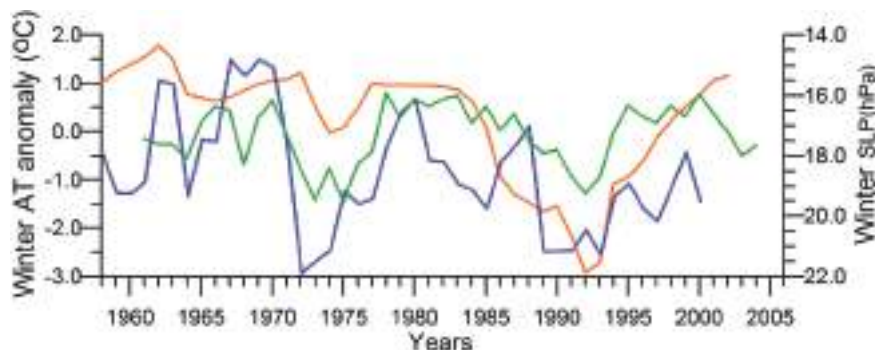


Fig. 1A.2.15. Winter (December-March) mean air temperature anomaly variations measured at the meteorological station near the Kerch Strait (red) and obtained by averaging of the GISST data for the basin (green), and winter (December-March) mean surface atmospheric pressure (hPa) obtained by averaging ERA40 data over the basin (blue). High frequency oscillations in the data have been filtered by the three point moving average.

The winter (December-March mean) basin-averaged sea level pressure (SLP) distribution over the Black Sea (Fig. 1A.2.15) follows closely the winter air temperature time series. The severe winters with low air temperatures tend to be associated with higher sea level atmospheric pressures (up to 1021 hPa), whereas lower pressures correspond to milder winter seasons. Decreasing winter air temperature trend during the 1985-1993 is supported by an increasing trend of the winter surface pressure and vice versa for the 1990s.

Link to teleconnection patterns over the Eurasia: The North Atlantic Oscillation (NAO) defined as an index representing the normalized sea level atmospheric pressure difference between Lisbon, Portugal (for the Azores high pressure system) and Stykkisholmur/Reykjavik, Iceland (for the Icelandic low pressure system) is an important mode of variability of the Northern Hemisphere atmosphere (Marshall et al., 1997). Its positive values for winter (December through March) indicate strong pressure gradient between these two pressure systems that brings cold and dry air masses to southern Europe and Black Sea region by strong westerly winds (Hurrell, et al., 2003). In these periods, the Black Sea region is affected by the Azores high pressure center and thus characterized by the higher surface air pressure values, reduced evaporation and colder air and sea surface temperatures (Fig. 1A.2.16). Conversely, the negative NAO index that implies lower surface atmospheric pressure differences gives rise to milder winters with warmer air temperatures and less dry/more wet atmospheric conditions transported over the Black Sea from the southwest. Various studies in the Mediterranean, Black and Caspian Seas (e.g., Reva, 1997; Ozsoy, 1999; Tsimplis and Josey, 2001; Stanev and Peneva, 2002; Oguz, 2005b; Oguz et al., 2006; Kazmin and Zatsepin, 2007) established a regional dynamical link to the NAO. The NAO signature has also been recorded in stream flow changes of the Tigris and the Euphrates Rivers (Cullen and deMenocal, 2000), as well as in the River Danube discharge (Polonsky et al., 1997; Rimbu et al., 2004).

The general consistency between periods of positive (negative) NAO index values and relatively low (high) sea surface and air temperatures, higher (lower) surface air pressures supports the presence of a teleconnection between the regional atmospheric conditions and the NAO-driven large scale atmospheric motion (Oguz et al., 2006, Kazmin and Zatsepin, 2007). In terms of duration and intensity of events, the sequence of mild and severe winter cycles follows the temporal pattern of the negative and positive NAO cycles, respectively. In particular, the strong cooling trend during 1980-1993 characterizes an extended strongly positive NAO index phase with an increasing trend. The subsequent warming trend in SST coincides with the weakening of positive NAO index and its decreasing trend.

Krichack et al. (2002) have shown that interannual variability of precipitation over the eastern Mediterranean can be explained more appropriately by the joint analysis of the NAO and EAWR indices which incorporates different possible combinations of a quadrupole system formed by the high and low surface pressure anomaly centers over the North Atlantic and the Eurasia as representative of different states of the eastern Mediterranean atmosphere. Oguz et al. (2006) later adopted this concept for the Black Sea in order to explain some peculiarities of the climatic variations which can not be described well by the NAO alone.

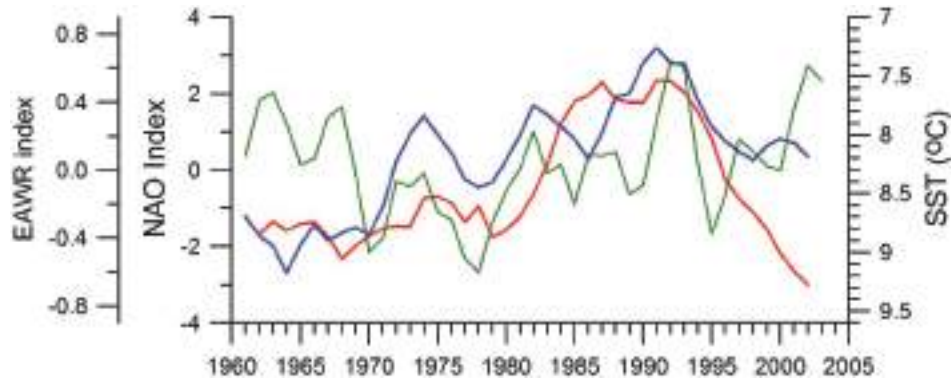


Fig. 1A.2.16. Long-term variations of the winter North Atlantic Oscillation index (blue), East Atlantic-West Russia (EAWR) index (green) and Iceland sea surface temperature (red). High frequency oscillations in the data have been filtered by the five point moving average.

The winter (December-January-February) mean East Atlantic-West Russia (EAWR) index represents the zonal shift between quasi-persistent high and low surface pressure anomaly centers over the Western Europe and the Caspian region (Fig. 1A.2.16). This system characterizes the second strongest mode of the North Atlantic climate (Molinero et al., 2005) and zonally modulates the NAO over the Eurasia continent. Its positive phase (EAWR index > 0) results from the joint effect of the increased anticyclonic anomaly center over the North Sea and the increased cyclonic anomaly center over the Caspian Sea. The Black Sea region is then exposed to cold and dry air masses from the northeast-to-northwest sector. Alternatively, its negative phase (EAWR index < 0) is associated with the cyclonic anomaly center over the North Sea and the anticyclonic activity over the Caspian Sea (i.e. relatively low pressure difference over the Europe). In this case, the Black Sea region is affected by warmer and wetter winter conditions under the influence of increased southwesterlies-to-southeasterlies. They resemble closely the North Sea-Caspian Pattern (NCP) index introduced using 500 hPa geopotential anomaly patterns by Kutiel and Benaroch (2002).

When both $NAO > 0$ and $EAWR > 0$, the system was governed by the low pressure anomaly centers over Iceland and Caspian Sea and a high pressure anomaly centers over Azores and the North Sea. This case leads to strongest cold winters in the Black Sea due to cold air mass outbreaks from the northwest and/or the northeast as in the case of early 1990s. When $NAO > 0$ and $EAWR < 0$, the Caspian low is replaced by an anticyclonic anomaly center, and the Black Sea region is then controlled by either cold air outbreaks from the northwest or warm air outbreaks from the southeast depending on the relative strengths and spatial coverages of the Icelandic low and Caspian high pressure systems. This case applies to the period of 1970-1975 and may be the reason for a weak cooling signature noted in the SST even if the NAO was in strong positive mode. The reverse case of $NAO < 0$ and $EAWR > 0$ gives rise to the cold winters with cold air outbreaks from the northern sector. Alternatively, the warm and mild winters may also prevail when the Azores high pressure system is sufficiently strong and protrudes towards the east. As suggested by the Black Sea hydro-meteorological time series data, the latter case occurred during the 1960s and 1990s. When both $NAO < 0$ and $EAWR < 0$, the system is affected by the warm air mass intrusions from the southwest-southeast sector giving rise to mild winters in the Black Sea. Its typical example was observed during the second half of the 1970s.

The decadal variations observed in the Black Sea hydro-meteorological properties are consistent to some extent solar (sun spot) variations having the 10-12 year periodicity. The periods of solar minima coincide with reduced air and sea surface temperatures, which generally correspond to the periods of positive NAO index values. In contrast, the periods of solar maxima coincide with the periods of higher air and sea surface temperatures characterized by negative values in the NAO index. A positive correlation exists between the SST and the sunspot number for each five year bins of the consecutive cold and warm cycles of the 1960-2000 phase. The in-phase variations between the sun spot number and the regional hydro-meteorological characteristics may suggest possible impact of the solar activity its link to the lower atmosphere and subsequently air and sea surface temperatures of the Black Sea.

References

- Afanasyev, Y.D., Kostianoy, A.G., Zatsepin, A.G., and Poulain P.M. (2002) Analysis of velocity field in the eastern Black Sea from satellite data during the Black Sea '99 experiment. *J. Geophys. Res.*, 107, 10.1029/2000JC000578.
- Beckers, J.M., Gregoire, M.L., Nihoul, J.C.J., Stanev, E., Staneva, J. and Lancelot C. (2002) Hydrodynamical processes governing exchanges between the Danube, the north-western continental shelf and the Black Sea's basin simulated by 3D and box models. *Estuarine, Coastal and Shelf Science*, 54, 453-472.
- Belokopytov, V. (1998) Long-term variability of Cold Intermediate Layer renewal conditions in the Black Sea. In *Ecosystem modeling as a management tool for the Black Sea*, NATO Sci. Partnership Sub-ser., 2, vol. 47, edited by Ivanov, L and Oguz, T., Vol 2, 47-52 pp, Kluwer Academic Publishers.
- Besiktepe, S.T., Lozano, C.J., and Robinson A.R. (2001) On the summer mesoscale variability of the Black Sea. *J. Mar. Res.*, 59, 475-515.
- Buesseler, K.O., Livingston, H.D., Ivanov, L. and Romanov, A. (1994) Stability of the oxic-anoxic interface in the Black Sea. *Deep-Sea Res. I*, 41, 283-296.
- Cullen, H.M., and de Menocal, P.B. (2000) North Atlantic Influence on Tigris-Euphrates streamflow. *Int. J. Climatol.*, 20, 853-863.
- Faschuk, D.Ya., Ayzatullin, T.A., Dronov, V.V., Pankratova, T.M. and Finkelshteyn, M.S. (1990) Hydrochemical structure of the layer of co-existence of oxygen and hydrogen sulfide in the Black Sea and a possible mechanism of its generation. *Oceanology (English transl.)*, 30, 185-192.
- Gawarkiewicz, G., Korotaev, G. Stanichny, S., Repetin, L. and Soloviev, D. (1999) Synoptic upwelling and cross-shelf transport processes along the Crimean coast of the Black Sea. *Cont. Shelf Res.*, 19, 977-1005.
- Ginsburg, A.I., Kostianoy, A.G., Soloviev, D.M., Stanichny, S.V. (2000) Remotely sensed coastal/deep-basin water exchange processes in the Black Sea surface layer. In *Satellites, Oceanography and Society*, D. Halperneds. Elsevier Oceanography Series, Amsterdam, 63, pp. 273-285.
- Ginsburg, A.I., Kostianoy, A.G., Nezlin, N.P., Soloviev, D.M., Stanichny, S.V. (2002a) Anticyclonic eddies in the northwestern Black Sea. *J. Mar. Syst.*, 32, 91-106.
- Ginsburg, A.I., Kostianoy, A.G., Krivosheya, V.G., Nezlin, N.P., Soloviev, D.M., Stanichny, S.V., Yakubenko, V.G. (2002b) Mesoscale eddies and related processes in the northeastern Black Sea. *J. Mar. Syst.*, 32, 71-90.
- Glazer, B.T., Luther III, G.W. Konovalov, S. K., Friederich, G. E., Trouwborst, R.E., Romanov, A.S. (2006) Spatial and temporal variability of the Black Sea suboxic zone. *Deep Sea Res. II*, 53, 1756-1768.
- Gregg, M. C. and Yakushev, E. V. (2005) Surface Ventilation of the Black Sea's Cold Intermediate Layer in the Middle of the Western Gyre. *Geophys. Res. Lett.* 32, L03604.

- Goryachkin, Yu. N., Ivanov, V. A., Lemeshko, E. M., and Lipchenko, M. M. (2003) Application of the altimetry data to the analysis of water balance of the Black Sea. *Physical Oceanography*, 13, 355-360.
- Hiscock, W.T. and Millero, F. J. (2006) Alkalinity of the anoxic waters in the Western Black Sea. *Deep Sea Res. II*, 53, 1787-1801.
- Hurrell, J.W. (1996) Influence of variations in extratropical wintertime teleconnections on Northern Hemisphere temperature. *Geophys. Res. Lett.*, 23, 665-668.
- Hurrell, J.W., Kushnir, Y., Ottersen, G., and Visbeck, M. (2003) An overview of the North Atlantic Oscillation. In *The North Atlantic Oscillation: Climatic Significance and Environmental Impact*, Geophysical Monograph 134, Edited by J.W. Hurrell, Y. Kushnir, G. Ottersen, M. Visbeck, 1-36pp, published by American Geophysical Union, Washington DC.
- Ilyin, Y.P. and Repetin, L.N. (2005) Long-term climatic trends in the Black Sea region and their seasonal features. *Proceedings of The First Biannual Scientific Conference: Black Sea Ecosystem 2005 and Beyond*, organized by Commission on the Protection of the Black Sea Against Pollution, May 2006, Istanbul.
- Ivanov, L.I. and Samodurov, A.S. (2001) The role of lateral fluxes in ventilation of the Black Sea. *J. Mar. Syst.*, 31, 159-174.
- Jannasch, H.W., Wirsén, C.O. and Molyneux, S.J. (1991) Chemoautotrophic sulfur-oxidizing bacteria from the Black Sea. *Deep-Sea Res.*, 38, Suppl.2A, S1105-S1120.
- Jørgensen, B.B., Fossing, H., Wirsén, C.O. and Jannasch, H.W. (1991) Sulfide oxidation in the anoxic Black Sea chemocline. *Deep-Sea Res.*, 38, Suppl.2A, S1083-S1104.
- Karl, D.M., and Knauer, G.A. (1991) Microbial production and particle flux in the upper 350 m of the Black Sea. *Deep Sea Res.*, 38, Suppl. 2A, S655-S661.
- Kazmin, A.S. and Zatsepin, A.G. (2007) Long-term variability of surface temperature in the Black Sea, and its connection with the large-scale atmospheric forcing. *J. Mar. Syst.*, 68, 293-301.
- Konovalov, S.K., and Murray, J.W. (2001) Variations in the chemistry of the Black Sea on a time scale of decades (1960-1995). *J. Mar. Syst.*, 31, 217-243.
- Korotaev, G.K., Saenko, O.A., Koblinsky, C.J. (2001) Satellite altimetry observations of the Black Sea level. *J. Geophys. Res.*, 106, 917-933.
- Korotaev, G.K., Oguz, T., Nikiforov, A., Koblinsky, C. J. (2003) Seasonal, interannual and mesoscale variability of the Black Sea upper layer circulation derived from altimeter data. *J. Geophys. Res.*, in press.
- Korotaev, G., Oguz, T., Riser, S. (2006) Intermediate and deep currents of the Black Sea obtained from autonomous profiling floats. *Deep Sea Res. II*, 53, 1901-1910.
- Krivosheya, V.G., Titov, V.B., Ovchinnikov, I.M., Kosyan, R.D., Skirta A.Yu. (2000) The influence of circulation and eddies on the depth of the upper boundary of the hydrogen sulfide zone and ventilation of aerobic waters in the Black Sea. *Oceanology (Eng. Transl.)*, 40, 767-776.
- Kuypers, M.M.M., Sliekers, A.O., Lavik, G., Schmid, M., Jørgensen, B.B., Kuenen J.G., Sinninghe, D.J.S., Strous, M. and Jetten, M.S.M. (2003) Anaerobic ammonium oxidation by anammox bacteria in the Black Sea. *Nature*, 422, 608-611.
- Lebedeva, L.P. and Vostokov, S. V. (1984) Studies of detritus formation processes in the Black Sea. *Oceanology (Engl. Transl.)*, 24(2), 258-263.
- Lee, B-S., Bullister, J.L., Murray, J.W. and Sonnerup, R.E. (2002) Anthropogenic chlorofluorocarbons in the Black Sea and the Sea of Marmara. *Deep-Sea Res. I*, 49, 895-913.
- Marshall, J., Kushnir, Y., Battisti, D., Chang, P., Hurrell, J., McCartney M., and Visbeck, M. (1997) A North Atlantic Climate Variability: phenomena, impacts and mechanisms. *Inter. Jour. Climatology*, 21(15), 1863-1898.
- Molinero, J. C., Ibanez, F., Nival, P., Buecher, E. and Soussi, S. (2005) North Atlantic climate and north-western Mediterranean plankton variability. *Limnol. Oceanogr.*, 50(4), 1213-1220.
- Murray, J.W., Jannasch, H. W., Honjo, S., Anderson, R. F., Reeburgh W.S., Top, Z., Friederich, G.E., Codispoti, L.A. and Izdar, E. (1989) Unexpected changes in the oxic/anoxic interface in the Black Sea. *Nature*, 338, 411-413.

- Murray, J. W., Top, Z. and Ozsoy, E. (1991) Hydrographic properties and ventilation of the Black Sea. *Deep-Sea Res.*, 38, Suppl.2A, S663-690.
- Oguz, T. (2005) Black Sea ecosystem response to climate teleconnections. *Oceanography*, 18(2), 118-128.
- Oguz, T. and Ediger, D. (2006) Comparison of in situ and satellite-derived chlorophyll pigment concentrations, and impact of phytoplankton bloom on the suboxic layer structure in the western Black Sea during May-June 2001. *Deep Sea Res. II*, 53, 1923-1933.
- Oguz, T., La Violette, P., Unluata, U. (1992) Upper layer circulation of the southern Black Sea: Its variability as inferred from hydrographic and satellite observations. *J. Geophys. Res.*, 97, 12569-12584.
- Oguz, T., Aubrey, D.G., Latun, V.S., Demirov, E., Koveshnikov, L., Sur, H.I., Diacanu, V., Besiktepe, S., Duman, M., Limeburner, R., and Eremeev, V.V. (1994) Mesoscale circulation and thermohaline structure of the Black sea observed during HydroBlack'91. *Deep Sea Research I*, 41, 603-628.
- Oguz, T., Malanotte-Rizzoli, P., and Aubrey, D. (1995) Wind and thermohaline circulation of the Black Sea driven by yearly mean climatological forcing. *J. Geophys. Res.*, 100, 6846-6865.
- Oguz, T., Ivanov, L.I., and Besiktepe, S. (1998) Circulation and hydrographic characteristics of the Black Sea during July 1992. In: *Ecosystem Modeling as a Management Tool for the Black Sea*, L. Ivanov and T. Oguz (eds). NATO ASI Series, Environmental Security-Vol.47, Kluwer Academic Publishers, Vol. 2, pp.69-92.
- Oguz, T., Deshpande, A. G. and Malanotte-Rizzoli, P. (2002a) On the role of mesoscale processes controlling biological variability in the Black Sea: Inferences from SeaWiFS-derived surface chlorophyll field. *Continental Shelf Research*, 22, 1477-1492.
- Oguz, T., Cokacar, T., Malanotte-Rizzoli, P. and Ducklow, H. W. (2003) Climatic warming and accompanying changes in the ecological regime of the Black Sea during 1990s. *Global Biogeochem. Cycles*, 17(3), 1088, doi:10.1029/2003.
- Oguz T., Dippner, J.W. and Kaymaz, Z. (2006) Climatic regulation of the Black Sea hydro-meteorological and ecological properties at interannual-to-decadal time scales. *J. Mar. Syst.*, 60, 235-254.
- Ozsoy, E. and Unluata, U. (1997) Oceanography of the Black Sea: A review of some recent results. *Earth Sci. Rev.*, 42, 231-272.
- Ozsoy, E. (1999) Sensitivity to global change in temperate Euro-Asian Seas (The Mediterranean, Black Sea and Caspian Sea): A review. In *The Eastern Mediterranean as a laboratory basin for the assessment of contrasting ecosystems*, NATO Sci. Partnership Sub-ser., 2, vol. 51, edited by Malanotte-Rizzoli, P., and Eremeev V., 281-300 pp, Kluwer Academic Publishers.
- Polat, S.Ç. and Tugrul, S. (1995) Nutrient and organic carbon exchanges between the Black and Marmara Seas through the Bosphorus Strait. *Continental Shelf Research*, 15, 1115-1132.
- Polonsky, A. B., Basharin, D.V. Voskresenskaya, E.N. and Worley, S. (2004) North Atlantic Oscillation: description, mechanisms, and influence on the Eurasian climate. *Phys. Oceanogr.*, 15(2), 96-113.
- Pierre-Marie P., Barbanti, R., Motychev, S. and Zatsepin A. (2005) Statistical description of the Black Sea near-surface circulation using drifters in 1999-2003. *Deep-Sea Res. I*, 52, 2250-2274.
- Repeta, D.J. and Simpson, D.J. (1991) The distribution and recycling of chlorophyll, bacteriochlorophyll and carotenoids in the Black Sea. *Deep-Sea Res.*, 38, Suppl.2A, S969-S984.
- Repeta, D.J., Simpson, D.J. Jorgensen, B.B. and Jannash, H.W. (1989) Evidence for anoxic photosynthesis from distribution of bacteriochlorophylls in the Black Sea. *Nature*, 342, 69-72.
- Reva, Yu.A. (1997) Interannual oscillations of the Black Sea level. *Oceanology (Eng. Transl.)*, 37, 193-200.
- Rimbu, N., Dima, M. Lohmann, G. and Stefan, S. (2004) Impacts of the North Atlantic oscillation and the El Nino-southern oscillation on Danube river flow variability. *Geophys. Res. Lett.*, 31, L23203, doi:10.1029/2004GL020559.
- Rozanov, A.G., Neretin, L.N. and Volkov, I.I. (1998) Redox Nepheloid Layer (RNL) of the Black Sea: Its location, composition and origin. In: *Ecosystem Modeling as a Management Tool for the Black Sea*. L. Ivanov and T. Oguz, eds. NATO ASI Series, 2-Environmental Security-47, Kluwer Academic Publishers, Vol. 1, pp.77-92.
- Shiganova, T. (2005) Gelatinous plankton surveys in the Ponto-Caspian Seas. *Proceedings of The First Biannual Scientific Conference: Black Sea Ecosystem 2005 and Beyond*, organized by

- Commission on the Protection of the Black Sea Against Pollution, May 2006, Istanbul.
- Sokolova, E., Stanev, E.V., Yakubenko, V., Ovchinnikov, I. and Kosyan, R. (2001) Synoptic variability in the Black Sea. Analysis of hydrographic survey and altimeter data. *J. Mar. Syst.*, 31, 45-63.
- Sorokin, Y.I. (1972) The bacterial population and the process of hydrogen sulfide oxidation in the Black Sea. *J. Conseil Int. pour l'Exploration de la Mer*, 34, 423-454.
- Stanev, E.V. (1990) On the mechanisms of the Black sea circulation. *Earth-Sci. Rev.*, 28, 285-319.
- Stanev, E. V. and Beckers, J.M. (1999) Numerical simulations of seasonal and interannual variability of the Black Sea thermohaline circulation. *J. Mar. Syst.*, 22, 241-267.
- Stanev, E.V. and Peneva, E. (2002) Regional sea level response to global climatic change: Black Sea examples. *Global and Planetary Changes*, 32, 33-47.
- Staneva, J.V., Dietrich, D.E., Stanev, E.V. and Bowman, M.J. (2001) Rim Current and coastal eddy mechanisms in an eddy-resolving Black Sea general circulation model. *J. Mar. Syst.*, 31, 137-157.
- Sur, H.I. and Ilyin, Y.P. (1997) Evolution of satellite derived mesoscale thermal patterns in the Black Sea. *Prog. Oceanogr.*, 39, 109-151.
- Sur, H.I., Ozsoy, E. and Unluata, U. (1994) Boundary current instabilities, upwelling, shelf mixing and eutrophication processes in the Black Sea. *Prog. Oceanogr.*, 33, 249-302.
- Sur, H.I., Ozsoy, E., Ilyin, Y.P., Unluata, U. (1996) Coastal/deep ocean interactions in the Black Sea and their ecological/environmental impacts. *J. Marine Systems*, 7, 293-320, 1996.
- Titov, V.B. (2000) Dependence of the formation of the winter hydrological structure in the Black Sea on the severity of winter conditions. *Oceanology (Engl. Transl.)*, 40, 777-783.
- Titov, V.B. (2002) Seasonal and interannual variability of climatic conditions over the Black Sea, in the Black Sea, in *Multidisciplinary investigations of the northeast part of the Black Sea*, edited by A.G. Zatsepin and M.V. Flint, pp.9-19, Moscow, Nauka.
- Trouwborst, R. E., Clement, B. G., Tebo, B. M., Glazer, B. T., Luther III, G. W. (2006) Soluble Mn(III) in suboxic zones. *Science*, 313, 1955-1957.
- Tsimplis, M.N. and Josey, S.A. (2001) Forcing of the Mediterranean Sea by atmospheric oscillations over the North Atlantic. *Geophys. Res. Lett.*, 28, 803-806.
- Tugrul, S., Basturk, O., Saydam, C. and Yilmaz, A. (1992) The use of water density values as a label of chemical depth in the Black Sea. *Nature*, 359, 137-139.
- Zatsepin, A.G., Ginzburg, A.I., Kostianoy, A.G., Kremenitskiy, V.V., Krivosheya, V.G., Stanichny, S.V., and Poulain, P-M. (2003) Observations of Black Sea mesoscale eddies and associated horizontal mixing. *J. Geophys. Res.*, 108, 3246, doi:10.19/2002JC001390.
- Zatsepin A. G. , Golenko, N. N., Korzh, A. O., Kremenetskii, V. V., Paka, V. T., Poyarkov, S. G., and Stunzhas, P. A. (2007) Influence of the dynamics of currents on the hydrophysical structure of the waters and the vertical exchange in the active layer of the Black Sea. *Oceanology*, 47(3), 301-312.

CHAPTER 1B GENERAL OCEANOGRAPHIC PROPERTIES: GEOGRAPHY, GEOLOGY AND GEOCHEMISTRY (N. Panin)

N. Panin

National Institute of Marine Geology and Geo-ecology - GeoEcoMar, Romania

1B.1 Geographic position and physiography

The Black Sea is one of the largest almost enclosed seas in the world: its area is about 420 thousands km², the maximum water depth 2.212 m, the total water volume of about 534,000 km³. The Black Sea is placed in the southeastern part of the Europe between 40° 54' 40" and 46° 34' 30" northern latitudes, 27° 27' and 41° 46' 30" eastern longitudes. The sea is roughly oval-shaped. The maximum extent of the sea in the east-west direction is about 1175 km, while the shortest distance is of some 260 km between the southernmost tip of the Crimea and the Cape Kerempe on the Turkish coast (Fig. 1B.1). The Black Sea is connected to the Mediterranean Sea to the west and to the Sea of Azov to the north. The connection with the Mediterranean Sea is limited to the Istanbul-Canakkale (Bosporus-Dardanelles) straits. The Istanbul Strait is a rather narrow (0.76 - 3.6 km large) and shallow strait (presently 32 - 34 m at the sill) restricting the two-way water exchange between the Black and Mediterranean Seas. The other connection, with the Sea of Azov is realized by the Strait of Kerch.

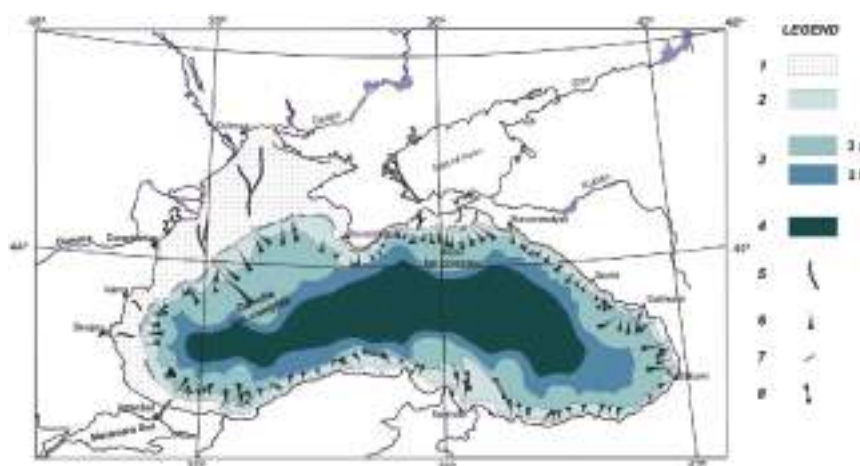


Fig. 1B.1. Geomorphologic zoning of the Black Sea (after Ross et al., 1974, Panin and Ion, 1997).

Legend; 1, continental shelf; 2, continental slope; 3, basin apron: 3 a - deep sea fan complexes; 3 b - lower apron; 4, deep sea (abyssal) plain; 5, paleo-channels on the continental shelf filled up with Holocene and recent fine grained sediments; 6, main submarine valleys - canyons; 7, paleo-cliffs near the shelf break; 8, fracture zones expressed in the bottom morphology.

The Black Sea is surrounded by high folded mountain chains represented by the Balkanides-Pontides belts to the south-west and south, by the Great and Little Caucasus to the east and by the Crimea Mountains to the north. There are low-standing plateaux and the Danube delta lowland only in the west and north-west. On the opposite eastern side there is the Kolkhida lowland of smaller extent. Consequently the relief energy is much higher on the eastern and southern coasts than on the northwestern shore.

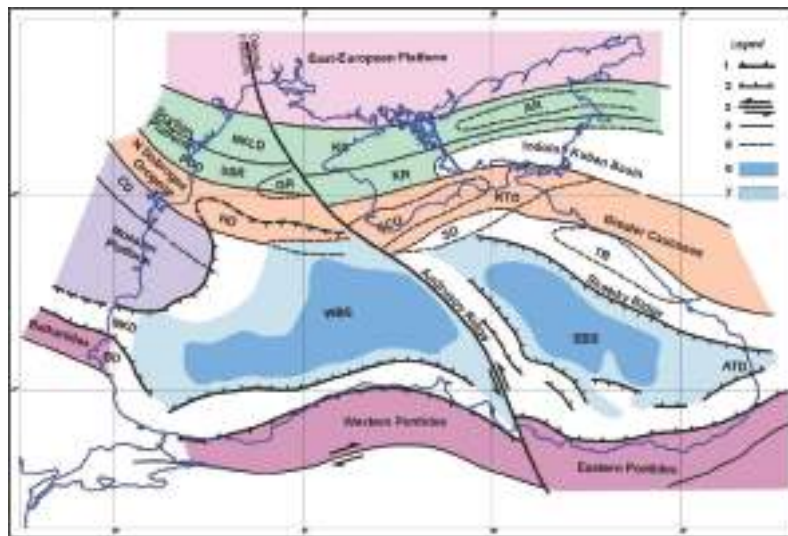


Fig. 1B.2. Tectonic sketch of the Black Sea Region (after Dinu et al., 2003; Panin et al., 1994).

Legend: 1, Orogenic overthrust front; 2, Gravitational faults of the rift; 3, Major strike-slip faults; 4, Major faults; 5, Limits of depressions and/or ridges; 6, Zone without granitic crust; 7, Thinned crust. Explanation of abbreviations: I. Platform regions: East European, Scythian, Moesian; II. Orogenic regions: North Dobrogea Orogene, Greater Caucasus, South Crimea Orogene - SCO, Balkanides, Western and Eastern Pontides; III. Depressions and ridges: PDD - Pre-Dobrogean Depression; NKLD - North Kilia Depression; KD - Karkinit Depression; HD - Hystria Depression; SD - Sorokin Depression; KTD - Kerchi-Taman Depression; NKD - Nijne-Kamchiisk Depression; BD - Burgas Depression; ATD - Adjaro-Trialet Depression; TB - Tuapse Basin; SSR - Suworov-Snake Island Ridge; KR - Krymskiy Ridge; AR - Azov Ridge; GR - Bubkin Ridge; IV. WBS - Western Black Sea; V. EBS - Eastern Black Sea;

The Black Sea basin can be divided into four physiographic provinces: the shelf representing about 29.9% of the total area of the sea, the basin slope - about 27.3% of the total area, the basin apron, with 30.6%, and the abyssal plain - 12.2% (Fig. 1B.1). One of the most prominent physiographic features is the very large shallow (less than 200 m deep) continental shelf within the northwestern Black Sea (about 25 % of the total area of the sea). The Crimean, Caucasian and southern coastal zones are bordered by very narrow shelves and often intersected by the submarine canyons.

1B.2. Geology of the Black Sea

Geologists consider the Black Sea a back-arc marginal extensional basin, which originated from the northward subduction of the Neo-Tethys along the southern margin of the Eurasian plate under a Cretaceous-Early Tertiary volcanic arc (Letouzey et al., 1977; Dercourt et al., 1986; Zonenshain and Le Pichon, 1986) as a result of the northward movement of the Arabic plate (Fig. 1B.2).

Since about 120 million years ago, the area has been a marine basin, with extremely dynamic development and large sediment accumulation of about 13 km of bottom sediment thickness in the central part of the basin. There are two extensional sub-basins with different geological history (Fig. 1B.2): (1) the Western Black Sea Basin, which was opened by the rifting of the Moesian Platform some 110 Ma ago (Late Barremian) followed by major subsidence and probable oceanic crust formation about 90 Ma ago (Cenomanian) (Astyushkov, 1992; Finetti et al., 1988; Görür, 1988) and (2) the Eastern Black Sea Basin, with rifting beginning probably in the Late Palaeocene (about 55 Ma

ago), and extension and probable oceanic crust generation in the Middle Eocene (ca.45 Ma ago) (Robinson et al., 1995).

1B.3. Water and sediment supply from rivers

The Black Sea has an extremely large drainage basin of more than 2 million km², collecting the water from almost all the European countries, except the westernmost ones. The northwestern Black Sea receives the discharge of the largest rivers in the Black Sea drainage area - the Danube River with a mean water discharge of about 200 km³/yr and the Ukrainian rivers Dniepr, Southern Bug and Dniestr contributing with about 65 km³/yr (Table 1B.1). Presently the influence of the Danube River is predominant for the sedimentation on the northwestern Black Sea shelf area.

The Danube influence extends far southward up to the Bosphorus region, as well as down to the deep sea floor. Presently the other three tributaries of the north-western Black Sea (Dniestr, Dniepr and Southern Bug) are not significant suppliers of sediments because they are discharging their sedimentary load into lagoons separated from the sea by beach barriers.

Table 1B.1. Fluvial water and sediment discharge into the Black Sea. *Data from Balkas et al. (1990); ** multiannual mean discharge before damming the River Danube after Bondar (1991); Panin (1996).

Rivers	Length (Km)	Drainage basin Area (Km ²)	Water discharge (Km ³ /yr)	Sediment discharge (Mt/yr)
I. North-Western Black Sea				
Danube	2,860	817,000	190.7	51.70**
Dniestr	1,360	72,100	9.8	2.50*
Dniepr	2,285	503,000	52.6	2.12*
Southern Bug	806	63,700	2.6	0.53*
Sub-total I:		1,455,800	255.7	56.85
II. Sea of Azov				
Don	1,870	442,500	29.5	6.40*
Kuban	870	57,900	13.4	8.40*
Sub-total II:		500,400	42.9	14.80
III. Caucasian coast rivers			41.0*	29.00*
IV. Anatolian coast rivers			29.7	51.00*
V. Bulgarian coast rivers			3.0*	0.50*
T O T A L :			372.3	152.15

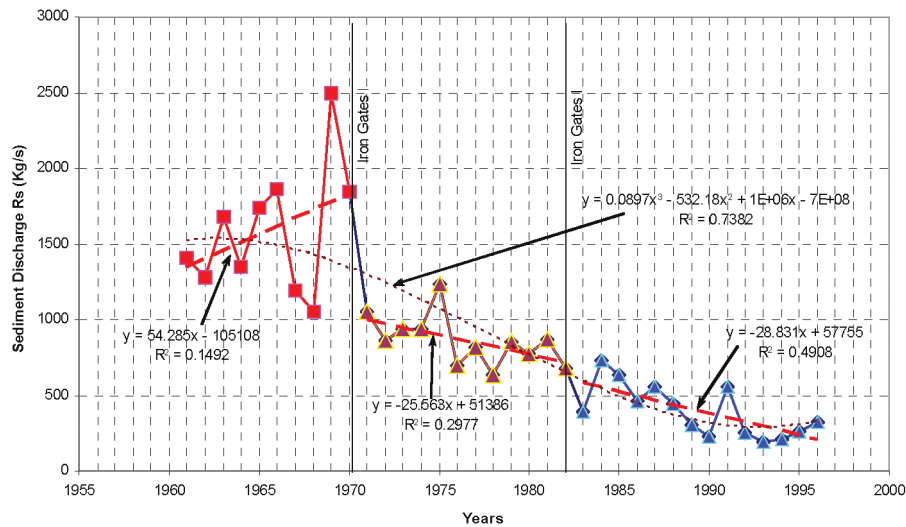


Fig. 1B.3. The decreasing trend of the Danube River sediment discharge after damming (Iron Gates I barrage in 1970, Iron Gates II barrage in 1983).

After the damming of the Danube River at Iron Gates I and II, the river sediment discharge diminished by almost 40-45 % (Fig. 1B.3), and the real sediment load brought by the Danube into the Black Sea is not larger than 30-40 million t/yr, of which only 10-12 % is sandy material and contributes to the littoral sedimentary budget of the delta front zone.

1B.4. Sedimentary systems of the Black Sea

The sedimentary systems in the Black Sea have been strongly influenced by the sea level changes driven by the processes of global glaciation and deglaciation. The surrounding relief and the physiography of the basin play also a very important role in defining the sedimentary systems. The eastern and southern parts of the sea are characterized by high relief energy and narrow continental shelf; this facilitates the direct transfer of sediments from the continent to the deep sea and determines a coarser grain size of these sediments. The western and north-western parts of the Black Sea have wide shelf and lower relief. Instead here the largest rivers are supplying important quantities of sediments, much finer (mainly silty-clay sediments).

North-western continental shelf: On the north-western Black Sea shelf area, the dispersal pattern of the Danube sediment supply indicates the existence of two main areas with different depositional processes (Panin et al., 1998): the Danube sediment-fed internal shelf and the sediment starving, external shelf (Fig. 1B.4).

Generally speaking, on the continental shelf the following sedimentary facies can be recognised (Shcherbakov and Babak, 1979):

Modiolus Mud: The *Modiolus* Mud is located at the top of the sedimentary sequence between 50 to 125 m of water depth. It is a light coloured mud, very rich in *Modiolus phaseolinus* coquinas whose thickness does not normally exceed 30 cm.

Mytilus Mud: The *Mytilus* (*Mytilus galloprovincialis*) mud is present from the shelf break till the depth of 50 to 40 m; further it is covered by the *Modiolus Mud*

Dreissena Mud: Around 130 m of water depth the surficial sediment is made of shells of *Dreissena*. Landward, this unit is covered by the *Mytilus Mud* and by the *Modiolus Mud*. The *Dreissena Mud* is outcropping only at the top of the continental slope.

The vertical transition in between *Dreissena Mud* to *Mytilus Mud* corresponds to the change from fresh/brackish to marine conditions in the Black Sea.

Internal, Danube sediment - fed shelf: The sediment-fed area in the neighbourhood of the Danube Delta includes the delta front unit (about 1,300 km²) and towards off-shore, at the base of the delta front to 50-60 m depth, the prodelta covering an area of more than 6,000 km². Its southern boundary is more difficult to define on account of the strong southward drift of fine grained sediment load discharged into the sea by the Danube, which is stumping the prodelta limit.

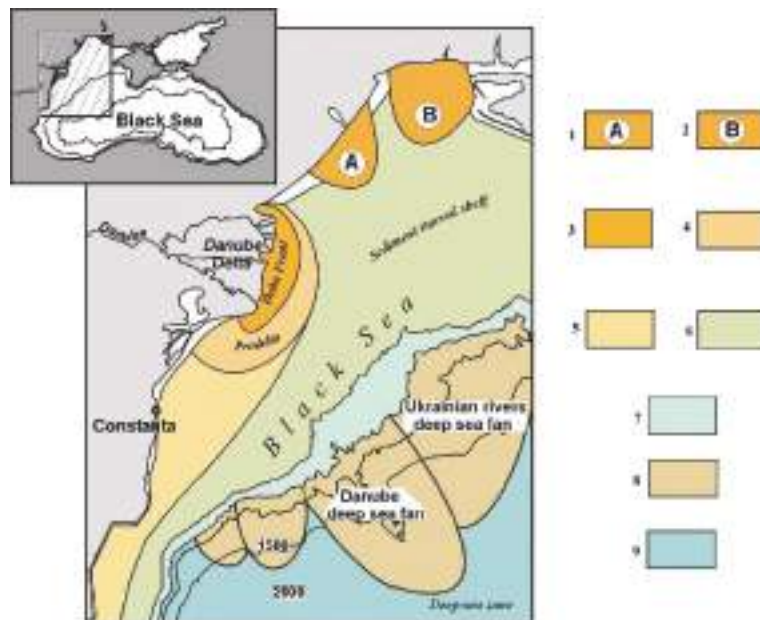


Fig. 1B.4. Main sedimentary environments in the northwestern Black Sea (after Panin et al., 1998).

Legend: 1-2, Areas under the influence of the Ukrainian rivers sediment discharge (A - Dniester and B - Dnieper); 3, Danube Delta Front area; 4, Danube Prodelta area; 5-6, Western Black Sea continental shelf areas (5, under the influence of the Danube-borne sediment drift; 6, sediment starved area); 7, Shelf break and uppermost continental slope zone; 8, Deep-sea fans area; 9, Deep-sea floor area.

Out of the area defined as the prodelta unit, the internal, western zone of the Romanian shelf stands out as the shallow marine area (less than 50 -60 m water depth), which receives clay and silty sediments, supplied by the Danube River. Moving as a suspended load, the sediment flux goes beyond the area in front of the Danube Delta but does not reach the eastern, external shelf zone. Under the influence of the dominant currents, the "clayey-silty" sediment flux moves southward toward the Bulgarian shelf, keeping within the western shelf area, close to the shoreline and finally discharging the sediment load in the deep-sea zone within the pre-Bosporus region.

External, sediment starving shelf: Situated outside the area covered by the Danube fed sediment flux the external, eastern part of the continental shelf represents an area practically deprived of clastic material (Fig. 1B.5). Within this sediment starving shelf area, the condensed sediment accumulation is of biogenic origin, producing an organic thin cover on relict sediments or concentrations of shells. The Danubian sediments seldom reach the shelf area north or northwest of the Danube mouths. Dniester and Dniepr, the main rivers north of Danube Delta, are themselves, as already mentioned, not significant suppliers of sediment for the north-western Black Sea shelf. Consequently, the sediment starving status characterizes almost all of the whole Black Sea continental shelf west of the Crimean Peninsula.

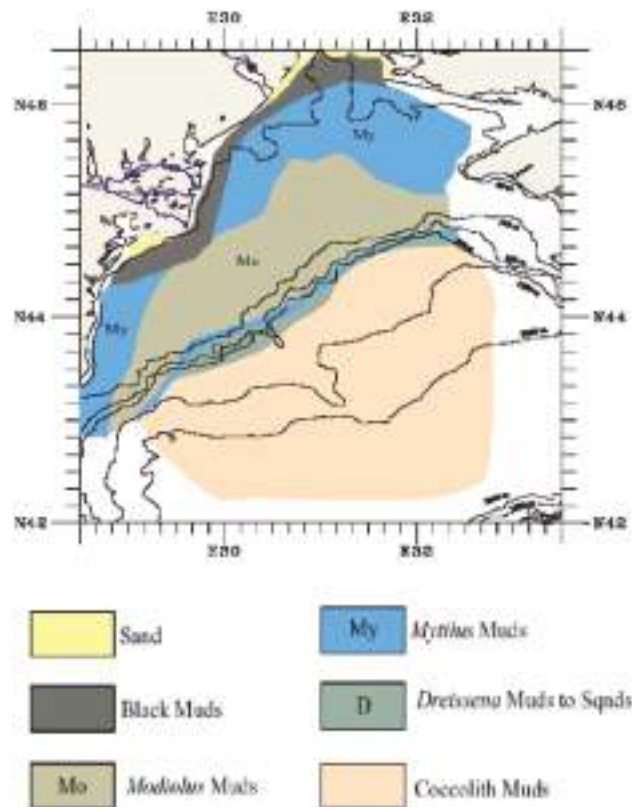


Fig. 1B.5. Repartition of litho-stratigraphic units on the sea floor in the NW Black Sea (from S. Radan, unpublished data).

Deep sea zone of the western Black Sea: During the Upper Quaternary, in correlation with the sea-level fluctuations of this period, very large accumulations of sediments were formed in the deep-sea zone of the north-western Black Sea, mainly on the continental slope and apron areas. This accumulation is represented by two distinct but interfingering fans: the Danube fan fed by the River Danube during fan accretion and the Dniepr fan built up by the Ukrainian rivers Dniepr, Dniestr and Bug. Eight seismic sequences have been identified within each of these fans (Wong et al., 1994, 1997). While the lowermost two consist mainly of mass transport-related deposits, the six upper sequences comprise typical fan facies associations, corresponding mainly to the low stands of the sea level related to the glacials.

The interpretation of seismic sequences show that the Danube and Dniepr fans were accreted during the past 480 k.yr (sequences 3 to 8). Average deposition rates for the fan

sequences range from 2.4 to 7.2 m/k.yr and the volume of material deposited within a sea level cycle lies between 4,300 km³ and 9,590 km³.

Within the deep-sea zone of the Black Sea, the existing accumulation of recent sediments is represented by coccolith ooze overlying sapropelic or organogen sediments (Ross et al., 1970) highlighting the domination of the organic component over the detrital one. Ross and Degens (1974) have defined the following succession of the upper sediment layers:

Unit I - coccolith ooze (0 - 3,000 yrs BP) : micro laminated carbonated sediment with *Emiliana huxleyi* Unit II - sapropel beds (3,000 - 7,000 yrs BP) - micro laminated sediment very rich in organic matter (sapropel)

Unit III - banded lutite (7,000 - 25,000 yrs BP) - banded lutites ± turbidites.

These units correspond to the Arkhangelskiy and Strakhov's (1938) stratigraphic units: (1) recent deposits; (2) Old Black Sea beds, and (3) Neoeuxinian deposits (Tables 1B.2 and 1.3). Very seldom and locally spread gravitationally transported material and mainly hemipelagic sediments occur within the slope, apron and abyssal zones, during this high stand sea level.

1B.5. Past environmental and sea level changes in the Black Sea

Large-scale sea level changes and consequently drastic reshaping of land morphology, large accumulation of sediments in the deep part of the sea and modifications of environmental settings occurred all along the Black Sea geologic history. The Quaternary was especially characterised by very spectacular changes, which have been driven by the global glaciations and deglaciations.

During these changes the Black Sea level behaviour was influenced by the restricted connection with the Mediterranean Sea by the Bosphorus - Dardanelles Straits. When the general sea level lowered below the Bosphorus sill, the further variations of the Black Sea level followed specific regional conditions, without being necessarily coupled to the ocean level changes. One of the main consequences of the lowstands was the interruption of the Mediterranean water into the Black Sea, which became an almost freshwater giant lake.

The main glacial periods of the Quaternary in Europe (Danube, Günz, Mindel, Riss and Würm) corresponded to the regressive phases of the Black Sea, with lowstands of the water level down to -120 m. As mentioned above, the regressions represent phases of isolation of the Black Sea from the Mediterranean Sea and the World Ocean. Only the connection with the Caspian Sea could sometimes continue through Manytch valley. Correspondingly, during regressions, under fresh water conditions, the particularities of fauna assemblages had a pronounced Caspian character. On the contrary, during the interglacials, the water level rose to levels close to the present level; the Black Sea was reconnected to the Mediterranean Sea, and the environmental conditions as well as the fauna characteristics underwent marine Mediterranean influences.

For example, during the Karangatian phase (since 125 ka BP to ~ 65 ka BP) of the Black Sea, which corresponds to the warm Riss-Würmian (Mikulinian) interglacial (Fig. 1B.6),

the water level exceeded the present-day level by 8 to 12 m. The saline Mediterranean water penetrated through the Bosphorus, and the Black Sea became saline (30 to 37‰), with a steno- and eury-haline marine Mediterranean type fauna (Nevesskaya, 1970). The sea covered the lowlands in the coastal zone.

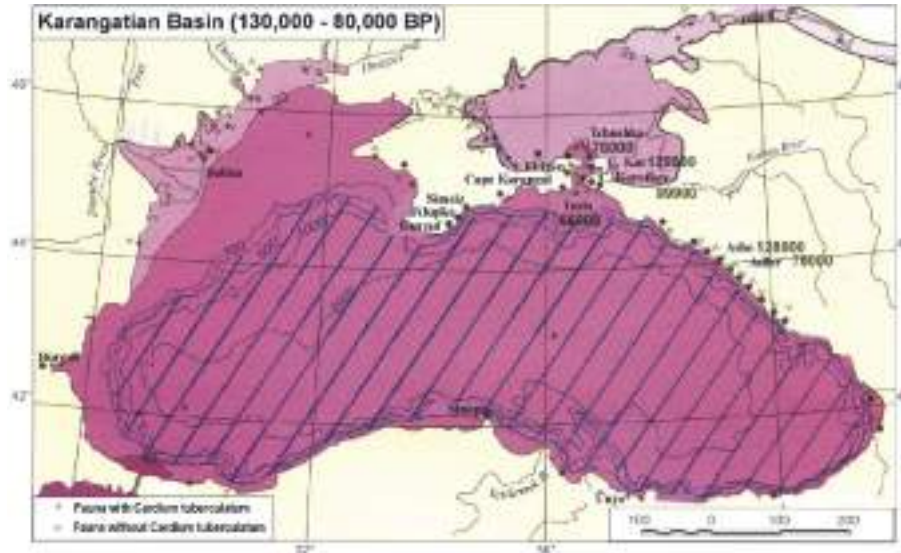


Fig. 1B.6. Plaeo-geographic reconstruction of the Black Sea during the Karangatian phase (Riss-Würmian or Mikulinian interglacial) (after Tchepalyga, 2002).

The last Upper Würmian glaciation (Late Valdai, Ostashkovian) corresponds to the Neoeuxinian phase of the Black Sea. This is a very low-stand phase, down to -110 - 130 m. The shoreline moved far away from the present-day position, especially in the north-western part of the Black Sea, and large areas of the continental shelf were exposed (Fig. 1B.7). The hydrographic network, especially the large rivers as Palaeo-Danube and Palaeo-Dniepr, incised up to 90 m the exposed areas. The Neoeuxinian basin, during the glacial maximum ($\sim 19 \div 16$ ka BP) was completely isolated from the Mediterranean Sea, and, correspondingly, the water became brackish and even fresh (3-7‰ and even less), well oxygenated, without H_2S contamination. The fauna was brackish to fresh water type with Caspian influence.

At about 16 - 15 ka BP, the postglacial warming and the ice caps melting started. As the supply of the melting water from the glaciers through the Dniepr and the Dniestr rivers, as well as the Danube river to the Black Sea was very direct and important, the Neoeuxinian sea-level rose very quickly, reaching and overpassing at ~ 12 ka BP the Bosphorus sill altitude. The majority of scientists, who studied the Black Sea, believe that in this phase it was a large fresh-water outflow through the Bosphorus-Dardanelles straits towards the Mediterranean (Aegean) Sea. Kvasov calculated (1975) that the fresh water outflow discharge was of about $190 \text{ km}^3/\text{year}$.

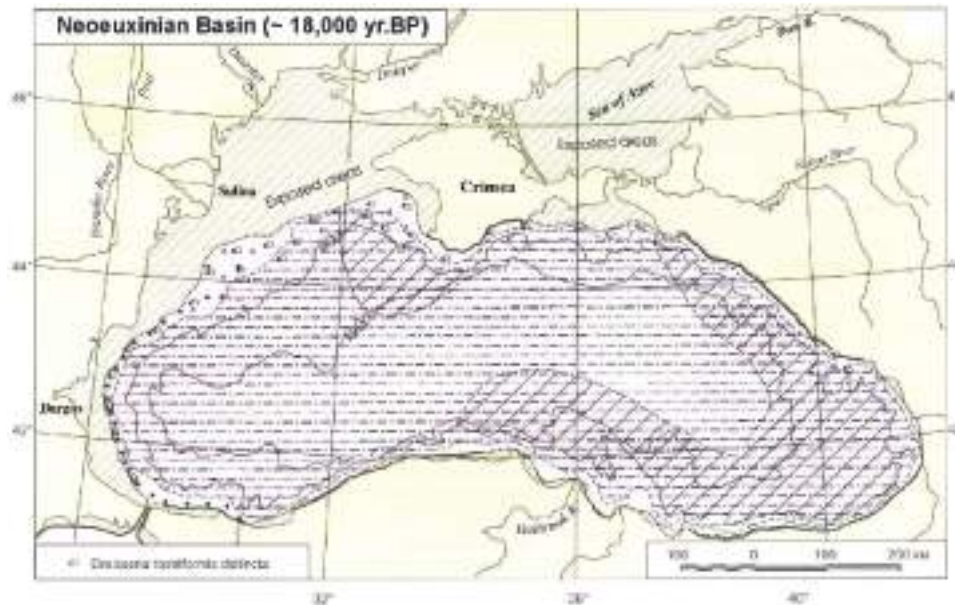


Fig. 1B.7. Palaeo-geographic reconstruction of the Black Sea during the Neoeuxinian phase (Upper Würmian) (after Tchepalyga, 2002).

At the beginning of the Holocene, some 9-7.5 ka BP, when the Mediterranean and the Black Seas have reached the same level (close to the present day one), the two-way water exchange was established, and the process of transformation of the Black Sea in an anoxic brackish sea started. During the last 3 ka BP, a number of smaller oscillations of the water level have been recorded ("Phanagorian regression", "Nymphaean" transgression, a lowering of 1-2 m in the X-th century AD, a slow rising continuing even today).

In the late nineties, a new hypothesis was formulated by Ryan et al. (1997). They considered that, when the deglaciation started during a short episode, the level of the Black Sea was high enough, and the fresh Pontic water flowed towards the Aegean Sea. At about 12 k.yr BP, the retreat of the ice-sheet front determined the reorienting towards the North Sea, for the limited period of time of melt-water supply. The Black Sea, without the inflow of the ice-melting water during the Younger Drias cooling (~11 ka BP) until 9 ka BP, under more arid and windy climate, experienced a new lowering of the level (down to -156 m). At the same time, the Mediterranean Sea continued to rise, reaching by 7.5 K.yr BP the height of the Bosphorus sill, and generating a massive input of salt water into the Black Sea basin. The flux was several hundred times greater than the world's largest waterfall, and it caused a rise of the level of the Black Sea, some 30 to 60 cm per day topping up the basin in few years time. More recent interpretation concludes that a deeper Bosphorus sill (~ -85 m) could lead to another scenario of mixing of Black Sea and Mediterranean waters (Major et al., 2002).

This new hypothesis is still under debate; numerous data from the straits of Bosphorus and Dardanelles, Marmara and Aegean Seas and the Danube Delta do not entirely support the Ryan's hypothesis. These data indicates that the "classical" scenario of Black Sea water outflow is rather credible. There are also some hydraulic incompatibilities for accepting a catastrophic flooding event in the Black Sea as well as a different time scale for reaching the present day salinity of the Black Sea waters (Myers et al., 2003). The

scenario proposed by the EU "Assemblage" project (Lericolais et al., 2006) after an extensive study of the western Black Sea is synthesized as shown in Fig. 1B.8.

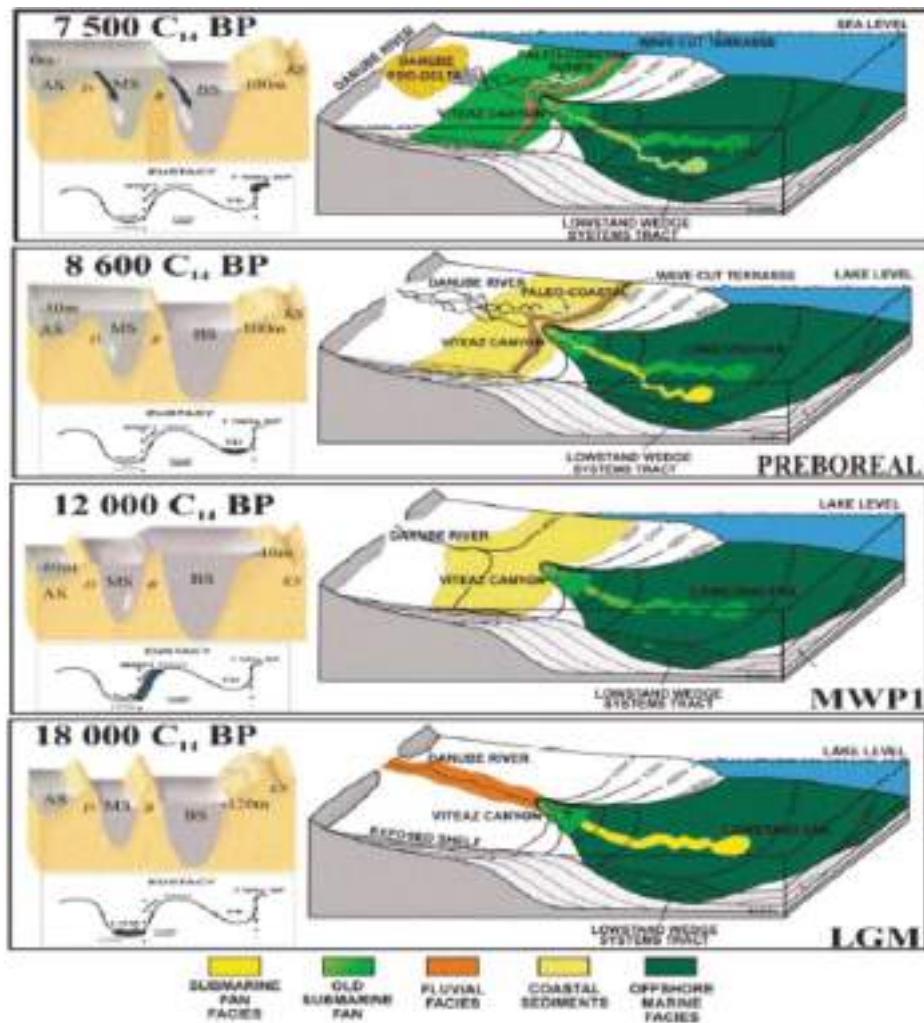


Fig. 1B.8. The scenario of the Black Sea water level fluctuation since the Last Glacial Maximum (after Lericolais et al., 2006, Final Report of the EU project "Assemblage")

The water brought to the Black Sea after the Melt Water Pulse 1A (MWP1A) at approximately 12,500 C_{14} BP (14,500 yr cal. BP) (Bard et al., 1990) was supposed to be sufficiently important that the water level rose up to between -40 m to -20 m, where the *Dreissena* layers were deposited. This water level would have brought the level of the Black Sea high enough for making possible an inflow of Mediterranean water with marine species of dinoflagellates (Popescu, 2004), and an outflow of Pontic waters towards Mediterranean Sea. Palynological studies show that during the Younger Dryas a cool and drier climate prevailed. The Younger Dryas climatic event had lowered the Black Sea water-level and cut again the connection with the Mediterranean Sea. Around 7.5 kyr BP, the Black Sea water level suddenly changed because of a quite abrupt flooding of the Black Sea by Mediterranean waters, as supposed by Ryan et al. (1997, 2003) supported with dinoflagellate cyst records (Popescu, 2004).

Table 1B.2. Stratigraphy and correlations of Upper Quaternary phases for the coastal and inner shelf zones (with slight modification from Fedorov, 1978).

General scale	Europe	European Russia	Black Sea region			
			General stratigraphic scale		W and NW Black Sea	Northern Black Sea
Holocene	Flandrian	Holocene	Black Sea Horizon	Nymphaean	Terrace at 2 m; sands with Cardium edule L. etc.	Crimea, Kerch, Taman Terrace at 2 m; Sands with Cardium edule L. etc.
				Phanagorian	Regression to - 6 - 8 m. Archeological layers V÷I c. BC	Regression to - 6 - 8 m. Archeological layers V÷I c. BC
				New Black Sea	Terrace at +4 +5 m; sands and shells with Cardium edule L., Chlamys, Ostrea, Mytilus	Terrace at +4 +5 m; sands and shells with Cardium edule L., Chlamys, Ostrea, Mytilus
				Old Black Sea	Clayey sands with Cardium edule L. etc. at -10 -20 m water depth on shelf	Clayey sands with Cardium edule L. etc. at -10 -20 m water depth on shelf
Upper	Grimaldian - Würm (regression to -100 -130 m)	Ostashkovian	Neoeuxinian	Late Neoeuxinian	Würmian loess; clays with Monodacna caspia Eichw., Dreissea polymorpha Pall., at -20 -30 m water depth on shelf	Clays with Monodacna caspia Eichw., Dreissea polymorpha Pall., at -20 -30 m water depth on shelf
	Neotyrhenian (terrace at 2-8 m above SL)	Mologo-Sheksnian		Early Neoeuxinian (Postkarangatian)	Regression to -60 - 80 (-130) m. Würmian loess. Deepening of the valleys incisions	Regression; deepening of the valleys incisions to -60 -80 m.
		Kalininian				
		Mykulinian	Karangatian	Upper Karangatian Lower Karangatian	Terrace at +15 +16 m Shells and sands with Cardium tuberculatum L., Paphia senescens (Coc.) etc.	Terrace at +12 +15 m (Pshady valley), +25 +30 m (in Sochi region); Shells with Cardium tuberculatum L., Paphia senescens (Coc.), Aporrhais pespelicani L., Paphia senescens (Coc.), Cerithium vulgatum Burg.etc.
Pleistocene						

Table 1B.2. Stratigraphy and correlations of Upper Quaternary phases for the coastal and inner shelf zones (with slight modification from Fedorov, 1978).

Black Sea region							
Middle	Regression (Riss II ?) Deepening of Bosphorus to - 100 m	Moskovian	Upper Euxinian-Uzunlarian	Regression	Regression. Clayey loess-like deposits.	Clayey deposits with Limneea, Planorbis ; pebbles with Viviparus	Regression. Alluvial pebbles, terminal moraine at Amtkheli.
	Eutyrrhenian (Tyrrhenian Ib) (terrace at 10-20 m)	Odyntzovian		Uzunlarian	Terrace at +35 +40 m (Bulgaria) Upper Babel layers, sands with Didacna nalivkini Wass. etc., Uppermost lagoonal clays	Clayey sands with Cardium edule L., Didacna nalivkini Wass. etc.	Terrace at +25 +30 m (Pshady) and +35 +37m (Pshady valley); pebbles, sands with Cardium edule L., Mactra stultorum L., Scrobicularia
	Regression (Riss I ?)	Dneprian		Late Paleoeuxinian		Sands and clays with Didacna nalivkini Wass., D.pontocaspia Pavl., Viviparus Regression	Terrace at 40÷43 m (Pshady valley); Sands, conglom., limestones with D.nalivkini Wass., D. subpyramidata Prav., at the base Balanus
			Lower Euxinian-Uzunlarian	Regression	Regression	Regression	Regression, Dilluvium
Lower	Paleotyrrhenian (Tyrrhenian I-a) (terrace at 18-30 m)	Lykhvinian		Paleouzunlarian	Sands, clays with Didacna pallasi Prav., D.nalivkini Wass. Lower Babel layers. Lagoonal clays with Didacna pseudocrassa Pavl. etc.	Continental deposits with- in the Mandzhil terrace	Terrace at +45 +50 m (at Ashe, Makopse, Magri); pebbles with C.edule, Paphia sp., Chione gallina
				Early Paleoeuxinian			Terrace at +60 +65 m (Dzhubgy); sands, pebbles with Didacna baericrassa Pavl., D.pallasi Prav., C.edule L.
	Mindel (Roman regression)	Okan	Regression		Alluvial sands with Viviparus and Tyraspol complex of mammals	Top deposits with Archidiscodon sp.	Regression
	Cromerian Terrace at 60 m	Dnestrian	Tchaudian	Upper Tchaudian		Shells, sands with Didacna pseudocrassa Pavl., D. tschoudae Andrus., D.rudis Nal.;Terrace " Large tables " (Bolshye stoly)	Terrace +40 +55 m(at Pshady), +100 +105 m (at Pshady valley), ~+130 m (at Sochi) ; Congl.,sands with D.pseudocrassa, D. Tschoudae, D.rudis

Black Sea region				
Eopleistocene	Sicilian I Terrace at 100 m	Günz (regression)	Gurian - Tchaudian	Lower Tchaudian
				Regression
		Günz (regression)	Gurian	Sands and clays with Archidiscodon meridionalis Nest. (late) within Nogaysk outcrop
				Continental deposits with Taman complex of mammalian fauna
	Emilian-Calabrian	Morozovian-Nogayskian	Gurian deposits	
				Clayey continental deposits Sands with Didacna baericrassa, D. parvula, V. pseudoachatinoides, Fagotia esperi
				Sandy-clayey deposits of Guria with D. tschaudae, D. tschaudae guriiana Livent., D. crassa guriensis Newesk., D. pleisto-pleura (Davit), D. pseudocrassa
				Deposits with Gurian-Tschaudian fauna
				Break
				Clays with Didacna digressa Livent. etc.

Table 1B.3. Stratigraphy and correlations of Upper Quaternary phases for shelf and bathyal zones (with slight modification from Scherbakov et al., 1979)

Northern Europe		BLACK SEA									
Stratigraphic subdivisions		Bathymetric zone 0-50 m			Bathymetric zone 50-200 m			Bathyal zone - northern part		Bathyal zone - southern part	
		Layers	Molluscs	Horizon	Molluscs	Diatomaea	Horizon	Diatoms, molluscs	Horizon	Nannopl.dino flagelates	Age
Upper	Subatlantic	Dzhemetinian	Divaricella divaricata Gafrarium minimum Pitar rudis Cardium papillosum	Phaseolinus muds	Modiolus phaseolinus	Coscinodiscus radiatus Thalassiosira excentrica Actinocyclus ehrenbergii Cyclotella kutzingiana Cyclotella accolata	Cocolith ooze	Coscinodiscus radiatus Endictia oceanica Thalassiosira excentrica Asteromphalus robustus Rhizosolenia calcar avis	Cocolith ooze Unit 1	Emiliania huxleyi Lingulodinium sp. Peridinium sp.	
	- 2,800 Sub-boreal - 4,800 Atlantic										
Middle	- 7,800 Boreal - 9,400	Kalamitian	Chione gallinaria Spisula subtruncata Mytilus galloprovincialis	Mytilus muds	Mytilus galloprovincialis Cardium edule	Coscinodiscus radiatus Thalassiosira excentrica Asteromphalus robustus	Sapropel-like muds		Sapropel muds Unit 2	Braarudosphaera bigelovi Peridinium trochoideum	
	Pre-boreal - 10,200 Younger Dryas Allerød Lower Dryas Bølling Gothiglacial	Bugazian-Viteazian	Cardium edule Abra ovata Corbula mediterranea Mytilaster lineatus Monodacna caspia Dreissena polymorpha	6,800 ± 140	Mytilus galloprovincialis Cardium edule Monodacna caspia Dreissena polymorpha	Thalassiosira excentrica Stephanodiscus astraea Synedra buculus Navicula palpebralis var. semipalpata	Terrigenous-biogenic muds		Terrigenous-biogenic muds Unit 3		7,090± 180 8,600± 200
Holocene											

Northern Europe		BLACK SEA									
	Lower	Neoeuxin	Monodacna caspia Dreissena polymorpha	8,550 ± 130	Monodacna caspia Dreissena rostriformis bugensis	Stephanodiscus astraea Melosira arenaria Diploneis domblitensis	Hydrotrillic muds	Stephanodiscus astraea	Nannofossil-rich terrigenous mud	Reworked Cretaceous. Paleogen, Neoge Cocoliths	
							Terrigenous brown "oxydated " muds			Tectatodinium spiriferites	
				13,500±1,500	Dreissena rostriformis distincta			Clayey muds	Fragments and young forms of : Dreissena rostriformis Monodacna caspia	Lacustrian phase	
			Dreissena polymorpha Viviparus fasciatus Unio sp.	17,760 ± 200	Dreissena rostriformis distincta						
Upper Pleistocene											
Würm (Valdai)											
Upper											
Ostashkovian glaciation											

References

- Aksu, A. E., Hiscott, R. N., Kaminski, M. A., Mudie, P. J., Gillespie, H., Abrajano, T., and Yasar, D., 2002a, Last glacial-Holocene paleoceanography of the Black Sea and Marmara Sea: stable isotopic, foraminiferal and coccolith evidence: *Marine Geology*, v. 190, no. 1-2, p. 119-149.
- Aksu, A. E., Hiscott, R. N., Mudie, P. J., Rochon, A., Kaminski, M. A., Abrajano, T., and Yasar, D., 2002b, Persistent Holocene outflow from the Black Sea to the eastern Mediterranean contradicts Noah's Flood hypothesis: *GSA Today*, no. May, p. 4-10.
- Aksu, A. E., Hiscott, R. N., and Yasar, D., 1999, Oscillating Quaternary water levels of the Marmara Sea and vigorous outflow into the Aegean Sea from the Marmara Sea Black Sea drainage corridor: *Marine Geology*, v. 153, no. 1-4, p. 275-302.
- Aksu, A. E., Hiscott, R. N., Yasar, D., Isler, F. I., and Marsh, S., 2002c, Seismic stratigraphy of Late Quaternary deposits from the southwestern Black Sea shelf: evidence for non-catastrophic variations in sea-level during the last ~10000 yr: *Marine Geology*, v. 190, no. 1-2, p. 61-94.
- Algan, O., Çagatay, N., Tchepalyga, A. L., Ongan, D., Eastoe, C., and Gökasan, E., 2001, Stratigraphy of the sediment infill in Bosphorus Strait: water exchange between the Black and Mediterranean Seas during the last glacial-Holocene: *Geo-Marine Letters*, v. 20, no. 4, p. 209-218.
- Algan, O., Gokasan, E., Gazioglu, C., Yucel, Z. Y., Alpar, B., Guneyusu, C., Kirci, E., Demirel, S., Sari, E., and Ongan, D., 2002, A high-resolution seismic study in Sakarya Delta and Submarine Canyon, southern Black Sea shelf: *Continental Shelf Research*, v. 22, no. 10, p. 1511-1527.
- Andrusov, N.I. 1892. Some results of the expedition of 'Tchernomoryetz': About the genesis of the hydrogen sulphide in the Black Sea waters. *Comm. Russian Geographical Soc.* 28, 5: 89-94 (in Russian).
- Andrusov, N.I., 1926. Paleogeographical maps of the Black Sea region in the Upper Pliocene, Pontic, Tchaudian and in the Euxinian Lake epoch" *Bull. MOIP, Sect. Geology* 4, 3-4: 35-46 (in Russian).
- Arkhangelskiy, A. D. 1927. "On the Black sea sediments and their importance in the knowledge of sedimentary deposits." *Bull MOIP, Sect. Geology* 5, 3-4: 199-264 (in Russian).
- Arkhangelskiy, A.D., and N. M. Strakhov. 1932. The geological structure of the Black Sea. *Bull MOIP, Sect. Geology* 10, 1: 3-104 (in Russian).
- Arkhangelskiy, A.D., and N. M. Strakhov, 1938. The geological structure of the Black Sea and its evolution. Moscow-Leningrad: Ed. Acad. Sc. USSR (in Russian).
- Arkipov, S. A., Ehlers, J., Johnson, R. G., and Wright, H. E. J., 1995, Glacial drainage towards the Mediterranean during the middle and late Pleistocene.: *Boreas*, v. 24, no. 3, p. 196-206.
- Ballard, R. D., Coleman, D. F., and Rosenberg, G., 2000, Further evidence of abrupt Holocene drowning of the Black Sea shelf: *Marine Geology*, v. 170, no. 3-4, p.253-261.
- Balkas, T., G. Dechev, R. Mihnea, O. Serbanescu, and U.Unlüata. 1990. State of marine environment in the Black Sea region. *UNEP Regional Seas Report and Studies* 124, UNEP.
- Berné, S., Auffret, J.-P., and Walker, P., 1988, Internal structure of subtidal sand waves revealed by high-resolution seismic reflection: *Sedimentology*, v. 35, p. 5-20.
- Berné, S., Lericolais, G., Marsset, T., Bourillet, J.-F., and De Batist, M., 1998, Erosional offshore sand ridges and lowstand shore-facies : examples from tide and wave dominated environments of France: *Journal of Sedimentary Research*, v. 68, no. 4, p. 540-555.
- Bondar, C., 1998, Hydromorphological relation characterizing the Danube river mouths and the coastal zone in front of the Danube delta: *Geo-Eco-Marina*, v. 3, p. 99-102.
- Calvert, S. E., and Fontugne, M. R., 1987, Stable carbon isotopic evidence for the marine origin of the organic matter in the Holocene Black Sea sapropel: *Chemical Geology*, v. 66, no. 3-4, p. 315-322.
- Carter, R. W. G., Hesp, P. A., Nordstrom, K. F., and Psuty, N. P., 1990a, Erosional landforms in coastal dunes, in Nordstrom, K. F., Psuty, N. P., and Carter, R. W. G., eds., *coastal dunes; processes and morphology*: Chichester (United Kingdom), John Wiley & Sons, p. 217-250.
- Carter, R. W. G., Nordstrom, K. F., and Psuty, N. P., 1990b, The study of coastal dunes, in Nordstrom, K. F., Psuty, N. P., and Carter, R. W. G., eds., *Coastal dunes; processes and morphology*: Chichester (United Kingdom), John Wiley & Sons, p. 1-14.
- Correggiari, A., Field, M. E., and Trincardi, F., 1996, Late Quaternary transgressive large dunes on the sediment-starved Adriatic shelf, in De Batist, M., and Jacobs, P., eds., *Geology of Siliciclastic Shelf Seas.*: London, Geological Society Special Publication, p. 155-169.

- Demirbag, E., Gökasan, E., Oktay, F. Y., Simsek, M., and Yüce, H., 1999, The last sea level changes in the Black Sea: Evidence from the seismic data: *Marine Geology*, v. 157, no. 3-4, p. 249-265.
- Dimitrov, P. S., 1982, Radiocarbon datings of bottom sediments from the Bulgarian Black Sea Shelf: *Bulg. Acad. Sci. Oceanology*, v. 9, p. 45-53.
- Evsylekov, Y. D., and Shimkus, K. M., 1995, Geomorphological and neotectonic development of outer part of continental margin to the south of Kerch Strait: *Oceanology*, v. 35, p. 623-628.
- Fairbanks, R. G., 1989, A 17,000-year glacio-eustatic sea level record; influence of glacial melting rates on the Younger Dryas event and deep-ocean circulation: *Nature*, v. 342, no. 6250, p. 637-642.
- Fedorov P.V., 1978. The Pleistocene of the Ponto-Caspian Region. *Trudy Geol.Inst. Acad.Sc.USSR*, Nauka, Moscow, 168 p. (in Russian).
- Fedorov, P. V., 1988, The problem of changes in the level of the Black Sea during the Pleistocene: *International Geology Review*, v. 30, no. 6, p. 635-641.
- Fedorov, P. V., 2000, Pleistocene climatic events in the geological history of the Black Sea: *Stratigraphy and Geological Correlation*, v. 8, no. 5, p. 491-497.
- Filipova-Marinova, M., 2004, Late quaternary palaeoenvironmental records from the southern Bulgarian Black Sea coast, in *ASSEMBLAGE first workshop*, Varna, Bulgaria, p. 10.
- Finetti, I., G. Bricchi, A. Del Ben, M. Papin, and Z. Xuan. 1988. "Geophysical study of the Black Sea area." *Bull. Geofis. Teor. Appl.* 30: 117-118, 197-234.
- Fouache, E., Porotov, A., Müller, C., and Gorlov, Y., 2003, The role of neo-tectonics in the variation of the relative sea level throughout the last 6000 years on the Taman Peninsula (Black Sea, Azov Sea, Russia), in *Rapid Transgressions in semienclosed Basins*, Gdansk - Jastarnia, Poland.
- Fryberger, S. G., Al Sari, A. M., and Clisham, T. J., 1983, Eolian dune, interdune, sand sheet, and siliciclastic sabkha sediments of an offshore prograding sand sea, Dhahran area, Saudi Arabia: *American Association of Petroleum Geologists Bulletin*, v. 67, no. 2, p. 280-312.
- Fryberger, S. G., Dean, G., and McKee, E. D., 1979, Dune forms and wind regime, A study of global sand seas: Reston, VA (USA), U. S. Geological Survey.
- Giosan, L., Bokuniewicz, H. J., Panin, N., and Postolache, I., 1997, Longshore sediment transport pattern along Romanian Danube delta coast: *Geo-Eco-Marina*, v. 2, no.11-24.
- Gökasan, E., Demirbag, E., Oktay, F. Y., Ecevitoglu, B., Simsek, M., and Yüce, H., 1997, On the origin of the Bosphorus: *Marine Geology*, v. 140, no. 1-2, p. 183-199.
- Gorur, N., Cagatay, M. N., Emre, O., Alpar, B., Sakinç, M., Islamoglu, Y., Algan, O., Erkal, T., Kecer, M., Akkok, R., and Karlik, G., 2001, Is the abrupt drowning of the Black Sea shelf at 7150 yr BP; a myth?: *Marine Geology*, v. 176, no. 1-4, p. 65-73.
- Gunnerson, C. G., and Oztuvgut, E., 1974, The Bosphorus, in Degens, E. T., and Ross, D. A., eds., *The Black Sea - Geology, Chemistry and Biology*: Tulsa, Amer. Assoc. Petrol. Geol., p. 99-114.
- Hay, B., Honjo, S., Kempe, S., Ittekkot, V., Degens, E., Konuk, T., and Izdar, E., 1990, Interannual variability of particle flux in the Northwestern Black Sea: *Deep Sea Research*, v. 37, p. 911-928.
- Hay, B. J., Arthur, M. A., Dean, W. E., Neff, E. D., and Honjo, S., 1991, Sediment deposition in the Late Holocene abyssal Black Sea with climatic and chronological implications: *Deep-Sea Research*, v. 38, no. Suppl.2, p. S1211-S1235.
- Jones, G. A., and Gagnon, A. R., 1994, Radiocarbon chronology of Black Sea sediments: *Deep Sea Research* 1, v. 41, no. 3, p. 531-557.
- Jousé, A. P., and Mukhina, V. V., 1978, Diatom units and the paleogeography of the Black Sea in the Late Cenozoic (DSDP, leg 42B).
- Kenyon, N. H., and Stride, A. H., 1968, The crest length and sinuosity of some marine sand waves: *Journal of Sedimentary Petrology*, v. 38, p. 255-259.
- Konyukhov, A. I., 1997, The Danube submarine fan: specific features of the structure and sediment accumulation: *Lithology and Mineral Resources*, v. 32, no. 3, p.197-207.
- Kuprin, P. N., Scherbakov, F. A., and Morgunov, I. I., 1974, Correlation, age, and distribution of the postglacial continental terrace sediments of the Black Sea: *Baltica*, v. 5, p. 241-249.
- Lericolais, G., Panin, N., Popescu, I., Berné, S., Ion, G., and Blason scientific crew, 1998, Danube and Dniepr paleovalleys : New discoveries during BlaSON survey on the north western Black Sea

- shelf, in 3rd International Conference on the Petroleum Geology and Hydrocarbon Potential of the Black and Caspian Seas Area., Neptun, Constanza (Romania), p. 34.
- Lericolais, G., Popescu, I., Guichard, F., Popescu, S. M., and Manolakis, L., 2007, Water-level fluctuations in the Black Sea since the Last Glacial Maximum, in Yanko-Hombach, V., Gilbert, A. S., Panin, N., and Dolukhanov, P.M., eds., *The Black Sea Flood Question: Changes in Coastline, Climate, and Human Settlement*.
- Lericolais, G., Popescu, I., Panin, N., Guichard, F., Popescu, S. M., and Manolakis, L., 2003, Could the last rapid sea level rise of the Black Sea evidence by oceanographic surveys have been interpreted by Mankind?, in CIESM Workshop Monographs, Fira, Santorini, Greece, p. 44-53.
- Major, C. O., 1994, Late Quaternary sedimentation in the Kerch area of the Black Sea shelf: response to sea level fluctuation [BA thesis]: Wesleyan University, 116 p.
- Major, C. O., Ryan, W. B. F., Lericolais, G., and Hajdas, I., 2002, Constraints on Black Sea outflow to the Sea of Marmara during the last glacial-interglacial transition: *Marine Geology*, v. 190, no. 1-2, p. 19-34.
- Mamaev, V. O., and Musin, O. R., 1997, Black Sea Geographic Information System, CD-ROM, in Programme, B. S. E. P.- U. N. D.P., ed.: New York, United Nations Publications.
- Muratov, M.V. 1951. "History of the Black Sea basin in relation to the development of surrounding areas." *Bull. MOIP, Section Geology*, NS 26: 1, 7-34 (in Russian).
- Muratov, M.V., and Yu. P Neprochnov, 1967. "Structure of the Black Sea depression and its origin." *Bull. MOIP, Section Geol.* 42: 5, 40-49 (in Russian).
- Neprochnov, Yu. P. 1958. "The results of seismic investigation in the Black sea in the neighborhood of Anapa." *Dokl. Acad. Sc. USSR* 121: 6, 1001-1004 (in Russian).
- Neprochnov, Yu. P. 1960. "The deep structure of Earth crust below the Black Sea based on seismic data." *Bull. MOIP, Section Geol.* 35: 4, 30-36 (in Russian).
- Neprochnov, Y. P., 1980, *Geologicheskaya istoriya Chernogo morya po rezul'tatam glubokovodnogo bureniya* - (Translated Title: *The geological history of the Black Sea from the results of deep-sea drilling*): Moscow, USSR, Nauka Press, 212 p.
- Nevesskaja, L. A., 1965, Late Quaternary bivalve mollusks of the Black Sea: Their systematics and ecology: *Akad. Nauk SSSR Paleont. Inst. Trydy*, v. 105, p. 1-390.
- Nevesskaja, L. A., 1970, Contribution to the classification of ancient closed and semiclosed bodies of water on the basis of the character of their fauna, in Obruchev, D. V., and Shimansky, V. N., eds., *Modern problems in paleontology*: Moscow, Nauka Press, p. 258-278.
- Nevesskiy, E. N. 1961. Postglacial transgressions of the Black Sea. *Dokl. Acad. Sc. USSR* 137: 3, 667-670 (in Russian).
- Nevesskiy, E. N. 1967. *Processes of sediment formation in the near-shore zone of the sea*. Moscow: Nauka (in Russian).
- Nikonov, A. A., 1995, Manifestations of young tectonic activity in the southern Azov and Kerch fault zones: *Geotectonics*, v. 28, no. 5, p. 381-390.
- Noakes, J. E., and Herz, N., 1983, University of Georgia Radiocarbon dates VII: *Radiocarbon*, v. 25, no. 3, p. 919-929.
- Ostrovskiy, A. B., Izmaylov, Y. A., Balabanov, I. P., Skiba, S. I., Skryabina, N. G., Arslanov, S. A., Gey, N. A., and Suprunova, N. I., 1977, New data on the paleohydrological regime of the Black Sea in the Upper Pleistocene and Holocene, in Kaplin, P. A., and Shcherbakov, F. A., eds., *Paleogeography and Deposits of the Pleistocene of the Southern Seas of the USSR*: Moscow, Nauka Press, p. 131-141.
- Ozsoy, E., Unluata, U., and Top, Z., 1993, The evolution of Mediterranean water in the Black Sea; interior mixing and material transport by double diffusive intrusions: *Progress in Oceanography*, v. 31, no. 3, p. 275-320.
- Panin, N., 1983, Black Sea coastline changes in the last 10,000 years: a new attempt at identifying the Danube mouths as described by the ancients: *Dacia N.S.*, v. 27, p.175-184.
- Panin, N., 1989, Danube delta: Genesis, evolution sedimentology: *Rev. Roum. Géol. Géophys. Géogr.*, v. 33, p. 25-36.

- Panin, N., 1997, On the geomorphologic and geologic evolution of the river Danube: Black Sea interaction zone: *Geo-Eco-Marina*, v. 2, p. 31-40.
- Panin, N., Jipa, D., 1998, Danube river sediment input and its interaction with the north-western Black Sea: results of EROS-2000 and EROS-21 projects: *Geo-Eco-Marina*, v. 3, p. 23-35.
- Panin, N., Jipa, D., 2002, Danube River Sediment Input and its Interaction with the north-western Black Sea: *Estuarine, Coastal and Shelf Science*, v. 54, no. 3, p. 551-562.
- Panin, N., Panin, S., Herz, N., and Noakes, J. E., 1983, Radiocarbon dating of Danube Delta deposits: *Quaternary Research*, v. 19, p. 249-255.
- Panin, N., Popescu, I., 2007, The northwestern Black Sea: climatic and sea level changes in the Upper Quaternary, in Yanko-Hombach, V., Gilbert, A. S., Panin, N., and Dolukhanov, P. M., eds., *The Black Sea Flood Question: Changes in Coastline, Climate, and Human Settlement*: Springer.
- Pazyuk, L. I., Rychkovskaya, N. I., Samsonov, A. I., Tkachenko, G. G., and Yatsko, I.Y., 1974, History of the northwestern margin of the Black Sea in light of the new data on the stratigraphy and lithology of Plio-Pleistocene bottom rocks in the area of Karkinitkiy Bay: *Baltika*, v. 5, p. 86-92.
- Popa, A., 1993, Liquid and sediment inputs of the Danube river into the north-western Black Sea Univ: *Mitt. Geol.-Paläont. Inst. Hamburg*, v. 74, p. 137-149.
- Popescu, I., 2002, Analyse des processus sédimentaires récents dans l'éventail profond du Danube (mer Noire) [PhD thesis]: Université de Bretagne Occidentale-Université de Bucarest, 282 p.
- Popescu, I., Lericolais, G., Panin, N., Normand, A., Dinu, C., and Le Drezen, E., 2004, The Danube Submarine Canyon (Black Sea): morphology and sedimentary processes: *Marine Geol.*, v. 206, no. 1-4, p. 249-265.
- Popescu, I., Lericolais, G., Panin, N., Wong, H. K., and Droz, L., 2001, Late Quaternary channel avulsions on the Danube deep-sea fan: *Marine Geology*, v. 179, no. 1-2, p. 25-37.
- Popov, G. I., 1970, Significance of fresh water molluscs for correlation of continental and marine Pleistocene of Ponto Caspian. In: *Geology and fauna of the lower and middle Pleistocene: Palaeogeography, Palaeoclimatology, Palaeoecology*, v. 8, no. 2-3, p. 251-260.
- Popov, G. I., 1975, New data on the stratigraphy of Quaternary marine sediments of the Kerch' Strait: *Transactions (Doklady) of the U.S.S.R., v. Academy of Sciences: Earth Science Sections*. 213(1973), no. 1-6, p. Pages 84-86.
- Popov, G. I., and Suprunova, N. I., 1977, Stratigraphy of Quaternary bottom sediments of the Kerch' Strait: *Transactions (Doklady) of the U.S.S.R., v. Academy of Sciences: Earth Science Sections*. 237, no. 1-6, p. 111-113.
- Robinson, A.G., J. H. Rudat, C. J. Banks, and R.L.F. Wiles. 1996. "Petroleum geology of the Black Sea. Mar." *Pet. Geol.* 13: 195-223.
- Ross, D. A., and Degens, E. T., 1974, Recent sediments of the Black Sea, in Degens, E. T., and Ross, D. A., eds., *The Black Sea - Geology, Chemistry and Biology*: Tulsa, Amer. Assoc. Petrol. Geol., p. 183-199.
- Ryan, W. B. F., 2004, The Black Sea flood; a seed for a Myth ?, in 32nd IGC Florence 2004, Florence, p. Session T17.05 - Myth and geology.
- Ryan, W. B. F., Major, C. O., Lericolais, G., and Goldstein, S. L., 2003, Catastrophic Flooding of the Black Sea: *Annu. Rev. Earth Planet. Sci.*, v. 31, no. 1, p. 525-554.
- Ryan, W. B. F., Pitman, W. C., IIIrd, Major, C. O., Shimkus, K. M., Moskalenko, V., Jones, G. A., Dimitrov, P. S., Gorür, G., Sakiñç, M., and Yüce, H., 1997, An abrupt drowning of the Black Sea shelf: *Marine Geology*, v. 138, no. 1-2, p. 119-126.
- V. Sedov. 1969. "Structure of the Earth's crust in the western part of the Black Sea." *Dokl. Acad. Sc. USSR* 186: 4, 905-907 (in Russian).
- Shcherbakov, F. A., Kuprin, P. N., Potapova, L. I., Polyakov, A. S., Zabelina, E. K., and Sorokin, V. M., 1978, Sedimentation on the continental shelf of the Black Sea: Moscow, Nauka Press, 211 p.
- Shcherbakov, F. A., and Babak, Y. V., 1979, Stratigraphic subdivision of the Neoeuxinian deposits in the Black Sea: *Oceanology*, v. 19, no. 3, p. 298-300.
- Shcherbakov F.A., Koreneva E.V., and Zabelina E.K., 1979. Late quaternary stratigraphy of the Black Sea. Late Quaternary History and Sedimentogenesis of Marginal and Inland seas. Nauka, Moscow (in Russian).

- Shimkus, K. M., Evsyukov, Y. D., and Solovjeva, R. N., 1980, Submarine terraces of the lower shelf zone and their nature, in Malovitsky, Y. P., and Shimkus, K. M., eds., Geological and Geophysical Studies of the Pre-Oceanic Zone: Moscow, P.P. Shirshov Inst. of Oceanology Acad. Sci. USSR, p. 81-92.
- Shnyukov, Y. F., and Trashchuk, N. N., 1976, A new region of occurrence of Karangatian deposits on the southern slope of the Kerch Peninsula: Ukrainian Academy of Sciences, Doklady, v. B, no. 12, p. 1078-1080.
- Shopov, V., Bozilova, E., and Atanassova, J., 1992, Biostratigraphy and radiocarbon data of Upper Quaternary sediments from western part of the Black Sea (In Bulgarian with English summary): Geol. Balcanica, v. 22, p. 59-69.
- Shopov, V., Chochov, S., and Georgiev, V., 1986, Lithostratigraphy of Upper Quaternary sediments from the northwestern Black Sea shelf between the parallels of the Cape Emine and Danube River mouth: Geologica Balcanica, v. 16, no. 6, p. 99-112.
- Sorokin, V. M., Roslyakov, A. G., and Yutsis, V. V., 1998, New data on the structure of the upper Danube deep-sea fan: Lithology and Mineral Resources, v. 33, no. 6, p.518-524.
- Stanley D. J., and Ch. Blanpied. 1980. Late Quaternary water exchange between the eastern Mediterranean and Black Sea. Nature 285: 537-541.
- Stanley D. J., and Ch. Blanpied. 1981. The Sea of Marmara, late Quaternary lithofacies and palaeoceanographic exchange between eastern Mediterranean and the Black Sea. Marine geology and geophysics. Rapp. 27th Congress of CIESM 27: 8, 57.
- Strakhov, N. M. 1954. Sedimentogenesis in the Black Sea. In Genesis of sediments in modern basins, 81-136. Moscow: Academy of Sc. USSR (in Russian).
- Strakhov, N. M. 1963. Some characteristics of diagenesis of the Black Sea deposits. Lithology and mineral resources 1: 3-21 (in Russian).
- Talling, P. J., 2000, Self-organization of river networks to threshold states: Water Resources Research, v. 36, no. 4, p. Pages 1119-1128.
- Tchepalyga, A. L., 1984, Inland sea basins, in Velichko, A. A., Wright, H. E. J., and Barnosky-Cathy, W., eds., Late Quaternary Environments of the Soviet Union: Mineapolis, MN, United States, Univ. Minn. Press., p. 229-247.
- Trashchuk, N. N., and Bolivets, V. A., 1978, A new area of occurrence of Karangatian deposits on the NW coast of the Black Sea: Ukrainian Academy of Sciences, Doklady, v. B, no. 8.
- Winguth, C., 1998, Pleistozäne Meeresspiegelschwankungen und Sedimentation im nordwestlichen Schwarzen Meer: Berichte aus dem Zentrum für Meeres- und Klimaforschung der Universität Hamburg, Reihe D, 129 p.
- Winguth, C., Wong, H. K., Panin, N., Dinu, C., Georgescu, P., Ungureanu, G., Krugliakov, V. V., and Podshuveit, V., 2000, Upper Quaternary water level history and sedimentation in the northwestern Black Sea: Marine Geology, v.167, no. 1-2, p. 127-146.
- Wong, H. K., Panin, N., Dinu, C., Georgescu, P., and Rahn, C., 1994, Morphology and post-Chaudian (Late Pleistocene) evolution of the submarine Danube fan complex: Terra Nova, v. 6, p. 502-511.
- Wong, H. K., Winguth, C., Panin, N., Dinu, C., Wollschläger, M., Ungureanu, G., and Podshuveit, V., 1997, The Danube and Dniepr fans, morphostructure and evolution: GeoEcoMarina, v. 2, p. 77-102.
- Yaranov, D. 1939. Correlation of the Quaternary of the Balkan peninsula, the Black Sea, of the Mediterranean Sea and of the Atlantic coasts of the Euro-African bloc." God. SU. 35: 187-204.
- Yevsyukov, Y.-D., and Shimkus, K. M., 1995, Geomorphological and neotectonic development of outer part of continental margin to the south of Kerch Strait: Oceanology, v. 35, no. 4, p. 623-628.
- Zonenshain, L. P., and X. Le Pichon. 1986. Deep basins of the Black Sea and Caspian Sea as remnants of Mesozoic back-arc basins. Tectonophysics 123: 181-212

CHAPTER 2 THE STATE OF EUTROPHICATION (T. Oguz *et al.*)

T. Oguz

Institute of Marine Sciences, Middle East Technical University, Erdemli, Turkey

V. Velikova

Inebolu Sokak 29, Kabatas, Istanbul, Turkey

A. Cociasu

National Institute for Marine Research and Development (NIMRD), Constanta,
Romania

A. Korchenko

GOIN, Moscow, Russian Federation

2.1. Introduction

Marine eutrophication of coastal waters is considered to be a significant problem worldwide. The Black Sea is no exception, where considerable increase in the nutrient load has led to marked changes in the ecosystem structure and functioning. Eutrophication is defined here as excessive supply of nutrients (silicate, nitrogen and phosphorus) into water that subsequently leads to accelerated growth and over-production of algae and species of higher trophic levels, high rate of oxygen depletion, development of hypoxia or anoxia near the bottom of productive areas and subsequent degradation of benthic community structure. A key to successful management of coastal waters is reliable scientific assessment of eutrophication and of its governing processes. This chapter evaluates the current state and the long-term trend of eutrophication in the Black Sea using the available data for river nutrient (both organic and inorganic) loads, dissolved inorganic and organic nutrient, chlorophyll-a, surface and subsurface oxygen concentrations along the coast with respect to the reference conditions of the interior basin. The coastal stations are chosen from the sites that either receive river loads (like Sulina station) or are in close proximity of industrial complexes (like Constanta) or urban settlements (like Bay of Bourgas). Unless otherwise specified, the data described below are from the data-base of the Commission on the Protection of the Black Sea Against Pollution.

2.2. Long-term changes in river nutrient loads

The excessive nutrient enrichment was originated predominantly by enhanced river-based nutrient supply into the northwestern shelf starting by the early 1970s. The River Danube was used to be the major supplier of nutrients during the 1970s and 1980s that amounted to almost 80% of the total load into the sea. They were derived by agriculture, industry and urban settlements and supplied mainly through diffuse sources (Table 2.2.1). Based on more recent measurements at the discharge point of the Sulina branch, the River Danube contribution was reduced to nearly 50% of the overall river-based DIN and P-PO₄ loads (Table 2.2.2). The remaining half was contributed almost equally by the

Ukrainian rivers along the northwestern coast (Dniepr, Dniester, Bug) and the Turkish Rivers along the southern coast (Table 2.2.2).

Table 2.2.1. The sources and causes of nutrient enrichment in the western coastal waters of the Black Sea.

Drivers of nutrient enrichment		Causes of nutrient enrichment
Agriculture/farming	Lack of fertiliser storage facilities Unsustainable/inefficient farming practices Intensive livestock production Intensive fertiliser utilization and detergents Lack of proper effluent treatments of discharges from livestock and agricultural farms	Point and diffuse sources from agriculture/farming, industry and settlements Deposition from atmospheric emissions originated from land-based sources Background emissions
Industry	Untreated or improperly treated industrial effluents due to outdated or absence of treatment technology Insufficient treatment plants and their poor management Lack of control for waste water treatment plants	

Table 2.2.2 Annual-mean river-borne nutrient loads (in kilotonnes y⁻¹) into the Black Sea from each country during 2003-2005 (from TDA, 2007). The superscripts (a) and (b) denote the estimates based on the TNMN measurements at Reni and the NMRD measurements at Sulina discharge point, respectively.

Nutrient Load	Ukraine	Romania	Bulgaria	Turkey	Georgia	Russia	Total
DIN	29.85	304.10(a) 68.86(b)	2.35	24.87	0.54	0.84	362.55(a) 127.31(b)
P-PO ₄	2.30	8.80(a) 8.52(b)	0.24	6.13	0.02	0.32	17.81(a) 17.53(b)

The total nitrogen emission from the River Danube catchments increased from about 400 kilotonnes (kt) y⁻¹ in the 1950s to 900 kt y⁻¹ in 1985-1990 and then reduced to 760 kt y⁻¹ in 2000-2005 (Fig. 2.2.1a). Phosphorus emission was an order of magnitude smaller and changed from 40 kt y⁻¹ in 1950s to its peak value of 115 kt y⁻¹ during the first half of the 1990s and then to 70 kt y⁻¹ in 2000-2005 (Fig. 2.2.1b). Both emissions are thus still roughly 1.5 times higher than the 1950s. The construction of Iron Gate 1 in 1975 was estimated to impose a minor influence on the total-N load but was more critical on controlling the total-P load (daNUbs Project Final Report, 2005). The nitrogen-based agricultural run-off contributed around half of the total nitrogen emission since 1955 and contribution from urban settlements was around 20-30% (Fig. 2.2.1a). The increase in nitrogen emission is evidently well-correlated with fertilizer consumption prior to 1990 that increased from 0.5 million tonnes (mt) y⁻¹ in the 1950s to 3.0 mt y⁻¹ during the green revolution era in the eastern block countries during the 1980s (Fig. 2.2.1). According to this data set, phosphorus emission was mainly supplied by urban settlements up to 80% in 1990; the contribution of agriculture remained less than 20% (Fig. 2.2.1b). The effect

of increase in phosphorus fertilizer consumption to 1.5 mt y⁻¹ did not appear to increase agricultural-based phosphorus emission.

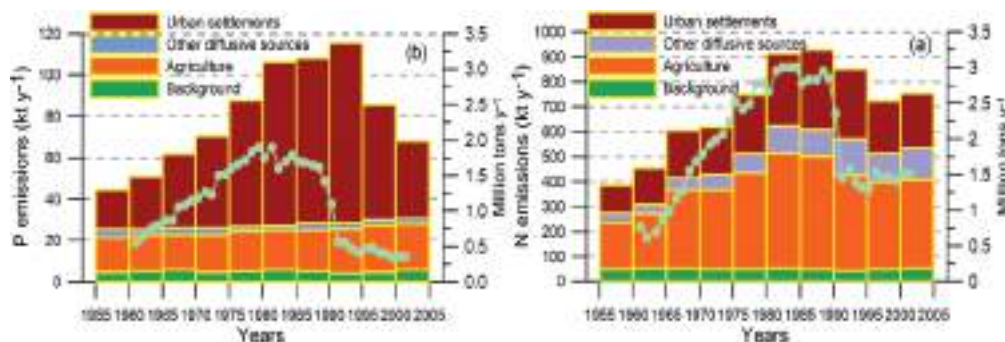


Fig. 2.2.1 Relative contributions of different point and diffuse sources to the emissions of (a) total nitrogen (N) and (b) total phosphorus averaged over 5 year bins and amounts of total nitrogen and phosphorus fertilizer consumption in the Danube catchments basin (solid circles). Redrawn from daNUbs Project Final Report (2005).

Following the collapse of their centrally-planned economy and economic recession, nitrogen and phosphorus fertilizer consumptions reduced to 1.5 mt y⁻¹ and 0.5 mt y⁻¹, respectively, during 1990-1991. Fig. 2.2.1 however suggests surprisingly minor change in agricultural nitrogen emission and no change in agricultural phosphorus emission. The phosphorus emission was reduced more predominantly by the improvement of regional environmental management, the introduction of phosphorus-free detergents, the improved nutrient removals at treatment plants (daNUbs Project Final Report, 2005).

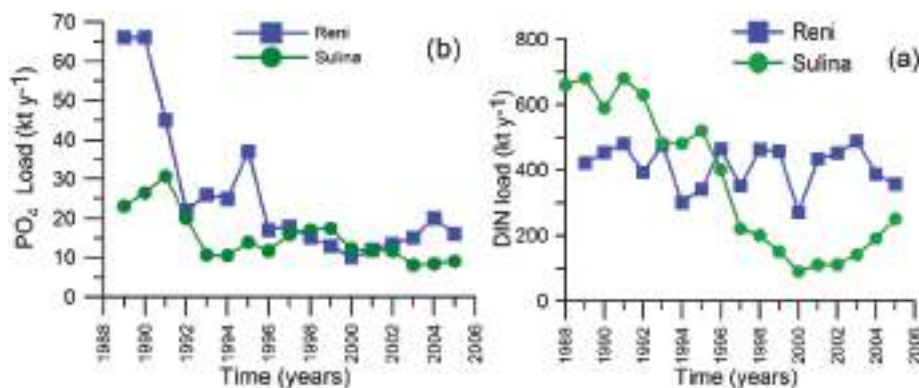


Fig. 2.2.2 Annual DIN and P-PO₄ loads measured at Sulina discharge point of the River Danube to the sea and at Reni located at the upstream end of the Sulina branch.

The lack of major reduction in nitrogen emissions from the Danube catchments basin is reflected in relatively high DIN load into the sea. At Reni (located at the upstream end of the Sulina branch), it fluctuated within the range of 300-500 kt y⁻¹ since the early 1990s (Fig. 2.2.2a) in consistent with the N-emission data (Fig. 2.2.1a). Such relatively high DIN load was explained by continuing emissions from large nitrogen stocks deposited in soils and groundwater in the catchments areas (daNUbs Project Final Report, 2005). On the basis of Reni data, a factor of three reductions is necessary to accomplish its pristine level prior to 1960 (~150 kt y⁻¹). According to the NIMRD (National Institute of Marine Research and Development, Romania) measurements at the

discharge point of Sulina branch of the River Danube, the DIN flux entering the sea tended to decrease gradually during the 1990s to $\sim 100 \text{ kt y}^{-1}$ at 2000 and increased afterwards to 250 kt y^{-1} in 2005 that was twice higher than its pristine level. It is hard to justify the considerable difference between two ends of the Sulina branch ($\sim 40 \text{ km}$), but the concomitant reduction in the interior basin subsurface nitrate peak (section 2.3) supports the Sulina data. On the other hand, both measurements reveal similar P-PO_4 load between 10 and 20 kiloton yr^{-1} after the mid-1990s (Fig. 2.2.2b).

No systematic data sets are available to assess the current state of organic nutrient loading from the northwestern rivers. But, the BOD₅ data may be used to deduce indirectly their DON loads. As inferred from Fig. 2.2.3, the total BOD₅ data from the Rivers Danube and Dniester, Dniepr and Bug display a gradual decreasing trend from the peak values close to 1000 kt y^{-1} during 1997-1999 to $\sim 500 \text{ kt y}^{-1}$ after 2000, which implies approximately 50% reduction. The Danube contribution to the total BOD load amounts to 80%. Assuming the DON (dissolve organic nitrogen)/ BOD₅ ratio ~ 0.3 (San Diego-Mcglone et al., 2000), the DON load into the northwestern Black Sea is estimated as 150 kt yr^{-1} in the present decade. The Danube contribution turns out to be approximately 130 kt yr^{-1} , which roughly corresponds to one-third of the Reni DIN load. This is a rather conservative estimate and represents an average condition over the NWS. It may in fact be locally much higher.

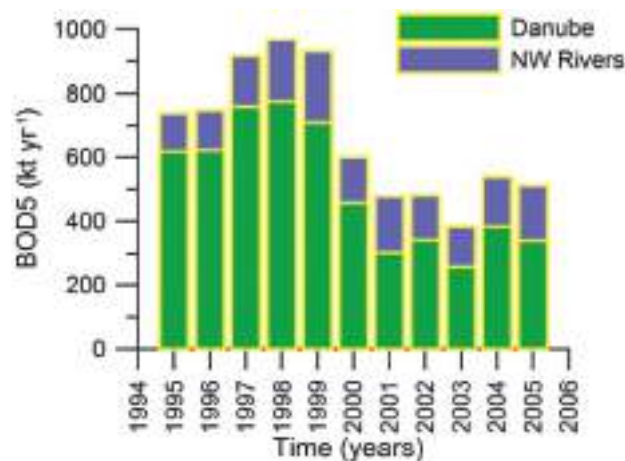


Fig. 2.2.3. BOD₅ load from the Danube River and other rivers (Dniester, Dniepr and Bug) discharging into the northwestern shelf during 1995-2005.

2.3. Long-term changes in nutrient concentrations

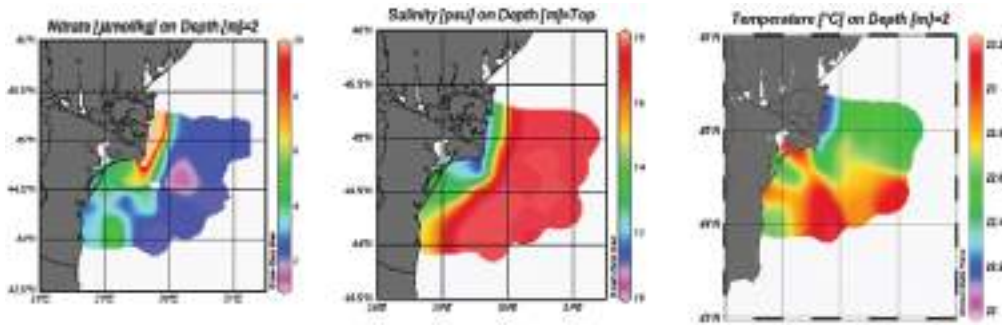


Fig. 2.3.1. Spatial distribution of surface temperature, salinity and nitrate concentration (μM) in Romanian coastal and offshore waters during September 2002 (Horstmann and Davidov, 2002).

Nutrients along the western coast acquire maximum concentrations in the Danube delta region that is characterized by relatively colder and less saline water mass and separated from offshore waters through a sharp frontal zone (Fig. 2.3.1). A predominant feature of the delta region is high rates of sediment deposition and resuspension mechanisms and rapidly changing physical conditions (in daily-to-weekly time scales) that introduce great deal of patchiness in nutrient concentrations. Almost 30-50% of nutrients supplied by the Danube is estimated to deposit near its mouth (Velikova and Cociasu, 2004) and thus does not contribute directly to the local biological production. At longer time scale (i.e. ~the last 50 years), sediment cores suggested 20% of total riverine nitrogen input accumulated in sediments of the western coastal waters, whereas denitrification eliminated 55% of the input (Teodoru et al., 2007). When the Danube plume extends southward, as shown in Fig. 2.3.1, low salinity and high nutrient water mass loses its character immediately to the south of the delta region and N-NO_3 concentration generally decreases by more than 50% (Fig.2.3.1).

Changes in nitrogen concentration: Consistent with the DIN load data shown in Fig. 2.2.2a, the annual-mean DIN concentration at Sulina discharge point shows a gradual reduction from $\sim 300 \mu\text{M}$ at 1990 to $\sim 40 \mu\text{M}$ at 2000 and then exhibits a slight rise to $\sim 70 \mu\text{M}$ at 2005 (Fig. 2.3.2). Albeit its large drop, recent values of DIN are still too high. The contribution of N-NH_4 to DIN remained negligibly small during the 1990s, but was around 10% after 2000. On the contrary, the annual-mean DIN concentration persistently varied around $150 \mu\text{M}$ at Reni during 1997-2005 (Fig. 2.3.2).

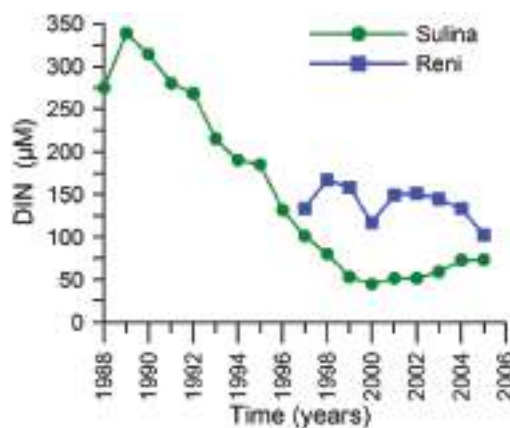


Fig. 2.3.2 Annual DIN concentration measured at Sulina discharge point of the River Danube to the sea and at Reni located at the upstream end of the Sulina branch.

As inferred by the amalgamated annual-mean surface NO_3 data (Fig. 2.3.3), following an increase in the first half of the 1990s, N-NO_3 concentration decreased during the second half and then started rising in the present decade. Its mean values for the previous and present decades are approximately $5 \mu\text{M}$ and $7 \mu\text{M}$, respectively. A notably similar long-term DIN structure also took place to the north of the Danube delta. Along the western coastal waters of Ukraine, DIN concentration increased from $1 \mu\text{M}$ in the 1960s to $9 \mu\text{M}$ in the 1980s and stabilized thereafter around $7.5 \mu\text{M}$ (Fig. 2.3.4) that was similar to that in the Romanian shelf. Although the eastern coastal waters of Ukraine had relatively better conditions with lower concentrations ($\sim 4 \mu\text{M}$ in the present decade) an increasing tendency over the last two decades is evident (Fig. 2.3.4).

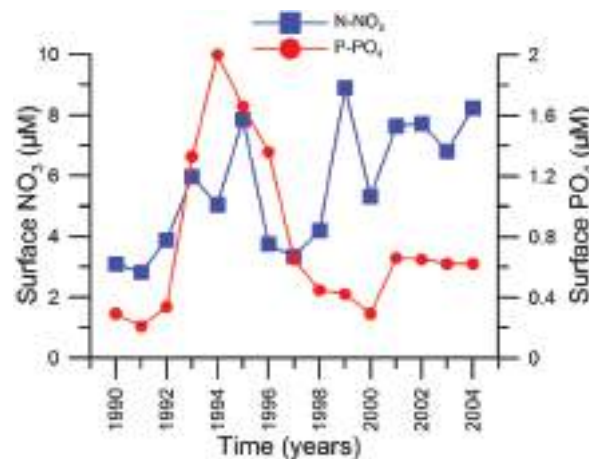


Fig. 2.3.3. Amalgamated annual-mean surface N-NO_3 and P-PO_4 concentration changes in Romanian waters (re-drawn from Parr et al., 2007).

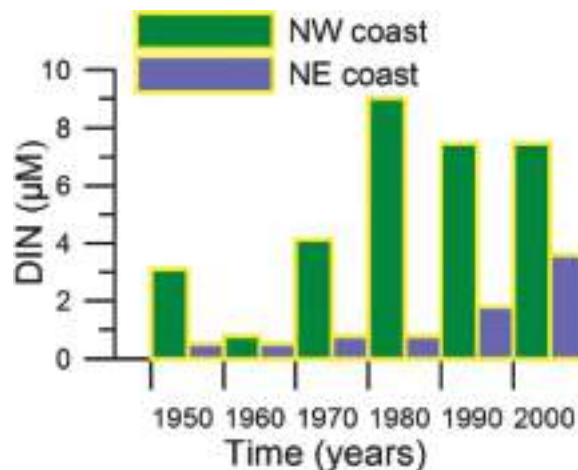


Fig. 2.3.4. Decadal variability of surface dissolved inorganic nitrogen (DIN) concentration along the western and eastern coastal waters of the NWS based on the averaging of available data from several stations at 5-year bins (after Loveya et al., 2006).

Surface nutrient concentrations measured monthly at the coastal sampling station near Constanta constitute the most comprehensive long-term data set to monitor their multi-decadal changes along the western coastal waters. Following a major reduction during the second half of the 1970s, N-NO_3 and N-NH_4 concentrations fluctuated within

5-10 μM during the 1980s and 1990s except a rising trend in 2004-2005 (Fig. 2.3.5). The decadal-mean N-NO_3 concentration reduced from 6.90 μM in the 1980s to 5.90 μM in the 1990s and then elevated to ~ 8 μM during 2000-2005 (Table 2.3.1). N-NH_4 concentration experienced an opposite trend and increased roughly 2.0 μM from the 1980s to the 1990s and then reduced by 1.0 μM during the present decade (Table 2.3.1). N-NO_2 concentration always remained around 1 μM and constituted only 6% of the total DIN. In general, the DIN possessed a slight rising trend from 12 μM in the 1980s to 13 μM in the 1990s and 14 μM in the 2000s (Table 2.3.1). This trend is consistent with the Sulina data (Fig. 2.2.2a) although the values are four-fold lower.

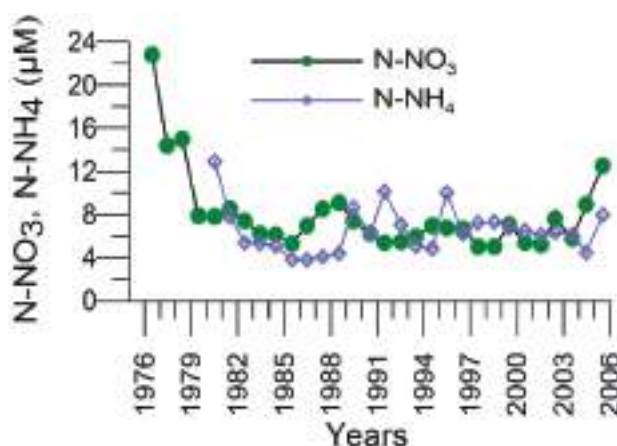


Fig. 2.3.5. Annual-mean surface concentrations of N-NO_3 (green) and N-NH_4 (blue) at Constanta station (A. Cociasu, per. com).

Table 2.3.1. Multi-annual mean surface nutrient concentrations (μM) in Constanta (after Velikova and Cociasu, 2004)

Period	1959-65	1983-90	1991-00	2001-05
N-NO_3	1.60	6.90	5.90	7.98
N-NH_4	-	5.11	7.06	6.12
P-PO_4	0.26	6.54	1.86	0.49
SiO_4	40.5	11.0	12.6	13.7

According to the monthly surface NO_3 and N-NH_4 concentration variations at Constanta during 2000-2006 (Fig. 2.3.5), the period 2000-2004 was characterized by a major N-NO_3 peak during April or April-May that coincides with the highest discharge period of the Danube. N-NO_3 concentration then decreased linearly up to September and then started increasing linearly up to next April. As an exception, a second and stronger peak appeared during the 2003 severe winter (January-February). This annual structure changed appreciably during 2005-2006 in terms of an extended spring peak to July and reduction in N-NO_3 concentration by September up to a minimum in November; thus the minimum N-NO_3 concentration phase shifted from August to November. Moreover, NO_3 concentrations from 2000 to 2006 indicated approximately 5 μM linear trend of increase. NH_4 concentration attained higher values predominantly in summer months.

Considerable interannual and local variabilities are also noted along the northwestern coastal waters (Fig. 2.3.7). N-NO_3 and N-NH_4 concentrations were exceptionally high (60-90 μM) near the waste water treatment plant sites Pivnichi and Pivdenna during 2003-2006 contrary to their much lower values during 2000-2002. N-NO_3 concentrations in the Odessa, Uzhnyi, and Ilichevsk ports were typically around 10-20 μM .

Measurements along the Romanian and Bulgarian coastal waters to the south of the Danube delta revealed comparable N-NO_3 and N-NH_4 concentrations with the Ukrainian coastal waters. N-NO_3 concentrations at Mamaia beach and two adjacent offshore stations along 5m and 20 m isobaths indicate uniformity of the Danube plume within 20 m isobath zone (Fig.2.3.8a). The features such as the April-May N-NO_3 peak within 10-20 μM range and relatively high spring concentrations during 2002 and 2005 resemble those observed at Constanta station (Fig.2.3.6).

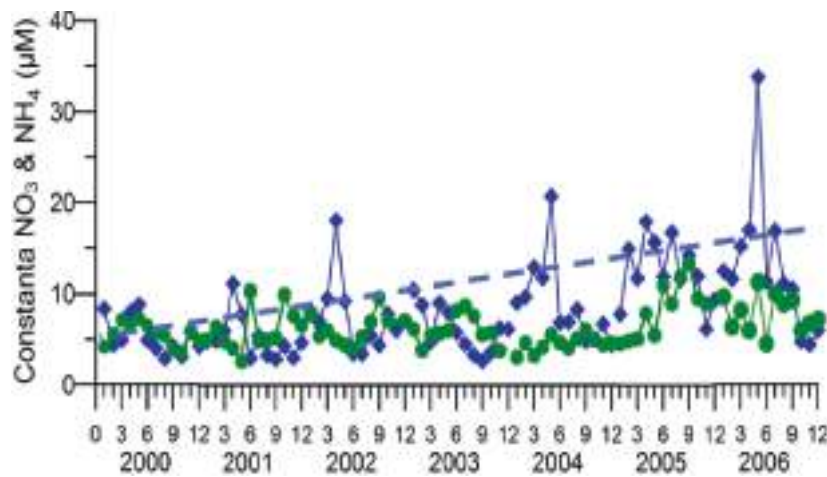


Fig. 2.3.6. Monthly changes of surface NO_3 (squares) and NH_4 (dots) concentrations and the trend of NO_3 concentration at Constanta monitoring station during 2000-2006.

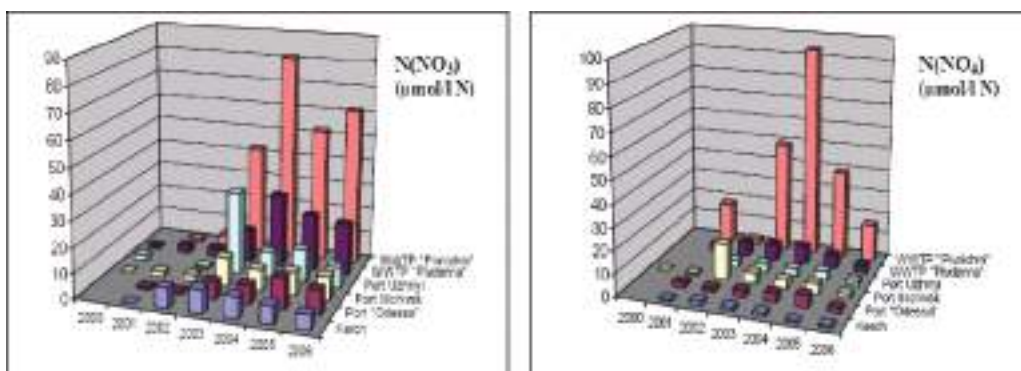


Fig. 2.3.7. Annual-mean N-NO_3 (left) and N-NH_4 (right) concentrations (μM) at various sites along northwestern Ukrainian waters during 2000-2006 (After PMA AG and AC Activities and Reporting, 2007).

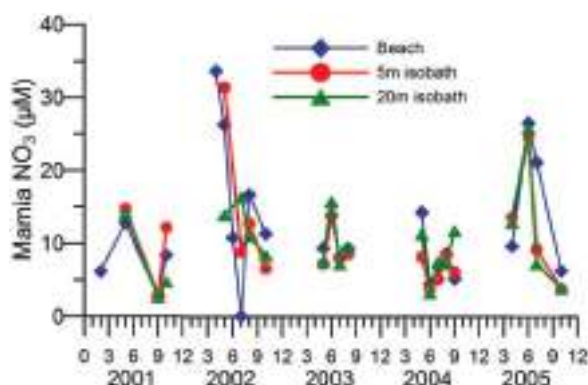


Fig. 2.3.8a. Monthly changes of surface NO_3 concentration at the Mamia beach and 5 m and 20 m isobaths further offshore during 2000-2005.

Further south along the southern Bulgarian coast, N-NO_3 and N-NH_4 at stations near Ahtopol and Bourgas Bay reveal concentrations as high as $20 \mu\text{M}$ in summer months that are comparable with their winter values (Fig. 2.3.8b,c). Their annual structure was therefore somewhat different than Constanta station, and likely signifies contribution from local sources in addition to the Danube upstream influence.

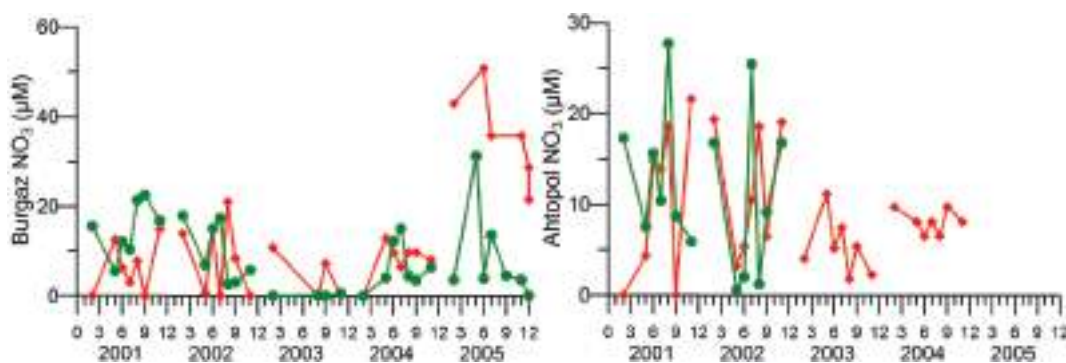


Fig.2.3.8b,c. Monthly changes of surface NO_3 and NH_4 concentrations at Ahtopol and Burgaz monitoring stations during 2000-2005.

More dense and regular measurements in the Bosphorus exit section during 1996-2003 possessed an order of magnitude lower N-NO_3 concentration (Fig. 2.3.8d). More importantly, they revealed a typical open-sea type annual structure with an N-NO_3 peak during winter due to enhanced vertical mixing, and N-NO_3 depletion in summer due to its uptake in phytoplankton production. An additional spring (April-May) peak exists during high Danube discharge years, reflecting efficiency of southward coastal transport. Opposite to the Bourgas Bay and Ahtopol, in the Bosphorus section the summer N-NO_3 concentration was low due to its intense uptake in phytoplankton production.

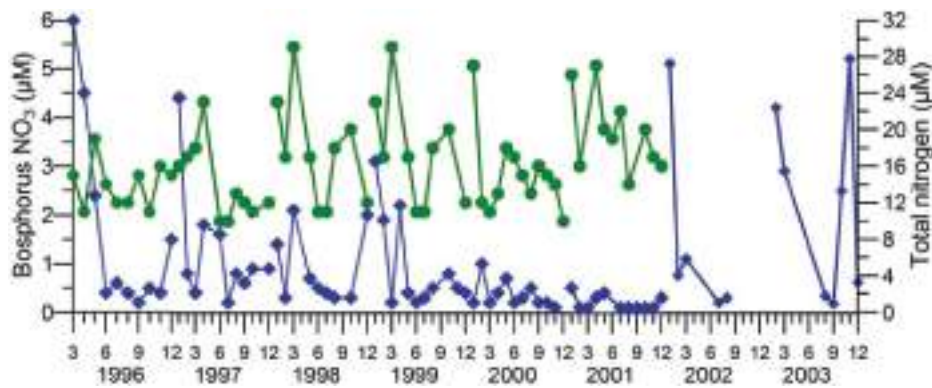


Fig. 2.3.8d. Monthly surface NO_3^- concentration (blue) and total nitrogen (organic + inorganic) concentration (green) (μM) at the Bosphorus northern entrance during 1996-2003 (redrawn after Okus, 2005).

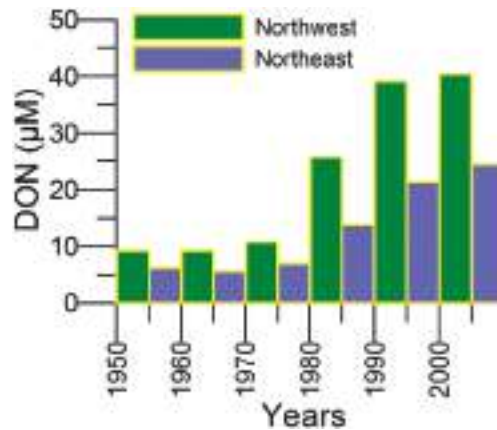


Figure 2.3.9. Decadal variability of surface dissolved organic nitrogen (DON) concentration along the western and eastern coastal waters of the NWS based on the averaging of available data from several stations at 5-year bins.

As inferred from the BOD₅ data (Fig. 2.1.3), the western Black Sea coastal waters seem to continue receiving considerable anthropogenic-based organic nitrogen. An estimate of 130 kt y^{-1} DON load inferred earlier from the Danube BOD₅ data implies $\sim 30 \mu\text{M}$ DON concentration supplied by the River Danube during the present decade that is comparable to $\sim 40 \mu\text{M}$ in the northwestern coastal waters (Fig. 2.3.9) due to continuous supply of high DON load from Dniepr, Dniestr and Bug Rivers as evident by a steady increase of its concentration since the 1970s. Similarly, the annual- and regional-average dissolved organic nitrogen concentration of $\sim 10 \mu\text{M}$ was observed along the Bulgarian coastal waters during 2001-2003 (Table 2.2.2). In addition, more than $10 \mu\text{M}$ difference between total nitrogen and N-NO_3^- concentrations in the Bosphorus exit station during the peak Danube discharge period (March-May) throughout 1996-2001 (Fig. 2.3.8d) provides a further support for organic nitrogen enrichment all along the western coastal waters.

Table 2.3.2. Annual and regional-mean concentrations of phosphorus and nitrogen species in Bulgarian coastal waters during 2001-2003. TP, TN and ON refer to total phosphorus, total nitrogen and organic nitrogen, respectively. All values are expressed in μM (after Velikova and Cociasu, 2004).

Years	P-PO4	TP	ON	TN
2001	0.27	0.45	10.29	12.40
2002	0.18	0.44	5.46	8.35
2003	0.23	0.42	10.98	14.87

On the basis of available data for 2000-2005, Fig. 2.3.10 summarizes the current status of the nitrogen enrichment along the periphery of the basin using different color codes for different ranges of annual-mean N-NO_3 concentration. According to this classification, the threshold for the highest N-NO_3 concentration in western coastal waters were set to $2.8 \mu\text{M}$ that in reality was far more higher and easily exceeded $10 \mu\text{M}$ as documented above. The entire southern coast is identified by the second highest N-NO_3 concentration that covers the range between $1.4 \mu\text{M}$ and $2.8 \mu\text{M}$. A small number of sites offshore of the Turkish/Georgian border show high levels of enrichment, which are likely to be the result of local discharges from mining industry. Northeastern and Crimean coastal waters are less eutrophic and characterized by N-NO_3 concentration less than $1.4 \mu\text{M}$. It is however important to note that, for southern and northeastern coastal waters, this classification scheme was based on rather limited measurements, such as twice a year (April and October) sampling during only 2004 and 2005 along the southern coast. Fig. 2.3.10 therefore should be interpreted with some caution. More frequent sampling strategy is highly desirable for more reliable coverage of the annual range of variations.

The surface productive zone of the interior basin has been nitrate limited even during the intense eutrophication phase (Oguz, 2005), and therefore the change of peak N-NO_3 concentration in the nitracline layer (see Chapter 1) is an important indicator for monitoring basin-scale response of eutrophication. The change in subsurface nitrate maximum concentration (Fig. 2.3.11) from $\sim 2\text{-}3 \mu\text{M}$ during the pristine state to $7\text{-}9 \mu\text{M}$ during the intense eutrophication period (i.e. the 1980s) confirms devastating effect of eutrophication for the entire sea that persisted up to 1992. Afterwards, the interior basin responded to the decline in the anthropogenic DIN load by reducing the peak subsurface nitrate concentration below $6 \mu\text{M}$ after the 1990s. The present value of this peak varies around $4.0\text{-}5.0 \mu\text{M}$ and thus implies a gradual shift of the system towards low nutrient conditions. As the nitrogen (both organic and inorganic) load supplied by the northwestern rivers was decreasing according to the Sulina measurements, primary production in the interior basin at present appears to consume nutrients which have already accumulated within during the intense eutrophication phase.

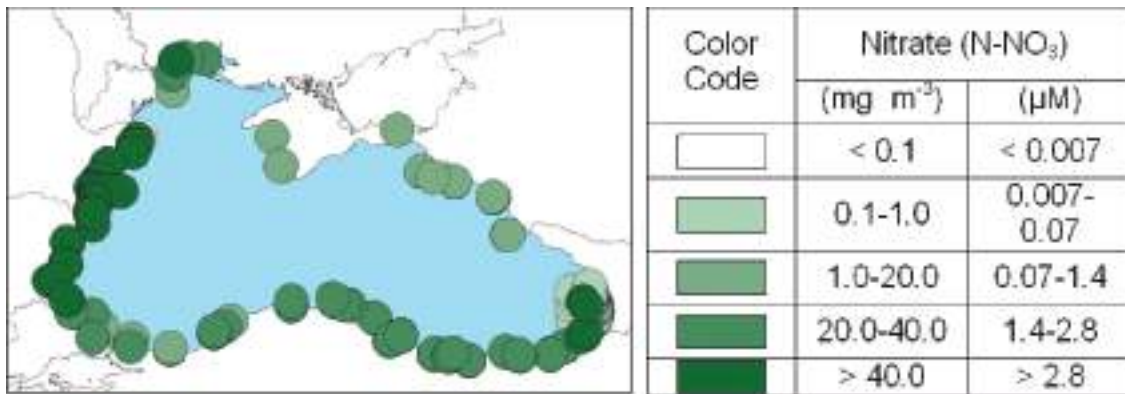


Figure 2.3.10. Ranges of mean nitrate (NO₃-N) concentrations during 2000-2005 in surface waters (0-10 m) along the coast of the Black Sea (modified from TDA Report, 2007).

Changes in phosphorus concentration: P-PO₄ concentration in the Sulina discharge point experienced an abrupt reduction from 7.5 μM at 1990 to 2.5 μM at 1993. It fluctuated afterwards between 2 μM and 3 μM, whereas it was changing between 1.0 and 2.0 μM at Reni (Fig. 2.2.12).

Along the northwestern coastal waters, it increased to around 3 μM in the mid-1970s and retained this level for a decade (Fig. 2.3.13a) reflecting upstream influence of the Danube in addition to local contributions from hot spots and discharges from Dniepr, Dniestr and Bug Rivers. This level was maintained until 2005 even though it locally acquired order of magnitude higher values during 2004-2005 (Fig. 2.3.13b). Long-term P-PO₄ data at Constanta monitoring station (Fig. 2.3.14) indicate two major peaks (~10-12) μM at 1975 and 1987 and minima (~2 μM) at 1981 and 1992 following its background values of <1 μM during the 1960s (the mean value = 0.26 μM). The decadal-mean P-PO₄ concentration was highest (~6.0 μM) during the 1980s and decreased to values less than 1.0 μM during 1990-1992 with a mean value of 0.49 μM for 1993-2005 (Table 2.3.1). The Constanta data is however biased due to the strong impact of the land-based source from the Navodari Factory and thus may not be representative for all the Romanian coastal waters. Further reduction to the mean value of ~0.2 μM is noted along the Bulgarian coast (Table 2.3.2) and northeastern coastal waters (Fig. 2.3.15).

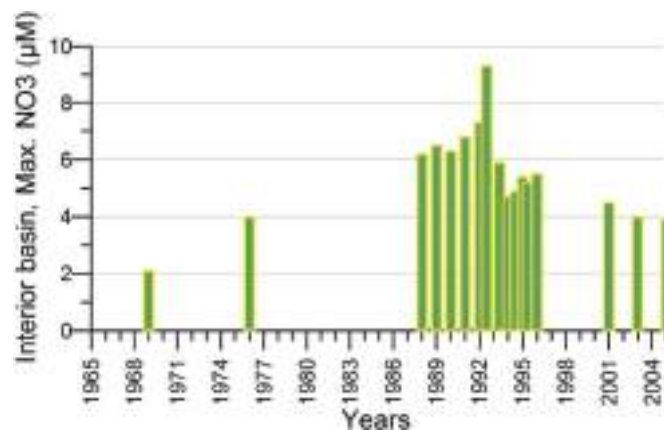


Fig. 2.3.11. Temporal variations of the subsurface peak nitrate concentration within the interior basin computed by averaging of all available data (after Kononov and Murray, 2001, modified with the recent data by T. Oguz).

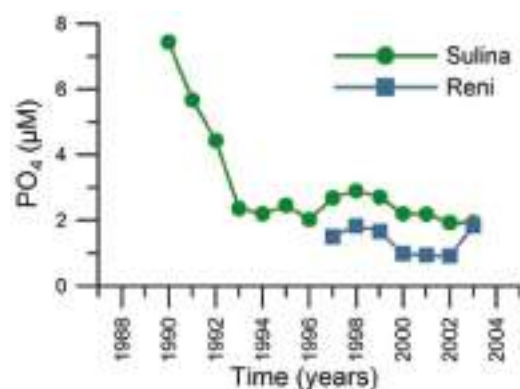


Fig. 2.3.12. Annual-mean P-PO₄ concentration measured at Sulina discharge point of the River Danube to the sea and at Reni located at the upstream end of the Sulina branch.

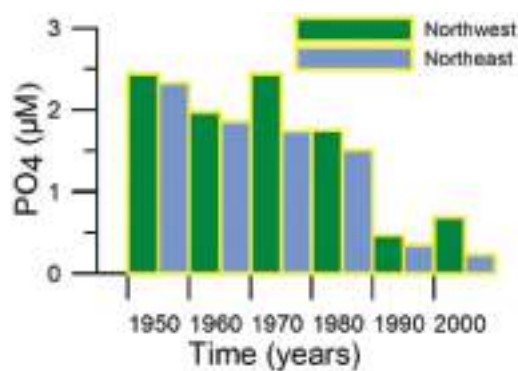


Fig. 2.3.13a. Decadal variability of surface phosphate (P-PO₄) concentration along the western and eastern coastal waters of the NWS based on the averaging of available data from several stations (redrawn from Loveya et al., 2006).

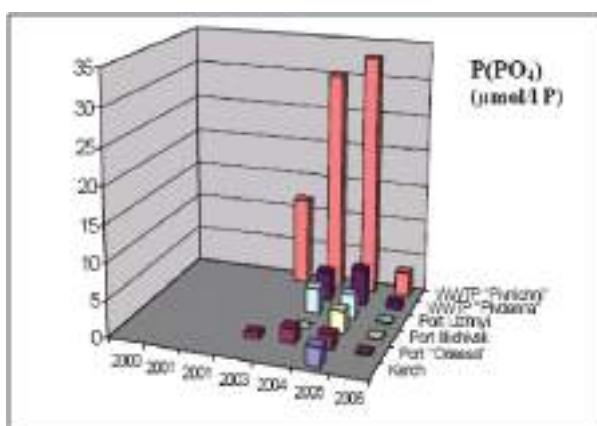


Fig. 2.3.13b. Annual-mean P-PO₄ concentration (µM) at various sites of northwestern Ukrainian coastal waters during 2000-2006 (After PMA AG and AC Activities and Reporting, 2007).

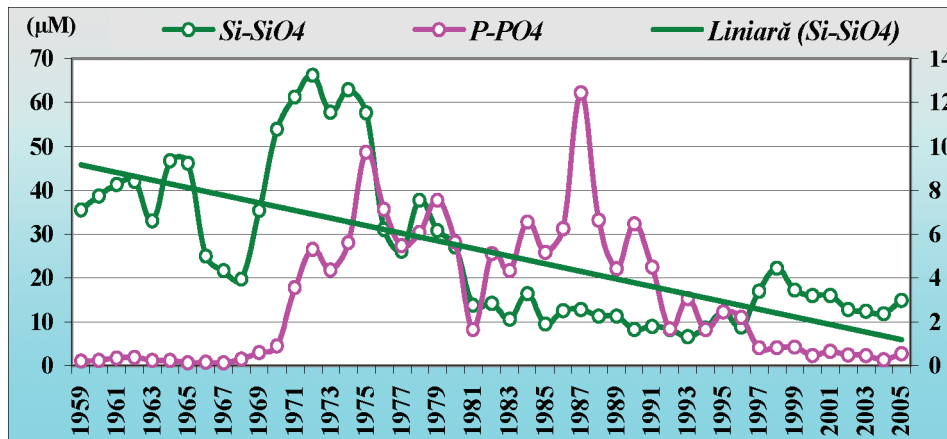


Fig. 2.3.14. Annual-mean surface concentrations of PO_4 (right hand side axis) and SiO_4 (left hand side axis) at Constanta station.

According to the colour-coded classification scheme (Fig. 2.3.16), the western coastal waters are classified as highest phosphate levels ($>0.39 \mu\text{M}$). A comparable level of elevated phosphate concentrations was assigned in Fig.2.3.16 for the Russian coast along the opposite side of the sea, but it disagrees with lower values shown in Fig. 2.3.15. The Turkish coast is characterized by relatively low P-PO_4 concentration albeit isolated sites of higher contamination exist presumably due to local industrial discharges.

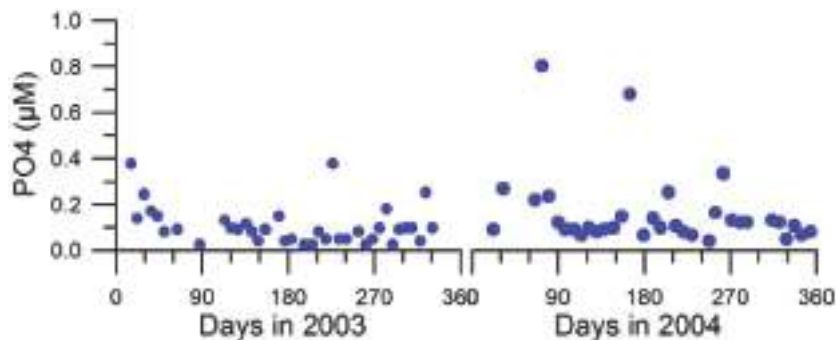


Fig. 2.3.15. Surface concentrations of P-PO_4 in near-shore waters of the Gelendzhik area during 2003-2004 (redrawn from Kucheruk, 2005).

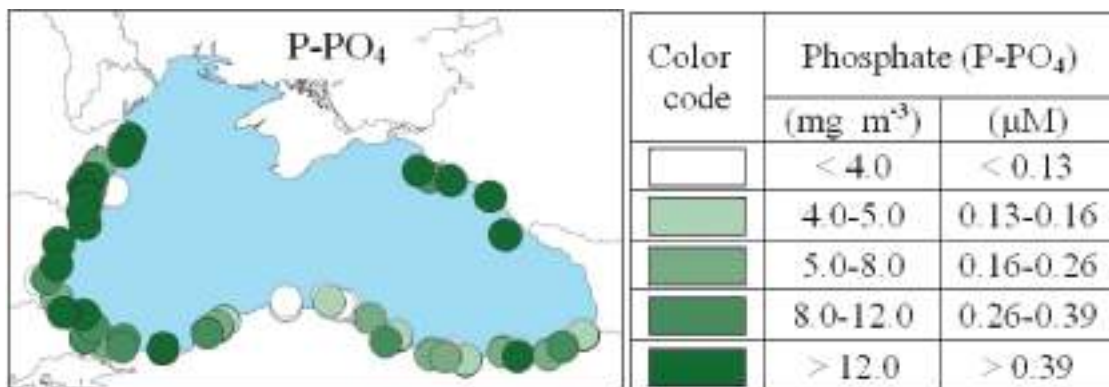


Fig. 2.3.16. Ranges of mean concentrations of phosphate (P-PO_4) during 2000-2005 in surface waters (0-10m) along the coast of the Black Sea (After TDA Report, 2007).

The annual-mean surface silicate concentration (SiO_4) measured at Constanta monitoring station prior to 1970s was quite high with an average value of $40 \mu\text{M}$ and reached at $65 \mu\text{M}$ at 1975 (Fig. 2.3.14). Following the construction of Iron Gate I during the early-1970s, it started reducing to around $10\text{--}20 \mu\text{M}$ within the second half of 1970s due to the retention mechanism in the upper reaches of the River Danube. The declining trend since the 1980s was disrupted by an abrupt increase from $10 \mu\text{M}$ in 1996 to $22 \mu\text{M}$ in 1998 and then declining trend continued up to $11.0 \mu\text{M}$ in 2004 except a minor increase to $13.7 \mu\text{M}$ in 2005.

Changes in nutrient ratios: Owing to relatively high DIN emissions, the River Danube has always been a phosphorus limited system and supplied DIN at much higher rate with respect to P-PO_4 . The P-limitation is evident at the Sulina discharge point where N/P ratio remained above its Redfield ratio even though both N-NO_3 and P-PO_4 concentrations tended to decrease since 1990 and P-limitation becomes weaker than the previous decades (Fig. 2.3.17a). The increasing trend during 1990-1993 reflects much faster decline of P-PO_4 concentration (Fig. 2.3.12), whereas the gradual decline during 1993-1999 and increase afterwards are largely controlled by the variations of N-NO_3 concentration (Fig. 2.3.2) as P-PO_4 concentrations remained rather steady after 1993. The data at Constanta monitoring station also support the P-limitation at an increasing rate after 1997 as compared to the N-limitation before (Fig. 2.3.18a). On the contrary, the amalgamated data (Fig. 2.3.17a) indicate preferentially N-limitation for the Romanian shelf waters. The data shown in Table 2.3.3 also support N-limitation for the 1980s and 1990s but not for the 2000-2003 period for which the N/P ratio value of 32 contradicts with a value of ~ 12 suggested by the amalgamated data. The difference seems to arise due to the bias of the data given in Table 2.2.3 by the Constanta N/P data (Fig. 2.3.18a) that showed P-limitation after 1999.

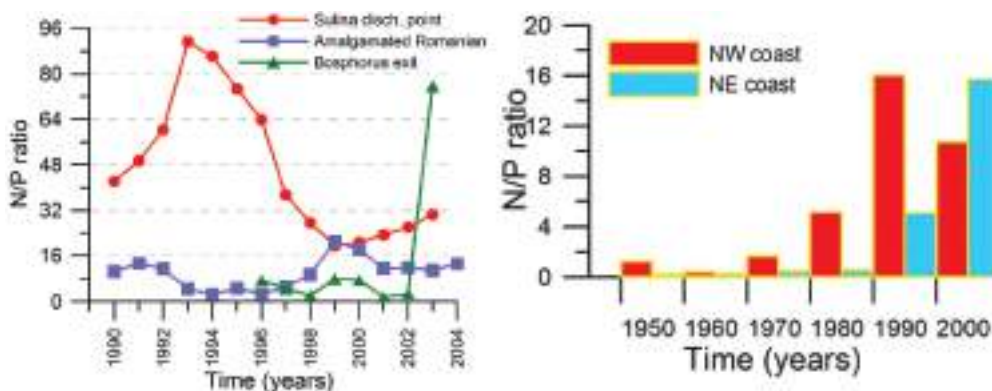


Fig. 2.3.17. Long-term changes of nutrient concentration ratios at (a) Sulina discharge point, Romanian shelf and Bosphorus exit region, and (b) Ukrainian coastal waters.

The N-limitation also applies for both the northwestern and northeastern Ukrainian coastal waters (Fig. 2.3.17b and Table 2.3.3) as well as the Bosphorus exit section (Fig. 2.3.17a), except for 2003 that was based on an average of only two measurements; one below the Redfield ratio and the other above and therefore the 2003 value of N/P ratio is not statistically significant. It is hard to identify precisely the type of nutrient limitation for Bulgarian waters because of the absence of systematic and sufficiently long time

series for all major nutrients. On the basis of available data summarized in Table 2.3.3, Bulgarian coastal waters appear to be P-limited during winter months due to their excessive nitrogen enrichment (Fig. 2.3.8b,c, 2.3.18b), while they attained either N-limitation or Redfield value the rest of the year (Fig. 2.3.18b). Bulgarian waters therefore switch seasonally between P- and N-limitation (Velikova and Cociasu, 2004). The seasonal alternation does not show a regular seasonal pattern, but varies interannually. On the basis of all these evidences, it appears that inner shelf along the western coast is currently P-limited (Fig. 2.3.18a) whereas the outer shelf is either weakly N- or P-limited (Fig. 2.3.17), and the interior basin is predominantly N-limited (Fig. 2.3.19a).

The long-term variation of Si/N ratio at Constanta (Fig. 2.3.18a) since 1980 falls into three phases. The first phase (1980-1988) was characterized by the monthly Si/N values varying between 0.5-1.5. In the second phase (1989-1997), Si/N values reduced to the range 0.4-1.2. The third phase (1998-2005) resembled the first phase with the values changing between 0.6 and 2.0. In general, Si/N ratio remained below 2.0 and favored Si limitation in the Constanta region. Because of the lack of comprehensive data coverage, it is not clear how well the Si limitation applies to other regions along the western coast. Because the deep interior basin is more severely limited by nitrogen, Si/N values are much higher than its threshold for Si limitation (Fig. 2.3.19b).

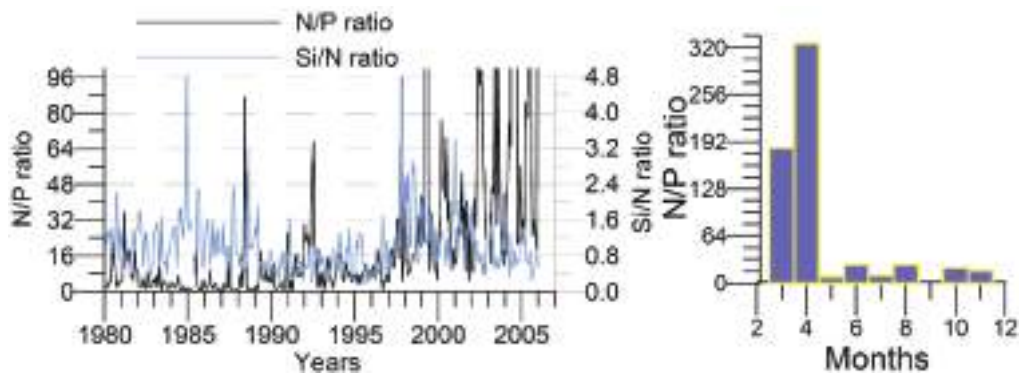


Fig. 2.3.18. Long-term changes of nutrient concentration ratios at (a) Constanta monitoring station, and (b) monthly changes in Bulgarian coastal waters during 2001-2003.

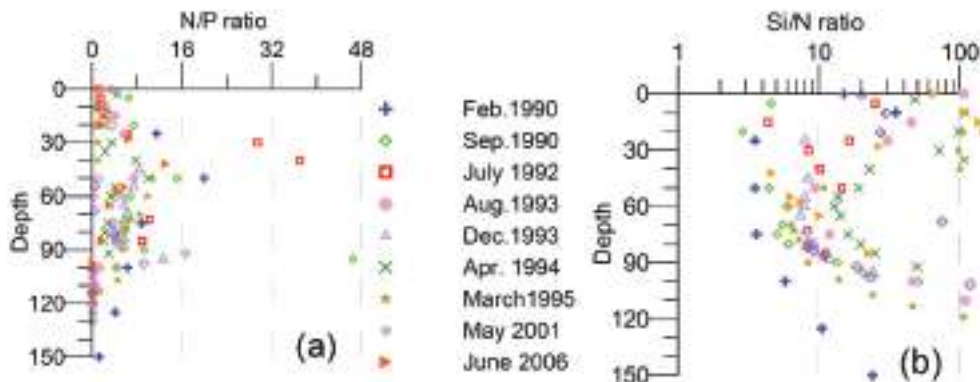


Fig. 2.3.19. Vertical profiles of N/P and Si/N ratios at different locations of the interior basin during different months and years.

Atmospheric input of nutrients: In addition to nutrient inputs from rivers, coastal sources and sediments, atmospheric wet and dry depositions may likely constitute an important component of the long-term nutrient enrichment of the Black Sea that however remains to be poorly studied. According to the State of Environment Report (2000), the atmospheric nutrient input onto the Black Sea surface was about 400 kt y⁻¹, and therefore higher than the present level of riverine supply.

Within the framework of BSERP/GEF monitoring program, atmospheric precipitation was sampled at a remote site Katsively near Sevastopol-Crimea during 2004-2005 (Chaykina et al., 2005). They measured the total DIN wet deposition as 550 mg m⁻² during March-December 2004 and 910 mg m⁻² during 2005 that amounts to atmospheric fluxes of 240 kt y⁻¹ and 400 kt y⁻¹, respectively, if extrapolated over the surface area of the Black Sea. Similar measurement at Zmeiny Island at 40 km offshore from Odessa during 2003-2007 indicated approximately 240 ktons y⁻¹ nitrogen and 16 ktons y⁻¹ of phosphorus fluxes from the atmosphere (Medinets and Medinets, 2008). Atmospheric deposition of nutrients is therefore comparable to the current loads from the River Danube and therefore appears to constitute an important element of the overall nitrogen budget of the sea.

Table 2.3.3. Multi-annual mean nutrient ratios in Romanian surface coastal waters, the Bay of Varna and Bulgarian coastal waters (BW) as an average of all measurements within the 50 km zone (after Velikova and Cociasu, 2004)

	Romania				Bulgaria		Ukraine	
Period	1960-1970	1980-1991	1992-1999	2001-2005	2001-03		2000-05	
					BW	Varna Bay	NW coast	NE Coast
Si / P	142.9	2.6	11.2	30.6	34.4	88.4	-	-
Si / N	-	0.9	0.9	1.2	9.0	7.0	-	-
N / P	-	3.1	10.2	32.0	55.2	31.0	10.7	15.7

2.4. Surface chlorophyll concentration

Few long-term data exist on *in situ* chlorophyll-a measurements in the Black Sea and therefore remote sensing ocean color data are used to infer its seasonal-to-interannual variations, even though chlorophyll signal is likely deteriorated by rich particulate material and dissolved organic substance along the western coastal waters. The average chlorophyll concentrations are computed from 9 km gridded, 8-daily SeaWiFS products for the northwestern (Ukrainian) coastal waters (the region 1), the Romanian and Bulgarian coastal waters (the regions 2 and 3), the Bosphorus-Black Sea junction region (the region 4), and the western interior basin (the region 5) (Fig. 2.4.1). The Danube delta region between the regions 1 and 2 is not included into the analysis because of its unrealistically high chlorophyll concentrations (≥ 20 mg m⁻³), most of which possibly reflect contributions from yellow substance and particulate matter discharged by the Danube. The analysis of the data is depicted in Fig. 2.4.2.



Fig. 2.4.1. The regions of the western basin used for the analysis of SeaWiFS chlorophyll concentration variations.

An immediate feature noted in Fig. 2.4.2 is approximately four-fold decrease in chlorophyll concentration from the northwestern shelf (region 1) to the Bosphorus-Black Sea junction zone (region 4). In the region 1, highest concentrations extend from early spring to late autumn in the range of $6\text{--}8\text{ mg m}^{-3}$. Lowest concentrations are observed in winter months and often exceed those in further south. The region 2 possesses three peaks; the first one comprises the late winter-early spring (February-March) and arises due to typical spring bloom dynamics. This is the weakest peak ($\sim 3\text{ mg m}^{-3}$). It is followed by a stronger late-spring peak (in May-June with $\sim 5 \pm 1\text{ mg m}^{-3}$) that evidently coincides with the period of high Danube discharge. For some years (i.e. 2006), these two peaks are combined to form one extended peak. The third one occurs in autumn ($\sim 4 \pm 1\text{ mg m}^{-3}$) and is often separated from the former one by a period of relatively low summer concentrations of $\sim 2\text{ mg m}^{-3}$. The measurements in Constanta monitoring station during 2001-2005 (Fig. 2.4.3) generally support these features with some differences such as a strong early autumn (September) bloom in 2002, a late winter (February-March) bloom in 2003, and a late autumn bloom (November) in 2004. The Bulgarian and the Bosphorus regions also possess three-peaks between 2 mg m^{-3} and 4 mg m^{-3} with considerable year-to-year changes whereas the lowest concentrations in summer months are about 0.5 mg m^{-3} .

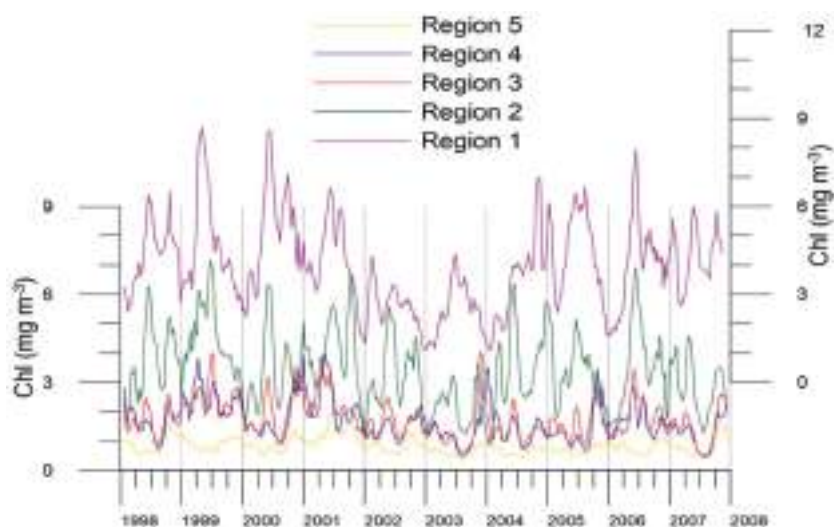


Fig. 2.4.2. Average surface chlorophyll concentration for five regions of the western Black Sea basin obtained from 8-daily 9 km resolution SeaWiFS ocean colour products after the original data is smoothed by 5 point moving average. The axis on the right hand side applies for the region 1, and the axis on the left hand side for all other regions.

The long-term monthly measurements at the Bosphorus exit section during 1996-2001 (Fig. 2.4.4) generally support the ocean colour data both in terms of timing and magnitude. The most pronounced features are the late winter and autumn peaks that are connected with low summer chlorophyll concentrations. The measurements in Bourgas Bay during 1987-1997 (Fig. 2.4.4) that comprises the period before the availability of satellite ocean color data suggest somewhat different seasonal chlorophyll concentration structure; the late winter-spring peak emerges the most dominant feature at either moderate ($\sim 4\text{--}5 \text{ mg m}^{-3}$) or high ($>8 \text{ mg m}^{-3}$) concentrations and is followed by a secondary peak during summer months. No appreciable chlorophyll peak however existed during autumn months. This annual structure persisted during 1987-1995 period, after which the annual structure seems to shift to the structure described for the region 4 with higher intensity of autumn concentrations.

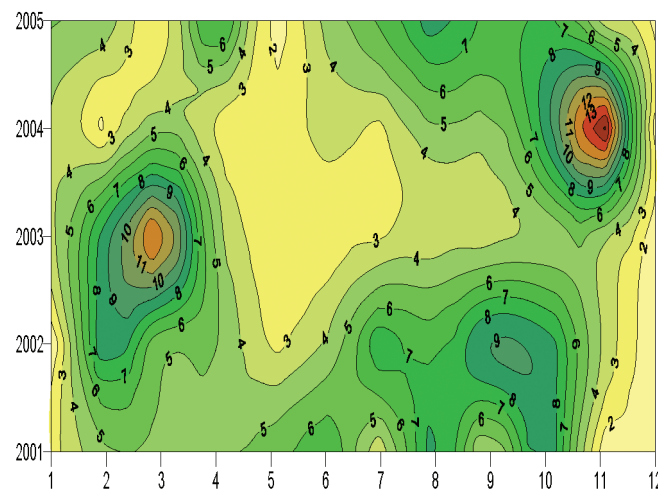


Fig. 2.4.3. Monthly surface chlorophyll concentration variations (mg m^{-3}) at Constanta station during 2001-2005.

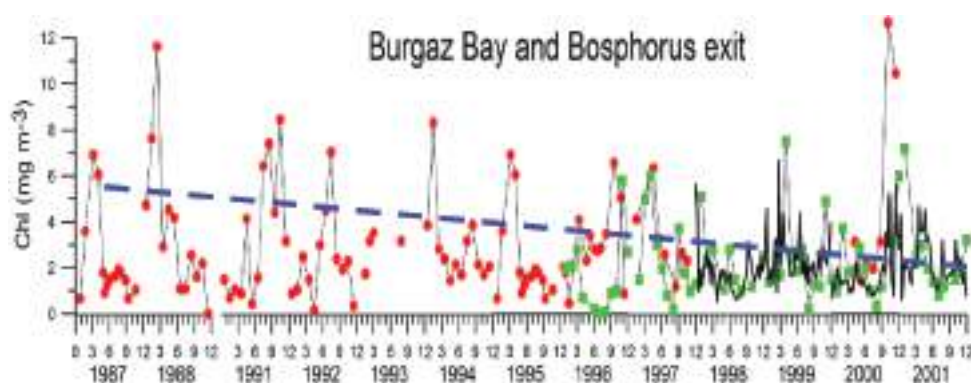


Fig. 2.4.4. Monthly surface chlorophyll concentration during 1987-2001 measured in the Burgaz Bay (red dots) and the Bosphorus northern exit (green squares), and the SeaWiFS ocean color data for the region 4 (bold lines). The dashed line shows decreasing trend of peak Chl concentration since the 1980s. The field data are provided by Hibaum (2005); Moncheva (2005) and Okus (2005) and satellite data by daily-8, 9 km resolution SeaWiFS ocean colour product.

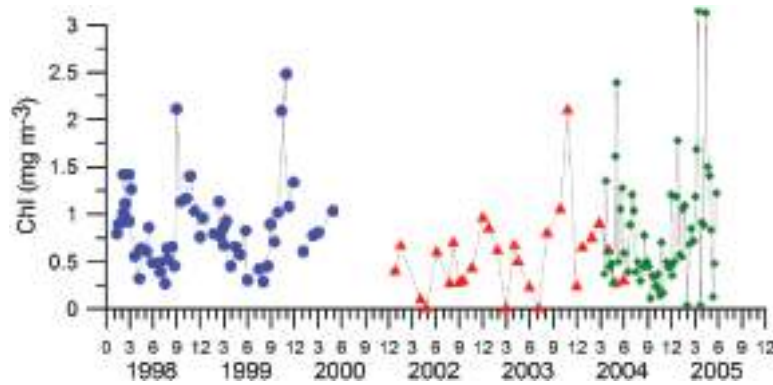


Fig. 2.4.5. Surface chlorophyll-a concentration measured along the Crimean topographic slope zone (dots; after Churiliova et al., 2005), near the Cape Sinop at the central part of the southern coast (triangles; after Feyzioglu, 2006; Bat et al., 2007), and Surmene Bay near the southeastern corner of the sea (squares; after Feyzioglu, 2006).

On the other hand, measurements at two coastal stations along the southern coast and along the topographic slope zone to the south of Crimea (Fig. 2.4.5) show peak concentrations in the range of 1.0-2.0 mg m^{-3} during February-March and November-December that are comparable to minimum concentrations measured at Bourgas and Bosphorus stations. The lowest concentrations which are generally observed during the summer were typically less than 0.5 mg m^{-3} .

The surface chlorophyll concentration variations within the central part of the western basin (region 5) vary within 0.5 - 2.0 mg m^{-3} (Fig. 2.4.2). The most notable feature that repeats almost every year is a linear decreasing trend from a peak in November (1.5 - 2.0 mg m^{-3}) to a minimum ($\sim 0.5 \text{ mg m}^{-3}$) in July followed by a sharp increase from August to November again. This annual structure differs from the western coastal waters (the regions 1-to-4) by the absence of additional spring peak due to the Danube nutrient supply. The only exception is the anomalously high concentrations in summer 2001 as also supported by direct measurements (Oguz and Ediger, 2007).

The long-term data using all available direct measurements within the interior basin ($> 1500 \text{ m}$) for the summer-autumn period (May-November) reveal surface chlorophyll values less than 0.6 mg m^{-3} during 1978-1987 followed by the phase of high concentrations up to about 2.0 mg m^{-3} during 1989-1992 during the anchovy collapse and *Mnemiopsis* population outburst period (i.e. the changes in top-down control) (Fig. 2.4.6). There is no sufficient data coverage to assess chlorophyll variations during the mid-1990s even though values up to 1.0 mg m^{-3} were measured during 1998-1999. The SeaWiFS summer (May-September) data for more recent period (averaged over the rectangular region defined by 31-41°E and 41.5-44°N) reveal two distinct phases: high summer chlorophyll concentrations ($\sim 1.4 \text{ mg m}^{-3}$) during 1998-2001 and the subsequent moderate chlorophyll concentrations ($\sim 0.8 \text{ mg m}^{-3}$) afterwards.

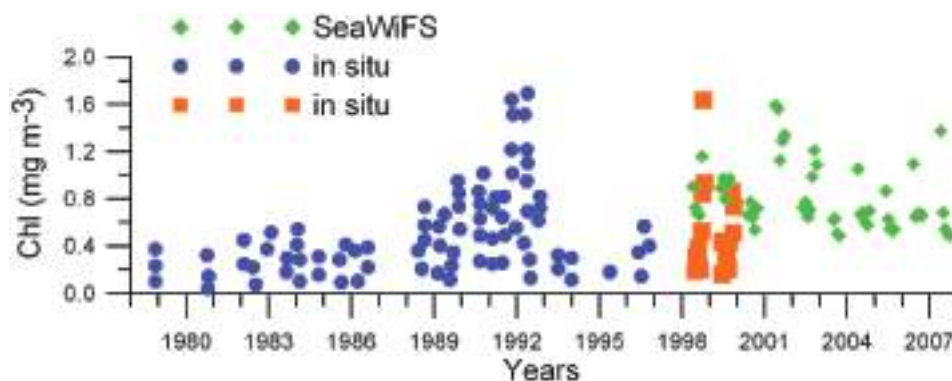


Fig. 2.4.6. Long-term changes of surface chl-a concentrations in the interior Black Sea (depth >1500m) for May-November period, 1978-1999. Each data point represents a single measurement taken from Yunev et al. (2002) (blue symbols) and Churilova et al (2004) (red symbols). This data set is complemented by the monthly-average 9 km gridded May to September-mean SeaWiFS data for the interior basin defined by 31-41°E longitudes and 41.5-44°N latitudes (green symbols).

The annual-mean chlorophyll concentrations deduced from the satellite ocean color data do not indicate appreciable interannual variability for the regions 3, 4 and 5 (Fig. 2.4.7), but attained relatively low values during 2003 in regions 1 and 2 due possibly to the anomalous cold winter (Chapter 1). The decrease in annual-mean concentrations from north-to-south and from 1998 to 2007 is also noted in Fig. 2.4.7.

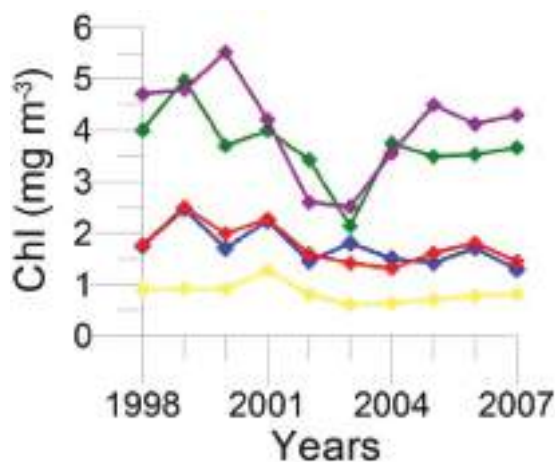


Fig. 2.4.7. Annual-mean surface chlorophyll concentration for five regions of the western Black Sea basin obtained from 8-daily 9 km resolution SeaWiFS ocean colour product. The colour code for the regions are as shown in Fig.2.4.2.

The surface chlorophyll maps presented in Fig. 2.4.8 provide the monthly average distributions for 2001, 2003 and 2005 that were chosen to represent examples for highly, weakly, and moderately productive years, respectively. Throughout these years, the northwestern part of the Black Sea possess highest chlorophyll concentrations (>10 mg m⁻³) especially in summer months. This over-productive zone weakens gradually southward along the Bulgarian and Turkish coastal waters that are characterized by the values around 2-4 mg m⁻³. The Danube effect is most often visible up to the Bosphorus coastal region, and its signature gradually weakens further eastward along the Anatolian

coast. Some localized moderately productive zones are occasionally observed along the south-eastern and eastern coasts. The northern coastal zone was identified by lowest concentrations. The Rim Current system forms a barrier between coastal and interior waters during winter and spring periods when it is relatively strong, but more efficiently distributes chlorophyll between coastal and interior waters during summer and autumn when it is weakly stable and prone to mesoscale instabilities.

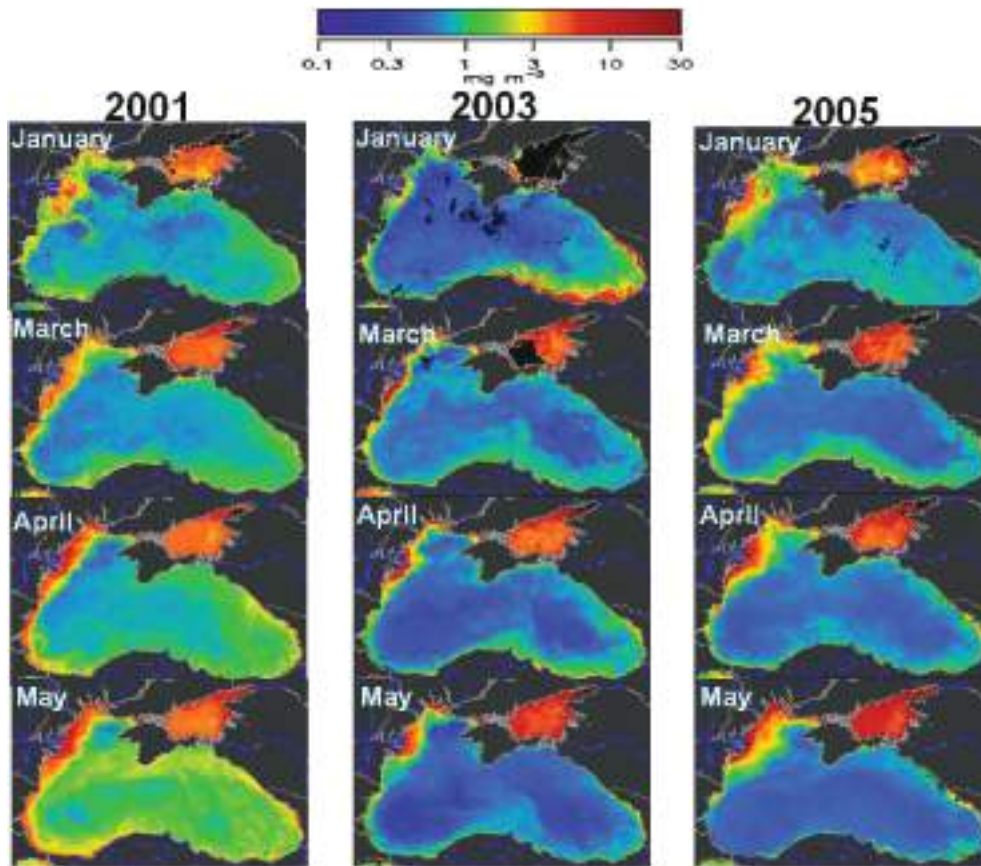


Fig. 2.4.8. Monthly composites of surface chlorophyll concentration derived from daily-2km resolution SeaWiFS (NASA) ocean colour products for 2001, 2003 and 2005 (*EC-Joint Research Centre, Global Environment Monitoring Unit Ocean Colour Archive, <http://oceancolour.jrc.ec.europa.eu/>*).

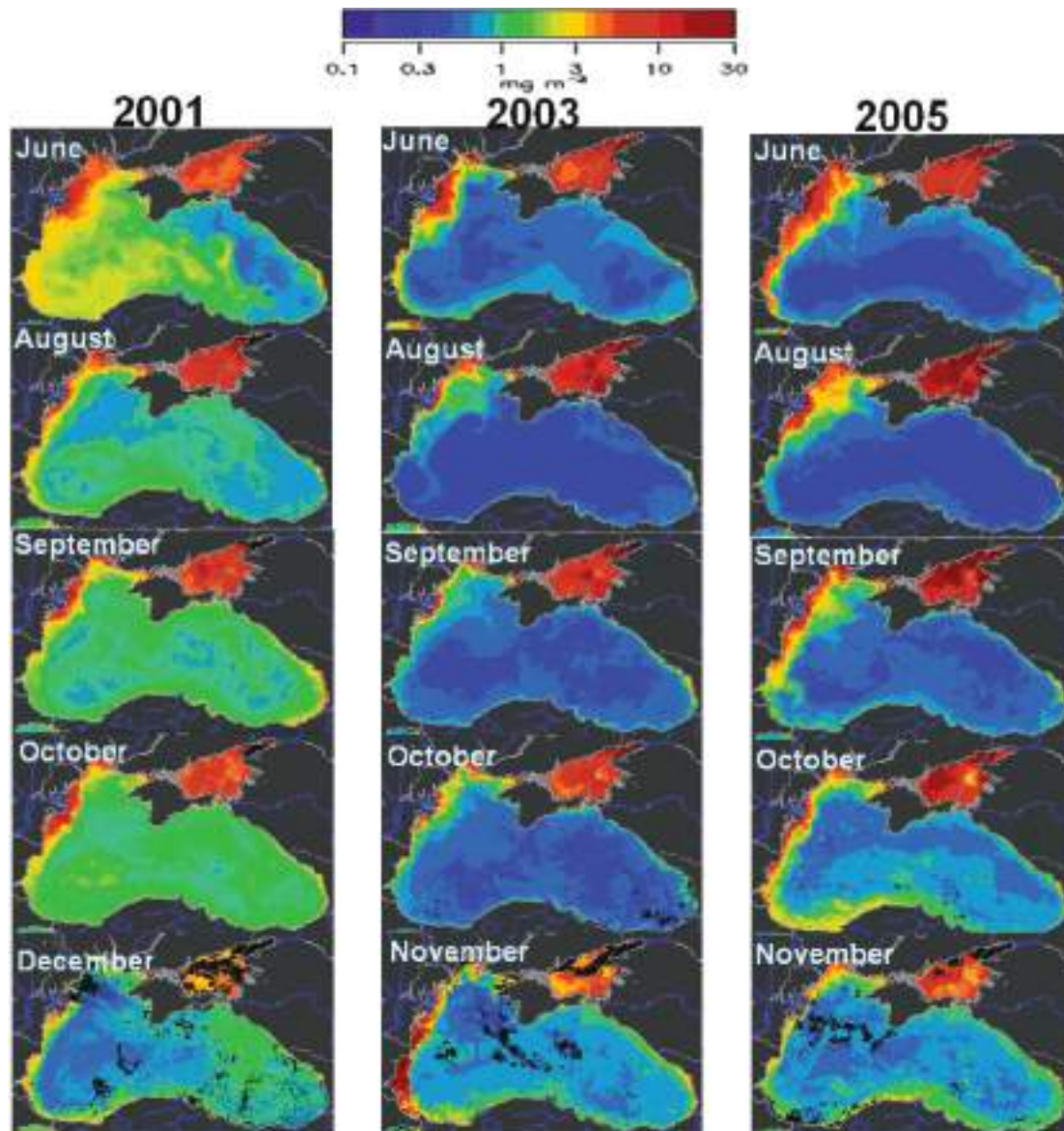


Fig. 2.4.8. (continued) Monthly composites of surface chlorophyll concentration derived from daily -2km resolution SeaWiFS (NASA) ocean colour products for 2001, 2003 and 2005 (EC-Joint Research Centre, Global Environment Monitoring Unit Ocean Colour Archive, <http://oceancolour.jrc.ec.europa.eu/>).

2.5. Surface and near-bottom oxygen concentrations

Northwestern shelf: Following the first sight of hypoxia (oxygen concentrations below 2 mg/l, or oxygen concentration less than 30% saturation value) in the coastal zone between Dnestr and Danube delta in August 1973, zones of seasonally low oxygen have been detected in the bottom waters of the northwestern shelf, most commonly within 30-40 mile zone along its north and west coasts; i.e. in the discharge regions of the northwestern rivers. Hypoxia development typically started in June-July, stretched towards offshore up to the depths of 20-30 m and attained its maximum coverage in August. In October, it largely retreated except in close vicinity of the Danube discharge region and near Odessa. According to the long-term observations (Loyeva et al., 2006),

the largest hypoxia coverage (about one-third of the NWS area or more) was observed in the years 1978, 1983, 1989, 1990, 1999 and 2000, among which the 1983 event covered 52% of the NWS total area (Fig. 2.5.1). A similar analysis by Zaitsev (1992) reported almost twice larger spatial coverage for the 1970s and 1980s. It was reported to decrease in Romanian coastal waters and no hypoxia case was observed in Bulgarian waters in 2001-2005, where lower oxygen concentrations tended to occur more predominantly in the northern sector (Parr et al., 2005).

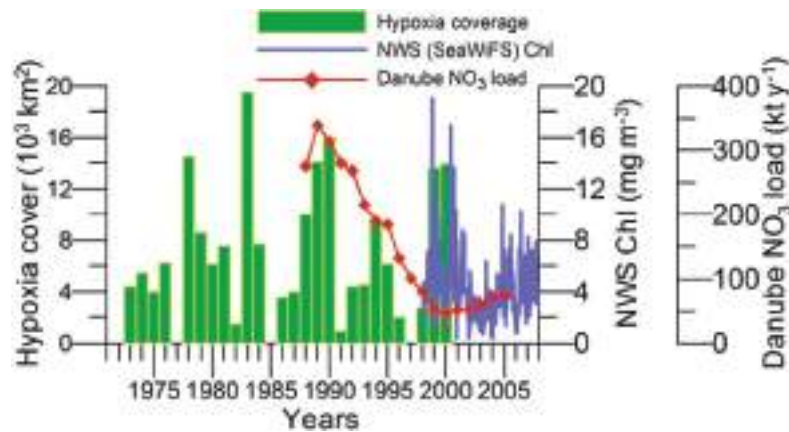


Fig. 2.5.1. Long-term variations of spatial coverage of hypoxia in the northwestern shelf (redrawn from Loyeva et al., 2006), average chlorophyll concentration (mg m^{-3}) for the northern part of the NWS provided by daily-8 km SeaWiFS ocean color sensor and the River Danube N-NO_3 discharge.

Berlinskii (1989; 2003) proposed a linear empirical relationship between the rate and timing of river discharge and the scale of hypoxic conditions. In years with high river discharge and hence high nutrient input and organic matter production, the oxygen concentration in bottom layers becomes $\sim 20\%$ lower in comparison with years of low river discharge. Frequency of hypoxic conditions in front of the Danube river mouth was found to decrease when roughly half of the fresh water discharge took place before the first half of April whereas the maximum river input in April-May favoured oxygen depletion later in June-October. Loyeva et al. (2006) suggested a close correlation ($r=0,86$) between spatial coverage of brackish water with salinity less than 17.5 psu and the area of near bottom hypoxia. The data shown in Fig. 2.5.1, however, suggest no clear correlation of the extent of hypoxia with neither Danube fresh water discharge nor NO_3 load, but it seems to correlate with the SeaWiFS chlorophyll concentration during 1998-2000 for the northern part of the NWS. In fact, hypoxia development depends not only the intensity of eutrophication but also circulation, stratification and meteorological (wind, heat flux, etc.) conditions and therefore may be subject to large year-to-year variations and a simple correlation to environmental factors may not always hold. Its sensitivity to different number of hydro-meteorological and biogeochemical factors complicates estimation of its spatial coverage by proxy data and therefore limits the use of such indirect approach as a reliable indicator of eutrophication. Fig. 2.5.1 does not indeed show stable tendency of increase or decrease in hypoxia coverage in the northwestern Black Sea.

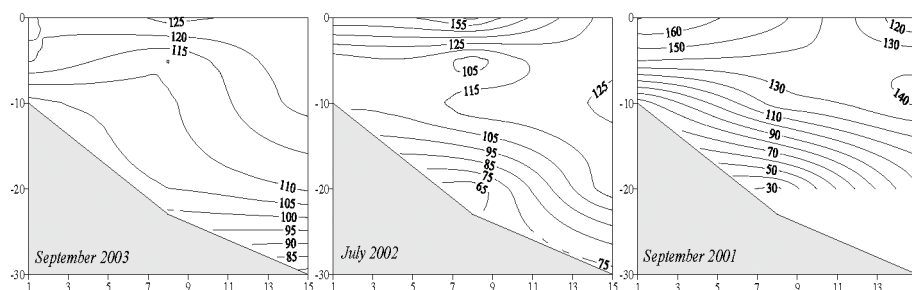


Fig. 2.5.2. Vertical distribution of oxygen saturation ratio along the Sulina transect during September 2001 and 2003, July 2002 (after Velikova and Cociasu, 2004).

Vertical distribution of oxygen saturation ratio along the Sulina transect exhibited oxygen depletion in summers 2001 and 2002 following relatively warm winters whereas bottom waters in the summer 2003 after the cold winter did not show any significant depletion (Fig. 2.5.2).

Long-term surface oxygen measurements in Constanta (Fig. 2.5.3) suggest persistently low concentrations (between 200-250 μM) from the late-May to the end of September during the 1980s and the 1990s. The recovery in oxygen status in surface waters is evident after 2000 which are further supported by benthic data (e.g. mussel bed and community age class distributions) in the following chapters.

Interior basin: Modification in sub-surface oxygen structure of the interior basin in the 1980s due to considerable increase in organic matter production has been monitored by long-term changes in the thickness of the suboxic layer (Orlova et al., 1999; Konovalov et al., 2001). This layer is defined in Fig. 2.5.4 by the sigma-t surfaces of 20 μM oxygen and 5 μM hydrogen sulphide concentrations and has been constructed using all available data from the interior basin since the 1960s. It is located at depths away from the direct impact of atmospheric ventilation and its temporal changes mainly reflect the changes due to biochemical processes. Its thickness had a relatively stable structure with a mean value of 20 m or equivalently $\Delta\sigma_t \sim 0.4 \text{ kg m}^{-3}$ up to the late 1970s. It was then broadened to $\sim 40 \text{ m}$ ($\Delta\sigma_t \geq 0.55 \text{ kg m}^{-3}$) during the 1980s and preserved this structure until the early-1990s due to higher rate of oxygen consumption associated with intensified biological production. This period was followed by a decline of the thickness to $\Delta\sigma_t \sim 0.35 \text{ kg m}^{-3}$ during the mid-1990s after which the data from 2001 and 2003 indicated further broadening due to intense phytoplankton bloom events.

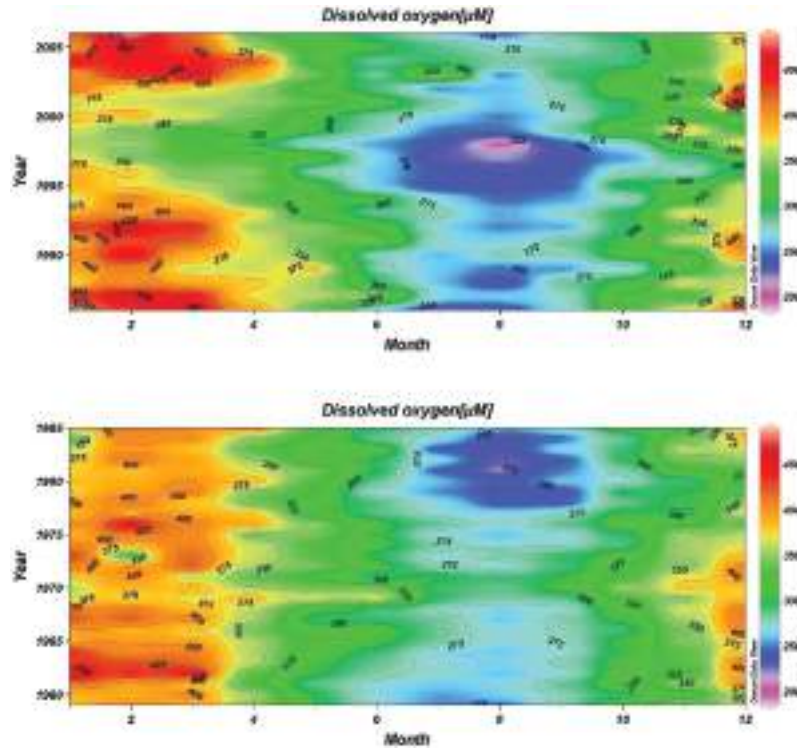


Fig. 2.5.3. Temporal variations of surface dissolved oxygen concentration in Constanta since the 1960s.

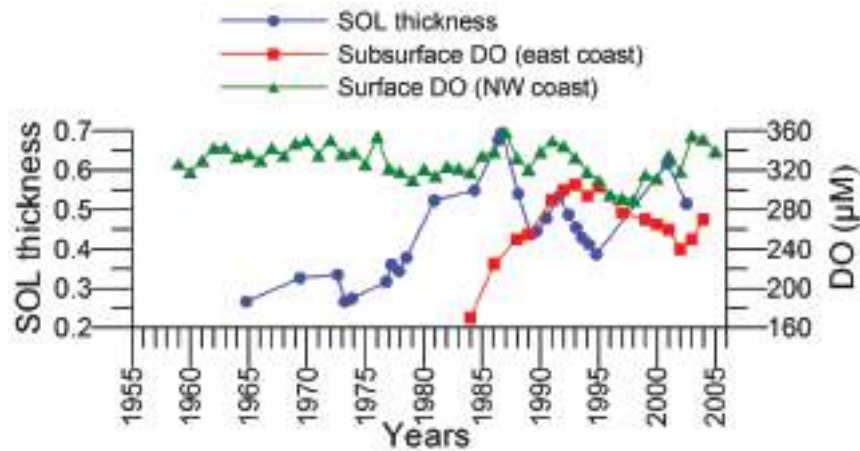


Fig. 2.5.4. SOL thickness measured as the difference between the sigma-t surfaces of 20 μM dissolved oxygen and 5 μM hydrogen sulphide concentrations deduced by all available data from the deep interior basin (after Konovalov et al., 2005), average dissolved oxygen concentration within the layer of $\sigma_t \sim 14.45$ and 14.6 kg m^{-3} surfaces in the region off the eastern coast (after Yakushev et al., 2005), and annual-mean surface dissolved oxygen concentration in northwestern coastal waters.

Fig. 2.5.4 further includes the long-term oxygen concentration variation of the layer between $\sigma_t \sim 14.45$ and 14.6 kg m^{-3} surfaces (roughly the base of euphotic zone) along the eastern coast formed by annual averages of all deep stations irrespective of their seasons and locations. In consistent with the period of maximum SOL thickness, oxygen concentration of this layer attained low values below 200 μM and then was followed by an increasing trend up to $\sim 300 \mu\text{M}$ during the 1990s at the time of

narrower SOL thickness. The mid-1990s represented best conditions of the subsurface oxygen concentration, after which it started to deteriorate again during the period of SOL broadening. The interior basin and the eastern part of the sea presently reflect an intermediate state of the subsurface oxygen structure between worst conditions of the 1980s and the best conditions of the mid-1990s.

The surface DO concentrations in the northwestern coastal waters (Fig. 2.5.4), mostly in the vicinity of Constanta, respond less markedly to adverse effects of eutrophication because of atmospheric ventilation of surface layers. Nevertheless, slight changes are observed between relatively higher concentrations during cold periods (e.g. 1985-1993, after 2003, and prior to 1975) and warm periods (1975-1985 and 1994-2002). Instead it responds more strongly to climatic effects as indicated by its elevated values during short term severe winter episodes of 1985-1987, 1992-1993, 2003-2004. Fig. 2.5.4 further indicates that subsurface concentration within the eastern basin and surface concentration in the northwestern coastal waters tend to have opposite interannual variations after 1998 due to different environmental factors governing oxygen concentration. The eastern coastal waters appear to be controlled primarily by physical mechanisms that are regulated directly by climatic cooling-warming cycles, whereas northwestern waters by the changes in Danube organic and inorganic nitrogen loading, in addition to the direct climatic forcing.

2.6. Conclusions and key assessments

Nitrogen and phosphorus emissions continue to reduce, but their 2000-2005 average values are still 1.5 times higher than their pristine levels at 1955-1965. P-PO₄ flux supplied by the River Danube declined considerably at 1990-1993, after which it maintained a steady level between 10-20 kt y⁻¹ at the Sulina discharge point to the sea. The River Danube DIN flux at the Sulina discharge point decreased gradually during the 1990s to about 100 kt y⁻¹ at 2000, but possessed a weak increasing trend to 250 kt y⁻¹ during 2005. The DON flux supplied by the northwestern rivers (Danube, Dniepr, Dniestr, and Bug) is currently even higher than the DIN load. Consequently, an increasing trend is observed in DIN concentration along the Ukrainian, Romanian and Bulgarian coastal waters in the present decade. The western coastal waters are presently subject to both dissolved inorganic and organic nitrogen enrichment, and they do not present an apparent status of improvement in terms of nitrogen during the last 10 years. DIN and PO₄ concentration levels along other coasts (southern, northeastern and northern) are, on the other hand, about 3-4 folds lower than the western coast. In spite of ongoing nitrogen enrichment, the western coastal waters tend to be weakly nitrogen limited as for the case of the interior basin, except the predominantly P-limited shallow inner shelf zone. The data suggest a weak Si limitation in western coastal waters as well. This is partially due to decreasing SiO₄ concentration and partially due to increasing DIN concentration. Limited measurements at Sevastopol-Crimea quantitatively supported the importance of atmospheric deposition of nitrogen species.

Monitoring winter nutrient concentrations as an indicator of eutrophication set by EEA does not suit well for the Black Sea western coastal waters, because they possess peaks

at April-May at the time of highest Danube discharge. More frequent (e.g. monthly) monitoring at less number of stations around the basin can be considered as an option of monitoring. Atmospheric deposition need to be monitored regularly around the basin in order to arrive at a more reliable nutrient budget of the sea. Moreover, nitrogen losses due to sedimentation and denitrification along the western coastal waters remain to be quantified in order to assess the fate of nitrogen enrichment of the system.

Surface chlorophyll concentration varies five-folds from its highest annual-mean values ($\sim 5 \text{ mg m}^{-3}$) in the northwestern region to lowest values ($\sim 1 \text{ mg m}^{-3}$) within the interior basin. The annual structure in the northwestern shelf is characterized by relatively high concentrations from early spring to late autumn. Lowest concentrations are observed in winter months. Romanian, Bulgarian and southwestern coastal waters generally reveal three peaks over the year; the first one comprises a weak late winter-early spring (February-March) algae bloom period in relation to typical spring bloom dynamics. This is the weakest one and does not exist for some years. It is followed by a stronger late-spring peak (in May-June) that evidently coincides with the period of high Danube discharge. The third one occurs in autumn and is separated from the former one by a period of relatively low summer concentrations. Interior basin depicts a different annual structure. Surface chlorophyll concentration decreases linearly from a peak in November to a minimum in July, followed by a sharp increase from August to November again. The autumn peak is the strongest one with an occasional weak chlorophyll peak in spring. Monitoring surface chlorophyll concentration only in summer months, as set by EEA monitoring strategy, therefore may not be well-suited for the Black Sea, and may even lead to a wrong assessment. While summer months possess lowest chlorophyll concentration at the surface, they tend to show high values below the seasonal thermocline (i.e. the subsurface chlorophyll maximum layer), which therefore need to be monitored systematically. Comparison of satellite ocean colour and in situ chlorophyll concentrations is encouraging, and indicate that satellite data provide a potential tool for chlorophyll monitoring.

According to recent studies, hypoxia decreased in Romanian coastal waters as compared to the previous decade, and no hypoxia case was observed in Bulgarian waters in 2001-2005. Relatively low oxygen concentrations tend to occur more predominantly in the northern sector upstream of the Danube delta region. Long-term data at Constanta monitoring station suggest surface oxygen concentration in 200-250 μM range during May-September period, including the intense eutrophication period of the 1980s. This information therefore is not particularly useful for assessment purposes. It is indeed essential to monitor the near-bottom summer oxygen concentration in addition to its surface value. On the other hand, the annual-mean surface oxygen concentration is a good indicator for monitoring long-term climate-induced modulations of eutrophication phenomenon in the western coastal waters. Subsurface oxygen concentration (below the eutrophic zone) data from the interior basin and the eastern part of the sea presently reflect an intermediate state between worst conditions of the 1980s and the best conditions of the mid-1990s.

References

- Bat, L., Şahin, F., Satılmış, H.H., Üstün, F., Birinci Özdemir, Z., Kıdeys A.E., ve Shulman, G.E. (2007). Karadeniz'in değişen ekosistemi ve hamsi balıkçılığına etkisi. *Journal of Fisheries Sciences*, 1 (4), 191-227.
- Berlinskii, N. (1989) Mechanisms of bottom hypoxia formation in shelf ecosystems. *Water Resources*, 4, 112-121.
- Berlinskii, N, Garkavaia, G., Bogatova, Y. (2003) Problems of anthropogenic eutrophication and evolution of hypoxic situations in the North-Western part of the Balcak Sea. *Ecology of Sea*, 17-22.
- Chaykina, A.V., V.V., Dolotov, Y.P., Ilyin, S.K., Konovalov, A.S., Kuznetsov, L.N., Repetin, O.V. Voitsekhovich (2005) Observational studies of nutrient loads on the Black Sea with atmospheric precipitations. *Proceedings of The First Biannual Scientific Conference: Black Sea Ecosystem 2005 and Beyond*, organized by Commission on the Protection of the Black Sea Against Pollution, May 2006, Istanbul.
- Churilova T., G. Berseneva, L.Georgieva. (2004) Variability in bio-optical characteristics of phytoplankton in the Black Sea. *Oceanology (English translation)*, 44(2), 192-204.
- Churilova, T., Z. Finenko, S. Tugrul, (2006) Light absorption and quantum yield of photosynthesis during autumn phytoplankton bloom in the western Black Sea. *Proceedings of The First Biannual Scientific Conference: Black Sea Ecosystem 2005 and Beyond*, organized by Commission on the Protection of the Black Sea Against Pollution, May 2006, Istanbul.
- Cociasu, A., L. Popa, S. Dineva, P. Ivanova, V. Velikova (2004) Summary report on field and laboratory work in 2001-2003 in comparison with previous observations in the Western Black Sea. Nutrient management in the Danube Basin and its impact on the Black Sea. daNUbs Projects (EVK1-CT-2000-00051), Deliverable 7.6, Nutrient Management in the Danube basin and its impact on the Black Sea. EVK1-CT-2000-00051.
- daNUbs Project Final Report (2005) Nutrient management in the Danube basin and its impact on the Black Sea. Final Report, December 2004.
- Feyzioglu, M., A. Guneroglu, I. Yildiz (2006) Weekly changes of *Synechococcus* spp. and pigment concentration in the Southeastern Black Sea coast. *Proceedings of The First Biannual Scientific Conference: Black Sea Ecosystem 2005 and Beyond*, organized by Commission on the Protection of the Black Sea Against Pollution, May 2006, Istanbul.
- Hibaum, G, V. Karamfilov (2005) Regime shifts in the annual dynamics of primary production and chlorophyll_a concentrations in the costal zone of the Bourgas Bay (Western Black Sea). *Proceedings of The First Biannual Scientific Conference: Black Sea Ecosystem 2005 and Beyond*, organized by Commission on the Protection of the Black Sea Against Pollution, May 2006, Istanbul.
- Horstmann, U., Davidov, A. (2002) IFM Annual Report. daNUbs project.
- Konovalov, S.K., and J.W. Murray (2001). Variations in the chemistry of the Black Sea on a time scale of decades (1960-1995). *J. Mar. Syst.*, 31, 217-243.
- Konovalov, S., J.W. Murray, and G.W. Luther III (2005) Basic Processes of Black Sea Biogeochemistry. *Oceanography*, 18, 25-35.
- Kucheruk, N. (2005) Integrated study of eutrophication and biodiversity in the Russian coastal waters. *Proceedings of The First Biannual Scientific Conference: Black Sea Ecosystem 2005 and Beyond*, organized by Commission on the Protection of the Black Sea Against Pollution, May 2006, Istanbul.
- Loyeva, I., I. Orlova, N. Pavlenko, Yu. Popov, V. Ukrainskiy, Yu. Denga, V. Komorin, V. Lepeskin (2006) Estimation of the ecological state of the north-western part of the Black Sea. *Proceedings of The First Biannual Scientific Conference: Black Sea Ecosystem 2005 and Beyond*, organized by Commission on the Protection of the Black Sea Against Pollution, May 2006, Istanbul.
- Medinets, S. and Medinets, V. (2008) Results of investigations of atmospheric pollutants fluxes to the surface of Zmeiny Island in western part of the Black Sea in 2003-2007. In: 2nd Biannual and Black Sea Scene EC project joint conference on climate change in the Black Sea - hypothesis, observations, trends, scenarios and mitigation strategy for the ecosystem. 6-9 October 2008, Sofia, Bulgaria.

- Moncheva, S. (2005) Phytoplankton shifts in the Black Sea - Driving forces and implication for reference conditions. Proceedings of the JRC Workshop, 26-28 October, 2005-Istanbul
- Okus, E. (2005) Time series analysis of nutrients in southwestern Black Sea and the Sea of Marmara. Proceedings of the JRC Workshop, 26-28 October, 2005-Istanbul
- Oguz, T. (2005) Long-Term Impacts of Anthropogenic Forcing on the Black Sea Ecosystem. *Oceanography*, 18, 112-121.
- Oguz, T. and D. Ediger (2007) Comparison of in situ and satellite-derived chlorophyll pigment concentrations, and impact of phytoplankton bloom on the suboxic layer structure in the western Black Sea during May-June 2001. *Deep Sea Res. II*, 53, 1923-1933.
- Parr et al. (2006) Impact of the Danube River on the Black Sea. Estimation of the ecological state of the north-western part of the Black Sea. Proceedings of The First Biannual Scientific Conference: Black Sea Ecosystem 2005 and Beyond, organized by Commission on the Protection of the Black Sea Against Pollution, May 2006, Istanbul.
- PMA AG and AC Activities and Reporting (2007) Final Report on Policy Measures, Development and Data Analysis for 2006/2007. Black Sea Commission, 20 November, 2007 San Diego-McGlone et al. (2000)
- State of the Environment of the Black Sea, 2002. Pressures and trends: 1966-2000. Commission on the Protection of the Black Sea Against Pollution. Istanbul. 101 pp.
- Teodoru, C. R., G. Friedl, J. Friedrich, U. Roehl, M. Sturm, B. Wehrli (2007) Spatial distribution and recent changes in carbon, nitrogen and phosphorus accumulation in sediments of the Black Sea. *Marine Chemistry*, 105, 52-69. TDA (2007) The Black Sea Transboundary Diagnostic Analysis.
- Yakushev, E.V., O.I. Podymov, and V.K. Chasovnikov (2005) Seasonal Changes in the Hydrochemical Structure of the Black Sea Redox Zone, *Oceanography*, 18, 49-55.
- Yunev, O. A., V. I. Vedernikov, O. Basturk, A. Yilmaz, A. E. Kideys, S. Moncheva, S. K. Konovalov (2002) Long-term variations of surface chlorophyll a and primary production in the open Black Sea. *MEPS*, 230, 11-28.
- Velikova, V. and Cociasu, A. (2004) Summary report on field and laboratory work in 2001-2003 in comparison with previous observations in the Western Black Sea Part. III. Comparison between Roumanian and Bulgarian waters. Nutrient management in the Danube Basin and its impact on the Black Sea. daNUbs Projects (EVK1-CT-2000-00051), Deliverable 7.6, Nutrient Management in the Danube basin and its impact on the Black Sea. EVK1-CT-2000-00051.
- Zaitsev Yu.P. (1992) Recent changes in the trophic structure of the Black Sea. *Fisheries Oceanography*, 1, 180-189.

CHAPTER 3 THE STATE OF CHEMICAL POLLUTION

(A. Korshenko *et al.*)

This chapter describes the state of petroleum hydrocarbon (TPHs), organochlorine pesticide, and trace metal pollution in water and sediments in the Black Sea during the last ten years. The pathways of these anthropogenic pollutants into sea ecosystem are different. Many pollutants are restricted to rather narrow zone in the vicinity of large cities, estuarine areas of the large rivers and industrial places. The petroleum hydrocarbon pollution mostly originates from transportation activity over the sea and mainly confines to the surface.

The data used for the assessment of spatial and temporal variability of the pollutants came from three main sources. The last five years were mainly covered by the international monitoring data collected by Secretariat of the Black Sea Commission. Despite some restriction in the number parameters these data sets were rather well and allowed to compare the pollution level of coastal zones in different countries. The second important source was the international Screening Cruise 1995 (for bottom sediments), the IAEA Cruise (11-20 September 1998) (for water column), the IAEA Cruise (22.09-9.10.2000) (for water column), the IAEA Cruise (24.09-3.10.2003) (for bottom sediments), the BSERP Cruise (6-19.06.2006) (for bottom sediments of Romania and Georgia). The third source was the national scientific expeditions.

3.1. The State Of Total Petroleum Hydrocarbons (TPHs)

A. Korshenko

State Oceanographic Institute, Moscow, RUSSIA

Depending on the analytical procedures applied in different cruises [5], the petroleum hydrocarbons data are expressed either in total amount or in terms of relative contributions of Aliphatic, Aromatic and Polyaromatic groups in the oil.

3.1.1. Water

The most intensive spatial investigations of the TPHs distribution over the whole Black Sea were carried out during two IAEA Cruises of RV "Professor Vodyanitskyi" during 11-20 September 1998 and 22.09-11.10 2000 [1]. In 1998, 16 stations were visited in the western central basin, the Danube offshore area and Romanian shelf. The average concentration for all sampled area is 0.084 mg/l, the maximum reached 0.23 mg/l in the shallow waters off Romania coast south of Constanta where active ship traffic, oil refinery and harbor activities could be the main reason of very high level of TPHs concentration. TPHs concentrations in the Danube discharge region were not high as compared with the Constanta region. Lowest concentrations (0.03 mg/l) were recorded near the entrance of Bosphorus Strait and near Odessa. In general, the spatial distribution of petroleum hydrocarbons in September 1998 was rather uniform and level was low (Fig. 3.1.1).

In the IAEA Cruise 2000, TPHs were measured at 32 stations in the Eastern and Central parts of the Sea. Its total concentration varied from negligibly low values to 0.73 mg/l

with an average value of 0.097 mg/l. The anomalously high concentration of 3.27 mg/l was recorded in the surface layer of a shallow station near Feodosiya in Crimea. This level exceeded the Russian standard Maximum Allowed Concentration, MAC, (0.05 mg/l) for marine waters more then 65 times. The second high value (0.73 mg/l) measured close to this site in front of Yalta. Two other stations near Yalta also had quite high TPHs concentrations varied in different horizons from 0.13 to 0.19 mg/l. Such local patch of oil pollution in the Southern Coast of Crimea was the biggest at this time in the Black Sea waters and could be the result either of local spill or municipal discharge of large tourist centers (Table 3.1.1).

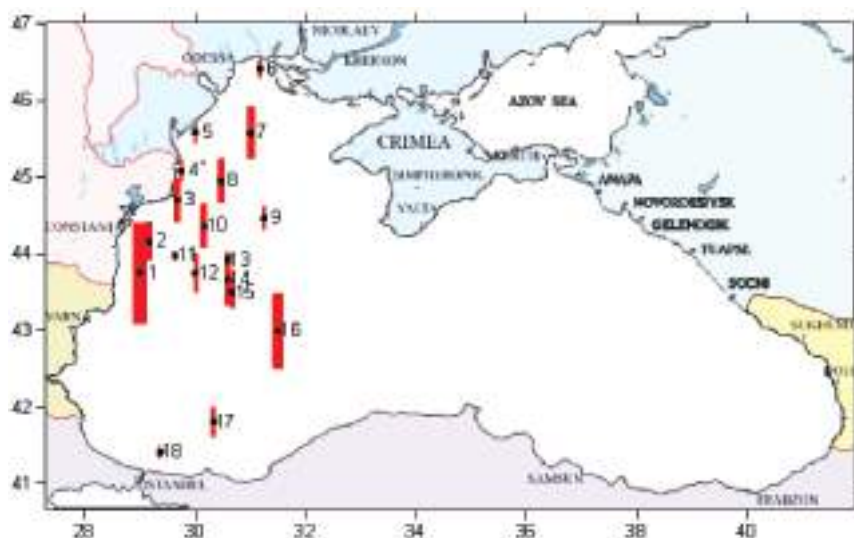


Fig. 3.1.1. Average Total Petroleum Hydrocarbons distribution (mg/l) at 11-20 September 1998.

Table 3.1.1. The average concentration of TPHs (mg/l) in different part of the Black Sea measured during the September-October 2000 IAEA Cruise.

Region	Central West	Crimea Cost	Kerch Strait	Georgians waters	Sinop polygon	Central East	Central open
Concentration	0.30	0.78	0.20	0.05	0.05	0.03	0.03

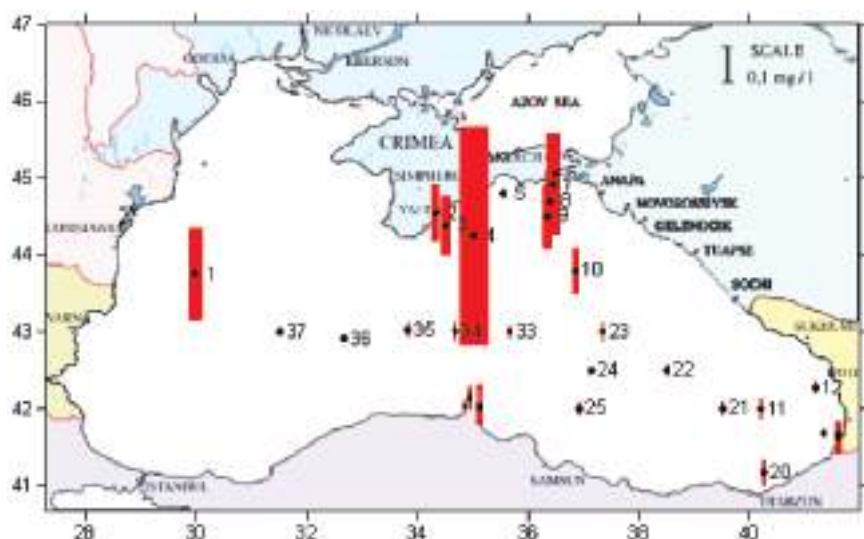


Fig. 3.1.2. Average Total Petroleum Hydrocarbons distribution (mg/l) at 22 September - 9 October 2000. The anomalous high concentration 3.27 mg/l near town Feodosiya is not shown on the map.

The waters at the Kerch transect was also relatively polluted by TPHs especially near the entrance of the Kerch Strait (Fig. 3.1.2) suggesting a discharge of oil pollution from the Kerch harbor and intensive ship traffic. On the contrary, the level of pollution in Georgian and Turkish waters was relatively low despite of a well-known center of oil processing in the Batumi area where the concentration of TPHs in surface and subsurface layers was lower than 0.09 mg/l and sometimes were under the detection limit of analytical procedure. In the Cape of Sinop region, the concentration varied from 0.02 to 0.12 mg/l. The Central part of the sea and the Eastern Basin showed only small concentrations of petroleum hydrocarbons which were often below the detection limit and never exceeded 0.05 mg/l.

Table 3.1.2. The average and maximum concentrations of TPHs (mg/l) in Ukrainian part of the Black Sea, 2000-2005.

Region	Kerch Strait	Crimean towns	Odessa Bay	Odessa region [11] 1988-99	Harbour Yuzhny	Harbour Illichevsk	Dnieper and South Bug Mouth	1992-99 [2] (140 samples)
Average	0.05	0.01	0.01	0.03-0.07	0.01	0.01	0.025	0.05
Maximum	0.18	0.06	0.08	-	0.07	0.07	0.05	1.2

Table 3.1.3. Annual average (above) and maximum concentrations (below) of TPHs (mg/l) in Ukrainian coastal waters of the Black Sea, 2000-2004 [4].

Region	2000	2001	2002	2003	2004	2004 TPHs (tons)*
Danube Delta	0.05	0.05	0.05	0	0	
	0.09	0.1	0.09	0.08	0.07	
Waterpasses in Danube Delta	0.06	0.06	0.04	0.05	0.01	
	0.10	0.12	0.08	0.08	0.07	
Suhoi Liman	0.05	0.05	0	0	0	
	0.3	0.25	0.28	0	0	
Harbour Illiechevsk**	0.05	0.05	0	0	0	
	0.08	0.16	0	0	0	
Harbour Odessa	0.09	0.12	0.12	0.11	0.12	0.17 (with Suhoi Liman)
	0.24	0.35	0.33	0.56	0.51	
South Bug Estuary & Bug Liman	0.2	0.28	0.16	0.17	0.19	43.59 (Dniper and South Bug Mouth)
	1.02	0.9	0.85	0.9	0.85	
Balaklava Bay (Crimea)				0	0.05	6.9 (Sevastopol)
				0.06	0.08	
Harbour Yalta (Crimea)	0	0.05	0	0	0.02	1.8 (Large Yalta)
	0	0.05	0.17	0.24	0.47	

* - estimation of petroleum hydrocarbons (tonns) discharge to the Black Sea in 2004.

** - Harbor Illiechevsk, the Channel and waste-water purification plant.

More recent (2000-2005) monitoring data from the northern part of the sea [3] indicated a maximum 0.18 mg/l in vicinity of Kerch Strait in September 2004 and an average concentration of 0.05 mg/l suggesting that concentrations were often close to analytical limit (Table 3.1.2). The TPHs concentration was very low in the Crimean towns Sevastopol and Evpatoriya despite their dense ship traffic and harbor activities. The monitoring data from the Odessa Bay also showed very low average concentration and moderate maximum level of 0.08 mg/l during 2000-2005. In the Yuzhny harbour, among 37 samples over last 5 years the only five had the concentration above zero. Practically the same situation in the waters of Illiechevsk harbour. At stations in the Dniper and South Bug Mouth the water were also free of TPHs.

According the other Ukrainian monitoring data for 2004, the water pollution by TPHs in the Danube Delta was moderate in August-October: the average value was 0.06 mg/l and maximum reached only 0.07 mg/l both in surface and near-bottom layers [4]. The TPHs was absent in the water slightly north along the coast in Suhoi Liman and Illiechevsk harbor (Table 3.1.3). On the other hand, very high concentrations were noted for the Odessa harbor where the TPHs content in the surface waters varied from 0.11 to 0.51 mg/l. Maximum occurred in October and monthly average value was high as 0.31 mg/l and 2-3 times higher than in January-August. The annual mean value was 0.12 mg/l. Near-bottom layer waters were less polluted and maximum reached 0.34 mg/l. The Bug Liman and South Bug estuarine area were characterized by the TPHs concentrations from zero to 0.85 mg/l in 2004 and the level of pollution slightly increased over the last few years. Similar high concentrations were also recorded in the Dniepr Liman and for the Dniepr river where maxima reached 0.68 and 0.50 mg/l, measured in deep waters in July and at surface in September correspondingly. The pollution increased in whole

water column about 1.3-1.8 times in these sites during the last few years. In the Crimean Balaklava Bay, the TPHs concentration varied from zero to 0.08 mg/l and mean value was 0.05 mg/l. Much higher mean values were recorded in the Yalta harbor where maximum in surface layer was as high as 0.47 mg/l in July and reached 0.17 mg/l near the bottom. The data for the 2004 were somehow higher than the average of the 5 years period (2000-2005). The difference could be high as 10 times, like in the Dnieper-South Bug area, Odessa Harbor or Crimean ports. The averaged data probably smoothed the real picks in the water.

On the basis of these data sets, it can be suggested that, apart from accidental spills at localized areas, this part of the Black Sea did not show a chronic TPHs pollution. In general, it can be stated that large spatial and temporal variability of petroleum hydrocarbons distribution were encountered during the last years. It seems that patches of oil pollution were often local and short time visible, therefore the maximums better describes the real level of pollution.

In Romanian coastal waters during 2001-2005, the level of water petroleum hydrocarbons pollution is presented in Table 3.1.4 [3]. In 2005, the average concentration was 0.14 mg/l with the maximum 0.20 mg/l (Portita, October) in the Danube Delta. Along the coast to the south near Mamaia, the TPHs content in the surface waters was much higher and maximum reached level 0.47 mg/l. Almost the same situation with a small variation was noted for all Romanian coast up to Bulgarian border.

Table 3.1.4. The average and maximum concentration of TPHs (mg/l) in the surface coastal waters of Romanian part of the Black Sea, 2001-2005.

Region	Year	Danube Delta	Mamaia	Constanta	Eforia Sud	Costinesti	Mangalia	Vama Veche
Average	2005	0.14	0.21	0.23	0.18	0.23	0.25	0.28
Maximum	2005	0.20	0.47	0.37	0.26	0.41	0.41	0.43
Average	2001-2004	0.22	0.17	0.15	0.14	0.16	0.22	0.14
Maximum	2001-2004	1.28	0.75	0.76	0.71	0.67	2.27	0.40
number of observation	2001-2004	41	47	68	47	46	48	48

Typically, the average concentrations in all Romanian coastal waters were highest in 2003. Nevertheless, extremely high mean values were also noted in the previous years. The absolute maximum reached 2.27 mg/l in June 2003 in shallow waters near Mangalia of the Romanian coast. Another high level (1.28 mg/l) was marked in the Danube delta near Portita in April 2004. It is important to note that high concentration like 0.50 - 0.70 mg/l was recorded many times in all regions of Romanian coast. In 2001, the average for 50 samples was 0.17 mg/l; a year later for 92 samples - 0.10 mg/l; in 2003 - 68 samples and the mean was 0.14 mg/l; in 2004 - 135 samples and the mean was 0.02 mg/l; in 2005 - 74 samples and 0.21 mg/l. In general, among 344 records of TPHs concentrations in Romanian waters during 2001-2004 only 72 were less then 0.05 mg/l and the other mean values indicated a high level of petroleum hydrocarbon pollution along the Romanian coast.

The seasonal changes of TPHs did not show any clear trend during 2001-2004 measurements due to different number of observations in different months: The averages were 0.12 mg/l in 4 samples in March; 0.21 mg/l in 17 samples in April, 0.23 mg/l in 74 samples in May; 0.18 mg/l in 44 samples in June; 0.08 mg/l in 54 samples in July; 0.14 mg/l in 55 samples in August; 0.20 mg/l in 61 samples in September; 0.15 mg/l in 36 samples in October.

Bulgarian monitoring data did not include petroleum hydrocarbons measurements during 2001-2005.

Turkish coastal TPHs monitoring data covered 2003-2005. Near the outlet of the Bosphorus Strait, the concentration at 3 shallow stations varied in the large range from 0.006 to 0.255 mg/l (exceeded 5 times the MAC according Russian legislation for marine waters) and the mean was 0.092 mg/l in January and February 2003. The general level of pollution of Turkish coastal waters was rather low and varied between 0.001 and 0.077 mg/l, the average was 0.011 mg/l next year mid-September. In August 2004 maximum (0.052 mg/l) was marked near the Sile to the east of the Bosphorus exit section. All other concentrations fell inside the range of 0.001 - 0.042 mg/l with heavier pollution levels observed in coastal waters near Samsun.

In April 2005, the average level of petroleum hydrocarbons content in 63 samples from the Turkish waters was 0.020 mg/l. Maximum was as high as 0.163 mg/l in Ordu area. Slightly lower pollution was recorded near Fatsa (eastern basin) and along the west coast. The situation however changed drastically by the end of September and beginning of October 2005. Some places could be considered as heavily polluted. The maximum concentration of TPHs reached incredible level of 25.466 mg/l at a station along the west coast characterized by surface waters of Danube origin; two other nearby stations had concentrations of 1.935 and 0.855 mg/l. Excluding these extreme values, the average of 60 samples was 0.199 mg/l. High values were spotted practically in all parts of the Turkish coast during October 2003: in Zonguldak, 1.279 mg/l, in Bartın, 0.573 mg/l, in Cide, 0.530 mg/l, in Akcaabat, 0.571 mg/l, in Sile, 0.900 mg/l. In general, very high water pollution was noted in the western part of the Black Sea where mean level for four stations occurred as high as 0.757 mg/l.

During the screening cruise in the Georgian waters in October 2000, the concentration of petroleum hydrocarbons was less than the detection limit of method used (0.04 mg/l) at 5 m depth as well as the near bottom layer at 114 samples out of 140. The overall average was 0.130 mg/l. In twenty four water samples, the TPHs content exceeded 1 MAC (0.05 mg/l) and reached the level of 1.13 mg/l, in average - 0.23 mg/l. But the concentration of petroleum hydrocarbons at two coastal stations on the 5 m horizon reached 4.72 and 6.81 mg/l (more then 136 MAC). The reason of such amount of oil products in the water is unknown, probably it was a slick.

The extensive monitoring investigations along Russian coastal waters showed a moderate level of petroleum hydrocarbons pollution in 1988-1996 that was in general characterized by 0.1-0.2 mg/l, e.g. 2-4 MAC according to the Russian regulation for marine waters [12, 13]. At the same time, concentrations at some sites were as high as 1.10 - 1.20 mg/l, 22-24 MAC. The maximum was recorded in Sochi area in 1990. The content of TPHs then decreased gradually.

Based on the topographical and hydrological conditions along the Russian coast, the shallow waters were divided into several zones (Fig. 3.1.3). To some extent the environmental parameters are uniform within each zone. The monitoring data from the each zone allowed estimation the magnitudes and local pollution sources.

The monitoring in these coastal waters over the last 5 years (2002-2006) provided 868 measurements with an average value of 0.073 mg/l. This level exceeds the Maximum Allowed Concentration (MAC) 0.05 mg/l according Russian regulation. At the same time the range of variation was extremely large and varied between analytical zeros (e.g. less than detection limit 0.002 mg/l) to 3.200 mg/l. The maximum was marked in 27 September 2003 in surface waters at the shallow station (8 m depth) in the vicinity of village Novaja Matsesta close to city Sochi. At the same time, the concentration of TPHs reached second maximum of 1.971 mg/l in the near-bottom layer. The other TPHs concentrations higher than 1.0 mg/l occurred two days earlier at the rather deep station (51 m depth) near the village Loo close to Lazarevskoe where it reached 1,380 and 1.548 mg/l in surface and bottom waters, respectively.

In general the high content of TPHs exceeded 1 MAC was measured in 421 cases, e.g. approximately in half of the samples. The mean was 0.131 mg/l. The mean concentration in other parts was 0.019 mg/l. The vertical distribution was rather uniform as well (Table 3.1.5) since almost 60% of measurement sites were less 20 m depth. In deep waters, the petroleum content in the water column was only occasionally studied, and the mean for the some measurements at the horizons between 50 m and bottom was 0.020 mg/l.



Fig. 3.1.3. Division of the Russian coastal waters in terms of TPHs pollution.

Table 3.1.5. TPHs concentrations in different water layers along the Russian coast in 2002-2006.

Layer	Number of measures	Mean, mg/l	Maximum, mg/l
Surface	371	0.083	3.200
Intermediate	176	0.033	0.200
Near bottom	321	0.084	1.971

Geographical pattern of TPHs distribution demonstrate increasing level of TPHs pollution in the coastal waters close to the towns Novorossiysk and Gelendzhik (Table 3.1.6). The most peculiar values were measured during September-October 2003-2005 and therefore could not be completely compared with the other data. The abundant samples from the southern part of the Russian coast and rather low sampling from the northern part showed concentrations in excess of 1 MAC in the surface and bottom waters. Relatively high values were recorded in all regions in September 2003 and October 2004. On the other hand, high TPHs were recorded only in waters between Inal Bight and village Divnomorskoe in July 2005. Interannual variations are not evident for such a short period of measurements (Table 3.1.7). One could suggest that TPHs concentration is slightly increased during the last years but the trend have to be confirmed with other data sets, if available. Seasonal variations are also not evident from this set of data (Table 3.1.8). The only conclusion which could be drawn by these data sets is higher TPHs pollution in the second part of the year with the mean value of 0.078 as compared to 0.050 mg/l for the first half of the year.

Summary: The mean concentration of petroleum hydrocarbons in the Black Sea in general were rather high and usually exceed standard Maximum Allowed Concentration (0.05 mg/l) almost everywhere in the sea (Table 3.1.9). The petroleum pollution appears a major problem for the whole sea during the last two decades. The same situation was in the previous period of 1980-th when the average of TPHs concentration for almost 4 thousands water samples exceeded the threshold of Maximum Allowed Concentration about 2 times [10]. The maximum concentrations could be extremely high, up to 25.5 mg/l, which were observed almost everywhere in the basin. Quite often, such high values were recorded along the tanker and shipping routes connecting the main harbors Odessa, Novorossiysk and Istanbul. The extremes in the coastal shallow waters should be a result of local spills from the ships or discharge from the waste water systems of the large cities. The ballast water discharge emerges one of the most important sources of petroleum pollution [14]. Black Sea rivers can also contribute significantly.

Table 3.1.6. Mean concentration of TPHs (mg/l) and number of measurements (in parantheses) in the different zones of Russian coastal waters in 2002 - 2006.

Parameter / Zone number	2	3	4	5	6	7	8	9
Surface	0.082 (208)	0.082 (48)	0.053 (49)	0.055 (8)	0.330 (9)	0.145 (12)	0.051 (27)	0.069 (6)
Intermediate	0.034 (98)	0.017 (45)	0.035 (23)	0.107 (3)	0.120 (2)	0.075 (2)	0.097 (3)	-
Near bottom	0.084 (168)	0.102 (41)	0.059 (47)	0.097 (8)	0.217 (9)	0.109 (12)	0.051 (27)	0.047 (6)
Average	0.073 (474)	0.066 (134)	0.052 (119)	0.081 (19)	0.258 (20)	0.123 (26)	0.054 (57)	0.058 (12)
Maximum	3.200	1.548	0.235	0.260	0.900	0.550	0.210	0.160
Date of Maximum value	27.09. 2003	25.09. 2003	18.10. 2004	16.07. 2005	18.10. 2004	18.10. 2004	13.10. 2004	13.10. 2004

Table 3.1.7. Annual variation of the mean concentration of TPHs (mg/l) in Russian coastal waters in 2002 - 2006.

Year	2002	2003	2004	2005	2006
Mean TPHs	0.027	0.058	0.091	0.082	0.064

Table 3.1.8. Seasonal variation of the mean concentration of TPHs (mg/l) in Russian coastal waters in 2002 - 2006.

Months	2	3	4	5	6	7	8	9	10	11
Mean	0.046	0.044	0.060	0.057	0.048	0.086	0.054	0.073	0.113	0.081
Maximum	0.210	0.160	0.080	0.300	0.110	0.640	0.260	3.200	0.900	0.820
Number of samples	22	38	4	52	32	111	178	239	128	64

Despite very high concentrations, about the half of samples can be considered as pollution-free implying very high level of spatial heterogeneity TPHs distribution. As a consequence, the current monitoring station network in the Black Sea appears to be not dense enough in terms of spatial coverage and temporal frequency to monitor oil spills. The field monitoring needs to be supported by satellite and/or aircraft images as routinely in Europe.

Satellite imagery can help identifying spills over very large areas. The Synthetic Aperture Radar (SAR) instrument, which can collect data independently of weather and light conditions, is an excellent tool to monitor and detect oil on water surfaces. This instrument offers the most effective means of monitoring oil pollution. It is currently on board the European Space Agency's ENVISAT and ERS-2 satellites and the Canadian Space Agency's RADARSAT satellite. In 2000-2004, JRC carried out a systematic mapping of illicit vessel discharges using mosaics of satellite images over all the European Seas (Fig. 3.1.4). These maps and the associated statistics were repeated on an annual basis in order to assess its evolution [6]. This action helped to reveal for the first time the dimension of the oil pollution problem, thus stressing the need for more

concerted international actions. For the Black Sea, 1227 oil spills were detected during 2000-2004.

Table 3.1.9. Maximum and mean concentration of Total Petroleum Hydrocarbons (mg/l) in the Black Sea waters in 1992 - 2006.

Area	Year	Waters	Max	Mean
IAEA	1998	Western shelf	0.23 (Constantia)	0.084
IAEA	2000	Eastern open	3.27 (Feodosia)	0.097
Ukraine	1992-1999	coastal	1.20	0.050
Ukraine	2000-2005	coastal	0.18 (Kerch)	0.050
Ukraine	2004	coastal	0.51 (Odessa)	0.12 (Odessa)
Ukraine	2004	coastal	0.85 (Dnieper - South Bug)	
Romania	2001-2005	coastal	2.27 (Mandalia)	0.14-0.28
Turkey	2003	coastal	0.255 (Bosphorus)	0.092
Turkey	2004	coastal	0.077 (Sile)	0.011
Turkey	2005	coastal	25.466 (Danube waters), 1.935 (Danube waters)	0.199 (without 3 extremes)
Georgia	2000	coastal	6.81 (Georgia)	0.13 (140 samples)
Russia	2002-2006	coastal	3.200 (Novaja Matsesta, Sochi)	0.073
Black Sea [10]	1978-1989 Winter	coastal + open, surface	0.89 (central Western shelf)	0.10 (519 samples)
Black Sea [10]	1978-1989 Spring	coastal + open, surface	0.59 (offshore of Crimea)	0.08 (379 samples)
Black Sea [10]	1978-1989 Summer	coastal + open, surface	0.55 (Odessa region)	0.08 (526 samples)
Black Sea [10]	1978-1989 Autumn	coastal + open, surface	1.29 (Sinop region)	0.09 (425 samples)
Black Sea [10]	1978-1989	coastal + open	1.29 (Sinop region)	0.09 (3828 samples)

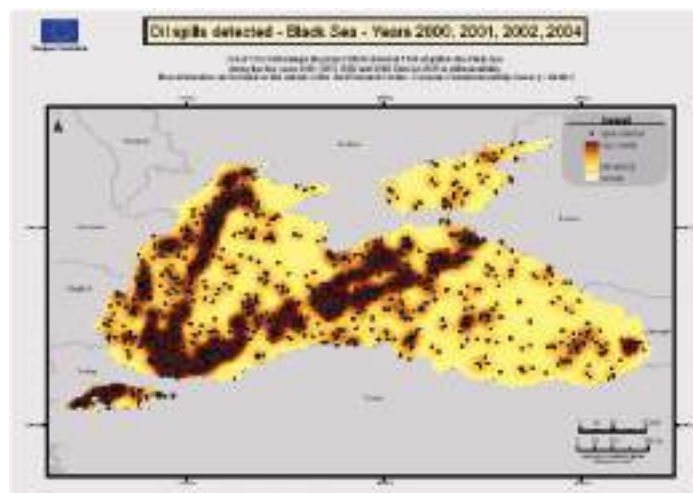


Fig. 3.1.4. The oil spills in the Black Sea for period 2000-2004. Map of oil spills based on images taken by Synthetic Aperture Radars (SARs) of European satellites ERS-2 and Envisat. The oil spill density has been spatially normalized to the spill widths and the number of images available for the detection <http://serac.jrc.it/midiv/maps/>.

Satellite detection of oil spills with synthetic aperture radar (SAR) can now provide reasonably reliable information, but it is still a major challenge for coastal environment. Difficulties are compounded when there is no a priori knowledge of the occurrence, location or timing of a spill, when volumes are small, or when the oil is mixed with water as it enters the sea - just the type of oil pollution that is most common. Thus, systematic multi-sensor routines represent an improvement. The Space Radar Laboratory of the Space Research Institute of RAS (http://www.iki.rssi.ru/asp/lab_554.htm) developed techniques for the synergistic use of satellite data to monitor pollution from pipe-line seeps, waste-water discharges, marine traffic and spillages from routine operations as part of offshore or tanker activities (<http://moped.iki.rssi.ru>). These techniques need to be implemented for operational monitoring system in coastal waters. First results were obtained during the semi-operational phase of satellite monitoring of the Russian coastal zones of the Black and Azov Seas in 2006-2007 [15, 16, and 17]. The ship routes to the ports of Novorossiysk and Tapes and oil terminal Zhelezny Rog were identified as the most polluted regions. Cumulative charts of oil spills based on the analysis of SAR data are presented (Fig. 3.1.5). Over the period of observations from April to October 2006, around 50 oil spills from ships were registered with the spill sizes of from 0.1 to 13 km². The integral area of spills detected over the period was around 120 km². Furthermore, approximately 70 oil spills from ships were detected in the north-eastern part of the Black Sea from April to October 2007, including the catastrophic 11 November 2007 event from the "Volgoneft-139" tanker accident for in the Kerch Strait which was estimated to disperse to 117.6 km². The total area of spills recorded during the observation period in 2007 was around 309 km².

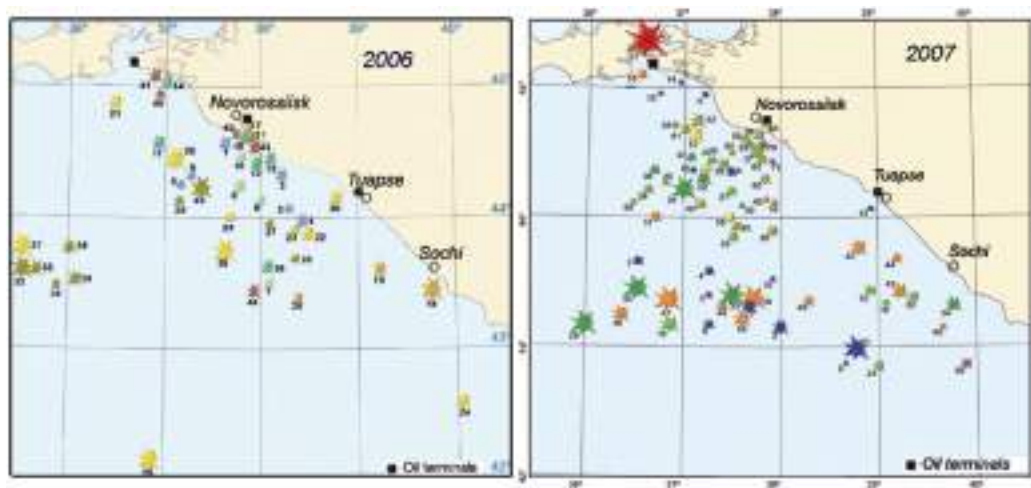


Fig. 3.1.5. Oil spills in the northeastern part of the Black Sea in 2006 and 2007.

3.1.2. Bottom Sediments

The first attempt to assess the level of TPHs pollution in the Black Sea bottom sediments was done in September-December 1995 during the international cruise aboard RV "V. Parshin" [8]. The samples were taken at 25 sites at the outlet of Bosphorus Strait and along

the Ukraine coast including the Danube Delta as well as the vicinity of city Sochi in the southern part of Russian coast (Fig. 3.1.6). In bottom sediments around Crimea peninsula, the content of petroleum hydrocarbons was below $6.6 \mu\text{g/g}$ near Yalta (depth 57 m), and 5.8 and $2.1 \mu\text{g/g}$ at the shallower stations in the vicinity of Feodosia (18 m) and Kerch (6 m), respectively. The TPHs concentration increased drastically to $310 \mu\text{g/g}$ with the mean value of $210 \mu\text{g/g}$ at two sites in the northwestern shelf (Odessa area) with the depth of 11 m and 17 m. Similarly, high concentration was recorded at one station in the Danube Delta ($220 \mu\text{g/g}$, 3 m depth) whereas it was $49 \mu\text{g/g}$ at another shallower site (12 m depth). In the Bosphorus vicinity the 10 samples were taken at rather deep places with about 80-130 m depth. The TPHs concentration was low and varied from 12 to $76 \mu\text{g/g}$ with the average of $38.7 \mu\text{g/g}$. In the Russian part the high content of hydrocarbons $170 \mu\text{g/g}$ was finding only at one station with 8 m depth placed near coast. Four other stations were much deeper (25-40 m) and the hydrocarbons pollution of bottom sediments reduced to $7.6 - 53 \mu\text{g/g}$ with mean $22.9 \mu\text{g/g}$.

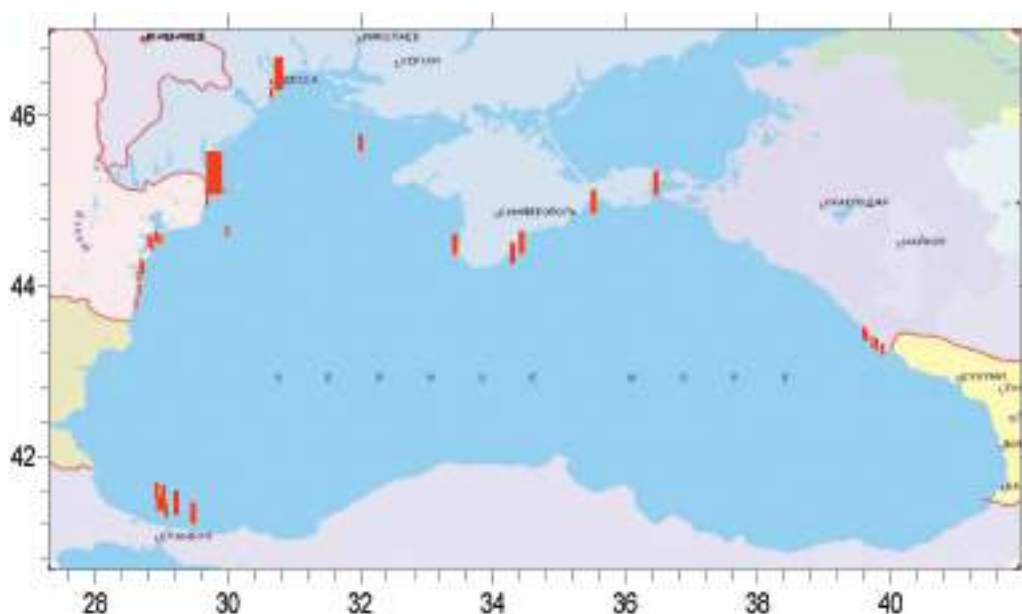


Fig. 3.1.6. Total Petroleum Hydrocarbons distribution in the bottom sediments of coastal area of the Black sea in September-December 1995 [8].

The petroleum hydrocarbons pollution of bottom sediment were sampled at shallow coastal stations with the depth less than 12 m as well as Odessa and Dnieper Deeps below 20 m in 1988-1999 [11]. At the slope of Dnieper Deep, the TPHs concentration varied in a range $1600 - 2000 \mu\text{g/g}$ dry weight close to the Odessa city, but apart from the ports it was slightly less as $800 - 1700 \mu\text{g/g}$. The Odessa and Yuzhny ports could be considered as a most important source of petroleum pollution. Beside this, the spectrum size of bottom sediment highly influenced on the TPHs level. The maximum numbers were recorded in the central part of the Odessa Deep in the fine clay sediments where the concentrations reached $3400 - 5700 \mu\text{g/g}$. At the same time, the minimum was $300 \mu\text{g/g}$ only in the sandy sediments close to the coast.

The other set of monitoring data from 169 samples received in the northwestern shelf during 1992-1999 [2]. The maximum reached $825.0 \mu\text{g/g}$ while the average value for the

whole set was 114.8 µg/g. The highest pollution was recorded in sediments of the Danube delta region - the average for 29 samples reached 210 µg/g, next was the Dniestr Lagoons outlet area with 169 µg/g for 23 samples. In the Dniepr-Bug Lagoon area the average of 6 samples was 133 µg/g. The mean concentration in the Odessa area close to the ports of Odessa, Illiechevsk and Yuzhny was 100 µg/g for 63 samples. The pollution level was, on the other hand, much lower (15.0 µg/g) in the central part of the shelf away from the main sources of pollution. After 2000, no data were available for petroleum hydrocarbons in bottom sediments along the Ukrainian coast.

Along Romanian coast the petroleum hydrocarbons in sediments were not sampled until 2005. In the period of April-October 2005, the concentration in bottom sediments of shallow parts of the Romanian coast (depths less 20 m) varied in a very large range from 25,6 to 11736,7 µg/g. The maximum was noted in June close to Constanta at the site of 5 m water depth. The two other very high values of 6729 and 10090 µg/g were recorded there in April and October, respectively. The concentrations at all other stations were significantly less with an average value 389.7 µg/g for 68 samples. The spatial distribution was rather uniform (Table 3.1.10). A very high level was recorded near the main harbor Constanta. A slightly increasing level of petroleum hydrocarbons pollution was noted in the Danube Delta and near the village Vama Veche in the south. In general, the Romanian bottom sediments could be considered as highly polluted by petroleum hydrocarbons. The average level for whole coastal line exceeded almost 8 times the concentration of Netherlands standard for bottom sediments, Permission Level 50 µg/g [7]. The average data for each part of the Romanian coast also was few times higher than 1 PL (Table 3.1.10).

Table 3.1.10. The mean concentration of TPHs (µg/g) and number of measurements within monitoring programme in the different sites of Romanian coast in 2005.

	Danube Delta	Mamaia	Constanta North	Constanta South	Eforie Sud	Consinesti	Mangalia	Vama Veche
Mean	339.2	273.6	221.5	4484.4	231.2	291.9	258.3	499.5
Number of samples	10	13	5	8	8	11	8	8

In June 2006 four samples were taken along the transect off Constanta at depths 14, 36, 45 and 53 m. Total content of petroleum hydrocarbons in the bottom sediments did not exceed 74.4 µg/g and the average was only 33.7 µg/g for all four samples with minimum 6.6 µg/g. Those data are highly different from almost 100 times higher values recorded in 2005. It could be explained by spatial heterogeneity of bottom sediment pollution depending from many factors.

The only petroleum hydrocarbons pollution monitoring of bottom sediments in Turkish coastal area was performed in April and September-October 2005. In April the level of TPHs was low and varied from 1.6 to 233.2 µg/g in the western part of the Turkish coast. The maximum reached 38.7 µg/g only, at stations with 12-51 m water depth in the vicinity of Sakarya River. However, near the town Zonguldak, the pollution level drastically increased up to the extremely high number of 11999.1 µg/g at a site with 13 m water depth, 9025.0 µg/g at 50 m and 475.5 µg/g at 100 m water depth. The bottom sediments from Cide to Fatsa in the eastern part were relatively clean with mean value of

165.0 µg/g for 16 stations placed at the depth range of 9-111 m. The minimum here was 2.3 µg/g, maximum reached 793.7 µg/g and was noted for the deepest station near Cide. The mean for 15 stations of the eastern part was 234.7 µg/g and maximum was 2512.4 µg/g near Pazar. In general, at 40 sites along the Turkish coast sampled in April 2005 the mean value was 700.3 µg/g. Almost ten times lower values were recorded in October 2005 with the mean of 77.4 µg/g for the 63 stations. The maximum was 1016.5 µg/g near Zonguldak.

According to forecasts the volume of oil and oil product transportation through Georgian ports is estimated to be about 50-60 million tonnes per year in 2010-2015. Intense development of marine infrastructure is expected to aggravate current complex ecological state of the marine ecosystem of the sea for which oil pollution is the most dangerous. Within the frame of the international project on the "Study of the background ecological status of the Eastern part of the Black Sea along the coast of Georgia", the concentration of petroleum hydrocarbons in the bottom sediments was determined during 2000. Samples of bottom sediments were taken from 75 stations on the Georgian shelf at the depth range from 10 to 1500 m. A gradually decreasing petroleum hydrocarbon concentration was observed along the topographic slope down to the depth of 200 m. The average concentration for the sites with depths less than 50 m was 26.9 µg/g, from 50 to 100 m - 19.5 µg/g, and from 100 to 200 m - 11.4 µg/g. High content of petroleum hydrocarbons was detected in the bottom sediments of the Poti harbour area, 35.3 µg/g on the average. In the bottom sediments to the north of the Batumi harbour, the concentration of petroleum hydrocarbons also increased up to 17.7 - 21.7 µg/g, on the average 10.5 µg/g. Apparently, flows of sediments contaminated with petroleum products moved from the Batumi area northwards. In the gorge of the Natanebi River petroleum deposits and oil manifestations, petroleum hydrocarbons content was measured at 152.7 µg/g.

Method used for identification of petroleum hydrocarbons was enabled to identify not only the groups of petroleum products, but the approximate time of oil spills as well [5,6,7]. The TPHs in the bottom sediment was of different origin and differed in terms of light and heavy fractions. Latest spills were mostly found in the regions of Batumi and Poti harbours as well as between estuaries of Khobi and Tsivi Rivers. Their origin was the man-made pollution due to the impact of ports and terminals. In the deep stations starting from the depth of 200 m, concentration of TPHs increased which may likely be due to re-deposition of petroleum products absorbed on the clay particles transported from the coastal water to the deep water area. At the same time, anoxic conditions prevented biogenic degradation of the hydrocarbons.

Table 3.1.11. The concentration of TPHs ($\mu\text{g/g}$) and other physical and chemical parameters of the bottom sediments of the Georgian part of the Black Sea in June 2006 [9].

Region	TPHs ($\mu\text{g/g}$)	EOM (mg/g)	Total Organic Carbon, TOC(%)	Grain Size Fines, <65.5 μm (vol%)	Total PAHs (ng/g)	Total HCHs (pg/g)	Total DDTs (pg/g)	Total PCBs (pg/g)
Batumi	6.1	0.031	0.13	42.55	145.1	318	496	864
Kobuleti	202.2	0.43	0.65	54.71	27384.8	1118	16550	4000
Natanebi	76.7	0.45	1.59	79.76	3944.5	1634	5090	6200
Supsa	70.3	0.18	1.66	75.86	4074.6	1336	3679	4320
Poti	15.6	0.042	0.24	9.92	710.3	664	1269	1445

In June 2006, at five sites at 60 m water depth along Georgian coast in vicinity of Batumi, Kobuleti, Poti and estuaries of the Natanebi and Supsa Rivers, the maximum was recorded near Kobuleti and reached the level 202.2 $\mu\text{g/g}$ [9]. The minimum was 6.1 $\mu\text{g/g}$ near Batumi and mean value was 74.2 $\mu\text{g/g}$. The concentration of extracted organic matter (EOM) in the bottom sediments varied between 0.03 and 0.45 mg/g and, in general, the high concentration of TPHs is correlated with the high EOM content. The same correlation was also evident with the grain size of bottom sediments. The coarse ground had less concentration of petroleum hydrocarbons (Table 3.1.11). Majority of fine sediment near estuary Natabeni and Supsa was not heavily polluted by hydrocarbons and could not be regarded as "hot spots".

Prior to 2000, high content of hydrocarbons (170 $\mu\text{g/g}$) was found only at one coastal station at 8 m depth in Russian coastal waters. At other deeper stations (25-40 m) the hydrocarbons pollution was in the range of 7.6 - 53 $\mu\text{g/g}$ with mean 22.9 $\mu\text{g/g}$ [8]. In December 2000, the southern part of the Russian coast from the town Gelendzhik to the village Adler (8 stations placed at 26-41 m water depth) was characterized by the minimum concentration level of 10.7 $\mu\text{g/g}$ (measured at the traverse of estuary Chyhykt River close to Lasarevskoe). The maximum reached 117.0 $\mu\text{g/g}$ at the traverse of the Sochi harbour. The average was 32.8 $\mu\text{g/g}$.

In June-July 2002, monitoring of the TPH pollution level of sediments showed drastic differences to south of Taman. The aliphatics fraction reached the level of 45-84 $\mu\text{g/g}$ and aromatics 35-62 $\mu\text{g/g}$ in deep parts, while they had only 5-9 $\mu\text{g/g}$ and 2 $\mu\text{g/g}$, respectively, in shallow stations. The 10-20 fold differences could be the result of size spectrum of bottom sediment particles, which is much smaller in the deep zone with active sedimentation.

In August 2004, the concentration of total petroleum hydrocarbons in the bottom sediments in the southern part of the Russian coast, between the rivers Hosta and Shapsukho near Tuapse, varied in a very wide range from 11.9 to 2840.0 $\mu\text{g/g}$ with the average of 394.4 $\mu\text{g/g}$. Two most extreme values were registered in the shallow estuaries of the rivers Tuapse (2840.0 $\mu\text{g/g}$) and Sochi (1400.0 $\mu\text{g/g}$) at 6-7 m water depth. Without these extremes, the average value still remained very high (221.8 $\mu\text{g/g}$, more than 4 PL [7]) and demonstrated a rather wide spreads of petroleum pollution along southern and central part of Russian coast. In estuaries of the Hosta and Sochi Rivers of the southern zone 2, the mean was 227.0 $\mu\text{g/g}$. The mean concentration near villages Loo,

Lazarevskoe and the Shahe River at the depth about 40-60 m, on the other hand, was much lower with a value 28.5 µg/g. Slightly to north, the pollution of bottom sediments by TPHs was below 1 MAC at all points at the distance 2 nm from the coast and depth 40-60 m up to the Shapsukho River.

In general, the TPHs pollution level in coastal bottom sediments can be divided into two groups: the offshore stations at more than 2 nm away from the coast located at depths 40-60 m and inshore shallow stations. The average level for the offshore sites was 31.3 µg/g and the variation was only from 11.9 to 74.1 µg/g. The inshore group contained the shallow estuaries of the Sochi River with the mean 481.0 µg/g, and estuary of the Tuapse River with the mean 787.0 µg/g. The difference in petroleum hydrocarbons concentration up to 10-20 times in inshore and offshore regions is evident and should be related to large volumes of municipal and manufacturing waste from two large cities and the discharges from two rivers.

The investigations of bottom sediments pollution by petroleum hydrocarbons in the northern part of Russian coast were carried out in October 2004. Inside the Gelendzhik Bight the concentration of TPHs in the bottom sediments was 61.2 µg/g. Significantly higher values between 122.0 µg/g were measured near the pear in Sheskhari and 1900.0 µg/g in the western part of Novorossiysk harbor. The mean value was 911.0 µg/g. An opposite situation was observed in the Anapa Bight slightly to north. Two samples from the 5 m water depth showed only 5.0 and 88.0 µg/g TPHs concentrations therefore much lower than the southern parts. Similar moderate values (59.5 µg/g) were received in bottom sediments of the port Kavkaz in the Kerch Strait at the point of 6 m depth.

In July 2005, several samples were collected in the southern part of the Russian coast from the River Sochi up to the village Dzankhot in the north near Gelendzhik. All samples were taken at the depth 30-50 m slightly away from the shore. The concentration was rather moderate and varied in the narrow range from 35.3 to 88.0 µg/g with the average value of 54.0 µg/g. The only station in the shallow estuary of the River Mzumta (9 m depth) showed the maximum recorded level.

Summary: During the last 10 years, the mean concentration of petroleum hydrocarbons in the bottom sediments of coastal parts of the Black Sea varied from very low level up to high value of about 0.8 mg/g (Table 3.1.12). Usually in the most sites of the coast the average concentration was about 1 PL (50 µg/g, [7]) but several maxima exceeded this threshold 13-16 times. Those extremely polluted sites are placed in Romania, Turkish and Russian waters, close to the main sources of TPHs, namely large ports, oil refinery or oil terminals for transportation. The maximum values around 12 mg/g were recorded at Romanian and Turkish coasts at the very shallow depths and most likely represented fresh oil spills in 2005. Due to high patchiness of oil distribution in the sea such occasional extreme values are expected.

Table 3.1.12. Maximum and mean concentration of TPHs ($\mu\text{g/g}$) in the bottom sediments of the Black Sea in 1995 - 2006.

Project	Year	Region	Max. value	Max. Depth (m)	Mean (Depth <20m)	Mean (Depth >20m)	Mean
Screening	1995	Crimea	310.0	11	116.2	4.7	71.6
Screening	1995	Russian	170.0	8	170.0	22.9	52.3
Screening	1995	Bosporus	76.0	107	-	38.7	38.7
Research	1988-1999	Ukraine	5700.0	-	-	-	-
Monitoring	1992-1999	Ukraine	825.0	-	-	-	114.8
Monitoring	2005	Romania	11736.7	5	775.4	-	775.4
BSERP	2006	Romania	74.4	36	6.6	42.8	33.7
Monitoring	04.2005	Turkey	11999.1	13	2078.1	457.2	700.3
Monitoring	10.2005	Turkey	1016.5	51	84.0	76.4	77.4
Research	2000	Georgia	152.7	88	19.0	19.0	19.0
BSERP	2006	Georgia	202.2	60	-	74.2	74.2
Research	2000	Russia	117.0	41	-	32.8	32.8
Research	2002	Russia	144.0	70	-	60.5	60.5
Research	2003	Russia	152.0	50	25.5	96.3	36.7
Monitoring	08.2004	Russia	2840.0	7	646.0	31.3	394.4
Monitoring	10.2004	Russia	1900.0	15	671.0	122.0	625.2
Monitoring	2005	Russia	88.0	9	88.0	49.1	54.0

TPHs concentrations in the bottom sediments decreased with increasing depth; i.e. towards offshore (Table 3.1.12). The average level of concentrations was usually highest at depths shallower than 20 m. Some uncertainties came from the sampling strategy; i.e. due to different number of sampling in each site. Irregular and often patchy sampling in many parts of the sea greatly limited a better evaluation of the TPHs pollution. In many cases, the pollution assessment was made on the basis of only few samples of bottom sediments taken during the last 10 years or even none at all. The further monitoring program is much desired for more reliable description of bottom sediments pollution by petroleum hydrocarbons especially in vicinity of main oil sources.

3.2. The State Of Chlorinated Pesticides

Alexander Korshenko

State Oceanographic Institute, Moscow, RUSSIA

Sergei Melnikov

Regional Centre "Monitoring of Arctic", Sankt-Petersburg, RUSSIA

3.2.1. Water

The pesticides investigation in the Black Sea waters significantly differs from the petroleum hydrocarbons studies. Due to low concentration of chlorinated hydrocarbons

in the marine water this parameter was not included into the measurements list neither during the international IAEA Cruise of the RV "Professor Vodyanitskyi" in 11-20 September 1998, nor in the second IAEA cruise of the RV "Professor Vodyanitskyi" during 22 September - 11 October 2000 [1]. The main source of the information on the pattern of pesticides distribution was provided by the national scientific and monitoring programs.

177 water samples were collected for chlorinated hydrocarbon measurements in the surface layer of shallow waters of the North-Western part of the Black from 1988 to 1999 [2]. In general, the level of pesticides was low. The average concentration of lindane (γ -HCH) was 0.48 ng/l (Table 3.2.1). The data varied within the range from analytical zero to 4.0 ng/l. The DDT and its metabolites DDE and DDD had a slightly higher level - average 1.08 ng/l with the range 0.0 - 14.4 ng/l; 0.55 ng/l (0.0 - 5.4 ng/l); 0.38 ng/l (0.0 - 6.3 ng/l), respectively. Important point is to note the predominance of DDT in comparison with its metabolites. It suggests a more recent and ongoing water pollution in the studied area. The method of liquid-gas chromatography applied at the end of this monitoring period allowed to identify very low concentrations of some other chlorinated pesticides like hexa-chlorobenzene, aldrin and heptachlor. Their average and maximum concentration in 1999 was 0.26 and 4.18 ng/l for hexa-chlorobenzene, 0.22 and 3.12 ng/l for aldrin, 0.01 and 0.22 ng/l for heptachlor, respectively.

57 samples analysis were taken for pesticide analysis in Romanian coastal waters during April, July and October 2005 within the framework of national monitoring program [3]. The stations were placed along Romanian coastline at shallow sites at depths less than 20 m. The pesticides concentration of the DDT group exceeded the detection limit of the method used (DL = 0.001 ng/l) only in 18 water samples. The maximum 14.75 ng/l total concentration of DDT group was recorded in April near Mangalia close to beach at 5 m depth isobath. Individual concentration of DDT there was 6.95, DDD 5.91 and DDE 1.89 ng/l. The DDT level exceeded the detection limit, DL, only in this one sample, and the DDT was not registered in other cases. Except this outstanding sample, DDD was recorded 5 times with an average 0.32 ng/l and the maximum 1.01 ng/l. DDE exceeded the DL 17 times. Its average was 0.12 ng/l and the maximum 0.47 ng/l.

Among pesticides of the HCH group, the lindane (γ -HCH) was found rather often in all places along the Romanian coast and in the Danube Delta. Its concentration exceeded the DL (0.001 ng/l) in 34 samples. The average of all samples was 0.064 ng/l and the maximum reached 0.3 ng/l in July near Costanesti. The average for samples where concentration of γ -HCH was higher than its DL was 0.108 ng/l.

No data were available to make an assessment of water pesticides pollution along the Bulgarian, Turkish and Georgian coasts. These pollutants were not included into routine national monitoring programs.

Water samples were collected along the Russian coastal waters from 23 May 2002 to 23 November 2006. Investigations were performed within the frame of national monitoring program. In May, October and November 2002, 48 water samples obtained in the southern region close to the city Sochi showed no pesticides concentration above the DL which seems to be rather unrealistic and suggest either false sampling or measurement. These monitoring data were thus excluded from the analysis. The same also applies for the February 2003 data set.

The September-October 2003 samplings were performed as a part of the "Aero visual monitoring program" and covered the southern and central parts of the Russian coast between the Cape Inal close to Dzubga [3]. The average of total DDT concentration was 0.84 ng/l and varied within range of 0.17-3.26 ng/l (Table 3.2.1). Maximum concentrations of total DDTs, as well as 2.30 ng/l for DDT and 0.96 ng/l for DDE were recorded in the near bottom layer at a shallow station (8 m depth) close to the village Novaja Matsesta in the Sochi region. The next highest total DDTs values of 2.20 ng/l and DDT of 1.36 ng/l were also recorded in the upper layer at the same station.

The spatial distribution of total DDTs group pesticides was rather uniform. The average for different zones of coastal waters was almost the same: for zone 2 - 0.81 ng/l, for zone 3 - 0.89 ng/l, zone 4 - 0.83 ng/l. The vertical variations were also small; the average for samples taken above 20 m depth horizon was 0.89 ng/l and slightly higher than 0.74 ng/l below 20 m. See Fig. 3.1.3 for the locations of these zones.

Among different DDTs forms and metabolites, the dominant role belonged to 4,4-DDT with the average for the whole set of data 0.42 ng/l and maximum 2.00 ng/l. The average and maximum of 2,4-DDT were 0.06/0.30 ng/l; metabolites 2,4-DDE - 0.04/0.27 ng/l; 4,4-DDE - 0.30/0.84 ng/l; 2,4-DDD - 0.00/0.18 ng/l; 4,4-DDD - 0.01/0.36 ng/l. This structure of group concentration suggests rather 'fresh' DDT pollution of marine coastal waters in the region.

Table 3.2.1. Maximum and average concentration of pesticides (ng/l), and number of observations (in parentheses) in marine waters of the Black Sea in 1992 - 2005.

Project	Year	Region	γ -HCH	A-HCH	β -HCH	HCH total	DDT	DDE	DDD	DDT total	HCB*	Other
Monitoring [2]	1992-1999	Ukraine	4.0/0.48 (177)	-	-	-	14.4/1.081 (77)	5.4/0.55 (77)	6.3/0.38 (77)	-	4.18/0.26 (**)	3.34/0.23 (***)
Monitoring [3]	2005	Romania	0.3/0.064 (57)	-	-	-	6.95/0.12 (57)	1.89/0.07 (57)	5.91/0.13 (57)	14.75/0.32 (57)	-	-
IAEA Cruise [1]	09.1998	Western Black Sea	-	-	-	-	-	-	-	-	-	-
IAEA Cruise [1]	09.2000	Eastern Black Sea	-	-	-	-	-	-	-	-	-	-
Monitoring [3]	2005	Bulgaria	-	-	-	-	-	-	-	-	-	-
Aero Visual Monitoring	2003	Russia	2.33/0.23 (40)	2.32/0.39 (40)	3.88/2.70 (40)	6.50/3.31 (40)	2.30/0.48 (40)	0.96/0.34 (40)	0.36/0.02 (40)	3.26/0.84 (40)	0.32/0.06 (40)	0.86/0.26 (40)
Aero Visual Monitoring	07-08.2004	Russia	3.60/0.14 (80)	0.59/0.11 (80)	4.99/3.14 (80)	7.21/3.38 (80)	1.28/0.17 (80)	0.39/0.04 (80)	0/0 (80)	1.66/0.21 (80)	0.28/0.06 (80)	0.18/0.01 (80)
Aero Visual Monitoring	10.2004	Russia	0.19/0.13 (100)	0.20/0.12 (100)	3.42/2.74 (84)	3.76/2.85 (100)	0/0 (84)	0.34/0.05 (84)	0/0 (84)	0.34/0.05 (84)	0.11/0.09 (84)	0/0 (84)
Aero Visual Monitoring	07.2005	Russia	0.35/0.16 (59)	0.68/0.43 (59)	6.81/3.98 (59)	7.80/4.55 (59)	0.64/0.15 (59)	0.23/0.02 (59)	0.77/0.08 (59)	1.29/0.20 (59)	0.14/0.07 (59)	0.18/0.09 (59)PCB

Notes: The **bold** number exceed the 1 MAC = 10 ng/l.

HCb* - hexachlorobenzene,

** - the only samples treated in 1999.

0.18/0.09/59PCB - pentachlorobenzene, maximum, average and number of samples.

The total HCH concentration was much higher than DDT and varied from 2.12 to 6.50 ng/l; the average for 40 samples was 3.31 ng/l. The highest concentrations of 6.50 and 5.78 ng/l were recorded in shallow places with 6-8 m depth close to villages Novaja Matsesta and Nizne-Nikolaevka situated between Hosta and Sochi where DDT pollution was also highest. Similar to DDT the spatial distribution of these pesticides was rather uniform. The average was 3.49 ng/l in the second zone; 2.98 ng/l in the third zone; 3.47 ng/l in the fourth. The average was 3.36 ng/l for shallow stations less than 25 m, and 2.95 ng/l for deeper stations.

Among different forms of HCH, the dominant one with the average level of 2.70 ng/l and maximum 3.88 ng/l was the β -HCH (Table 3.2.1). The lindane and γ -HCH had the mean concentrations of 0.23/2.33 ng/l and 0.39/2.32 ng/l, respectively.

Hexachlorobenzene content exceeded the DL = 0.01 ng/l in 19 samples. The average for all studied area was 0.06 ng/l and the maximum reached 0.32 ng/l. Heptachlor had a maximum (0.86 ng/l) in vicinity of Sochi and the average value for all stations was 0.06 ng/l. Aldrin concentration (maximum 0.48 ng/l) was also marked near Sochi. Cis-chlordane concentration exceeded the DL only in 7 samples, maximum was 0.11 ng/l, cis-nonachlor spreaded much wider over the whole area and was registered in 24 samples; the average was 0.14 ng/l and maximum reached 0.40 ng/l at a coastal station close to the village Chemitokvazhe near Lazarevskoe. The concentration of octachlorostyrene, heptachlorepoxyde, trans-chlordane, trans-nonachlor, photomirex and mirex did not exceed the DL in all samples.

In the second round of "Aero visual monitoring programme" during July-August 2004, 80 water samples were taken within the central and southern parts of the Russian coast. The total DDT concentration exceeded DL=0.05 ng/l in 39 samples and reached the maximum 1.66 ng/l at a station located 2 nautical miles away from the coast off the River Shapsukho mouth close to the town Tuapse. The average for the whole set of samples was 0.21 ng/l. The DDT content was much higher in the central part of coast in the fourth zone (average was 0.34 ng/l), 5 times lower (0.07 ng/l) in the third zone, and slightly higher in the second zone (0.16 ng/l).

Among the forms of DDT group, 4,4-DDT exceeded the DL in 36 samples and reached 0.94 ng/l and the average was 0.14 ng/l. The spatial distribution of 4,4-DDT showed a maximum (average 0.219 ng/l) in the central part of Russian coast (zone 4). It reduced southward to 0.06 ng/l in the zone 3 and was twice higher in the Sochi area (0.11 ng/l). The 2,4-DDT reached maximum 0.54 ng/l but average was as low as 0.03 ng/l. The average content of another form 4,4-DDE, although measured up to 0.39 ng/l, was 0.04 ng/l only. The 2,4-DDE was practically absent and its maximum was only 0.07 ng/l. The concentration of both DDD forms did not exceed DL in all samples.

Similar to previous year, the HCHs concentration was an order of magnitude higher than the DDT group. The maximum of total HCHs reached 7.21 ng/l and average was 3.38 ng/l. The maximum was recorded in the subsurface layer off Tuapse at a distance 7 nm from the coast. In general the HCH was distributed evenly over the investigated area of coastal waters. The averages for three different zones were very close: 3.65 ng/l for the zone 2, 3.05 ng/l for the zone 3, and 3.41 ng/l for the zone 4. Also there was no appreciable difference between the shallow and deep stations; the average was 3.52 ng/l at stations shallower than 20 m, and 3.26 ng/l for deep ones.

The maximum of β -HCH concentrations reached 4.99 ng/l and average was 3.14 ng/l. Much lower concentrations were recorded for α -HCH (0.59/0.10 ng/l) and lindane (3.60/0.14 ng/l). Among other pesticides, hexachlorobenzene was recorded rather often in all places along the Russian coast with the maximum and average concentrations of 0.28, 0.06 ng/l, respectively. Pentachlorobenzene seldom traced in the water column at a maximum concentration 0.18 ng/l. The concentrations of heptachlor, aldrin, octachlorstyrene, heptachlorepoxyde, transchlordan, cischlordan, cisonachlor, transnonachlor, photomirex and mirex did not exceed the DL in all samples.

During 9-19 October 2004, the entire Russian shelf was studied from Sochi in the south and to the Kerch Strait in the north. Among 84 samples of marine waters collected, the concentration of DDE exceeded the DL (0.05 ng/l) only in 25 cases. The average level was 0.05 ng/l. The maximum of DDE (0.34 ng/l) was measured inside the Novorossiysk port. Other forms of this group never exceeded the DL (Table 3.2.1). The HCH was again significantly higher and rather uniform. No special place or patches with high concentration was found. The average for the 100 samples was 2.85 ng/l and they varied within a narrow range from 0.90 to 3.76 ng/l and no single sample was free of these pesticides. The maximum was recorded at station placed at 2.5 miles away from the coast near the village Olginka in the zone 4. The averages for different zones varied between 2.44 and 3.17 ng/l. The mean level of α -HCH for 40 samples was 0.12 ng/l and the maximum was 0.20 ng/l. The corresponding values were 2.74 and 3.42 ng/l for β -HCH and 0.13 and 0.19 ng/l for γ -HCH. The concentrations of other pesticides did not exceed the DL in all samples with the exception of relatively high hexachlorobenzene (0.07 and 0.11 ng/l) measured in two samples from Novorossiysk Bight.

During the 4-18 July 2005 "Aero visual monitoring" measurement program, the DDT pesticides were found in low quantities (Table 3.2.1). However, in contrary to the previous investigations, the DDT and DDD were also recorded in the samples. The average and maximum levels of total DDT for the entire Russian coastal stations were 0.20 ng/l and 1.29 ng/l, respectively that exceed the 0.1 MAC level. The pattern of geographical distribution showed decreasing of DDT content in the waters from south to north (Table 3.2.2). The highest concentration was found in near-bottom layer of 50 m deep station in the vicinity of Katkova Szel close to Lazarevskoe (zone 3). DDTs showed a vertically uniform distribution with the equal mean concentration of 0.25 ng/l in the subsurface and near-bottom layers.

Table 3.2.2. The average concentration of chlorinated pesticides (ng/l) in the different zones of Russian costal waters in July 2005.

	Average	2	3	4	5	6	7	8	9
DDT total	0.24	0.43	0.73	0.21	0.18	0.40	0.00	0.04	0.07
HCH total	4.55	4.61	4.79	4.95	5.15	4.91	3.79	4.45	3.08

The concentration of pesticides from HCH group was almost 5 times higher than DDT mainly due to a high contribution of β -HCH (Table 3.2.1). The dominance of this form of HCH could be the sign of old pollution and contrasted with low lindane concentrations with the average 0.16 ng/l and the maximum 0.35 ng/l observed near Cape Codosh close to Tuapse. The concentration of β -HCH reached the maximum level 6.81 ng/l in near

bottom waters at 60 m depth close to the Cape Uch-Dere and Dagomys River estuary. Their content in the near-bottom layer was slightly higher than in the surface; 4.26 ng/l and 3.73 ng/l, respectively. The HCH distribution did not exhibit a visible geographical trend. All coastal zones were almost equally polluted by HCH (Table 3.2.2).

The concentrations of chlororganic pesticides heptachlor, aldrin, octachlorstyrene, heptachlorepoxyde, transchlordan, cischlordan, cisonachlor, transnonachlor, photomirex, 1,2,3,4 TCB, 1,2,3,5 TCB, 1,2,4,5 TCB and mirex were lower than their detection limit 0.05 ng/l in all samples. Hexachlorobenzene occurred in 11 samples in the range from DL to 0.14 ng/l (Table 3.2.1). Maximum content was measured in the near bottom layer at depth 47 m off the village Ashe in the zone 3. Pentachlorobenzene occurred only in five samples with the maximum 0.18 ng/l in bottom waters at 50 m depth in the vicinity of Cape Codosh in the zone 4.

Summary: The measurements of pesticide concentration in water were performed rather seldom due to their very low concentrations (Table 3.2.1) and in the frame of international monitoring programme on the Black Sea (BSIMAP) their measurements in water were optional as well as in most of the international monitoring programs. Despite the fact that most of the samples practically free from pesticides due to their concentrations below the Detection Limit (0.05 ng/l), some very condense patches were however detected. Their patchiness may be related to unusual physical conditions like stormy weather or large freshwater discharge into the sea after floods. The densest patch was recorded in Romanian coastal waters (along 5 m isobath) near town Mangalia in April 2005. In this sample the BOD₅ also low probably due to the stabilization effect of high pesticides concentration on microbiological community. This patch was a local feature since no pesticides were found in the neighboring stations along 20 m isobath.

The results of Russian monitoring programs suggested very low DDT concentrations in marine waters. Their maxima reached 0.1-0.3 MAC. The DDT pollution in southern part of the Russian coastal waters was much higher than the northern part. The HCH content was about 10 times higher mainly because of the accumulation of 'old' β -HCH. Nearly uniform pesticide concentrations in surface and near bottom layers support the idea of their spreading from coastal point sources.

In summary, very low level pesticide pollution was observed in coastal waters in general except some occasional patches with very high pesticides concentrations in different layers. The pollution by pesticides could be considered as an 'old' pollution due to low contributions of DDT and lindane in comparison with its metabolites.

3.2.2. Bottom Sediments and Biota

During the first international cruise in September 1995, 10 samples were taken along the Ukraine coastline from the town Kerch on the eastern side of the Crimea peninsula to the Danube delta on the west (Table 3.2.3). The depths of sampling were in the range from 3 m to 78 m. The bottom sediments around Crimea (sampling sites were Karkinitzky Gulf, Balaklava, Yalta, Feodosiya, Kerch) practically free from the HCH pesticides. Their amount varied from 0.016 to 0.189 ng/g. The strong contrast was observed in sediments from the northern-western shelf. The total concentration of HCH had a minimum 1.25 ng/g, average 1.69 ng/g and maximum 2.25 ng/g in Illichevsk port, Odessa bay and Danube Delta region. Among metabolites, α -HCH and β -HCH were slightly

more important than lindane. Hexachlorobenzene (HCB) had a similar spatial distribution with the average 0.221 ng/g, and the maximum 1.300 ng/g was measured in the Danube Delta.

The DDT had extremely high concentration in the NW Shelf sediments contrary to its absence around Crimea. The maximum of total DDTs concentration reported for Odessa Bay exceeded highest level of the Crimean concentrations more than 110 times (Table 3.2.3).

For the NW Shelf of the Black Sea, the historical data from the period 1992-1999 showed rather low concentrations of γ -HCH in the bottom sediments. The average of the data from 182 samples was 0.38 ng/g varying in the range between analytical zero and 4.5 ng/g [2]. This data set showed lindane concentration in zooplankton at an average value of 12.74 ng/g comprising a wide range between zero and 78.92 ng/g. Similar estimation for benthic animals was one order of magnitude lower: with the average of 1.54 ng/g for the range from below the detection limit to 16.2 ng/g (Table 3.2.3). The average concentration of lindane varied within the narrow range of 0.26-0.79 ng/g during 1992-1999 (Table 3.2.3).

The average and maximum concentrations were 2.38, 54.2 ng/g for DDT, 2.65, 54.3 for DDE and 3.08, 48.8 for DDD. They were not significant except in the Danube area where their total average concentration was 20.4 ng/g exceeded the permission level, PL, almost 10 times (Table 3.2.3). Very high level of DDT group was registered in zooplankton organisms, one order of magnitude higher than in sediments. Approximately equal concentrations of DDT and its metabolites appear to indicate a mixture of new and old pollution. In all sub-regions of the NWS the total concentration of DDT averaged over the period 1992-1999 exceeded the PL for bottom sediments.

Table 3.2.3. The average concentration of pesticides in the bottom sediments in the North-Western Shelf of Ukrainian waters, ng/g.

1992-99[2]	Odessa region	Dnieper-Bug	Dniester	Danube	Open part of NWS	Zoo-plankton	Zoo-benthos	Suspended matter
γ -HCH	0.36	0.47	0.33	0.79	0.26	12.74	1.54	0.23
DDT	1.22	1.24	2.81	6.38	2.14	17.11		
DDE	2.35	1.89	3.19	5.30	1.27	19.1		
DDD	1.92	1.16	4.14	8.76	0.56	5.08		
DDTtotal*	5.49	4.29	10.14	20.44	3.97		7.01	345.0
DDTtotal 2000[1]		2.50		19.57				
DDTtotal 2005[3]	18.86	16.52	6.1	6.5	Sevastopol 0.53	Kerch 0		

- total concentration of DDT and its metabolites (sum of DDT, DDE, DDD).

The **bold** values show higher than the permission level (PL) according Neue Niederlandische Liste. Altlasten Spektrum 3/95: total of DDT group is 2.5 ng/g, for γ -HCH is 0.05 ng/g.

Rather moderate level of the total DDT concentration (2.50 ng/g) measured at two samples of bottom sediments in June 2000 near the Tendra split of the Ukrainian Coast compared well with the previous data (Table 3.2.3). The same also occurred in the

Danube region reflecting its traditional high level of DDT pesticides pollution. In the bottom sediments of the Odessa harbor the pesticides measurements in May and October 2004 showed that the γ -HCH content varied from 0.12 to 0.17 ng/g of dry bottom sediments, DDT from 2.91 to 3.24 ng/g, DDE from 0.16 to 0.31 ng/g, and DDD from 0.21 to 0.39 ng/g. The important feature was the predominance of the 'fresh' pollution, and lower level of metabolites than DDT itself.

In the vicinity of Odessa harbor at the depth 24 m, the sediment core was sampled in 6 October 2003 and then split into 10 samples for the analysis of organic contaminants [18]. The most polluted part by pesticides of HCH group was the upper 9 cm. In this thin layer the average concentration of total HCH was 3,59 ng/g (maximum 5,04 ng/g) whereas it was only 0,42 ng/g (max 0,59 ng/g) within the rest of the core. The average value in the whole column of core was 1,69 ng/g. In general the HCH pollution of bottom sediments here was not too high and agreed with the previous data.

An opposite situation was however noted for the DDT group. These pesticides showed extremely high concentration all around the Black sea. The main feature was a "fresh" character of pollution due to dominance of DDT. In the upper 9 cm its concentration reached the extremely high level of 58000 ng/g. Further below in the sediment core DDT concentration decreased almost 2000 times. The total content of the DDT group attained here 63950 ng/g or 25580 PL according the Neue Niederlandische Liste [7].

During the observation at five stations in 4-19 January 2005, an extremely high concentration of DDT and its metabolites were found in the Odessa harbor (72.83 ng/g). Without this extreme value, the average DDT content was only 3.37 ng/g. At nearby stations (Dnieper and Bug Liman), the DDT concentration was also high, 16.52 ng/g, but about three times lower in the Dniester region to the south. In general, one can note that the concentration of DDT group was relatively low in the Danube region during 2005. In the Sevastopol harbor, the total concentration of DDT was also low.

First extended investigation of bottom sediments pollution by wide spectrum of pesticides in the coastal waters of Romania was done in 1993 by sampling at 15 stations from the Danube Delta to the southern border of Romania [8]. The total concentration of HCH group for 4 stations in the Danube Delta was very high and reached the level of 40.0 ng/g with an average value of 13.15 ng/g. The maximum concentration of 3.02 ng/g was recorded near the port Constanta while the average for the marine stations was 1.48 ng/g only. The lindane (γ -HCH) was widely presented in the bottom sediments, especially in the Danube area. Its averages for Danube and the rest of Romanian coast were 8.63 and 0.65 ng/g, respectively. For α -HCH those numbers were 3.70 and 0.36 ng/g; for β -HCH - 0.82 and 0.46 ng/g. Pesticides of DDT group were widely presented in the bottom sediments off Romanian coast in 1993 as well. The total content was very high and reached the level 71.63 ng/g and the average for all fifteen stations was 12.73 ng/g. DDD was the second most abundant after DDT. The most polluted region by DDD was the sediments in the Danube delta (the average 16.5 ng/g, and the maximum 43.1 ng/g) followed by the Constanta port (31.5 ng/g). The average DDT concentration in the Danube delta was 7.08 ng/g and maximum - 20.00 ng/g. The concentration of hexachlorobenzene (HCB) varied from analytical zero to 23.00 ng/g. The most polluted region by HCB was, once again, two stations in the Danube delta and two stations near Constanta. Heptachlor, aldrin, dieldrin and endrin

occurred mainly in the port Constanta with rather low concentrations in the range 0.17-0.25 ng/g.

Three sediment cores were sampled in the Danube delta and near the Constanta port in autumn 2003 [18]. The average concentration of HCH for the whole column of bottom sediments was 1.55 ng/g. Among single metabolites, lindane was less abundant. Among the sampling sites, the Danube delta was generally found much more polluted by HCH due to its high lipid content. In the Romanian shelf sediments DDTs concentration was very high with the average total content of 25.67 ng/g and maximum 83.80 ng/g. In particular, the DDT pollution in the Danube delta exceeded 10-folds the Constanta area with the respective average values of 29.48 ng/g and 2.94 ng/g. Among different forms of DDT group the DDD dominated wherever DDT had 20.3% from the total.

In April, June, July and October 2005 the average level of total concentration of pesticides from DDT group in 34 monitoring samples of bottom sediments was 0.047 ng/g. In most samples the concentration was rather low and only much higher at five stations. Its maximum was recorded in July at 5 m depth near Constanta Sud where total DDT reached 1.26 ng/g and consisted of 0.79 ng/g DDT, 0.43 ng/g DDD and 0.045 ng/g DDE. The lower values for metabolites could be a sign of 'fresh' pollution. The maximum of lindane concentration (0.98 ng/g) was recorded in April 2005 at shallow place in the vicinity of Sf. Gheorghe in the Danube Delta. The second highest concentration 0.82 ng/g was also recorded during the same period in the Danube Delta near Buhaz and varied between 0.002 and 0.37 ng/g in other stations. The average for the whole data set was 0.13 ng/g.

In June, 7, 2006 during the international cruise "Monitoring Survey for the Black Sea - 2006", bottom sediments were sampled along a transect at 1, 10, 20 and 30 nm from the city Constanta. The depth at these points was 14, 36, 45 and 53 m. The total concentration of pesticides of DDT group was rather high and varied between 1.29 and 9.87 ng/g. The highest concentrations (8.71 - 9.87 ng/g) were recorded in the central stations while it was much lower (1.29 - 1.36 ng/g) near both ends. It could be due to the size spectrum of bottom sediments particles. In the central stations, the percentage of small-size fractions less than 65 μm was as high as 42-43.4 % while its contribution was only 32% at other stations. The positive correlation between organic pollutants concentration and increasing the percentage of small particles is well-known.

The Total Organic Carbon (TOC) and Extracted Organic Matter (EOM) contents were also found to be higher at central stations (1.25-1.44 %; 0.110-0.270) with respect to others (0.16-0.61 %; 0.047-0.064 mg/g). Among different forms, the metabolites of DDT took the main role. The average of DDD concentration was 2.82 ng/g, DDE 1.43 ng/g and DDT only 0.46 ng/g. It could be considered as an 'old' pollution by the DDT group. The total HCH concentration in the area near Constanta varied from 0.36 to 2.37 ng/g. As for other pesticides the maximum was recorded in the centre of transect. The mean lindane concentration was only 0.12 ng/g, but β -HCH reached 1.70 ng/g (average 0.77 ng/g) and α -HCH 0.38 ng/g (average 0.17 ng/g). Among other pesticides, the hexachlorobenzene (HCB) occurred in relatively high concentrations up to 0.42 ng/g and the average for four samples was 0.18 ng/g. The others, including *cis* Chlordane, *trans* Chlordane, *trans*-Nonachlor, Heptachlor, Aldrin, Dieldrin, Endrin, Heptachlor epoxide, Methoxychlor, a-Endosulfan, b-Endosulfan and Endosulfan sulfate, all together, did not

exceed 0.20-0.22 ng/g. The total concentration of all pesticides in June 2006 was 3.59; 22.77; 22.32 and 3.67 ng/g at four stations at Constanta transect.

No routine monitoring data were available on pesticides concentration in the bottom sediments along Bulgarian coast line. These substances were not included into the national monitoring program. During international cruise "Assessment of Marine Pollution in the Black Sea Based on the Analysis of Sediment Cores" 24-27 September 2003, three sediment cores were sampled in the vicinity of Bourgas, Varna and Cape Kaliakra at 15 m depth [18]. At all stations the upper 10 cm layer of bottom sediments was found to be most polluted by all types of pesticides, but the pollution level significantly decreased at deeper levels. The average total HCH concentration was measured in the upper layer as 1.27 ng/g and the highest value of 2.12 ng/g was spotted near Bourgas. The pollution level in the vicinity of Varna was comparable to Bourgas, but the Cape Kaliakra site attained significantly lower level of HCH content with an average value of 0.21 ng/g. The different forms of HCH contributed to the pollution at an almost similar rate, but the DDT took 37% of total DDTs. The average DDTs concentration in the Varna core was 8.32 ng/g, in the Bourgas area 1.98 ng/g, and reduced to 0.35 ng/g in the Cape Kaliakra site. Among other pesticides cis-chlordane, trans-nonachlor, heptachlor, aldrin and dieldrin had average concentration 0.01 ng/g, and trans-chlordane was twice higher. Almost all concentration of endrin, α -endosulfan, β -endosulfan and endosulfan sulfate was lower then detection limit (0.001 ng/g).

During international cruise in September 1995 in the Bosphorus outlet area, 10 samples were taken at depth range 80-131 m [8]. Among DDT group all metabolites were presented almost in equal proportion. The total values reached 7.21 ng/g and the average was 3.54 ng/g. The concentration of pesticides from HCH group were about ten times lower in the studied area. The average level of total content for the group was 0.30 ng/g. Similar to the total DDT, its different forms were in relatively equal concentrations. No hexachlorobenzene pollution was recorded in bottom sediments. From other pesticides only aldrin (maximum concentration 0.18 ng/g) and dieldrin (maximum concentration 0.077 ng/g) were recorded in all samples. Endrin was found in a few samples but reached the maximum concentration 0.25 ng/g in one sample. Heptachlor occurred in two places with negligible amount.

In 15-19 June 2006 during the international cruise "Monitoring Survey for the Black Sea - 2006" in vicinity of Georgian towns and rivers Batumi, Kobuleti, Natanebi, Supsa and Poti the bottom sediments were sampled at depth 60 m [9]. The total HCH average concentration for the all sampled sites was 1.01 ng/g. The ratio between metabolites was 1:2.6:7.4 for γ -HCH, α -HCH and β -HCH, respectively. The maximum and minimum HCHs were recorded near Natanebi and Batumi. Similar to other regions, DDTs concentration along Georgian coast was much higher in comparison with HCH. Maximum DDT total concentration reached 16.55 ng/g (6.6 times of the PL) close to Kobuleti. The ratio of metabolites was approximately 1:3:15 for DDT, DDE and DDD. Other chlorinated hydrocarbons were found at lower quantities: HCB (maximum 0.42 ng/g), cis-chlordane (0.04 ng/g), trans-chlordane (0.09 ng/g), trans-nonachlor (0.003 ng/g), heptachlor (0.02 ng/g), aldrin (0.002 ng/g), dieldrin (0.06 ng/g), endrin (0.04 ng/g), heptachlor epoxide (0.02 ng/g), methoxychlor (0.02 ng/g), α -endosulfan (0.02 ng/g), β -endosulfan (0.05 ng/g), endosulfan sulfate (0.05 ng/g).

Along the Russian coast, five samples of bottom sediments were taken from the depth 8 m inside of port Sochi, and 25-40 m from other sites in the area between cities Sochi and Adler close to Georgian border during the December 1995 cruise. The maximum of total content of HCH group was 0.81 ng/g. Among their metabolites the β -HCH dominated. The concentration of γ -HCH exceeded the permission level (PL) for bottom sediments almost two times [7]. The DDTs were much more abundant in the bottom sediments. Their total concentration reached 12.36 ng/g (4.9 PL). In contrary with HCH, in the metabolites structure the DDT played main role and it can be considered as a "fresh" pollution.

Table 3.2.4. The concentration (ng/g) of organic pollutants in biota and bottom sediments along the Russian coast in August-September 2003.

2003	Kerch Strait	Anapa	Novorossiysk	Gelendzhik+ Blue	Arkhipo-Osipovka	Tuapse	Lazarevskaya	Sochi	Adler
HCHtotal	0.14	0.05	0	0.37	1.29	0.75	0.81	0.98	0.94
HCHbiota**	3.11			2.10					
DDT total	0.86	0.33	1.370	8.73*	5.29*	2.04	4.83*	8.40*	5.82*
DDTbiota	0.75			3.74					
Other Pesticides	0.20	0	0	0.10	0.38	0.11	0.31	0.24	0.18

- The **bold** value exceeds the permission level (PL) according Neue Niederlandische Liste. Altlasten Spektrum 3/95: Total of DDT group is 2.5 ng/g, for γ -HCH is 0.05 ng/g[7].
- ** biota - Bivalvia.

Along the Russian coastline, bottom sediment pollution by organic substances was investigated in the shallow waters in June-July 2003. In the Kerch Strait near the island Tuzla, the concentration of HCH in the bottom sediments was under the detection limit (0.05 ng/g of dry material). Slightly to the south at the anchor place near the Cape Panagia, the concentration of α -HCH (0.05 ng/g) and β -HCH (0.09 ng/g) exceeded the detection limit (Table 3.2.4). At the same time all forms of HCH were 10-20 times higher in the body of bottom invertebrates; α -HCH 0.56 ng/g, β -HCH 1.99 ng/g, γ -HCH 0.56 ng/g (maximum). Not all forms of the DDT group existed in bottom sediments at significant values, but 4,4 DDE (0.60 ng/g) and 4,4 DDD (0.45 ng/g) reached rather high concentrations. This type of pesticides was however found only in a minor level in the body of mollusks in this area.

Other types of chlorinated hydrocarbons, namely heptachlor, aldrin, octachlorstyrene, heptachlorepoxyde, trans-chlordane, cis-chlordane, trans-nonachlor, cis-nonachlor, photo-mirex and mirex were not recorded in sediments at this time, even if their heavy agricultural use around the Azov Sea. The only hexachlorobenzene was observed in bottom sediments near the island Tuzla with concentration 0.20 ng/g and few times more in the tissue of the benthic animals - 0.79 ng/g.

Slightly to the south along the coastal line (in shallow waters) at the traverse of the Bugaz Lagoon, β -HCH (0.05 ng/g), 4,4 DDE (0.16 ng/g) and 4,4 DDD (0.09 ng/g) were detected. Near the town Anapa only 4,4 DDE (0.22 ng/g) was found in sediments. In the vicinity of harbor Kabardinka, near Novorossiysk, almost all forms of the group DDT

were presented in rather significant quantity - 2,4 DDE (0.06), 4,4 DDE (0.48), 2,4 DDD (0.24), 4,4 DDD (0.53), 2,4 DDT (0.06 ng/g). Other pesticides were below the detection limit. From two places close to the Gelendzhik Bay and Blue Bay only the latter had a visible content in sediments (α -HCH 0.08 ng/g, β -HCH 0.67 ng/g) and a high level of this group was recorded in the tissues of bottom invertebrates near Gelendzhik Bay: α -HCH 0.57 ng/g, β -HCH 1.44 ng/g, γ -HCH 0.09 ng/g. Again, sediments in the Blue Bay consisted of very high concentrations of DDT group: 2,4 DDE 0.21 ng/g, 4,4 DDE 5.21 ng/g, 2,4 DDD 1.21 ng/g, 4,4 DDD 5.04 ng/g, 2,4 DDT 0.34 ng/g, 4,4 DDT 1.99 ng/g. Maximum total DDT level of 14.00 ng/g was recorded for the whole Russian coast. In the Gelendzhik Bay these pesticides were found approximately at equal levels in bottom sediments and in biota but they were about five times lower than in the Blue Bay. Among other pesticides, only hexachlorobenzene was in relatively significant concentrations in bottom sediments (0.09 ng/g) and biota (0.20 ng/g). A slightly to south along coast in vicinity of the village Arkhipo-Osipovka the content of pesticides in bottom sediments was rather high not only for the groups HCH (α -HCH 0.05 ng/g, β -HCH 1.24 ng/g) and DDT (2,4 DDE 0.09 ng/g, 4,4 DDE 1.60 ng/g, 2,4 DDD 0.58 ng/g, 4,4 DDD 2.64 ng/g, 4,4 DDT 0.39 ng/g), but for also for phenylpolychloride (0.12 ng/g), hexachlorobenzene (0.15 ng/g) and cis-nonachlor (0.11 ng/g).

In shallow waters near the town Tuapse, the concentration of pesticides from the HCH group was not too high, α -HCH 0.08 ng/g, β -HCH 0.67 ng/g. Almost all forms of DDT were marked in bottom sediments with the maximum level 1.85 ng/g for 4,4 DDD. Also minor quantity of phenylpolychloride (0.07 ng/g) and hexachlorobenzene (0.16 ng/g) were found in a single sample. Concentrations of α -HCH (max. 0.14 ng/g) and β -HCH (max. 1.15 ng/g) were not high in the bottom sediments near "Lazarevskaya". The DDT group was much higher in 4 samples; the maximum reached 0.08 ng/g for 2,4 DDE, 1.70 ng/g for 4,4 DDE, 1.09 ng/g for 2,4 DDD, 4.40 ng/g for 4,4 DDD, 0.10 ng/g for 2,4 DDT and 0.68 ng/g for 4,4 DDT. The average level exceeded twice the permission level for the bottom sediments. Like in the other parts of the Russian coast, the phenylpolychloride (0.07-0.10 ng/g) and hexachlorobenzene (0.09-0.46 ng/g) were also detected in the samples. For the area around the town Sochi, the concentration of HCH in 5 samples was not high and the variation of the data was very small suggesting a rather uniform spatial distribution in this part of the basin: α -HCH varied from 0.10 to 0.14 ng/g; β -HCH varied from 0.30 to 1.16 ng/g in bottom sediments. Among DDT group, some parts of the area showed abnormally high peaks. For instance, the maximum of 4,4 DDE (3.960 ng/g) and 4,4 DDT (5.100 ng/g) were recorded in the sediments inside of the Sochi harbor. At the same time maximum 4,4 DDD concentration (6.49 ng/g) was recorded in another sample. In general, the DDT was very high in this area and comparable with the Gelendzhik and Blue Bay areas. Among other pesticides the phenylpolychloride (0.07 ng/g) and hexachlorobenzene (0.07-0.71 ng/g) were found at quantities above the detection limit. The part of the area bordering Georgia often considered as highly polluted due to high discharge from the river Mzumta. Nevertheless, the concentration of pesticides was not too high. The content of α -HCH (0.18-0.24 ng/g) and β -HCH (0.58-0.85 ng/g) was similar to other parts of this area. The same also applies for the DDT metabolites with the exception of 4,4 DDD showing a maximum 5.81 ng/g, and consequently total DDT content reached 10.28 ng/g. The hexachlorobenzene was presented in all 4 samples (0.05-0.16 ng/g, average level 0.09 ng/g); phenylpolychloride - only in two (0.17-0.19 ng/g).

The pesticides content in bottom sediments along Russian coast had several main features during August-September 2003. The concentration of γ -HCH (lindane) never reached the detection limit in sediments, but this pesticide were found at large quantities in bodies of bottom invertebrates. The other isomers of HCH were widely distributed but never occurred at high quantities; maximum was less 2.00 ng/g. The DDT pesticides occurred more often at high concentration especially in the south. The maximum reached 14.00 ng/g and was beyond the permission level about 3.6 times. The average values for DDT and its metabolites (DDT 1.10 ng/g, DDE 3.07 ng/g and DDD 1.29 ng/g) clearly showed the dominance of metabolites over DDT that suggested an old pollution. Among others pesticides, only hexachlorobenzene and phenylpolychloride were generally observed in minor quantities, and cis-nonachlor and cis-chlordane were detected in bottom sediments only once.

In August and October 2004 the study of bottom sediment pollution was performed along the entire Russian coasts. In comparison with the similar investigations in 2004, a significant increase in the level of pesticides pollution was recorded in bottom sediments of the Novorossiysk, Tuapse and Sochi harbors. The maximum concentration of γ -HCH and total DDT reached 0,50 ng/g (9,8 PL) and 155 ng/g (61,9 PL), respectively.

Summary: Among the chlorinated pesticides, the HCHs and DDTs were most important pollutant in bottom sediments of the Black Sea during the last several decades. They both belong to the group of very dangerous chemical substances and their consumption was prohibited long time ago in the Black Sea basin. Nevertheless, their huge amount stored in the agricultural fields or old dilapidated storage places in the past are still the source of pollution today. In the absence of the quality standards for sediment pollution in the Black Sea riparian countries, the Netherlands Permission Levels (PL) for pollutants in the sediments [7] are used as the guidelines of the pollution levels in the Black Sea sediments. The permission level is 0.05 ng/g for lindane and 2.5 ng/g for DDTs total. Based on the Russian standards for the level of Extremely High Pollution (EHP) that is "5 times higher than the level of Maximum Allowed Concentration", the EHP levels are considered to be 0.25 ng/g for γ -HCH and 12.5 ng/g for DDTs total.

HCH pollution. Maximum lindane concentration exceeded the EHP level practically in all measurements performed during the last 13 years (Fig. 3.2.1). Each country had specific hot spots with very high lindane concentration in sediments due to fresh lindane discharges into the sea. The highest values of 4.5 ng/g in Ukrainian shelf in 1992 and 29.0 ng/g in Romanian coastal area in 1993 were never repeated again despite that highly polluted lindane patches exceeding the EHP level were recorded in Romania (the Danube Delta and port Constanta in 2003, the Danube Delta in 2005), Bulgaria (Varna and Bourgas Bays in 2003), Turkey (Bosporus Outlet in 1995), Russia (Kerch Strait in 2003, Novorossiysk harbor and estuary river Sochi in 2004), and Ukraine (the Danube Delta and Odessa Bay in 1995, Odessa Bay in 2003). Maximum concentrations of HCH metabolites were usually comparable with lindane (Table 3.2.5).

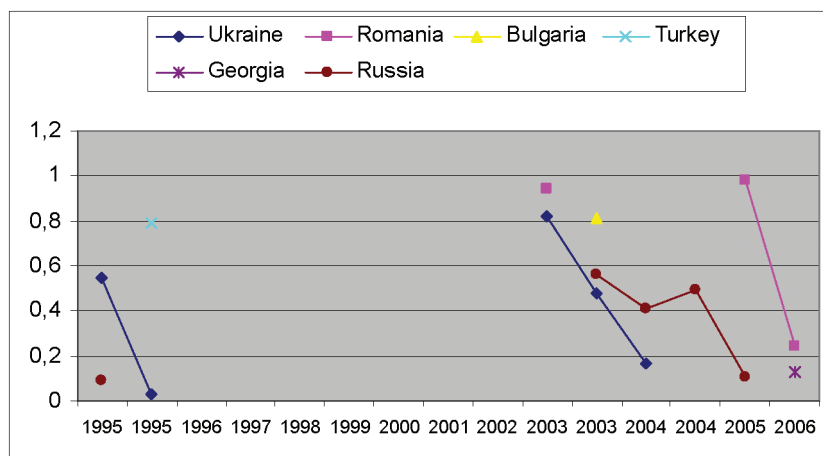


Fig. 3.2.1. The maximum concentration of γ -HCH (ng/g) in the different regions of the Black Sea (the maximums 4.5 ng/g in Ukrainian waters 1992 and 29.0 ng/g in Romanian water 1993 are not presented in the figure). The duplication of some years means different seasons of expeditions.

The average γ -HCH concentration was about two-fold lower than its extremes, nevertheless many average data exceed the PL (Fig. 3.2.2 and Table 3.2.6). Based on a rather sparse data set, it is difficult to assess the long-term trend of γ -HCH concentration in sediments of the basin. Taking into account the historical data, it is appropriate to set $EHP = 0.25$ ng/g as a measure of extremely high local pollution of γ -HCH.

Table 3.2.5. Maximum and mean concentration of pesticides (ng/g), and number of measurements (in parentheses) in the bottom sediments of the Black Sea in 1993 – 2006.

Project	Year	Region	γ -HCH	α -HCH	β -HCH	HCH total	DDT	DDE	DDD	DDT total	HCB*	Depth range
Monitoring [2]	1992-1999	Ukraine	4.5/0.38 (182)	-	-	-	54.2/2.38 (182)	54.3/2.65 (182)	48.8/3.08 (182)	-	-	-
Screening [8]	1995	Ukraine, NW Shelf	0.55/0.33 (4)	1.10/0.74 (4)	0.90/0.63 (4)	2.25/1.69 (4)	20.00/11.74 (4)	4.47/2.56 (4)	40.50/23.68 (4)	65.0/38.0 (4)	1.30/0.54 (4)	3-17 m
Screening [8]	1995	Ukraine, Crimea	0.027/0.016 (6)	0.048/0.015 (6)	0.14/0.038	0.19/0.07	0.002/0.01 (6)	0.28/0.13 (6)	0.38/0.18 (6)	0.59/0.31 (6)	0.024/0.01 (6)	6-78 m
Monitoring	2000	Ukraine	-	-	-	-	-	-	-	19.6/11.0 (2)	-	18-23 m
Screening [18]	2003	Ukraine (0-9 cm)	0.82/0.55 (4)	0.56/0.43 (4)	3.90/2.60 (4)	5.04/3.59 (4)	58000/16224 (4)	2840815 (4)	3110/1155 (4)	63950/18194 (4)	0.42/0.34 (4)	24.0
Screening [18]	2003	Ukraine (9-36 cm)	0.48/0.31 (6)	0.09/0.06 (6)	0.08/0.05 (6)	0.59/0.42 (6)	29.60/8.58 (6)	5.20/1.55 (6)	6.90/2.77 (6)	41.7/12.9 (6)	0.33/0.20 (6)	24.0
Monitoring	2004	Russia Odessa	0.17/- (-)	-	-	-	3.24/- (-)	0.31/- (-)	0.39/- (-)	-	-	-
Monitoring	2005	Ukraine	-	-	-	-	-	-	-	72.8/12.4 (10)	-	2-23 m
Screening [8]	1993	Romania	29.00/2.78 (15)	8.60/1.25 (15)	2.40/0.56 (15)	40.00/4.59 (15)	20.00/2.43 (15)	8.53/2.28 (15)	43.18/0.2 (15)	71.6/12.7 (15)	23.00/2.28 (15)	-
Screening [18]	2003	Romania	0.94/0.37 (27)	2.10/0.50 (27)	2.00/0.71 (27)	5.04/1.55 (59)	41.20/5.20 (27)	7.00/2.61 (27)	57.00/17.86 (27)	83.80/25.67 (27)	22.00/1.87 (27)	14-18 m
Monitoring	2005	Romania	0.98/0.13 (34)	-	-	-	0.79/0.03 (34)	0.05/0.004 (34)	0.43/0.014 (34)	1.26/0.047 (34)	-	0-20 m
Screening [9]	2006	Romania	0.24/0.12 (4)	0.38/0.17 (4)	1.70/0.77 (4)	2.37/1.08 (4)	0.89/0.46 (4)	2.78/1.42 (4)	5.10/2.82 (4)	9.87/5.31 (4)	0.42/0.18 (4)	14-53 m
Screening [18]	2003	Bulgaria	0.81/0.23 (28)	0.42/0.18 (28)	0.90/0.32 (28)	2.12/0.74 (28)	5.23/1.08 (28)	3.9/1.24 (28)	7.0/1.87 (28)	14.0/4.18 (28)	10.00/0.94 (28)	15.0-15.8 m
Screening [8]	1995	Turkey	0.79/0.14 (10)	0.21/0.09 (10)	0.22/0.07 (10)	1.10/0.30 (10)	1.54/1.15 (4)	2.85/1.49 (7)	4.32/2.03 (10)	7.21/3.54 (10)	0.25/0.09 (10)	80-131 m

Project	Year	Region	γ -HCH	α -HCH	β -HCH	HCH total	DDT	DDE	DDD	DDT total	HCB*	Depth range
Screening [9]	2006	Georgia	0.13/0.09 (5)	0.41/0.23 (5)	1.10/0.67	1.63/1.01	0.89/0.41 (5)	2.78/1.10 (5)	13.3/3.35 (5)	16.55/5.4 (5)	0.42/0.17 (5)	60 m
Screening [8]	1995	Russia, Sochi	0.09/0.05 (5)	0.19/0.15 (5)	0.56/0.36 (5)	0.81/0.57 (5)	8.69/3.43 (5)	2.74/1.60 (5)	5.56/2.86 (5)	12.36/7.8 (9) (5)	0.26/0.08 (5)	8-40 m
Aero-Visual Monitoring	2003	Russia**	0.56/0.03 (25)	0.57/0.13/25	1.99/0.68 (25)	3.11/0.83 (25)	5.73/0.71 (6)	5.42/1.25 (25)	7.88/2.82 (25)	14.0/4.78 (25)	1.26/0.20 (25)	6-100 m
Aero-Visual Monitoring	2004 August	Russia	0.41/0.04 (22)	1.07/0.20 (22)	1.57/0.64 (22)	3.06/0.88 (22)	25.87/4.84 (22)	10.97/2.98 (22)	72.79/9.53 (22)	89.0/17.34 (22)	1.30/0.43 (22)	6-68 m
Aero-Visual Monitoring	2004 October	Russia	0.49/0.07 (12)	0.44/0.15 (12)	0.89/0.40 (12)	1.63/0.63 (12)	28.43/11.89 (12)	40.24/9.38 (12)	120.13/28.9 (12)	154.7/50.17 (12)	0.89/0.30 (12)	5-25 m
Aero-Visual Monitoring	2005 July	Russia	0.11/0.04 (8)	0.32/0.15 (8)	0.69/0.41 (8)	0.86/0.59 (8)	2.07/0.82 (8)	7.20/3.24 (8)	8.82/3.96 (8)	18.09/8.0 (8)	0.50/0.25 (8)	9-52 m

HCB* - hexachlorobenzene

Russia** - averaged for all Russian coastal waters in 2003.

Table. 3.2.6. The repetitions of high γ -HCH concentration in the bottom sediments exceeds the PL 0.05 ng/g in the different sets of samples (in per cent).

Project	Year	Region	Max γ -HCH (ng/g)	Average γ -HCH (ng/g)	γ -HCH > PL 0.05 ng/g(%)
Screening	1995	Ukraine, NW Shelf	0.55	0.33	100
Screening	1995	Ukraine, Crimea	0.027	0.016	0
Screening	2003	Ukraine (0-9 cm)	0.82	0.55	100
Screening	2003	Ukraine (9-36 cm)	0.48	0.31	100
Screening	1993	Romania	29.0	2.78	100
Screening	2003	Romania	0.94	0.37	100
Monitoring	2005	Romania	0.98	0.13	41.1
Screening	2006	Romania	0.24	0.12	75
Screening	2003	Bulgaria	0.81	0.23	100
Screening	1995	Turkey	0.79	0.14	50
Screening	2006	Georgia	0.13	0.09	80
Screening	1995	Russia, Sochi	0.09	0.05	50
Monitoring	2003	Russia	0.56	0.03	4
Monitoring	2004	Russia, Southern	0.41	0.04	22.7
Monitoring	2004	Russia, Northern	0.49	0.07	50
Monitoring	2005	Russia	0.11	0.04	50

DDT pollution. Similar to the HCH group, maximum concentration of the DDTs group in sediments exceeded the EHP level of 12.5 ng/g practically at all regions of the Black Sea (Fig. 3.2.3). Enormously high pollution (63950 ng/g) in the Odessa area in 2003 can only be explained as an accidental event. Nevertheless, other sites in coastal zones around the Black Sea were also highly polluted by DDTs. Those "hot spots" are - Danube Delta, Odessa Bay and Illichevsk port (1995), Danube River mouth (2000), Odessa Bay (2003), Odessa and Uzhnui ports, Dniepr and South Bug Mouth (2005) in Ukraine; the Danube Delta, port Constanta and Sinoe (1993), Sf.Gheorghe and Sulina (2003) in Romania; - Varna (2003) in Bulgaria; Kobuleti (2006) in Georgia; Sochi port and Adler Canyon (1995), Sochi harbour, Sochi river estuary, Tuapse river estuary, Loo village, Blue Bight (Gelendzhik), Novorossiysk harbor (2003) in Russia (Fig. 3.2.4).

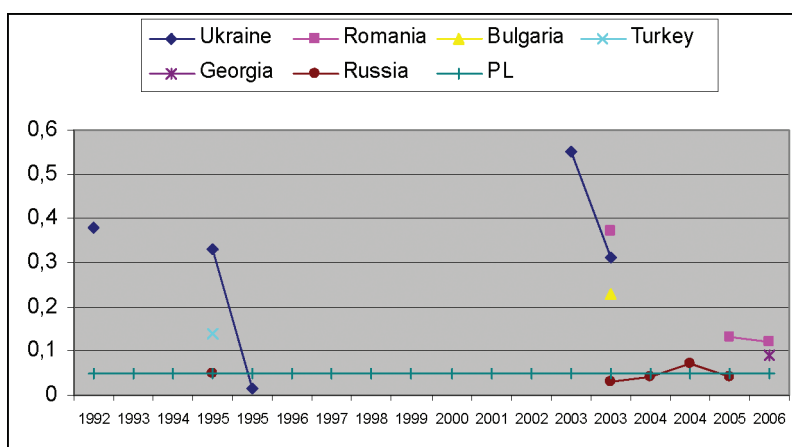


Fig. 3.2.2. The repetition factor of exceeding of PL by average concentration of γ -HCH (ng/g) in the bottom sediments of different regions of the Black Sea. The outstanding 2.78 ng/g in Romania 1993 is not presented in the figure. The duplication of some years means different seasons of expeditions. The Permission Level is 0.05 ng/g.

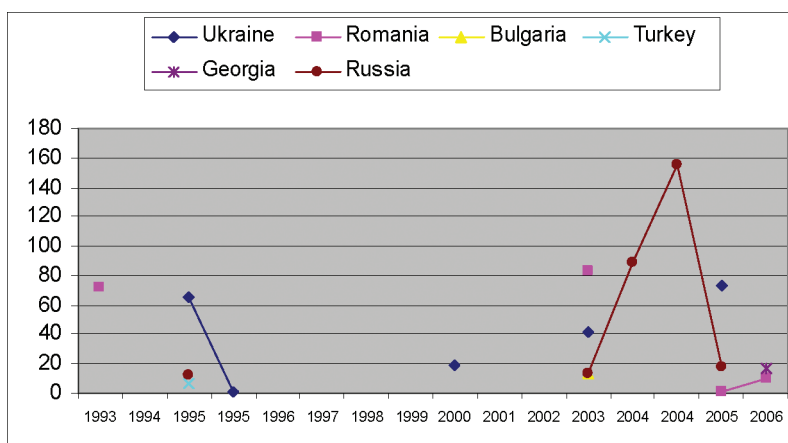


Fig. 3.2.3. The maximum concentration of pesticides DDTs group (ng/g) in the bottom sediments of different regions of the Black Sea (the maximum 63950 ng/g in Ukrainian waters 2003 is not presented in the figure). The duplication of some years means different seasons of expeditions. Total number of analyzed bottom sediments samples is 217.



Fig. 3.2.4. The "hot spot" sites in the coastal zone of the Black Sea with total DDTs concentration in sediments exceeding the level of Extremely High Pollution (12.5 ng/g) level during 1993-2006.

Table. 3.2.7. The repetitions of high DDTs concentration in the bottom sediments exceeds the PL 2.5 ng/g in the different sets of samples (in per cent).

Project	Year	Region	Max DDTs (ng/g)	Average DDTs (ng/g)	DDTs > PL 2.5 ng/g(%)
Screening	1995	Ukraine, NW Shelf	64.97	37.97	100
Screening	1995	Ukraine, Crimea	0.59	0.31	0
Monitoring	2000	Ukraine	19.57	11.03	100
Screening	2003	Ukraine (0-9 cm)	63950	18194	100
Screening	2003	Ukraine (9-36 cm)	41.7	12.9	83.3
Monitoring	2005	Ukraine	72.83	12.40	40
Screening	1993	Romania	71.63	12.73	100
Screening	2003	Romania	83.8	25.67	77.8
Monitoring	2005	Romania	1.26	0.05	0
Screening	2006	Romania	9.87	5.31	50
Screening	2003	Bulgaria	14.03	4.18	46.4
Screening	1995	Turkey	7.21	3.54	70
Screening	2006	Georgia	16.55	5.37	60
Screening	1995	Russia, Sochi	12.36	7.89	100
Monitoring	2003	Russia	14.03	4.18	64.0
Monitoring	2004	Russia, Southern	89.0	17.34	81.8
Monitoring	2004	Russia, Northern	154.71	50.17	83.8
Monitoring	2005	Russia	18.09	8.01	87.5

High level of pollution by pesticides from DDTs group in bottom sediments are also clearly evident in the data set consisting of 222 samples since 1995. Almost all samples collected in the coastal zone around the Black Sea showed total concentration of pesticides of DDT group higher than 50% of the Permission Level. The relatively low concentrations in sediments around the Crimea peninsula should be related to their low level discharges from local rivers into the sea, even though the usage of pesticides in grape and wine manufacturing is common in the region. Along the Russian coast with highly developed wine industry (e.g. Gelendzhik region), the pollution by DDTs pesticides in general much higher. When the entire data set was taken into account, 61.3% of samples contained the DDTs concentration comparable with its PL level of 2.5 ng/g (Table 3.2.7).

As a conclusion, practically the entire coastal waters around the sea contained a very high level of DDTs pollution in bottom sediments without any clear indication of reduction in such highly dangerous anthropogenic pollution.

Other pesticides were close to their detection limits for all costal zones of the Black Sea, except rather high concentrations of hexachlorobenzene in sediments along the Romanian and Bulgarian coasts (Table 3.2.7). It could be clear the absence of worries concerning different marked in the bottom sediments usually. The content of these modern chlorinated pesticides in the Black Sea therefore contradicted with high concentration of lindane and DDT.

3.3. The State Of Trace Metals

Alexander Korshenko

State Oceanographic Institute, Moscow, RUSSIA

Yury Denga

Ukrainian Scientific Centre of the Ecology of Sea, Odessa, UKRAINE

B.Gvakharia and Nino Machitadze

"Gamma", Tbilisi, GEORGIA

Andra Oros

National Institute for Marine Research and Development, Constanta, ROMANIA

3.3.1. Ukrainian sector of the Black Sea - Northwestern region

Water: The most recent trace metals measurements in Ukrainian coastal waters were performed within the framework of the marine ecological monitoring programme in December 2004-January 2005. These measurements clearly indicated a low level trace metal pollution in coastal waters. The trace metal contents at all measurement sites were typically one or two order of magnitude below the Maximum Allowed Concentration (MAC) accepted for Ukrainian waters (Table 3.3.1).

According to the earlier measurements conducted during 1995-2000, trace metal concentrations in different marine waters of the northwestern Black Sea were also found to be rather low. These concentrations represented the sum of the dissolved and suspended forms due to the conservation of samples aboard by nitric acid. A summary of the trace metal levels are provided below.

Cadmium: The contamination of marine waters by cadmium could be evaluated as insignificant since its concentration was persistently 30-50 times lower than the MAC value in all investigated regions, except the dredged materials dumping site close to Odessa where maximum cadmium concentration near the bottom reached 0,56 $\mu\text{g/l}$ in 1999 (Fig. 3.3.1).

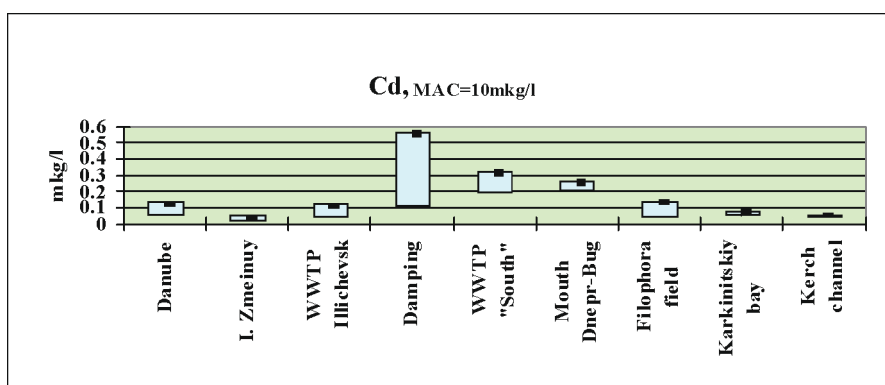


Fig. 3.3.1 Concentration of cadmium ($\mu\text{g/l}$) in Ukrainian marine waters in 1995-2000.

Mercury: Like cadmium, mercury concentration did not exceed 0.1 MAC (Fig. 3.3.2) except the damping sites where it was roughly 0.2 MAC.

Lead: Maximum lead concentration of 17.0 µg/l exceeded 1 MAC level by 1.7 times only at the Waste Waters Treatment Plant (WWTP) site of the town Illiechevsk in 2000 (Fig. 3.3.3). In other regions of the Black Sea, concentration in marine waters varied mainly in the range 0.5-2.0 µg/l with slightly higher values in the Danube discharge region (3.1 µg/l) and Dnieper- South Bug lagoon (5.2 µg/l).

Table 3.3.1. The trace metals concentration (µg/l) in Ukrainian waters of the Black Sea in December 2004 - January 2005 (25th cruise of R/V "Vladimir Parshin").

No of station	Areas	Hg	Cd	Co	Cu	Pb	Zn	As	Fe
MAC (µg/l)	0,1	10	5	5	10	50	10	50	
1	External raid of Odessa port	0,012	0,06	<0,5	3,0	5,8	11,3	1,8	<50
3	Waste waters discharge "North" in Odessa	0,012	0,09	<0,5	1,0	9,3	7,1	1,6	<50
4	Mouth of port Yuzhny in Odessa Bay	<0,010	<0,05	<0,5	1,8	1,7	2,0	2,0	<50
6	Mouth of Dnieper -Bug lagoon	<0,010	<0,05	<0,5	2,0	1,9	5,8	1,2	<50
8	Odessa shallows	<0,010	<0,05	<0,5	0,6	2,5	3,5	1,5	<50
10	Odessa shallows	<0,010	<0,05	<0,5	0,9	<1,0	2,1	1,6	<50
11	Place of damping	<0,010	<0,05	<0,5	0,4	<1,0	1,4	2,0	<50
12	Waste waters discharge "Sourth" in Odessa	0,011	0,08	<0,5	2,0	<1,0	2,8	1,4	<50
13	Mouth of port Illiechevsk in Odessa Bay	<0,010	0,08	<0,5	0,7	<1,0	0,5	1,9	<50
14	Place of damping	<0,010	0,15	<0,5	2,1	1,7	3,8	2,2	<50
15	Mouth of Dniestr lagoon	<0,010	<0,05	<0,5	0,7	<1,0	7,4	1,2	<50
24	Centre of Northern-Western shelf	<0,010	0,07	<0,5	2,3	<1,0	2,1	<1,0	<50
30	Mouth of Danube (north)	<0,010	<0,05	<0,5	1,7	1,2	4,9	1,4	<50
56	Cup Tarkhankut in Crimea	<0,010	0,06	<0,5	0,7	<1,0	5,4	2,0	<50
60	Yalta	<0,010	<0,05	<0,5	0,3	<1,0	1,7	<1,0	<50
73	Kerch Strait (centre)	<0,010	<0,05	<0,5	0,7	<1,0	2,5	1,2	<50
75	Kerch Strait (exit)	<0,010	<0,05	<0,5	1,3	<1,0	4,1	1,4	<50

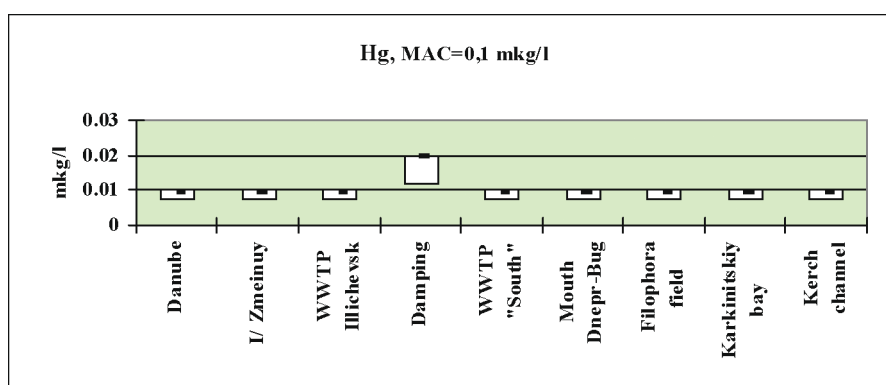


Fig. 3.3.2 Concentration of mercury (µg/l) in Ukrainian marine waters in 1995-2000.

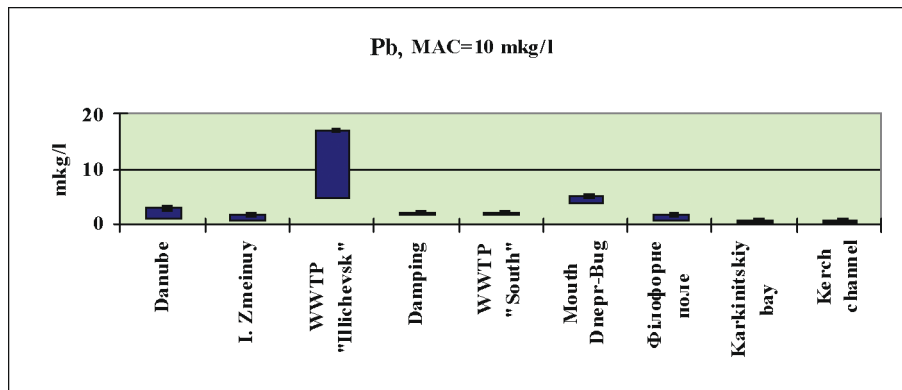


Fig. 3.3.3. Concentration of lead ($\mu\text{g/l}$) in Ukrainian marine waters in 1995-2000.

Zinc: Concentration of zinc higher than 1 MAC was observed in the dumping area ($145 \mu\text{g/l}$) and the Illiehevsk WWTP site, where the maximum concentration ($823 \mu\text{g/l}$, more than 16 MAC) was measured in 2000 (Fig. 3.3.4). In comparison with other areas, zinc concentration attained slightly higher values of $20 \mu\text{g/l}$ and $30 \mu\text{g/l}$ in the Danube and Dniepr estuaries, respectively.

Copper: In four of the total 11 measurement sites, copper concentration in marine water was higher than 1 MAC. These sites are as follows: near Odessa WWTP "South" (1.4 MAC), dumping site (1.6 MAC), Dnieper and Bug estuarine zone (5.0 MAC) and the Illiehevsk WWTP (30 MAC) (Fig. 3.3.5).

Arsenic: Concentration of this metal in marine waters was insignificant and did not exceed 1 MAC. In comparison with other places, the arsenic content was slightly higher in the Danube estuarine waters and in Karkinit'skiy Gulf (Fig. 3.3.6).

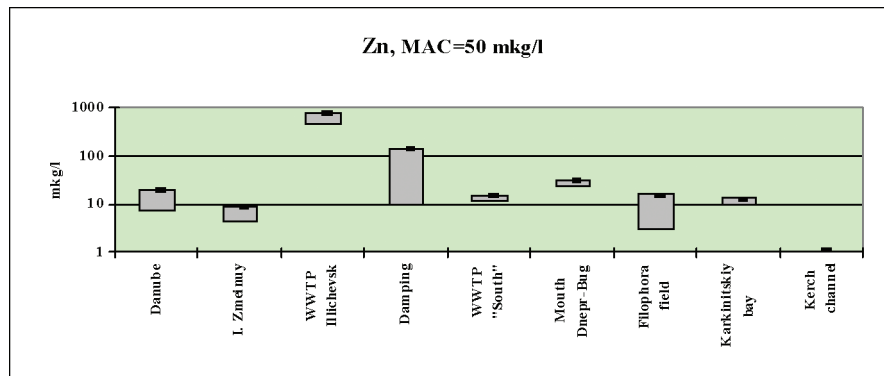


Fig. 3.3.4 Concentration of zinc ($\mu\text{g/l}$) in Ukrainian marine waters in 1995-2000.

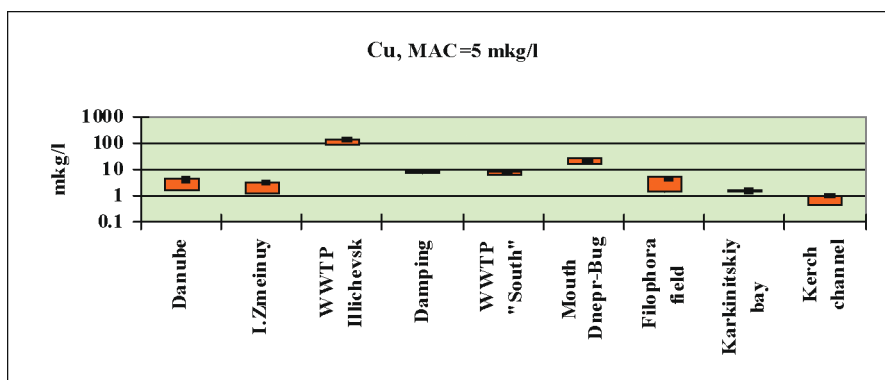


Fig. 3.3.5 Concentration of copper ($\mu\text{g/l}$) in Ukrainian marine waters in 1995-2000.

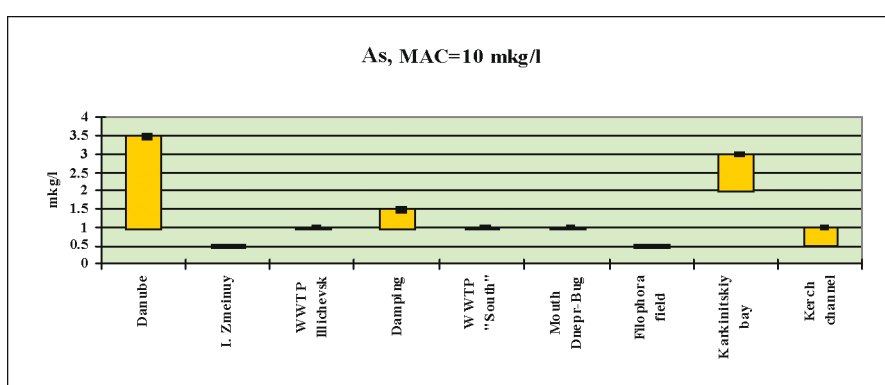


Fig. 3.3.6 Concentration of arsenic ($\mu\text{g/l}$) in Ukrainian marine waters in 1995-2000.

Chromium. Chromium concentration was below 1 MAC level at all measurement sites with the highest concentration of 2.8 $\mu\text{g/l}$ in the Danube discharge area and 1.0 $\mu\text{g/l}$ in the Odessa damping site and the WWTP "South" site (Fig. 3.3.7).

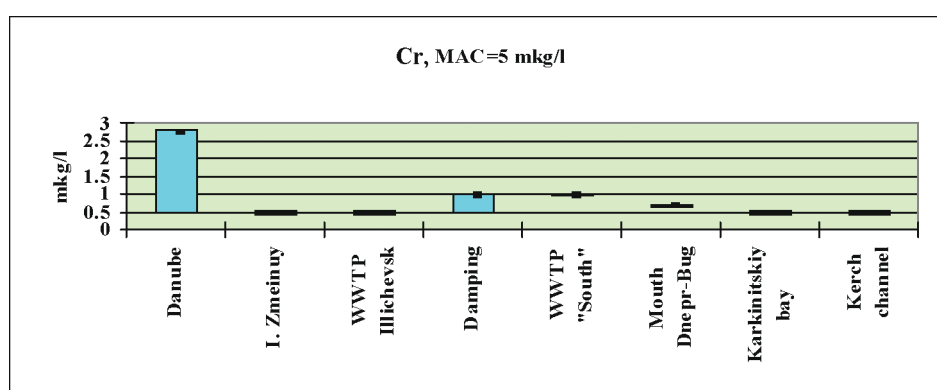


Fig. 3.3.7 Concentration of chromium ($\mu\text{g/l}$) in Ukrainian marine waters in 1995-2000.

In summary, higher metal concentrations were observed mostly in coastal areas with clear anthropogenic influence from the main land-base sources. They were, however, lower than the MAC levels. In the open areas of the Black Sea, they were close to their natural background values.

Bottom Sediments: The current data on metals concentration in the bottom sediments in the Ukrainian coastal zone of the northwestern Black Sea were obtained during the R/V "Vladimir Parshin" cruise in December 2004-January 2005. In contradiction with marine waters, bottom sediments often showed a rather high level metal pollution with maximum concentrations measured in the Danube discharge region (Table 3.3.2). Even though **mercury** content, known to be the most toxic metal, never exceeded the Permission Level (PL), it increased significantly close to the Odessa port, the vicinity of Danube estuarine zone, and the Crimean cities Sevastopol and Alushta. **Cadmium** concentration varied in the range from 0.1 PL to 0.7 PL measured in the Danube discharge region. A similar distribution was also noted for **cobalt** where data from different sites varied between 3.1 and 12.1 µg/g (0.2-0.6 PL).

On the contrary, **copper** concentration in bottom sediments, in general, was high and exceeded the PL in 8 cases; close to the Odessa port (82 µg/g), the dumping site, the Danube discharge area, and the vicinity of Crimean towns Sevastopol, Balaklava, Yalta and Alushta. The average for the Ukrainian shelf was 26.36 µg/g. **Lead** concentration varied in the range of 5.2 - 46.2 µg/g, and the average was 20.92 µg/g. This level was significantly less than the threshold. **Zinc** concentration exceeded the PL more than twice in the dumping place and only slightly in the Danube estuarine region. The North-Western shelf was not found to be polluted by **arsenic**. Its content was high only near Crimea and in the Kerch Strait. Pollution of bottom sediments by **chromium** exceeded the PL at several sites. Maximum level of metal pollution was noted for **nickel**. Its content varied from 7.0 up to 71.7 µg/g with an average value of 31.06 µg/g. Its concentration therefore was higher than its PL in 16 cases from 39 samples (41%).

Table 3.3.2. The trace metals concentration (µg/g) in the bottom sediments of Ukrainian part of the Black Sea in December 2004 - January 2005 (25 cruise of R/V "Vladimir Parshin").

No of station	Areas	Hg	Cd	Co	Cu	Pb	Zn	As	Cr	Ni	Al*
PL (µg/g) [7]		0.3	0.8	20	35	85	140	29	100	35	n.a
1	External raid of Odessa port	0.150	0.49	7.3	81.9	26.2	117	9.00	164	27.0	28900
3	Waste waters discharge "North" in Odessa	0.037	0.20	3.1	6.30	5.20	38.0	6.20	12.4	7.0	5640
4	Mouth of port Yuzhny in Odessa Bay	0.034	0.41	8.1	34.8	25.4	97.6	11.4	63.8	43.6	30300
6	Mouth of Dnieper - Bug lagoon	0.034	0.35	4.7	19.8	12.1	61.7	5.70	40.0	9.2	21600
8	Odessa shallows	0.038	0.42	6.5	31.2	30.3	78.1	1.5	67.4	35.4	27300
10	Odessa shallows		0.50	5.3	27.9	18.9	59.9	6.50	71.6	15.7	30600
11	Place of damping	0.020	0.25	8.2	19.7	16.5	64.1	7.30	72.6	17.7	38900
12	Waste waters discharge "South" in Odessa	0.098	0.38	7.2	31.8	24.8	97.3	6.00	89.5	28.0	27600
13	Mouth of port Illiechevsk in Odessa Bay	0.056	0.34	6.4	28.8	22.3	88.8	14.4	135	37.8	28200
14	Place of damping	0.063	0.39	7.5	39.7	29.7	302	10.2	71.8	29.5	33500
15	Mouth of Dniestr lagoon	0.021	0.12	3.1	4.60	8.00	29.7	2.80	32.0	10.6	12600
24	Centre of Northern-Western shelf	0.020	0.10	3.0	8.87	9.87	22.0	3.4	13.4	20.1	6540
29	Mouth of Sasyuk lake	0.094	0.28	6.7	30.8	29.1	92.7	15.7	69.2	36.9	30600
30	Mouth of Danube (north)	0.067	0.17	4.7	9.60	10.8	34.8	2.60	26.6	16.0	18800
34	Mouth of Danube (north)	0.250	0.52	9.6	54.2	37.3	144	10.4	108	60.6	45600
35	Mouth of Danube (south)	0.283	0.58	10.6	71.6	46.2	177	16.1	120	71.7	53000
39	Mouth of Danube (east)	0.048	0.15	6.1	16.2	18.1	51.6	9.00	46.7	21.0	23900
40	Mouth of Danube (east)	0.025	0.09	3.1	8.48	9.10	24.5	6.40	22.0	14.2	16600
41	Mouth of Danube (east)	0.042	0.10	3.9	11.1	11.7	30.8	6.20	24.6	14.8	15400
42	Mouth of Danube (east)	0.041	0.16	3.2	12.2	11.3	26.6	5.30	18.1	11.7	12200

No of station	Areas	Hg	Cd	Co	Cu	Pb	Zn	As	Cr	Ni	Al*
43	Mouth of Danube (east)	0.058	0.14	5.4	15.1	13.0	46.8	7.80	38.2	23.4	19700
44	Mouth of Danube (east)	0.049	0.21	7.4	24.6	18.8	67.8	12.2	68.8	34.6	29800
45	Mouth of Danube (east)	0.064	0.20	5.5	18.3	18.1	56.4	12.2	41.8	19.7	23300
46	Mouth of Danube (east)	0.142	0.37	9.2	35.4	44.2	115	20.4	88.2	47.7	30000
47	Mouth of Danube (east)	0.042	0.18	5.4	20.4	13.2	58.6	13.1	45.9	33.5	18500
49	Mouth of Danube (east)	0.038	0.16	5.3	16.9	6.10	35.5	10.1	20.2	22.2	9460
54	Karkinit'skiy Gulf	0.020	0.16	3.3	12.3	17.5	44.2	6.40	52.3	44.5	26800
56	Cup Tarkhankut in Crimea	0.030	0.16	5.8	30.2	28.1	76.9	5.30	53.1	30.1	31400
57	Mouth of port Sevastopol	0.136	0.24	8.1	39.7	24.1	97.0	25.2	77.5	42.1	53400
58	Mouth of port Balaklava	0.085	0.20	7.8	38.6	32.0	101	24.0	81.5	41.1	50800
60	Yalta	0.072	0.17	9.2	37.6	27.4	110	13.9	86.0	55.3	35000
61	Alushta	0.205	0.14	10.5	35.6	32.0	120	31.5	106	46.2	62200
62	Feodosia	0.075	0.20	9.1	34.7	24.0	108	14.8	94.1	45.4	50200
69	Kerch Strait (centre)	0.019	0.13	6.5	8.60	14.6	61.6	6.40	81.0	14.5	25600
70	Kerch Strait (centre)	0.020	0.08	6.0	4.70	11.4	42.1	10.5	81.6	17.0	25600
71	Kerch Strait (centre)	0.028	0.09	6.0	6.80	10.2	53.5	45.2	49.3	15.2	17900
73	Kerch Strait (centre)	0.086	0.22	11.9	31.9	25.2	113	15.6	97.2	51.5	53200
74	Kerch Strait (centre)	0.060	0.27	12.1	33.7	26.2	120	22.2	108	48.7	64400
75	Kerch Strait (exit)	0.059	0.32	10.8	33.5	27.0	118	10.6	106	50.3	51200

* - Aluminum used only as indicator of fine fraction of bottom sediments

n.a - not available

Trace metal concentrations in bottom sediments of the *Phyllophora* field occupying the central part of the northwestern shelf was monitored during July-August 2007 (26th cruise of R/V "Vladimir Parshin"). This data set indicated low level of mercury, cadmium, lead, arsenic and chromium pollution (Table 3.3.3). Nickel concentration exceeded the PL in 75% of the samples and reached the maximum 92.1 µg/g. Copper concentration was also above PL in 50% of the samples but the level of pollution wasn't too high. Cobalt and arsenic in bottom sediments were detected in moderate levels, mostly below the PL.

In general for the Ukrainian coastal zone not too much cases of high pollution of bottom sediments were noted during last 10 years. The copper and chromium pollutions were wide spread over the NWS (Fig. 3.3.8a,b). High chromium concentration was also found along the Crimea coast. Over the last decade the tendency of decreasing of maximum mercury and cadmium concentration in the Danube region were noted. No appreciable level of lead pollution was registered in bottom sediments.

3.3.2. Russian sector of the Black Sea - Northeastern region

Bottom Sediments: Metal concentration measurements in bottom sediments performed in June-July 2002 to the south of Taman showed large variations irrespective of sampling depths at 20m, 40m, 70m, and 100m (Table 3.3.4). Minimum concentrations of aluminum, vanadium, chromium, manganese, nickel, copper and arsenic were measured at 40 m depth. The opposite case occurred at 70 m depth where these elements attained maximum values, except manganese. Lead concentration increased to nearly 7.6 µg/g along the shore at 20m depth. The cadmium was below the detection limit at all sites.

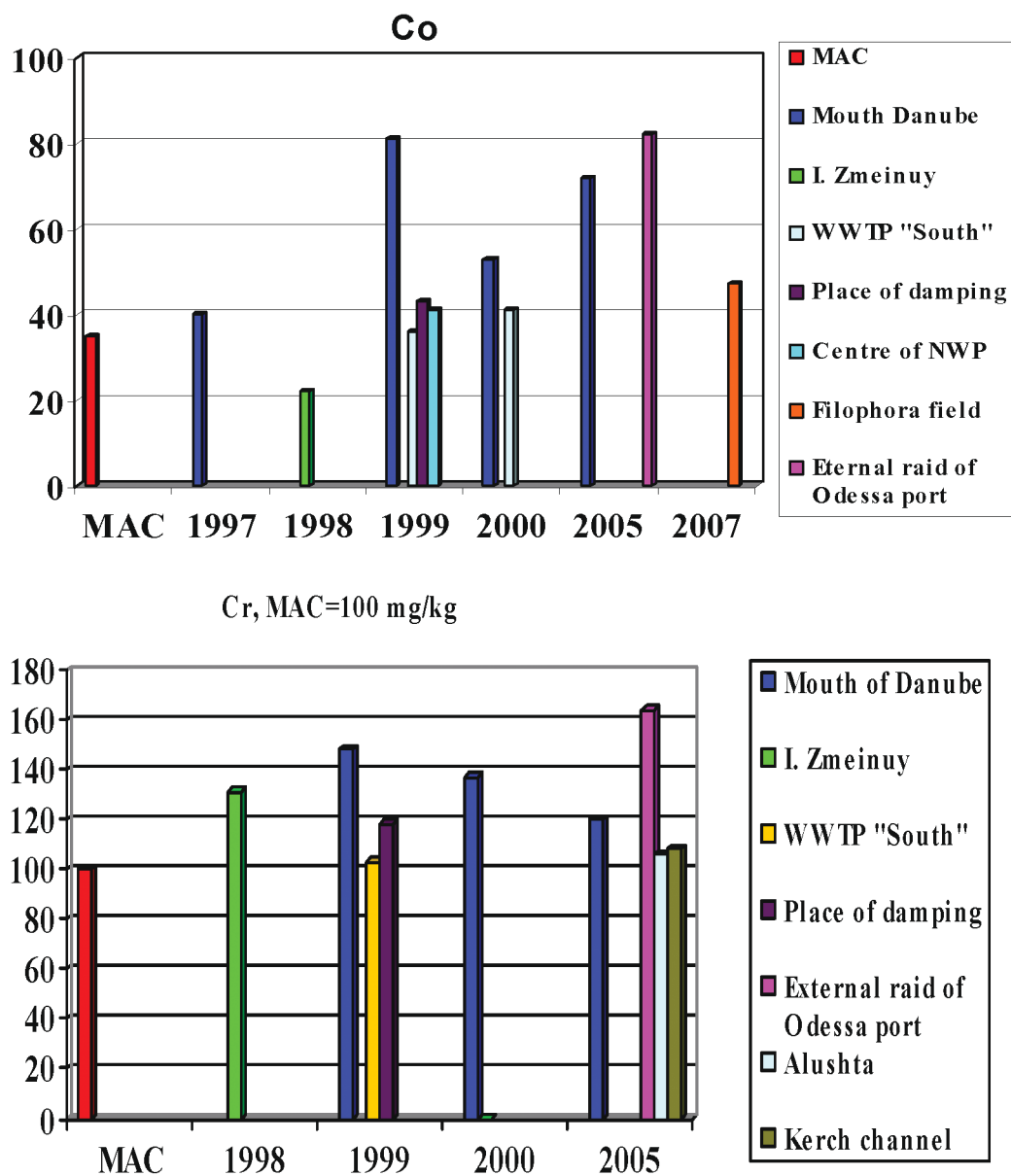


Figure 3.3.8. The high copper and chromium concentration ($\mu\text{g/g}$) in the bottom sediments of Ukrainian part of the Black Sea.

Table 3.3.3 The trace metal concentration (µg/g) in the bottom sediments of Phyllophora field and NW Shelf of the Black Sea in July-August 2007 (26 cruise of R/V "Vladimir Parshin").

		Hg	Cd	Co	Cu	Pb	Zn	As	Cr	Ni
		PL (µg/g) [7]								
Number of stations	Depth m	0.3	0.8	20	35	85	140	29	100	35
2	32	<0.001	0.02	0.92	1.60	3.60	5.3	0.98	4.30	7.5
39		0.043	0.30	8.13	34.8	28.9	73.7	6.90	41.4	46.2
45		0.039	0.33	12.2	44.0	37.0	96.2	8.00	55.1	55.9
75		0.020	0.17	4.90	12.7	10.2	35.3	4.00	13.1	24.2
84	44	0.023	0.29	7.92	27.5	19.4	57.2	5.90	25.2	41.6
142	39	0.033	0.31	11.2	27.4	19.9	80.3	8.80	32.3	49.0
157	39	0.032	0.27	10.4	22.6	26.2	66.2	5.30	29.2	35.4
177		0.088	0.31	11.0	37.3	37.4	166	8.00	53.3	67.7
221	50	0.080	0.29	22.8	46.9	32.1	99.2	22.1	46.7	92.1
234	66	0.028	0.22	15.6	38.7	38.2	104	17.6	52.4	62.3
246	32	0.127	0.46	17.4	38.0	18.6	95.7	9.70	52.8	71.2
262	1000	0.095	0.50	14.6	38.2	20.7	70.7	9.80	58.2	54.4

Table 3.3.4 Metal concentration (?g/g) in bottom sediments measured during June-July 2002 to the south of Taman.

Depth, m	Al	V	Cr	Mn	Ni	Cu	Zn	As	Cd	Pb
20	2184	128,4	47	661	28,6	53	31,06	7,25	0	7,6
40	876	54	27	163,5	5,5	38	30,08	2,02	0	4,3
70	3206	293	64	377,5	44	92	56,28	4,47	0	0,6
100	1488	115,2	42	255	32,2	79	25,61	5,35	0	5,0

3.3.3. Georgian sector of the Black Sea - Southeastern region

Bottom Sediments: Concentrations of Fe, Mn, Cu, Zn, Cr, V, Ni, Pb, Mo were measured in 186 samples of bottom sediments during 1993-1995 at shallow areas (3-15 m depth range) of the Georgian shelf. Additional trace metal measurements (Fe, Al, Cu, Zn, Cr, As, Ba and Pb) were performed in 2000 [19, 23, 24, 25]. 170 samples from 75 stations of the sea were collected throughout the entire Georgian shelf covering the depth range from 10 to 1500 m. A summary of these measurements is provided in Table 3.3.5.

Table 3.3.5. The metals concentration (µg/g) in the bottom sediments of Georgian shelf in 1993-1995 and 2000.

	Cr	Mn	Cu	Zn	As	Pb
1993-1995						
min/max	10/1300	700/9300	40/900	60/300	-	7,0-48
Average	215	1937	50	136	-	17,7
2000						
min/max	40/700	-	20/325	60/260	5,0/95	7-50
Average	81	-	81	102	15	20

Copper and Zink: High concentrations of Cu (325 µg/g) and Zn (260 µg/g) were found in bottom sediments collected from shallower depths near the estuary of Chorokhi River in response to the wastes discharged from mining enterprises in Murgul and Artvin regions of Turkey, in the immediate proximity of the boundary with Georgia and from Meria (Adjara) within the Georgian sector. They however decreased to the north. In sediments of the underwater slope of Kolheti lowland, Cu and Zn were distributed evenly at their background levels ranging from 20 to 45 (the average: 30 µg/g) for Cu and from 62 to 170 (the average: 110 µg/g) for Zn.

Arsenic: The distribution of arsenic in the shallow bottom sediments within Adjara section of underwater slope was analogous with distribution of Cu and Zn. Arsenic was introduced as a part of the sulphide minerals discharged into the sea together with other chalcophilic elements from the mining regions of Georgia and Turkey.

Chromium: This metal was distributed unevenly in bottom sediments. It mainly accumulated in sediments of the Chakvistskali-Supsa inter-mouth region with maximum concentrations 700 µg/g in the estuarine regions of the Chakvistskali and Natanebi Rivers. The main carriers of chromium are dark minerals (magnetite, biotite, pyroxene), the rock-forming minerals of the volcanic ores of basic composition (basalts, andesites, porphyrites, tuffs, tuff breccias, etc.) by the small rivers of the region (Korolistskali, Chakvistskali, Choloki, Natanebi, Supsa) [20]. In contrast to the copper and zinc, accumulation of chromium is natural, since it is not connected with any anthropogenic action. The difference between 1995 and 2000 was mainly related to the difference in sampling depths.

Lead: Lead was distributed evenly throughout the Georgian shelf. The maximum concentration did not exceed 50 µg/g, minimum was 7 µg/g, and the average for all Georgian shelf was 18 µg/g that corresponded to the local background level. Situation has not changed since mid-1990s.

Barium: High content of barium in bottom sediments was mainly confined into coastal zone of the Georgian shelf. The maximum concentration (in the limits of 0.1-0.2%) was found in the region between the Chorokhi River mouth to Batumi. Its distribution was related to the products of weathering of the barites- polymetallic layers of the South Caucasus, transported to the sea by the Chorokhi River. Accumulation of barium was also observed in the estuary sediments of Kintrishi River (0.05-0.1%). In coastal regions of the West Georgia, metamorphic geological formations containing clay minerals (in particular zeolites), rich in barium, were found. Possibly, that terrigenous material was enriched by above mentioned minerals, which explains comparatively high content of barium along the coast.

Aluminium: Being one of the basic rock-forming elements, aluminium constituted 2% to 7.5% of sediments of the Georgian shelf which are found at higher proportions in the area of Kolkheti lowland. On the average, in the northern part of the Georgian shelf, aluminium content was 3-4% higher than in south because of gradually increase of clay fractions in sediments in the northwards direction.

Iron: Coastal region of the shelf located in the inter-mouths of Korolistskali, Chakvistskali, Kintrishi, Natanebi and Supsa Rivers was characterized by high content of iron (>11%). These rivers drain the western extremity of Adjara-Trialeti folded system

and carry the products of red soil crust weathering into the sea. High content of iron is related with the dark minerals (magnetite, black mica, etc.) [21, 22]. In this region, high content of iron coincided with high content of chromium, which pointed to their common source. Within the limits of Kolkheti lowland, iron content varied from 3% to 5% in sediments of the underwater slope.

Manganese: In sediments from Chorokhi River estuary to the town Kolkheti, Mn distribution was practically homogeneous and equal to the natural background level from 0.07 to 0.27% with 0.13% on the average. This level corresponds to Mn concentration in the red-colored soil of coastal zone of Adjara and Gurii. In the area between Natanebi and Supsa Rivers, thickness of this type of soil is maximal and the discharge into the sea is therefore most intensive. To the north of the Supsa estuary, Mn content in sediments increased stepwise up to 0.93%, on the average 0.25%. It came into the sea in a large volume with suspended solids and particles of the Rioni River waters. In 1950-to-80s, Mn content in river particles was as high as 5.0-5.9%, and reached 5.0-14.8% level in sediments close to the northern branch of Rioni. That was however decreased to 0.3% in 1995. The decreasing Mn content in the Rioni discharge depends upon reduction of activity at the Chiature mining factory.

3.3.4. Romanian sector of the Black Sea - Western region

The investigations carried out in 2000-2005 on trace metals levels in water and sediments along the Romanian coastal zone evinced the following mean values and ranges:

Seawater (total concentrations): copper 14.09 $\mu\text{g/l}$ (1.46 - 27.31 $\mu\text{g/l}$); cadmium 2.15 $\mu\text{g/l}$ (0.27 - 4.60 $\mu\text{g/l}$); lead 11.58 $\mu\text{g/l}$ (1.03 - 30.04 $\mu\text{g/l}$); nickel 4.23 $\mu\text{g/l}$ (0.65 - 8.74 $\mu\text{g/l}$); chromium 5.28 $\mu\text{g/l}$ (1.50 - 12.23 $\mu\text{g/l}$); manganese 17.01 $\mu\text{g/l}$ (2.72 - 36.58 $\mu\text{g/l}$); zinc 9.06 $\mu\text{g/l}$ (0.40 - 26.98 $\mu\text{g/l}$).

Sediments: copper 61.83 $\mu\text{g/g dw}$ (18.71 - 134.35 $\mu\text{g/g dw}$); cadmium 1.81 $\mu\text{g/g dw}$ (0.37 - 3.35 $\mu\text{g/g dw}$); lead 55.52 $\mu\text{g/g dw}$ (15.71 - 107.35 $\mu\text{g/g dw}$); nickel 32.24 $\mu\text{g/g dw}$ (4.30 - 89.05 $\mu\text{g/g dw}$); chromium 12.01 $\mu\text{g/g dw}$ (3.01 - 23.34 $\mu\text{g/g dw}$); manganese 185.13 $\mu\text{g/g dw}$ (78.90 - 399.67 $\mu\text{g/g dw}$); zinc 117.90 $\mu\text{g/g dw}$ (26.98 - 181.63 $\mu\text{g/g dw}$).

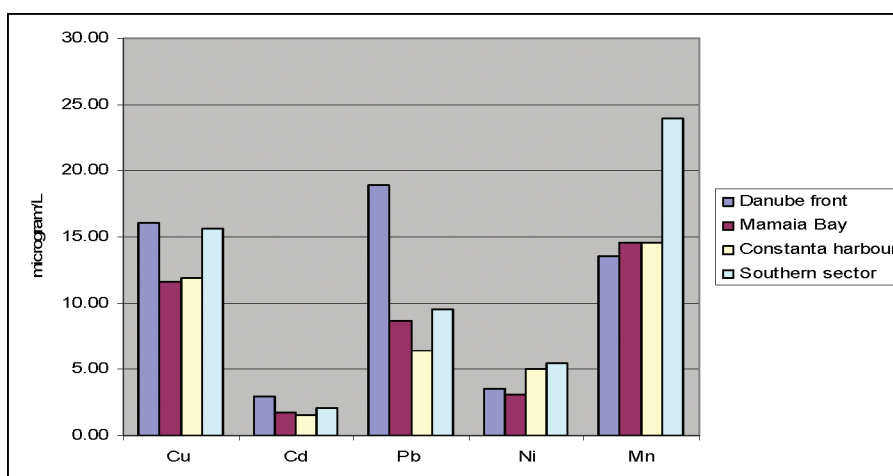


Fig. 3.3.9. Trace metal average values (2000 - 2005) in seawater along Romanian littoral

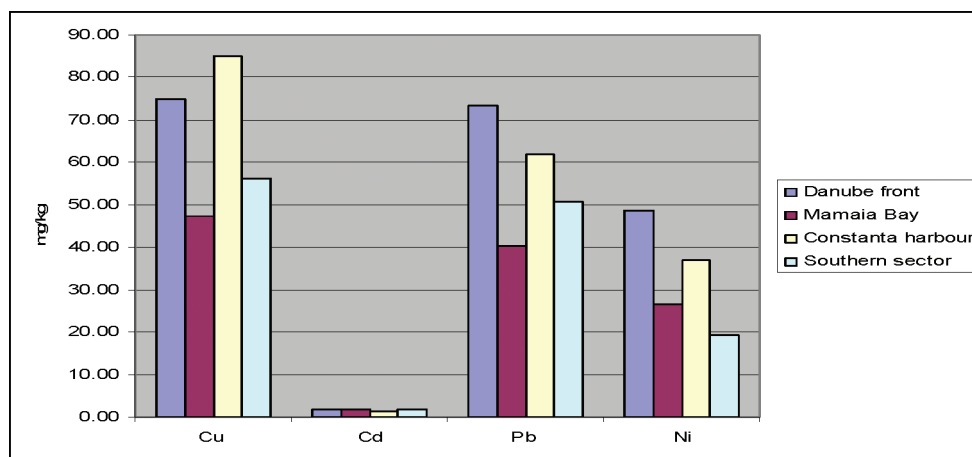


Fig. 3.3.10. Trace metal average values (2000 - 2005) in sediments along Romanian littoral

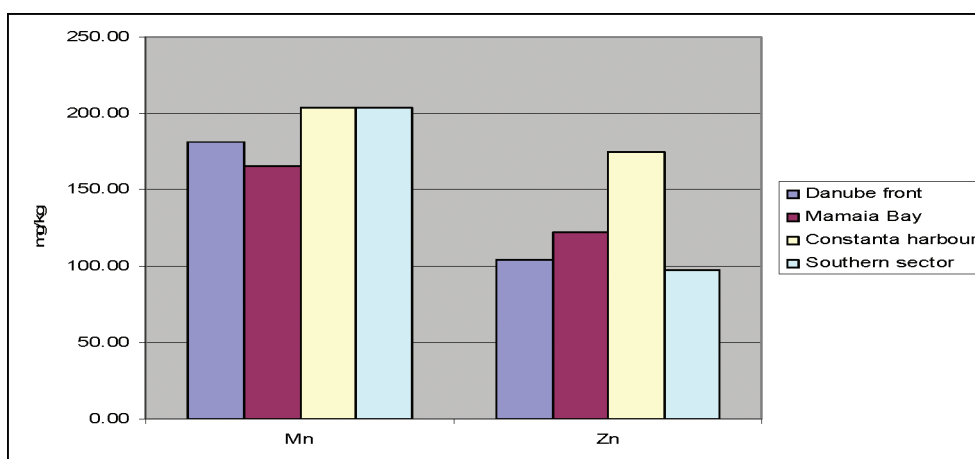


Fig. 3.3.10. (cont'd) Trace metal average values (2000 - 2005) in sediments along Romanian littoral

Trace metals distribution in seawater and sediments along the Romanian littoral during 2000-2005 presented a wide range of concentrations, under the influence of natural and anthropogenic factors. Strong impact of human activities was reflected, for instance, in the increased values of some metals in harbour sediments (Constanta Port). In comparison with the central sector of the littoral (Mamaia Bay) and the southern extremity, that were characterized by moderate values, in front of the Danube mouths higher concentrations of metals were measured, both in water and sediments. (Fig. 1B; Fig. 2).

Acknowledgments. The authors are grateful to the Secretariat of Black Sea Convention for providing the data collected for riparian countries used for this assessment. Special thanks to the personnel who were involved with sampling at sea and their analysis, particularly those working in "Typhoon" in Obninsk, O. Mjakoshin and Y. Yurenko in Sochi Hydrometeorological Centre, and Vakhtang Gvakharia (Georgia).

References

1. IAEA Regional Technical Co-operation Project RER/2/003 (2004) Marine Environmental Assessment of the Black Sea Region, working paper: Project Report, 356 p.
2. State of the Black Sea Environment. National Report of Ukraine. 1996-2000. - Chapter 4: Chemistry. V.Mikhailov, Yu.Denga, I.Orlova, V.Lepeshkin, R.Lisovsky, M.Pavlenko, L.Fetisov, V.Solovyov. - Odessa, Astroprint, p.34-53.
3. BSC - Black Sea Commission Annual Reports.
4. Marine Water Pollution. Annual Report 2004 By Korshenko A.N., I.G. Matveichuk, T.I. Plotnikova, V.P. Luchkov, V.S. Kirianov. - Moscow, Meteoagency of Roshydromet, 2006, 200 p.
5. Oradovsky S.G. (1993) Guidance on the methods of chemical analysis of seawater, Ed., St.Petersburg, Hydrometeoizdat, 220 pp.
6. Ferraro G., D. Tarchi, J. Fortuny, A. Sieber (2006) Satellite monitoring of accidental and deliberate marine oil pollution. In: Marine Surface Films Chemical Characteristics, Influence on Air-Sea Interactions and Remote Sensing. Eds. M. Gade, H. Hühnerfuss and G.M. Korenowski. Springer, 273-288.
7. Neue Niederlandische Liste. Altlasten Spektrum 3/93.
8. Black Sea Pollution Assessment. Ed. L.D. Mee and G. Topping, United Nations Publications, New York, 1998, 380 pp.
9. BSERP-2006 Cruise Report
10. Modern state of the Black sea waters pollution. Ed. Simonov A.I., Ryabinin A.I. "Seas project", Vol.IV, Black Sea, Issue 3, Sevastopol, "EKOSI-Hydrophysika", 1996, 230 p.
11. Savin P.T., N.F. Podpletnaya. Comparative characteristics of oil pollution of the nearshore and open areas of Odessa Region. - Problems of the sea coastal zone management and sustainable development. Abstracts of XXII International Coastal Conference, Gelendzhik, 16-20 May, 2007, 278-280.
12. Geoecology of shelf and coasts of Russian seas. Ed. N.A.Aibulatov. - M.: Noosphere, 2001, p. 314-316.
13. The list of fishing norms: maximum allowed concentrations (MAC) and as a guide safe levels of influence (OBUV) by harmful substances for the waters of basins having fishery importance. - Moscow, VNIRO, 1999, 304 p.
14. Patin S.A. Ecological problems of oil and gas resources development on the marine shelf. - M.: VNIRO Publishing, 1997, p. 131-140.
13. Mityagina M., O. Lavrova & T. Bocharova. Detection and Discrimination of Sea Surface Films in the Coastal Zone of Northeastern Black Sea Using SAR Data. ESA-ed., vol.1: ESA-SP-636, 2007.
16. Shcherbak S.S., O.Y. Lavrova, M.I. Mityagina, T.Y. Bocharova, V.A. Krovotyntsev, A.G. Ostrovskii. Multisensor satellite monitoring of seawater state and oil pollution in the north-eastern coastal zone of the Black Sea. International Journal of Remote Sensing. 2008. (in print).
17. Lavrova Olga, Marina Mityagina and Tatiana Bocharova, Satellite monitoring of sea surface state of Russia's coastal zone of the Black and Azov Seas // The 2nd International Workshop on Advances in SAAR Oceanography from Envisat and ERS Missions, January 2008, EASA-Esrin, Frascati, Italy.
18. Black Sea 2003 Cruise. Contaminant screening. Project Technical Report. Monaco, April 2004, 44 p.
19. Manual for the Geochemical analyses of Marine Sediments and Suspended Particle Mater. Reference Methods for Marine Pollution Studies. No. 63. UNEP 1995.
20. Machitadze N., V. Gvakharia, A. Tvalchrelidze (2001). Vanadium and chromium content in present sediments of Georgian sector of the Black sea. - Bull. of Georg. acad.of Sci., 164, No 3, p. 501-503.
21. Machitadze N., M. Tvalchrelidze, V. Gvakharia (2001). Particularities of geochemical zones formation in the sediments of south-eastern sector of the Black sea Georgia. - Bull. of Georg. acad.of Sci., 163, No 2, p. 297-300.
22. Gvakharia V.G., N.O. Machitadze, A.G. Tvalchrelidze (2002). Distribution Cu, Zn, Mo and Fe in contemporary marine sediments of the Georgian sector of Black sea. - A. Janelidze Geological Institute, Proceeding, New Series, Vol. 117, p. 424-429.

23. USEPA Method 418.1, TNRCC Method 1006.
24. Gvakharia V.G., Gelashvili N.E., Gvakharia T.A., Adamia T.M., Janashvili N.D., Maisuradze G.B. (2004). Method for determination of petroleum hydrocarbons and the study of pollution level of bottom sediments within the Georgian section of the Black Sea water area. - Georgian Engineering News, No2, p. 108-110.
25. Gvakharia V., Tsitsishvili V., Maisuradze G., Gelashvili N., Loria Kh., Girgvliani D. (2002). Use of Chromatography in Ecological Audit of Water Areas and Neighboring Territories of Black Sea coast of Georgia. - Second West Ukrainian Symposium on Adsorption Chromatography, p. 151-155.

CHAPTER 4 THE STATE OF RADIOACTIVE POLLUTION (V. Egorov et al.)

V.N. Egorov, S.B. Gulin, N.Yu. Mirzoyeva, G.G. Polikarpov, N.A. Stokozov

The A.O. Kovalevsky Institute of Biology of the Southern Seas, NASU,
Sevastopol, Ukraine

G.V. Laptev, O.V. Voitsekhovych

Ukrainian Hydrometeorological Institute, Kiev, Ukraine

A.I. Nikitin

SE SPA "Typhoon" of Roshydromet, Obninsk, Russia

Chapter co-ordinator: I. Osvath,

Marine Environment Laboratories, International Atomic Energy Agency, Monaco

4.1. Introduction

Due to its geographical location and limited water exchange with the rest of the World Ocean, the Black Sea has been one of the marine basins most contaminated with artificial radioactivity. Anthropogenic radionuclides originated primarily from two sources: the large-scale atmospheric nuclear weapons tests carried out before 1963 and the Chernobyl Nuclear Power Plant accident in April 1986 (Buessler and Livingston, 1996). The Black Sea received relatively high levels of atmospheric deposition from nuclear weapons testing, the global fallout reaching its maximum in the 40°-50°N latitude band (UNSCEAR, 2000), which runs across the Black Sea. The Chernobyl accident further led to direct contamination by fallout on the sea-surface. Secondary contributions from the deposition of radionuclides released to the atmosphere on the drainage basin entered the sea through river discharges, principally through the Danube and Dnieper Rivers (Livingston et al., 1988; Polikarpov et al., 1992). ^{137}Cs and ^{90}Sr are the most significant radionuclides reaching the Black Sea from these sources, due to their inventories, half-life and dosimetry. Additional relatively long-lived (e.g. Pu isotopes, ^{241}Am) or short-lived radionuclides (e.g. $^{95}\text{Zr}/^{95}\text{Nb}$, ^{103}Ru , ^{106}Ru , ^{110m}Ag , ^{125}Sb , ^{131}I , ^{134}Cs , $^{140}\text{Ba}/^{140}\text{La}$, ^{141}Ce , ^{144}Ce) have been reported and were traceable to the above-mentioned sources. There is no official record and no environmental evidence of radioactive waste dumping into the Black Sea (IAEA, 1999) as an additional pollution source. Monitoring of ^{137}Cs and ^{90}Sr in water, sediment and biota and significant research on marine radioactivity were carried out in the Black Sea since the early 1960s. In the period 1986-2005, within the framework of various international and national field campaigns and monitoring programmes, the Black Sea riparian countries collaborated in numerous studies. The present chapter provides an overview of these studies and assesses recent levels of radioactive pollution.

4.2. Concentrations and inventories of radionuclides in the water column

The regionally-averaged vertical profiles of ^{137}Cs and ^{90}Sr concentrations for the central deep basin (Fig. 4.1) indicate a three layer structure formed by high-concentrations in the

surface mixed layer, decreasing concentrations in the gradient layer, and low concentrations in the deep layer underneath. This structure has evolved by the progressive penetration of radionuclides to greater depths and the decrease in surface concentrations.

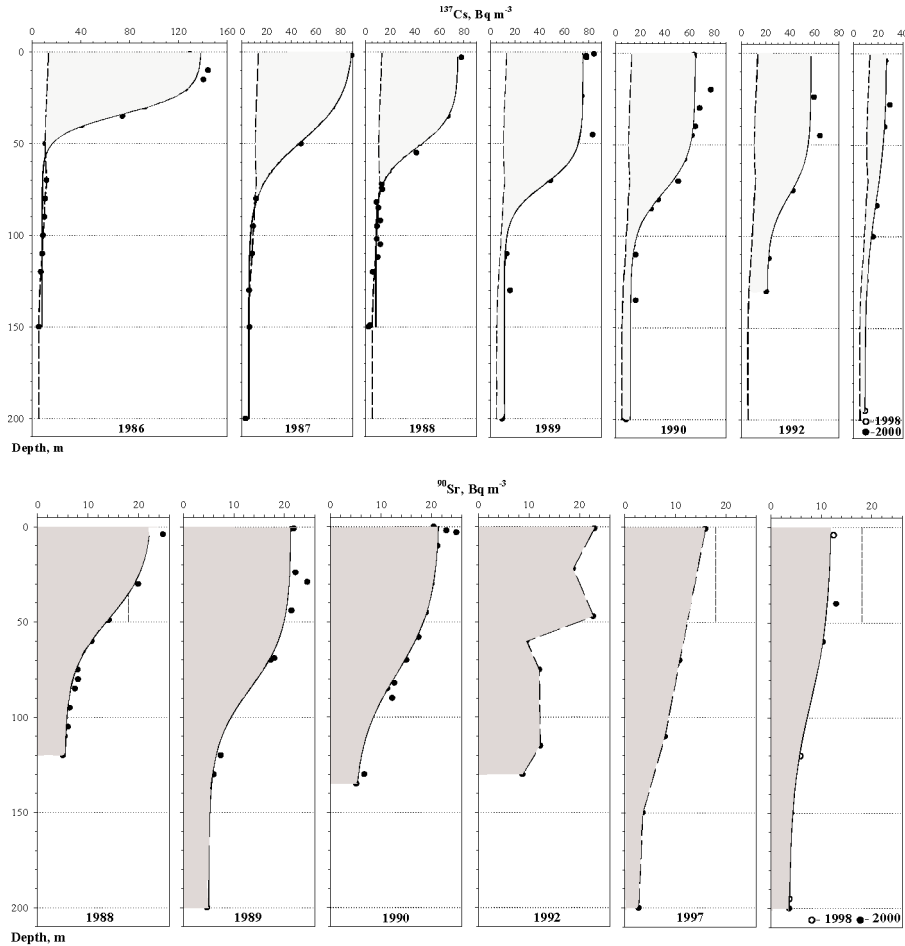


Fig. 4.1. Vertical distributions of ^{137}Cs (on top) and ^{90}Sr (below) concentrations in the Black Sea central basin in 1986-2000 (circles), curve-fitted profiles (solid lines) and average levels of ^{137}Cs concentration in the 0-200 m layer and ^{90}Sr in the 0-50 m layer before the Chernobyl NPP accident (dashed lines) (Stokozov and Egorov, 2002)

The atmospheric fallout deposited on the surface of the entire Black Sea during the first days of May 1986 was estimated at 1700-2400 TBq of ^{137}Cs , which corresponded to nearly 2% of the total ^{137}Cs release into the environment following the Chernobyl NPP accident (Nikitin et al., 1988; Polikarpov et al., 1991; Egorov et al., 1993). Shortly after the accident, the ^{137}Cs inventory in the surface 0-50 m layer reached 2700 TBq, exceeding its pre-Chernobyl value by a factor of 6-10. This inventory decreased abruptly to 1600 TBq in 1987 and then more gradually to around 500-600 TBq in 1998-2000 and 350 ± 60 TBq in 2001-2004 (Fig. 4.2). The ^{137}Cs input of 26 TBq from the Danube and the Dnieper Rivers over the period 1986-2000 was negligible in comparison with the direct contribution of atmospheric fallout (Voitsekhovich, 2001). The outflow of ^{137}Cs through the Bosphorus Strait was 250 TBq over the period 1986-2000 (Egorov et al., 2002, 2005).

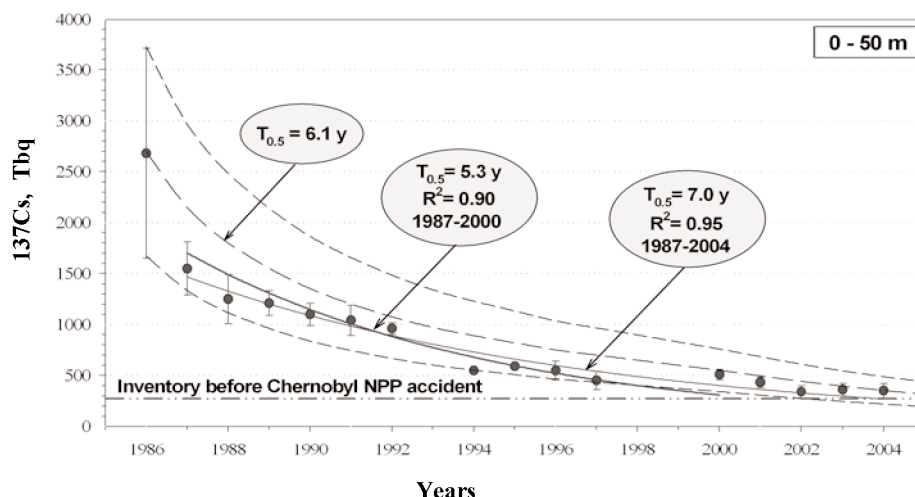


Fig. 4.2. Temporal evolution of the ^{137}Cs inventory in the 0-50 m water layer of the Black Sea after the Chernobyl NPP accident: estimates based on measured water concentrations (circles) and modeling (solid and dashed lines) (Egorov et al., 1993). A corresponding average environmental half-life of 5-7 y can be estimated for ^{137}Cs in surface waters.

The contribution of Chernobyl-origin ^{90}Sr deposition on the sea-surface was estimated to be 100-300 TBq, which resulted in a rapid increase of concentrations in the surface mixed layer (Egorov et al., 1999). The Dnieper and Danube Rivers added around 160 TBq of ^{90}Sr into the sea during 1986-2000, comparable in magnitude to the amount introduced by fallout after the Chernobyl NPP accident (Voitsekhovych, 2001). The ^{90}Sr outflow through the Bosphorus was 110 TBq over the period 1986-2000 (Egorov et al., 2002, 2005). Estimates given by Egorov et al. (2006) indicate a ^{90}Sr inventory of 1770 ± 790 TBq in the waters of the Black Sea in 1998-2000, 20% of which are attributable to the Chernobyl NPP accidental release, the majority of the ^{90}Sr inventory being contributed by global fallout. An area of particular interest due to secondary releases through the Dnieper from flooding of contaminated areas in the vicinity of the Chernobyl NPP, constituting an additional regional contamination source for the Black Sea, is the Dnieper-Bug estuary area. NW Black Sea annual mean surface concentrations of $16\text{--}21 \text{ Bq m}^{-3}$ ^{90}Sr were reported for 2001-2005, representing an increase as compared to the 1998-2000 annual means of between $10\text{--}15 \text{ Bq m}^{-3}$ ^{90}Sr (Egorov et al., 2006).

The evolution of ^{137}Cs and ^{90}Sr levels in coastal waters is illustrated by the values reported for the North-Eastern Black Sea (Table 4.1). Higher maximum post-Chernobyl levels in water were recorded in Sevastopol Bay, reaching up to 815 Bq m^{-3} and 157 Bq m^{-3} for ^{137}Cs and ^{90}Sr respectively (Fig. 4.4). As compared to initial levels measured after the Chernobyl accident, variations in average ^{137}Cs concentration values reported for 2001-2006 in coastal surface water narrowed down considerably, being mostly attributable to seasonal freshwater inflow and generally correlating well with salinity. Values between $12\text{--}21 \text{ Bq m}^{-3}$ were reported for Varna, Bulgaria in 2002-2004 (Veleva, 2006), $11\text{--}26 \text{ Bq m}^{-3}$ in 2003-2005 at the Georgian coast (Pagava, 2006), $15\text{--}36 \text{ Bq m}^{-3}$ in 2001-2005, with a single value close to 50 Bq m^{-3} in September 2004, for Constanza, Romania (Puscasu and Dima, 2006), being similar to those reported for the Russian coast (Table 4.1).

Relatively few data were published recently on Pu isotopes in Black Sea water. Values reported for $^{239+240}\text{Pu}$ over the period 1989-1998 range between 3 mBq m^{-3} in surface water and 13 mBq m^{-3} at 150-200 m depth.

Table 4.1. The dynamics of ^{137}Cs and ^{90}Sr levels (Bq m^{-3}) in surface waters of the North-Eastern Black Sea near the Russian Coast.

Year	^{137}Cs		^{90}Sr	
	Range	Average	Range	Average
Before Chernoby (1) NPP accident1	Homogeneous distribution	18.5	Homogeneous distribution	22.2
1986, June-July (2)	250-470	360 ± 50	74-100	86 ± 8
1986, October (2)	104-159	127 ± 17	22-37	28 ± 4
1987, June (2)	48-59	56 ± 4	-	-
2000-20013	20.0-28.0	23.5 ± 3.0	12.3-16.3	14.5 ± 2.0
2004	20.0-23.5	21.7 ± 1.8	10.3-11.0	10.7 ± 0.4
2005	20.2-22.6	21.4 ± 1.2	11.5-12.9	12.2 ± 0.7

Sources: (1) Vakulovsky et al. (1980, 1994), (2) Nikitin et al. (1988), (3) IAEA (2004)

4.3. Concentrations and inventories of radionuclides in sediment

The highest ^{137}Cs concentrations measured in 1992-1994 in the upper 5-cm layer of NW-W Black Sea shelf bottom sediments were found near the Danube Delta, the Dnieper-Bug Estuary, and around the Tarkhankut Cape of the Crimea peninsula (Egorov et al., 2006). A similar pattern of contamination was found in 2003-2004 (Voitsekhovych et al., 2006), reflecting the contributions of the post-Chernobyl initial atmospheric deposition, further river inflow and sediment transport and deposition. Total inventories of ^{137}Cs in bottom sediments near the river mouths in 1990-1994 were in the range $10\text{-}40 \text{ kBq m}^{-2}$, one order of magnitude higher than at shelf break ($2\text{-}5 \text{ kBq m}^{-2}$) and two orders of magnitude higher than at the continental slope and deep-water basin ($0.2\text{-}0.3 \text{ kBq m}^{-2}$) (Egorov et al., 2006). Pre-Chernobyl inventories of ^{137}Cs in bottom sediments ranged between $1\text{-}8 \text{ kBq m}^{-2}$ in coastal and shelf areas and were below 0.2 kBq m^{-2} in deeper areas (Vakulovsky et al, 1982). Maximum pre-Chernobyl ^{137}Cs concentrations in superficial bottom sediments of about $100 \text{ Bq kg}^{-1} \text{ d.w.}$ were reported by Vakulovsky et al. (1982). Maxima in the range of $500 \text{ Bq kg}^{-1} \text{ d.w.}$ ^{137}Cs were reported offshore the Danube mouths in September 1986 (Osvath et al., 1990), with current maxima reaching up to $100 \text{ Bq kg}^{-1} \text{ d.w.}$ ^{137}Cs according to Voitsekhovych et al. (2006).

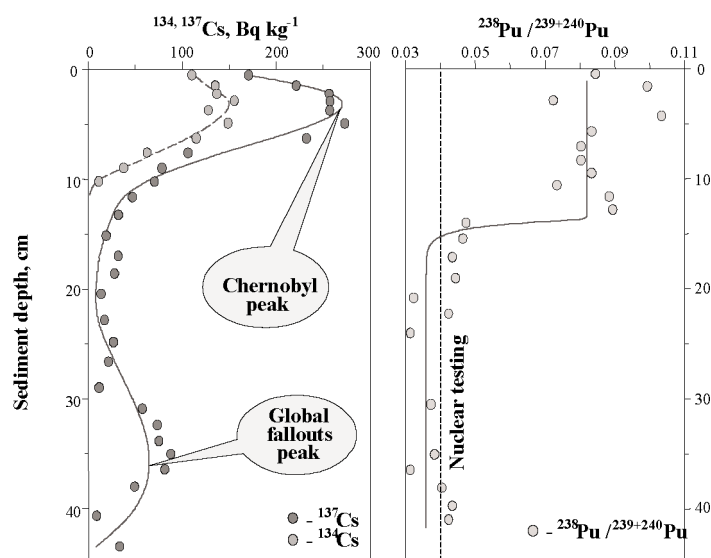


Fig. 4.3. Vertical distributions of ^{134}Cs , ^{137}Cs activities (Bq kg^{-1} d.w.) and the $^{238}\text{Pu}/^{239+240}\text{Pu}$ activity ratio versus sediment depth (cm) in the Danube delta region in 1997.

Well-preserved ^{137}Cs profiles in the deep basin and NW Black Sea bottom sediments (Egorov et al., 2006; Voitsekhovych et al., 2006) showed two subsurface peaks attributable to global fallout from atmospheric nuclear weapons testing and the Chernobyl accident. The Chernobyl origin of the upper peak in the ^{137}Cs activity profile was documented using the activity ratio of $^{134}\text{Cs}/^{137}\text{Cs}$, as the activity ratio of the short-lived ^{134}Cs ($T_{1/2} = 2.06$ years) to the longer-lived ^{137}Cs ($T_{1/2} = 30.17$ years) is known to be 0.53 in the Chernobyl release (Pentreath, 1988). A further differentiation of the pre- and post-Chernobyl sediments was carried out using the activity ratio $^{238}\text{Pu} / ^{239+240}\text{Pu}$, that was of about 0.04 for the pre-Chernobyl global fallout (Fig. 4.3) compared to 0.47 in the Chernobyl release (Pentreath, 1988). ^{210}Pb dating for well preserved cores, corroborated with indications from markers such as ^{137}Cs and Pu isotopes, was used for evaluating contributions from both radioactive and non-radioactive contamination sources and also sediment mass accumulation rates (Voitsekhovych et al., 2006; Gulin et al., 2002; IAEA, 2004).

Post-Chernobyl $^{239+240}\text{Pu}$ concentrations up to 0.4 Bq kg^{-1} d.w. were reported for sediments from both coastal and deep basin areas, depending on location and sediment composition (Egorov et al., 2006), with estimated $^{238}\text{Pu} / ^{239+240}\text{Pu}$ activity ratios varying in the range 0.105-0.165. These analyses indicated that about 75% of the total plutonium contamination in the Black Sea bottom sediments was caused by global fallout.

^{90}Sr being a soluble radionuclide, its levels in sediments remain generally low in the Black Sea. Pre-Chernobyl maxima of around 45 Bq m^{-2} ^{90}Sr inventory and 1.3 Bq kg^{-1} d.w. ^{90}Sr concentrations were reported by Vakulovsky et al. (1982) for superficial bottom sediments. Following the Chernobyl accident, in the Black Sea at large concentrations of ^{90}Sr in superficial bottom sediments remained in the same range as their pre-Chernobyl levels. Higher values were reported for the NW Black Sea, in particular offshore the Dnieper-Bug estuary area, where Mirzoyeva et al. (2005) reported concentrations of ^{90}Sr in the 0-5 cm layer of bottom sediments ranging up to 45 Bq kg^{-1} d.w. in 1986, 80 Bq kg^{-1}

¹ d.w. in 1989, 45 Bq kg⁻¹ d.w. in 1990-1996 and 150 Bq kg⁻¹ d.w. in 1997-2000. They relate the differences observed to river input, as previously mentioned, periods of high water inflow through the Dnieper and, to a lesser extent, through the Danube, resulting in increases of ⁹⁰Sr levels in offshore superficial sediments.

Radionuclides in beach sand are typically reported for radioprotection purposes. Concentrations in the past years range between roughly 0.5-12 Bq kg⁻¹ d.w. for ¹³⁷Cs, 0.2-10 Bq kg⁻¹ d.w. for ⁹⁰Sr and are below 0.2 Bq kg⁻¹ d.w. for ²³⁹⁺²⁴⁰Pu (IAEA, 2004).

4.4. Radionuclides in marine biota

The results of radioecological monitoring of the Sevastopol bays have shown that the increase of ¹³⁷Cs and ⁹⁰Sr concentrations in seawater recorded in May 1986 were followed by increases in the respective concentrations in marine biota (Fig. 4.4). Egorov et al. (2002) approximated the decrease recorded during the following years with exponential functions and estimated environmental half-lives for ⁹⁰Sr of 8.4 y for water, 4.9 y for seaweed, 6.7 y for mussels; and for ¹³⁷Cs 6.1 y for water, 4.7 y for seaweed, 7.5 y for mussels in the Sevastopol Bays. The doses delivered to the Black Sea biota by the anthropogenic radionuclides ⁹⁰Sr and ¹³⁷Cs after the Chernobyl NPP accident did not exceed the chronic exposure levels and the post-Chernobyl ⁹⁰Sr and ¹³⁷Cs contaminations did not introduce significant effects on biota in the Sevastopol Bay (Polikarpov, 1998; Mirzoyeva and Lazorenko, 2004). Maximum dose rates from anthropogenic radionuclides recorded in 1986 were found around 17%, 5.5% and 20% of the doses received from the natural ²¹⁰Po by fish, molluscs and seaweed, respectively.

Coastal monitoring results in countries around the Black Sea for the period 2000-2005 (Nikitin et al., 2006; Patrascu, 2006; Veleva, 2006; Pagava, 2006) indicate low levels of anthropogenic radionuclides in seaweed, molluscs and fish (Table 4.2). ²³⁹⁺²⁴⁰Pu concentrations up to 17 mBq kg⁻¹ w.w. in seaweed, 2.4 mBq kg⁻¹ w.w. in mollusks and 1 mBq kg⁻¹ w.w. in fish were reported at the NE Black Sea coast in 2000-2005 (Nikitin et al., 2006). Variations are observed between species and also depending on location, age etc., however, levels are generally low, with no radiological significance either for the biota themselves or for the human populations consuming edible species of marine biota.

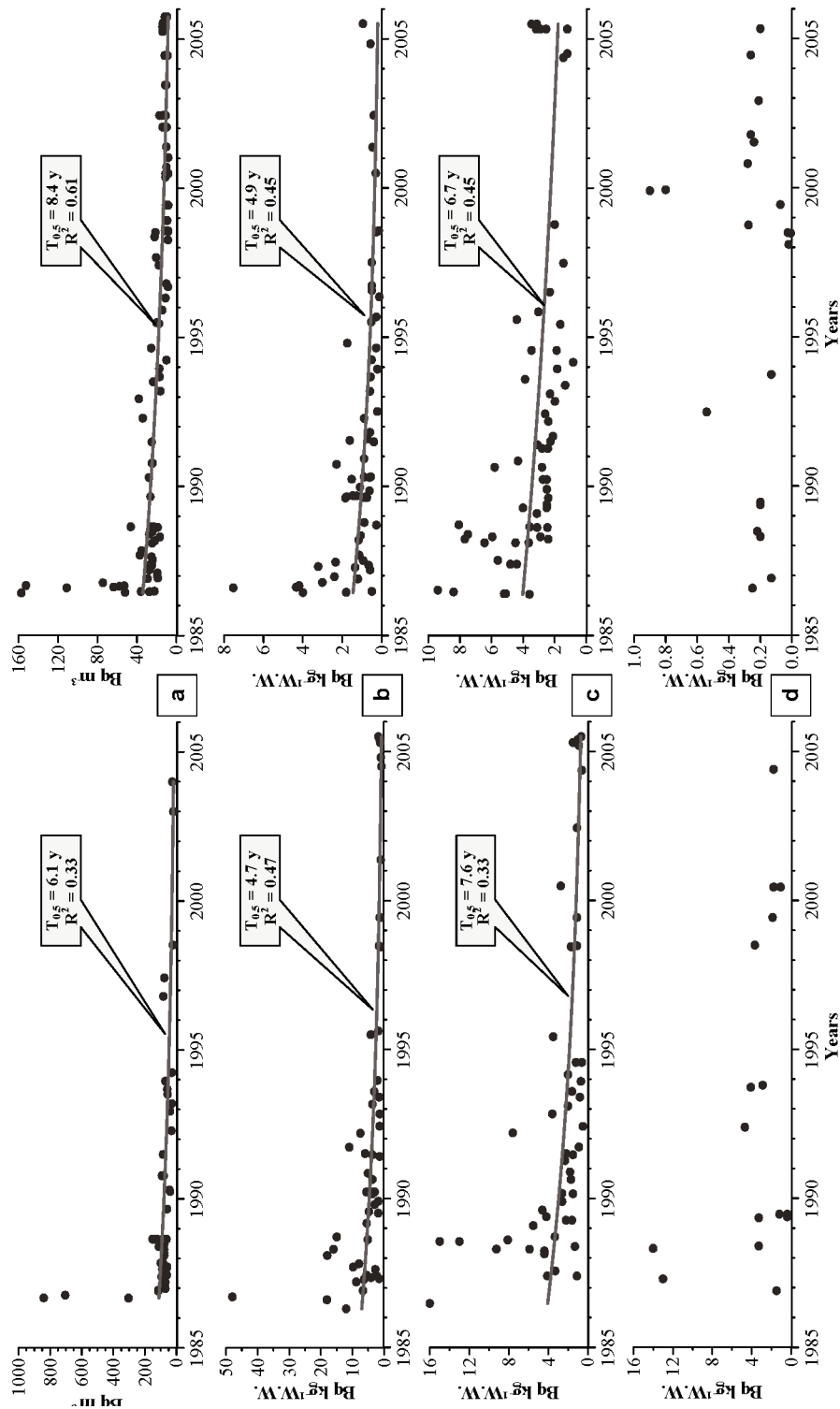


Fig. 4.4. Temporal evolution of ^{137}Cs (on the right) and ^{90}Sr (on the left) concentrations in water (a), algae *Cystoseira crinita* (b), mollusc *Mytilus galloprovincialis* (c) and fish *Merlangius merlangus euxinus* (d) in the Sevastopol bays in 1986-2005.

Table 4.2. The ranges of ^{137}Cs and ^{90}Sr concentrations in marine biota (Bq kg^{-1} w.w.) from coastal measurements performed by the riparian countries in the years 2000-2005.

Table 4.2. The ranges of ^{137}Cs and ^{90}Sr concentrations in marine biota (Bq kg^{-1} w.w.) from coastal measurements performed by the riparian countries in the years 2000-2005.	^{137}Cs	^{90}Sr
Biota		
Seaweed	0.3-3	0.4-2.5
Molluscs	0.3-2	0.02-3.2
Fish	0.8-3	0.02-3.2

4.5. Conclusions

Chernobyl atmospheric fallout deposited 1.7-2.4 PBq of ^{137}Cs into the Black Sea surface, which temporarily increased the ^{137}Cs inventory of the 0-50 m surface layer by a factor of 6-10 in comparison with its pre-Chernobyl value. The contribution of Chernobyl-origin ^{90}Sr (0.1-0.3 PBq) from atmospheric fallout was lower in comparison with that of ^{137}Cs . A subsequent ^{90}Sr input from the Danube and the Dnieper Rivers (about 0.16 PBq) was an important contribution to the budget of this radionuclide in the Black Sea, but the riverine ^{137}Cs input (0.02-0.03 PBq) was insignificant. The decrease of the ^{137}Cs inventory in the surface layer after Chernobyl has been mainly controlled by vertical mixing, loss through the Bosphorus Strait, and radioactive decay. The loss through the Bosphorus accounted for 2-2.5% of the ^{137}Cs inventory. In the case of ^{90}Sr , these processes have been compensated by river inputs from the Dnieper and Danube Rivers up to 1994-1995 and partially after 2000. The vertical mixing of ^{137}Cs and ^{90}Sr was mainly effective within the 0-200 m layer. Sediment inventories of ^{137}Cs in the Danube and Dnieper delta regions exceeded with one order of magnitude the values in the slope zone and two orders of magnitude those in the deep basin. Marine biota along the coastal areas of the Black Sea presented very low levels of anthropogenic radionuclides.

Although the Black Sea was ranked at the level of the year 2000 amongst the marine regions of the World Ocean as the 2nd highest in terms of ^{90}Sr concentrations in surface seawater (after the Irish Sea) and 3rd highest in ^{137}Cs concentrations (after the Baltic and Irish Seas) (IAEA, 2005), the levels of anthropogenic radionuclides found in the Black Sea environment associate insignificant radiological doses to human populations.

References

- Buesseler, K.O. and Livingston, H.D. (1996). Natural and man-made radionuclides in the Black Sea. In: P. Guéguénat, P. Germain and H. Métivier, Editors, *Radionuclides in the Oceans: Inputs and Inventories*, Editions de Physique, IPSN.
- Buesseler, K.O. and Livingston, H.D. (1997). Time-series profiles of ^{134}Cs , ^{137}Cs and ^{90}Sr in the Black Sea. In *Sensitivity to change: Black Sea, Baltic Sea and North Sea*. Eds. Ozsoy, E. and Mikaelyan A. Dordrecht: Kluwer Academic, 239-251.
- Egorov, V.N., Polikarpov, G.G., Kulebakina, L.G., Stokozov, N.A., Yevtushenko, D.B. (1993). *Model of*

- large-scale contamination of the Black Sea with the long-lived radionuclides ^{137}Cs and ^{90}Sr resulting from the Chernobyl NPP accident. *Water Resources*, 20 (3), 326-330 (in Russian).
- Egorov, V.N., Povinec, P.P., Polikarpov, G.G., Stokozov, N.A., Gulin, S.B., Kulebakina, L.G., Osvath, I. (1999). ^{90}Sr and ^{137}Cs in the Black Sea after the Chernobyl NPP accident: inventories, balance and tracer applications. *J. Environmental Radioactivity*, 49 (3), 137-156.
- Egorov, V.N., Polikarpov, G.G., Osvath, I., Stokozov, N.A., Gulin, S.B., Mirzoyeva N.Yu. (2002). The Black Sea radioecological response to the ^{90}Sr and ^{137}Cs contamination after the Chernobyl NPP accident. *Marine Ecological J.*, 1(1), 5-15. (In Russian).
- Egorov, V.N., Polikarpov, G.G., Stokozov, N.A., Mirzoeva N. Yu. (2005). Estimation of ^{90}Sr and ^{137}Cs transfer from the Black Sea to the Mediterranean basin after Chernobyl NPP accident. *Marine Ecological J.*, 4(4), 33-41.
- Mirzoyeva, N.Yu., Egorov, V.N., Polikarpov, G.G. (2005) Content ^{90}Sr in the Black Sea bottom sediments after the Chernobyl NPP accident and its using as a radiotracer for the assessment of the sedimentation rate. *System control of Environment (means and monitoring): collected scientific articles, NAS of Ukraine. MHI, Sevastopol*, 2005, 276 - 282 (in Russian)
- Egorov V.N., Polikarpov G.G., Gulin S.B., Osvath I., Stokozov N.A. Lazorenko G.E., 2006. XX years of radioecological response studies of the Black Sea to the Chernobyl NPP accident. Presented at the First Biannual Scientific Conference "Black Sea Ecosystem 2005 and Beyond", Istanbul, 8-10 May 2006.
- Gulin, S.B., Polikarpov, G.G., Egorov, V.N., Martin, J.M., Korotkov, A.A., Stokozov, N.A. (2002). Radioactive contamination of the north-western Black Sea sediments. *Estuarine, Coastal and Shelf Science*, 54 (3), 541 - 549.
- IAEA (1999). Inventory of radioactive waste disposals at sea. International Atomic Energy Agency, IAEA-TECDOC-1105, August 1999.
- IAEA (2004). Regional Technical Co-operation Project RER/2/003 "Marine Environmental Assessment of the Black Sea". Working material. Reproduced by the IAEA, Vienna, Austria, 2004.
- Livingston, H.D., Buesseler, K.O., Izdar, E., & Konuk, T. (1988). Characteristics of Chernobyl fallout in the Southern Black Sea. In: *Radionuclides: a tool for oceanography*. J.C.Guary, P. Guegueniat, & R.J.Pentreath (Eds.), Essex: UK Elsevier. 204-216.
- Nikitin A.I., Medinets V.I., Chumichev V.B., Katrich I.Yu., Vakulovsky S.M., Kozlov A.I., Lepeshkin V.I. (1988) Radioactive contamination of the Black sea caused by the Chernobyl NPP accident as of October 1986, *Atomnaya Energia*, 65 (2), 134-137 (in Russian).
- Nikitin A.I., Chumichev V.B., Valetova N.K., Katrich I.Yu., Kabanov A.I., Yurenko Yu.I. (2006) Monitoring of artificial radionuclides in the marine environment of the Russian Coast of the Black Sea: results obtained during the years 2004-2005.
- Osvath I., Dovlete C., Bologa A. (1990). Radioactivity in the Romanian sector of the Black Sea. *Proc. International Symposium on post-Chernobyl environmental radioactivity studies in East-European countries*. Kazimierz, Poland, 1990, pp108-112.
- Pagava S. (2006). Report on the Black Sea environmental pollution by radioactivity, Georgia 2003-2005. I. Javakhishvili Tbilisi State University, Tbilisi, Georgia. Report to the IAEA, 2006.
- Pentreath R.J. (1988). Sources of artificial radionuclides in the marine environment. In: *Radionuclides: A Tool for Oceanography*. Guary J.C., Guegueniat P., Pentreath R.J. (Eds.), Essex: UK Elsevier, 12-23.
- Polikarpov, G.G., Kulebakina, L.G., Timoshchuk, V.I., Stokozov, N.A. (1991). ^{90}Sr and ^{137}Cs in surface waters of the Dnieper River, the Black Sea and the Aegean Sea in 1987 and 1988, *J. Environmental Radioactivity*, 13, 25-28.
- Polikarpov G.G., Livingston H.D., Kulebakina L.G., Buesseler K.O., Stokozov N.A., Casso S.A. (1992). Inflow of Chernobyl ^{90}Sr to the Black Sea from the Dnieper River. *Estuarine, Coastal and Shelf Science*, 34, 315 - 320.
- Polikarpov G.G. (1998). Conceptual model of responses of organisms, populations and ecosystems in all possible dose rates of ionizing radiation in the environment. *Procc. of RADOX 96-97 conference, Norwich/Lowestoft*, 8-11 April, 1997. *Radiation Protection Dosimetry*, 75(1-4), 181-185.
- Patrascu, V. (2006). Romanian contribution by NIMRD Constanza to radioactivity assessment in Black Sea biota. Report to the IAEA, 2006.

- Puscasu C., Dima D. (2006). Assessment of marine radioactivity in the Romanian sector of the Black Sea. Environmental Protection Agency, Constantza, Romania. Report to the IAEA, 2006.
- Stokozov N.A. & Egorov V.N. (2003). Vertical water mixing in the Black Sea: evidences from long - term post - Chernobyl ^{137}Cs profiles. Procc. of NATO Advanced Research Workshop on Past and Present Water Column Anoxia, Sevastopol, Ukraine, 4-8 October 2003. 88-89.
- UNSCEAR (2000). Sources and effects of ionizing radiation. United Nations Scientific Committee on the Effects of Atomic Radiation UNSCEAR 2000 Report to the General Assembly with Scientific Annexes. Vol I: Sources. UN, New York, 2000
- Vakulovsky, S.M., Katrich, I.Yu., Krasnopevtcev, U.V., Nikitin, A.I., Chumichev, V.B., Shkuro, V.M. (1980). Spatial distribution and balance of H^3 and Cs-137 in the Black Sea in 1977. Atomic Energy, 49 (2), 105-108 (in Russian).
- Vakulovsky, S.M., Krasnopevtsev, Yu.V., Nikitin, A.I., Chumichev, V.B. (1982). Distribution of ^{137}Cs and ^{90}Sr between the water and bottom sediments in the Black sea in 1977. Okeanologia, v.XXII, issue 6, Moscow, 1982, pp.966-969 (in Russian)
- Vakulovsky, S.M., Nikitin, A.I., Chumichev, V.B., Katrich, I.Yu., Voitsekhovich, O.V., Medinets, V.V., Isarev, V.I., Bovkun, L.?, Khersonsky E.S. (1994) Cesium-137 and strontium-90 contamination of water bodies in the areas affected by releases from the Chernobyl nuclear power plant accident: An overview. J. Environmental Radioactivity, 23, 103-122.
- Veleva B. (2006). Report on results obtained in Bulgaria on Black Sea environmental pollution, with a focus on marine radioactivity. National Institute of Meteorology and Hydrology, Sofia, Bulgaria. Report to the IAEA, 2006.
- Voitsekhovych, O.V. (2001). Project status report of the Ukrainian Hydrometeorological Institute (UHMI), Central geophysical observatory (CGO), Marine Branch of UHMI (2001). National Report for the IAEA Regional Technical Co-operation Project RER/2/003 "Marine Environmental Assessment in the Black Sea". UHMI, Kiev-Sevastopol, 83 p.
- Voitsekhovych, O.V. , Kanivets V.V., Laptev G.V. (2006). Current state of radioactivity studies in the Ukrainian Hydrometeorological Institute (UHMI) 2002-2005. Progress Report to the IAEA, 2006.